



PROJECT NO.
5050



UV-Chlorine AOP in Potable Reuse: A Guidance Manual to Assessment and Implementation

UV-Chlorine AOP in Potable Reuse: A Guidance Manual to Assessment and Implementation

Prepared by:

Erin D. Mackey, PE, PhD

Brown and Caldwell

Ron Hofmann, P Eng, PhD

University of Toronto

Adam Festger, MS

Brown and Caldwell

Catherine Vanyo, PE

Brown and Caldwell

Co-sponsored by: California State Water Resources Control Board

2022



The Water Research Foundation (WRF) is the leading research organization advancing the science of all water to meet the evolving needs of its subscribers and the water sector. WRF is a 501(c)(3) nonprofit, educational organization that funds, manages, and publishes research on the technology, operation, and management of drinking water, wastewater, reuse, and stormwater systems—all in pursuit of ensuring water quality and improving water services to the public.

For more information, contact:

The Water Research Foundation

1199 North Fairfax Street, Suite 900
Alexandria, VA 22314-1445
P: 571.384.2100

6666 West Quincy Avenue
Denver, Colorado 80235-3098
P: 303.347.6100

www.waterrf.org
info@waterrf.org

©Copyright 2022 by The Water Research Foundation. All rights reserved. Permission to copy must be obtained from The Water Research Foundation.

WRF ISBN: 978-1-60573-603-7

WRF Project Number: 5050

This report was prepared by the organization(s) named below as an account of work sponsored by The Water Research Foundation. Neither The Water Research Foundation, members of The Water Research Foundation, the organization(s) named below, nor any person acting on their behalf: (a) makes any warranty, expressed or implied, with respect to the use of any information, apparatus, method, or process disclosed in this report or that such use may not infringe on privately owned rights; or (b) assumes any liabilities with respect to the use of, or for damages resulting from the use of, any information, apparatus, method, or process disclosed in this report.

Prepared by Brown and Caldwell and the University of Toronto

This document was reviewed by a panel of independent experts selected by The Water Research Foundation. Mention of trade names or commercial products or services does not constitute endorsement or recommendations for use. Similarly, omission of products or trade names indicates nothing concerning The Water Research Foundation's positions regarding product effectiveness or applicability.

Acknowledgments

Research Team

Principal Investigators:

Erin Mackey, PE, PhD
Brown and Caldwell

Ron Hofmann, PhD
University of Toronto

Project Team:

Adam Festger, Catherine Vanyo, PE
Brown and Caldwell

Tianyi Chen, Nathan Moore, Liz Taylor-Edmonds
University of Toronto

WRF Project Advisory Committee

Troy Walker
Hazen and Sawyer

Bryan Trussell
Trussell Technologies

June Leng
HDR

Participating Utilities and Manufacturers

Cornwall, Canada

Hampton Road Sanitation District, USA

Los Angeles Sanitation District, USA

Orange County Water District, USA

Region of Peel, Canada

Region of Waterloo, Canada

Water Replenishment District, USA

West Basin Municipal Water District, USA

DeNora

Trojan Technologies

Xylem

WRF Staff

John Albert, MPA, Chief Research Officer

Ashwin Dhanasekar, Research Program Manager

Contents

Acknowledgments.....	iii
Tables.....	vi
Figures.....	vii
Acronyms and Abbreviations	viii
Chapter 1: Introduction.....	1
1.1 Why Include UV-AOP as Part of a Treatment Strategy?	1
1.2 Overview of UV-AOP	2
1.2.1 Lamp and Oxidant Type Considerations	3
1.2.2 UV Dose for Disinfection and Oxidation	4
1.2.3 Sizing UV-AOP systems	6
1.2.4 Selecting the Oxidant for Use in an AOP Application	7
Chapter 2: The Basics of UV-AOP Photochemistry	9
2.1 UV-AOP Uses UV Light to Catalyze the Formation of Radicals that Degrade Contaminants	9
2.2 UVT is a Key Design Parameter.....	10
2.3 Radical Scavenging is also Important for System Sizing.....	10
Chapter 3: Influence of Background Water Chemistry on UV-AOP Efficacy.....	13
3.1 Nitrogen Species: Ammonia, Chloramines, Nitrate, and Nitrite	13
3.2 pH.....	18
3.3 Alkalinity.....	19
3.4 Chloride and Bromide.....	19
3.5 Organic Matter	20
Chapter 4: Design Considerations for UV-AOP Systems	21
4.1 Setting Design Criteria	21
4.2 Flow Rate and Redundancy	23
4.3 Oxidant Dosing Design.....	24
4.4 Source Water Characterization.....	25
4.5 Understanding the Dynamic Chemistry of the UV-Cl ₂ Process Is Essential to Good Design	26
4.6 Water Quality Considerations	29
4.7 Selection of UV Dose and Oxidant Dose Impact Both Efficacy and Cost Considerations.....	32
4.8 Hydroxyl Radical Scavenging Demand	34
4.9 Fouling Potential.....	35
4.10 Critical Control Point Monitoring.....	36
4.11 Monitoring of UV-AOP Systems.....	38
Chapter 5: Economic Analysis of UV-Cl₂ vs. UV-H₂O₂.....	47

5.1	Capital Cost Comparison in an RO-Based Application.....	47
5.2	Operation and Maintenance Cost Comparison in an RO-Based Application	48
5.3	Comparison of the Cost of Chlorine vs. Hydrogen Peroxide (Oxidant)	51
5.4	Increases in the Costs of Oxidants Related to Market Forces.....	53
5.5	Economic Impacts of Lamp Type Selection.....	56
5.6	Cost Impact of Alternate Target Contaminants	57
5.7	Costs of Quenching Residual Oxidant.....	58
5.8	Cost Impact of Nitrite	58
5.9	Non-Monetary Considerations	59
Chapter 6: Selecting the Right UV-AOP: A User’s Decision Tree.....		61
6.1	Is pH in an Acceptable Range to Consider UV-Cl ₂ ?	62
6.2	Is Ammonia Well Controlled?.....	63
6.3	Is Bromide Not an Issue or Well Controlled?.....	64
6.4	Is Nitrite in an Acceptable Range?.....	65
6.5	UV-Cl ₂ is Viable	66
6.6	UV-H ₂ O ₂ May be a Better Option	66
6.7	Decision Tree Summary.....	66
Chapter 7: Testing and Startup		69
7.1	Considerations for Bench- and Pilot-Testing in the Pre-design Phase	69
7.2	Performance Testing the Installed UV-Cl ₂ AOP System	70
7.2.1	Creating the Performance Test Matrix.....	74
7.2.2	Steady State/Mixing Test.....	75
7.2.3	Regulatory Involvement.....	76
7.2.4	Adjusting UVT	76
7.2.5	Indicator Compounds—The Surrogate Question	76
7.2.6	Performance Test Issues Related to the Dynamic Chemistry of UV-Cl ₂	77
Chapter 8: Pulling It All Together		79
References		85
Appendix A: Current State-of-the-Science of UV Chlorine AOP		89
Appendix B: Reaction Rate Coefficients of Microcontaminants with RCS and •OH		173
Appendix C: Kinetics Models.....		185
Appendix D: Variation and Removal of OH Radical Scavenging Capacity		217
Appendix E: DBPs and Toxicity		229

Tables

3-1	OH Radical Scavenging of Nitrogen Species Post-RO (pH 5.5)	15
4-1	Considerations for Developing Design Criteria	22
4-2	Sodium Hypochlorite Injection Best Practices	24
4-3	Feed Water Quality Parameters Important to UV-Cl ₂ System Sizing	25
4-4	Chlorine Chemistry through the UV-Cl ₂ Process	26
4-5	UV-AOP Alert and Alarm Level Summary	36
4-6	Chlorine Analyzer Comparison.	42
4-7	Summary of UV-AOP System Monitoring Requirements and Options.....	44
5-1	Conditions for Full Advanced Treatment Scenario with UV-Cl ₂ and UV-H ₂ O ₂	49
6-1	Potential Treatment Process Modifications to Address Elevated Ammonia and Nitrite in the Feed Water in Potable Reuse	65
7-1	Checklist for a Successful Performance Test.....	71
7-2	Example Performance Test Matrix	75
8-1	Key Considerations and Takeaways in the Evaluation of the UV-Cl ₂ AOP.	79

Figures

1-1	Illustration of UV-AOP Treatment.....	3
1-2	UV Lamp Emission Spectra and Absorbance of Oxidants Versus Wavelength	4
2-1	Lewis Dot Diagram of (a) Hydroxide Ion and (b) Hydroxyl Radical with an Unpaired Electron.....	9
3-1	Summary of the Roles of Nitrogen-Containing Species in Potable Reuse Applications of UV-AOP	14
3-2	Impact of Nitrogen Species on UV Absorption Spectra	15
3-3	Example of the Fate and Impact of Chloramines in a Post-RO UV-Cl ₂ Treatment Process at pH 5.5.....	17
3-4	Relative Proportions of HOCl and OCl ⁻ as a Function of pH.....	18
4-1	Travel Distance to the UV Reactor Can Affect the Required Free Chlorine Dose	29
4-2	Hypothetical Change in UVT and Monochloramine through a UV-AOP Reactor	40
4-3	Sample Line Design.....	41
4-4	Monitoring Locations and Monitor Options for UV-Cl ₂ and UV-H ₂ O ₂	44
5-1	Comparison of Annual O&M Costs for UV-Cl ₂ and UV-H ₂ O ₂ for a 12-mgd FAT Installation with Low Ammonia and Nitrite	50
5-2	Relative Cost Comparison of Annual O&M costs for UV-Cl ₂ and UV-H ₂ O ₂ with Low Ammonia and Nitrite	51
5-3	Comparison of Annual Oxidant Costs for UV-Cl ₂ and UV-H ₂ O ₂ for a 12-mgd FAT Installation.....	52
5-4	Detail of Annual O&M costs for UV-Cl ₂ and UV-H ₂ O ₂ for a 12-mgd FAT Installation.....	53
5-5	PPI for Water Treatment Compounds January 2007 through April 2022	54
5-6	Sensitivity Analysis of the Impact of the Price of Chlorine on O&M Costs.....	55
5-7	Annual O&M Cost of LPHO versus MP Lamp-Based Systems in a 12-mgd FAT Application with Low Ammonia and Nitrite.....	56
5-8	Impact of Increasing Nitrite on Annual O&M Cost	59
6-1	UV-Cl ₂ vs. UV-H ₂ O ₂ Evaluation Process Decision Tree	62
8-1	Water Replenishment District of Southern California UV/Cl ₂ Case Study.	82
8-2	LA Sanitation UV/Cl ₂ Case Study.....	83

Acronyms and Abbreviations

$\mu\text{g/L}$	micrograms per liter
CaCO_3	calcium carbonate
CB	collimated beam
CCP	critical control point
CBAT	carbon-based advanced treatment
Cl_2	chlorine
ClO^\bullet	chlorine oxide radical
CO_3^{2-}	carbonate
$\text{CO}_3^{\bullet-}$	carbonate radical
COC	chain of custody
DBP	disinfection byproduct
EED	electrical energy dose
EEO	electrical energy per order
FAT	full advanced treatment
GAC	granular activated carbon
gal	gallon
HAA5	(regulated) haloacetic acids
HCO_3^-	Bicarbonate
H_2O_2	hydrogen peroxide
HOCl	hypochlorous acid
HRT	hydraulic retention time
J/m^2	joules per square meter
k	bimolecular reaction rate coefficient
kWh	kilowatt hour
LI	log inactivation
LP	low-pressure
LPHO	low-pressure high-output
LRV	log removal value
LSA	ligno-sulfonic acid
$\text{M}^{-1}\text{s}^{-1}$	per molar per second
mgd	million gallons per day
mg/L	milligrams per liter
mg/L as N	milligrams per liter as nitrogen
mJ/cm^2	millijoules per square centimeter
MP	medium-pressure

NDEA	N-nitrosodiethylamine
NDMA	N-nitrosodimethylamine
ng/L	nanograms per liter
NH ₄ ⁺	ammonia
NO ₃ ⁻	nitrate
NO ₂ ⁻	nitrite
nm	nanometer(s)
O&M	operations and maintenance
OCl ⁻	hypochlorite ion
•OH	hydroxyl radical
PLC	programmable logic controller
PPI	producer price index
RCS	reactive chlorine species
RED	reduction equivalent dose
RO	reverse osmosis
SCADA	supervisory control and data acquisition
S ₀	UV intensity from a new lamp/lamps at 100% lamp power
SWRCB	(California) State Water Resources Control Board
TOC	total organic carbon
US EPA	U.S. Environmental Protection Agency
UF	ultrafiltration
UV	ultraviolet light
UV-AOP	ultraviolet light advanced oxidation process
UV-Cl ₂	ultraviolet light-free chlorine advanced oxidation process
UVDGM	UV Disinfection Guidance Manual
UV-H ₂ O ₂	ultraviolet light-hydrogen peroxide advanced oxidation process
UVT	ultraviolet transmittance at 254 nm
WRF	The Water Research Foundation
WWTP	wastewater treatment plant

CHAPTER 1

Introduction

This document provides an overview of the basic science of UV-Cl₂ and provides guidance on the practical issues related to the implementation and operation of UV-Cl₂ processes with an emphasis on potable reuse applications.

The ultraviolet light-hydrogen peroxide advanced oxidation process (UV-H₂O₂) has been used for contaminant removal for many years, but the UV-free chlorine advanced oxidation process (UV-Cl₂) is gaining interest. UV-Cl₂ can be cost-effective for potable reuse applications, but it may also apply to conventional drinking water treatment to control taste and odor and other regulated and emerging contaminants, such as 1,4-dioxane. A recent analysis indicated that of the active-design and under-construction potable reuse UV-AOP projects, 76 percent were pursuing UV-Cl₂ versus UV-hydrogen peroxide (Festger et al. 2021). The reasons for this shift will be discussed in this document, as will a view on what questions should be asked and what water quality considerations should be considered in making this selection.

While UV-Cl₂ has many similarities to conventional UV-H₂O₂ AOP, there are differences that deserve attention related to implementation. These factors include different optimum water quality conditions, different efficiencies when using low-pressure high-output (LPHO) or medium-pressure (MP) UV lamps, and the potential formation of by-products. The information that exists on UV-Cl₂ AOP is still mostly scattered throughout the research literature, which makes it difficult for end users to identify key issues that must be addressed if considering UV-Cl₂, and the important questions to ask of the UV manufacturers.

This guidance manual consolidates information about the state of the art in UV-Cl₂ in a single reference to inform agencies, consultants, and regulators considering its use. It includes an overview of the basic science of UV-Cl₂ and guidance regarding the practical issues related to implementing and operating UV-Cl₂ processes, with a special emphasis on potable reuse applications. Two case studies of current potable reuse applications using UV-Cl₂ are provided in Section 8 that capture design, operation, and monitoring approach at each facility, as well as lessons learned through operation of the process. A literature review, “Current State-of-the-Science of UV-Chlorine AOP” (UV-Cl₂ Review presented in Appendix A), is included with this guidance manual. It is a resource for more in-depth discussion of the UV-AOP-related physics, photochemistry, and water chemistry concepts referenced herein.

This guidance manual considers only UV-Cl₂ treatment. Because UV/monochloramine has not been proven to be an effective UV-AOP treatment and there are no full-scale applications, it is not included herein.

1.1 Why Include UV-AOP as Part of a Treatment Strategy?

Best practice for implementing advanced treatment for potable water reuse requires that water providers implement multiple treatment barriers. The reasons for taking this multi-barrier

approach are two-fold. First, if one process fails there are others to support the treatment requirement (i.e., there is always some treatment, even if full log reduction values (LRV) are not met), and second to accomplish the required total process log reduction for microbiological targets, multiple barriers are required. Regarding the latter, the California State Water Resources Control Board (SWRCB) requires 12-log removal of virus and 10-log removal of *Cryptosporidium* and *Giardia* (12/10/10), respectively, for groundwater injection in indirect potable reuse applications and is anticipated to require higher LRVs for direct potable reuse. This credit is earned through treatment. In groundwater replenishment applications, virus credit can also be earned through soil aquifer treatment (i.e., extended travel time through the aquifer to the withdrawal point). Other states, however, may require different LRVs for potable reuse. The SWRCB caps the treatment of any one process at 6-log, and at least three treatment processes must achieve a minimum of 1-log removal each. For these reasons, advanced treatment plants use multiple barriers.

UV-AOP accomplishes several objectives in an advanced treatment system:

- **UV-AOP removes chemical contaminants that may pass through upstream treatment processes.** Upstream processes may include microfiltration (MF) and reverse osmosis (RO), as in the case of so called “full advanced treatment (FAT),” or may include ozone and biofiltration in ozone/carbon-based advanced treatment trains (ozone-CBAT). In the case of RO-based treatment, contaminants that are not well removed by RO tend to be low in molecular weight (<100 atomic mass units) and non-polar. This can limit the ability of membrane separation processes to remove the compounds. Compounds in the nitrosamine group, e.g., *N*-nitrosodimethylamine (NDMA) or *N*-nitrosodiethylamine (NDEA), and others, such as 1,4-dioxane, are common examples.
- **UV-AOP processes earn up to 6-log inactivation credit for virus, *Cryptosporidium*, and *Giardia* in the California protocol.** It is, therefore, a potentially large contributor to the total LRV in a treatment process with high required LRVs, although strictly speaking, high-level disinfection can be accomplished with lower UV doses than those used for UV-AOP.
- **UV-AOP is a photochemical process versus a filtration or separation process.** The value of this different approach is twofold. First, by using a treatment process that uses high-energy UV light to destroy potentially harmful compounds in water, a process that the public can understand, it assists in building public confidence in the overall treatment strategy. Second, the use of an alternate process for treatment builds inherent redundancy and robustness and increases the treatment train’s overall strength.

1.2 Overview of UV-AOP

The term “advanced oxidation process” refers to a water treatment method that uses radicals. Collins and Bolton (2016) define AOPs as processes that “involve the use of powerful oxidizing intermediates (e.g., the hydroxyl radical, or $\cdot\text{OH}$) that can oxidize and degrade primarily organic pollutants from contaminated air and water.” The use of this treatment process is increasing in municipal applications as recalcitrant contaminants are more frequently discovered in water supplies (due to more extensive monitoring and lower analytical detection levels) and as scarcity drives the use of water sources that have been impacted by contamination. In practice, UV-AOP involves first the addition of an oxidant, such as hydrogen peroxide or free chlorine,

and subsequent treatment with a relatively high dose of UV light (Figure 1-1). Radical reactions are very fast and happen within the reactor.

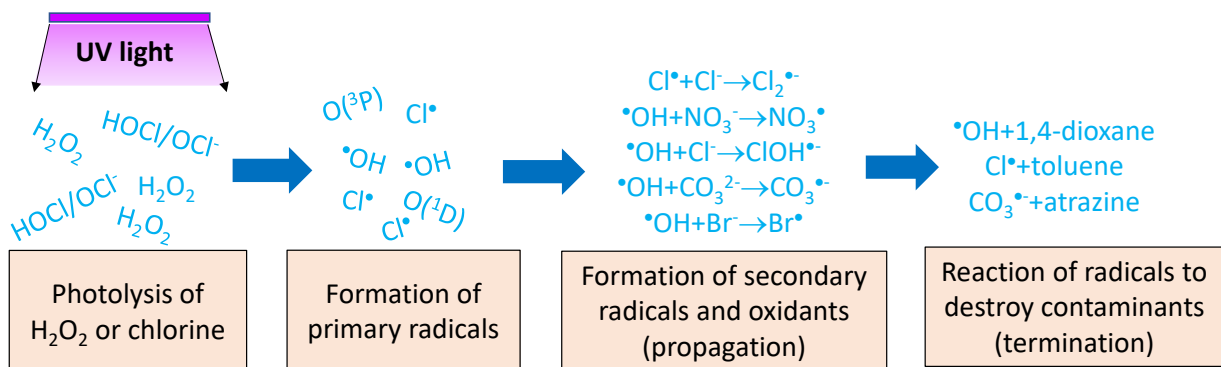


Figure 1-1. Illustration of UV-AOP Treatment.

Note: these radical reactions all occur in the reactor.

Some may object to the term “UV light,” since by strict definition “light” is visible to the human eye and UV wavelengths are invisible. The correct term is UV radiation. It is advisable, however, to avoid the word “radiation” when communicating to the public about water treatment due to the obvious opportunity for misunderstanding. In this document, we refer to “UV light.”

1.2.1 Lamp and Oxidant Type Considerations

One principle of a UV-based AOP is that the photons emitted by the lamp are absorbed by the oxidant (H₂O₂ or chlorine) so that the absorbed energy causes the oxidant to break down to form radicals. The ability of oxidants to absorb photons varies with wavelength. Hydrogen peroxide absorbs less strongly as wavelengths increase. For example, at acidic pH (i.e., <6) where hypochlorous acid predominates, chlorine absorbs UV light more strongly than H₂O₂ at wavelengths higher than ~220 nanometers (nm). When using an LPHO lamp that emits photons almost entirely at 254 nm, H₂O₂ is approximately one-third as effective as chlorine in terms of absorbing photons (Feng, Smith and Bolton, 2007, and Figure 1-2). Conversely, if an MP lamp is used, there are many photons being emitted at higher wavelengths that are not absorbed by H₂O₂. This tends to make MP lamps less energy efficient than LPHO lamps for UV-H₂O₂ processes. By contrast, at neutral or elevated pH, the higher wavelength photons can be absorbed by chlorine, which may enhance MP efficiency at higher pH for UV-Cl₂ AOP. Overall, the subject of which type of UV lamp (LPHO or MP) and which type of oxidant (H₂O₂ or chlorine) is preferred in different circumstances is very complex, and is discussed in more detail in Appendix A.

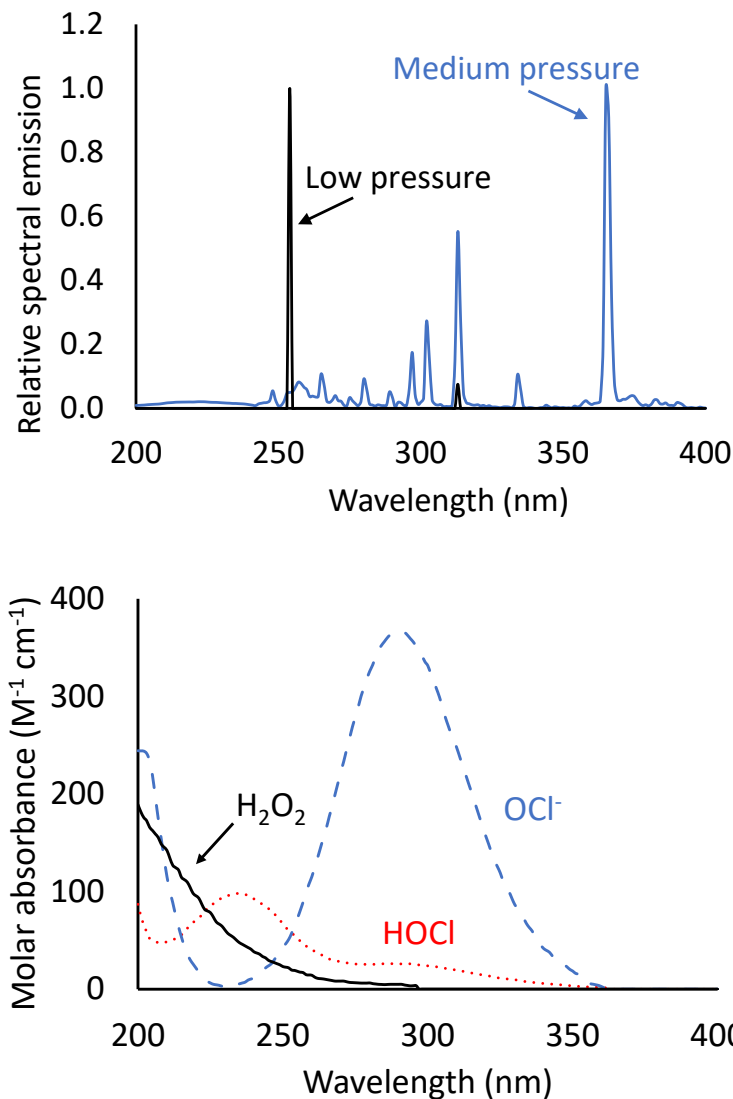


Figure 1-2. UV Lamp Emission Spectra and Absorbance of Oxidants Versus Wavelength.
Lamp emissions are not to scale. MP emission is typically much higher than LP.

1.2.2 UV Dose for Disinfection and Oxidation

While a detailed discussion of the approaches to quantify, model, and report reduction UV dose is beyond the scope of this manual, we provide a summary and refer the reader to the U.S. Environmental Protection Agency’s (USEPA) *Ultraviolet Disinfection Guidance Manual (UVDGM)* and *Innovative Approaches for Validation of Ultraviolet Disinfection Reactors for Drinking Water Systems* (USEPA 2006 and 2020, respectively, and Collins and Bolton 2016). Additional information may be found in Chapter A1.5 in Appendix A.

In UV applications, the UV energy applied to the water by way of the UV lamps can be quantified and is referred to as the “UV dose” or “UV fluence.” The UVDGM defines UV dose as “the UV energy per unit area incident on a surface, typically reported in units of mJ/cm² or J/m². [It]...accounts for the effects on UV intensity of the absorbance of the water, absorbance

of the quartz sleeves, reflection and refraction of light from the water surface and reactor walls, and the germicidal effectiveness of the UV wavelengths transmitted” (pp. xvii, USEPA 2006). Contaminant degradation by UV-AOP is achieved through the application of relatively high UV doses (i.e., relative to the levels used for UV disinfection only) and a combination of two photochemical processes: UV-photolysis (UV dose alone) and UV-oxidation (UV light plus an oxidant to form $\cdot\text{OH}$ or other radicals). The dose per log of a given contaminant (that is, the UV dose required to reduce the concentration of a target contaminant by one-log or 90%) is a function of such factors as oxidant concentration and UV absorbance properties, background water quality (e.g., $\cdot\text{OH}$ radical scavenging demand), contaminant reactivity with $\cdot\text{OH}$, and lamp emission spectrum. Accurate prediction of UV-AOP performance requires both mathematical models and empirical data, and at the time of publication is an evolving science. Regarding the UV emission spectrum, LPHO systems emit at predominantly 254 nm. MP lamps emit across a broad wavelength range, including wavelengths higher and lower than 254 nm that are potentially relevant for creating radical species (particularly in the UV-Cl₂ process, see Figure 1-2).

The UVDGM presents the concept of reduction equivalent dose (RED) in a UV or UV-AOP system. In short, RED is a practical means by which to quantify UV dose. It is computed by measuring the response of a surrogate organism or contaminant to UV dose at bench scale (creating a “dose-response curve”), then inferring the dose delivered by a full-scale UV system by correlating the reduction observed at the full scale to the dose required to accomplish that reduction in the dose-response curve. Because direct measurement of UV dose in a UV system is not currently possible, this process is required to quantify UV dose. At the high UV doses required for UV-AOP applications, this process presents certain challenges. Specifically, UV dose validation using microorganisms (described in UVDGM 2006) is limited to relatively low UV doses. The upper range of RED quantification in a traditional validation using MS2 bacteriophage is 100 to 140 millijoules per square centimeter (mJ/cm²). Note that a UV reactor “validation” is a comprehensive performance test, normally done by a third party, to determine the operating conditions of flow, ultraviolet transmittance at 254 nm (UVT), and power level under which a UV reactor delivers a given UV dose. The selected surrogate(s) leads to the validated range of UV dose, with surrogates such as T7 and T1 defining the lower range (1 to 5 mJ/cm²). MS2 and *Bacillus subtilis* are also commonly used surrogates. Please refer to the USEPA’s *Innovative Approaches* (2020) document for more information on the log inactivation (LI) method and the use of MS2 for demonstration of larger ranges of UV dose, specifically for viruses.

Using a high-resistance surrogate such as *Bacillus pumilus* or *Aspergillus brasiliensis* allows direct RED measurement of up to approximately 400 mJ/cm², although there are practical challenges associated with sampling and dosing if using these surrogates in a full-scale application for the field measurement of RED. Neither is sufficient, however, for encompassing the UV dose range of UV-AOP, which typically requires UV doses near to well above 1,000 mJ/cm². For such a high dose, chemical surrogates, such as NDMA, have been used with mixed success. Dose response curves using NDMA have been generated that result in dose-per-log values that vary widely, from 700 to 1,100 mJ/cm² (e.g., Sharpless and Linden 2003). Field trials have provided even lower dose-per-log values. The reason for this wide range is not clear,

but NDMA dose-response curves should be carefully scrutinized if used to verify UV dose as part of a performance test for a specific water quality. Other surrogate compounds that undergo degradation by photolysis only are under evaluation, also with mixed success, and this topic is included in the Research Needs section in Chapter A5 of Appendix A.

The full-scale UV-AOP system typically computes the UV dose delivered using a programmable logic controller (PLC)-based algorithm. Common inputs to a typical RED or LI equation are:

- Water flow rate
- Sensor intensity
- UVT
- Number of rows or groups of rows in operation
- Dose response of the target contaminant or oxidant

It may also include a factor to account for radical scavenging and the dosed oxidant concentration, depending on the system and manufacturer. Note that LI is related to the RED by way of the dose per log determined from bench-scale dose-response experiments in the same water matrix. These models are proprietary and manufacturer specific.

Most UV systems use some combination of an RED, LI, or contaminant log-reduction calculation algorithm to control operation of the system in a full-scale UV-AOP application. In one control approach, the calculated RED and oxidant concentration are maintained above a set threshold determined in pilot testing. Provided that the test conditions for determining the UV and oxidant dose requirements were representative of the application's operating full-scale water quality, this RED/oxidant combination should achieve the contaminant treatment target(s). RED, in conjunction with results of monitoring oxidant concentration, can be reported to the regulatory body as evidence of operational compliance as required by the permit.

Performance testing following startup and commissioning should verify the ability of the UV-AOP system to meet treatment requirements under the full range of expected operating conditions. The performance test should also verify the ability of the proposed control approach to govern treatment. In one example, the Terminal Island Water Reclamation Plant in Los Angeles (detailed in a case study provided in Section 8) is permitted to operate with a minimum RED of 920 MJ/cm² with an associated required minimum oxidant dose and minimum UVT. This threshold was determined based on site-specific acceptance testing and has been verified in ongoing verification tests. Other approaches to control and permit UV-AOP systems are discussed in Section 4.10.

Recommendations for performance testing UV-AOP systems are included in Section 7.2 of this Guidance Manual.

1.2.3 Sizing UV-AOP systems

There are two fundamental design variables for a UV-AOP system: its UV dose and the oxidant (type and concentration). Most manufacturers offering UV-AOP systems use proprietary models to determine the optimal UV-AOP sizing of their systems. Differing approaches between manufacturers, however, can make direct performance and cost comparisons of various UV-

AOP systems difficult, especially during initial sizing when sizing is not guaranteed. In addition, designers should take care in specifying UV dose targets for design of UV-AOP systems. Given the challenges associated with determining UV dose at the high levels required for UV-AOP, it is recommended that, if a minimum UV dose is specified, it be accompanied by performance targets to reduce a target contaminant(s). Further, UV dose targets should be well supported by the literature and past project experience.

There are two general approaches used for UV-AOP equipment sizing. The first is development and use of a reactor-specific deterministic mathematical model that uses an empirically measured scavenging factor (dependent on site-specific water quality) to determine combinations of UV and oxidant doses that will meet the treatment objective. The second is an empirical approach that leverages laboratory-, pilot-, and full-scale data to determine the UV dose and oxidant concentration required to achieve the treatment objective. Either approach is often coupled with a reactor's disinfection-level validation to govern disinfection sizing.

In either case, the manufacturer will need water quality data and the treatment objective(s) to size a reactor and develop a cost proposal. These methods are described in more detail in Chapter A2 in Appendix A.

Given uncertainties in sizing accuracy, the equipment specification should require field performance testing following installation. The designer and owner may require the manufacturer to pay damages (in the form of performance penalties) if the guaranteed manufacturer-sized UV system fails to accomplish treatment targets.

1.2.4 Selecting the Oxidant for Use in an AOP Application

The question of what oxidant to use in an AOP application requires consideration of numerous factors. In potable reuse applications, the decision primarily depends on the upstream treatment processes selected. Each of these factors is included in the Decision Tree portion of this Guidance Manual (Chapter 6).

There are two general treatment approaches taken in potable reuse. The first is ultrafiltration (UF) or MF, followed by RO, then UV-AOP. It uses membranes in combination with UV-AOP to produce a water with very low total organic carbon (i.e., <0.5 milligrams per liter [mg/L]). Current California SWRCB regulations for groundwater injection and reservoir augmentation and pending direct potable reuse rules will *require* the use of RO to reduce total organic carbon (TOC) to below 0.5 mg/L, and it is generally recognized that RO is required to accomplish this level. Alternatives to RO-based treatment are explored in detail elsewhere (e.g., Stanford et al. 2017; Funk et al. 2018, Bukhari et al. *In Press*), including those involving ozone and biofiltration with or without a pretreatment UF or MF system. This upstream treatment process generally results in a finished water with higher (relative to RO permeate) TOC, but the process can remove a wide range of microbial and chemical contaminants while avoiding the production of a brine concentrate stream.

As of this Guidance Manual's publication, several projects have received approval to operate in California using the UV-Cl₂ process, including the Water Replenishment District's Albert Robles Center for Water Recycling, Los Angeles Sanitation's Terminal Island Water Reclamation Plant, and City of Oceanside's Pure Water Oceanside facility. Each has unique permit conditions. The number of UV-H₂O₂ systems in operation exceeds the number of UV- Cl₂ systems, but as noted above, the majority of potable reuse treatment plants are preferentially selecting UV- Cl₂ as new projects move forward.

CHAPTER 2

The Basics of UV-AOP Photochemistry

UV advanced oxidation is a process that uses added oxidizing chemicals (e.g., hydrogen peroxide or chlorine) that absorb photons; this drives the production of radicals that can subsequently react with and decompose contaminants in the water. AOPs are typically used for applications such as potable reuse treatment and removal of contaminants or when water is contaminated with compounds that are resistant to conventional treatment like 1,4-dioxane. This chapter provides an overview of UV-AOP photochemistry. A more detailed description, including background water quality considerations, is included in Chapter A2 of Appendix A.

2.1 UV-AOP Uses UV Light to Catalyze the Formation of Radicals that Degrade Contaminants

As mentioned, advanced oxidation processes refer to water treatment that uses radicals. A radical is a chemical species that has one or more unpaired electrons (Figure 2-1), but a simpler way to consider it is an atom or molecule that is “missing” an electron, which makes it unstable and strongly reactive as it attempts to regain that electron. Such radicals can be stronger oxidants than traditional chemicals, such as chlorine or ozone.

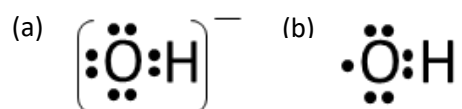


Figure 2-1. Lewis Dot Diagram of (a) Hydroxide Ion and (b) Hydroxyl Radical with an Unpaired Electron.

The most common radical used for UV-AOP is the hydroxyl radical ($\cdot\text{OH}$). The hydroxyl radical is extremely reactive and normally persists in water for less than one millionth of a second before reacting to regain its missing electron (Kohen and Nyska, 2002). If that electron is taken from a nearby contaminant, the contaminant is broken down. UV light plus H_2O_2 is a common means by which to generate $\cdot\text{OH}$. UV plus chlorine is also used to generate radicals. UV light causes the decomposition of chlorine species into $\cdot\text{OH}$, $\text{ClO}\cdot$, and other radical species. In general, UV- H_2O_2 processes only result in 5% to 20% decomposition of the H_2O_2 , whereas much more chlorine can be photolyzed across the UV reactor under typical conditions (often greater than 50%) due to its strong UV absorbance and its higher quantum yield of oxidant decomposition. The quantum yield is the ratio of how many molecules are either destroyed or produced per photon absorbed by the parent molecule (see Chapter 1.7 of Appendix A for details). It should be said, however, that while the overall process is understood reasonably well for UV- H_2O_2 , the fundamental chemistry of UV- Cl_2 AOP is very complex and not yet well understood. This makes it challenging to predict the performance of a UV- Cl_2 system without laboratory-, pilot- or full-scale testing, especially in waters other than RO permeate (e.g., drinking water with higher concentrations of organic compounds).

2.2 UVT is a Key Design Parameter

Good understanding of background UVT is important for proper UV system sizing regardless of oxidant or target contaminant(s).

UVT is defined as the fraction of light at a specific wavelength that passes through a medium (water in this case) over some specific distance (typically one centimeter [cm]). The units of measurement are, therefore, typically in units of % per cm (often shortened to simply “%”). For example, water with a UVT of 80%/cm means that for every cm of distance that the photons travel from the lamp out into the flow, 20% are absorbed. The cost of UV-AOP treatment is generally inversely proportional to the UVT of the water (with higher UVT water being less expensive to treat and vice versa).

UV absorbance and UVT are inversely related through the following relationship:

$$UVT = 100 \times 10^{-UVA_{254}} \quad \text{Equation (2.1)}$$

where UVT is in %/cm and UVA₂₅₄ is the absorbance of UV light (per cm) at 254 nm as measured by a spectrophotometer.

In practice, the lower the absorbance (i.e., the higher the UVT), the greater the efficiency of UV-AOP treatment. A very high UVT water, such as an RO permeate, may have a UVT of greater than 97% cm⁻¹, while the UVT of a non-RO-based treatment train can vary widely, from less than 90% cm⁻¹ to greater than 95% cm⁻¹, depending on the concentration and nature of the organic and inorganic species present in the water.

2.3 Radical Scavenging is Important for System Sizing

The number of radical scavengers in a water to be treated is a critical design parameter, since it dictates the amount of UV energy and oxidant that must be applied to generate sufficient radicals to destroy the target contaminants.

The goal of the AOP is to generate radicals (predominantly •OH, but also reactive chlorine species [RCS] in a UV-chlorine process), which can then react with and destroy the target contaminants. The radicals typically react indiscriminately, and many will react with other material in the water (e.g., organic carbon, nitrite, alkalinity) instead of the targets, which leads to inefficiencies. Stated another way, the amount of UV energy and oxidant must be high enough to generate enough radicals such that after accounting for those that are “scavenged” unproductively by other components in the water, the remaining radicals can accomplish the treatment objective. Scavenging by different background water constituents is discussed in detail in Chapter 3.

The relationship between a specific reactor’s UV dose, oxidant concentration, the UVT and radical scavenging of the water, and resulting treatment of a target contaminant is something that can only be interpreted by UV reactor models. UV manufacturers have invested in these models, which are specific to the geometry and performance of their UV equipment. While end users and consultants can understand in a general sense that waters with more scavenging

potential are more expensive to treat (e.g., ozone/biologically active carbon (BAC) effluent versus RO permeate), UV-AOP system sizing is generally provided by UV-AOP manufacturers. Best practice places the responsibility of system performance on the manufacturer, so these models are critical in the prediction of system sizing under specified conditions and the eventual guarantee of performance included, by the manufacturer, in the equipment procurement.

It is important to recognize that if water quality is known to vary, the radical scavenging potential will also likely vary. As part of the preliminary design process for a new AOP system, the potential variation in this parameter must be considered to ensure that the resulting AOP system can achieve its treatment goals over the range of expected water quality conditions.

More information on radical scavenging can be found in Chapter A2.1 of Appendix A.

CHAPTER 3

Influence of Background Water Chemistry on UV-AOP Efficacy

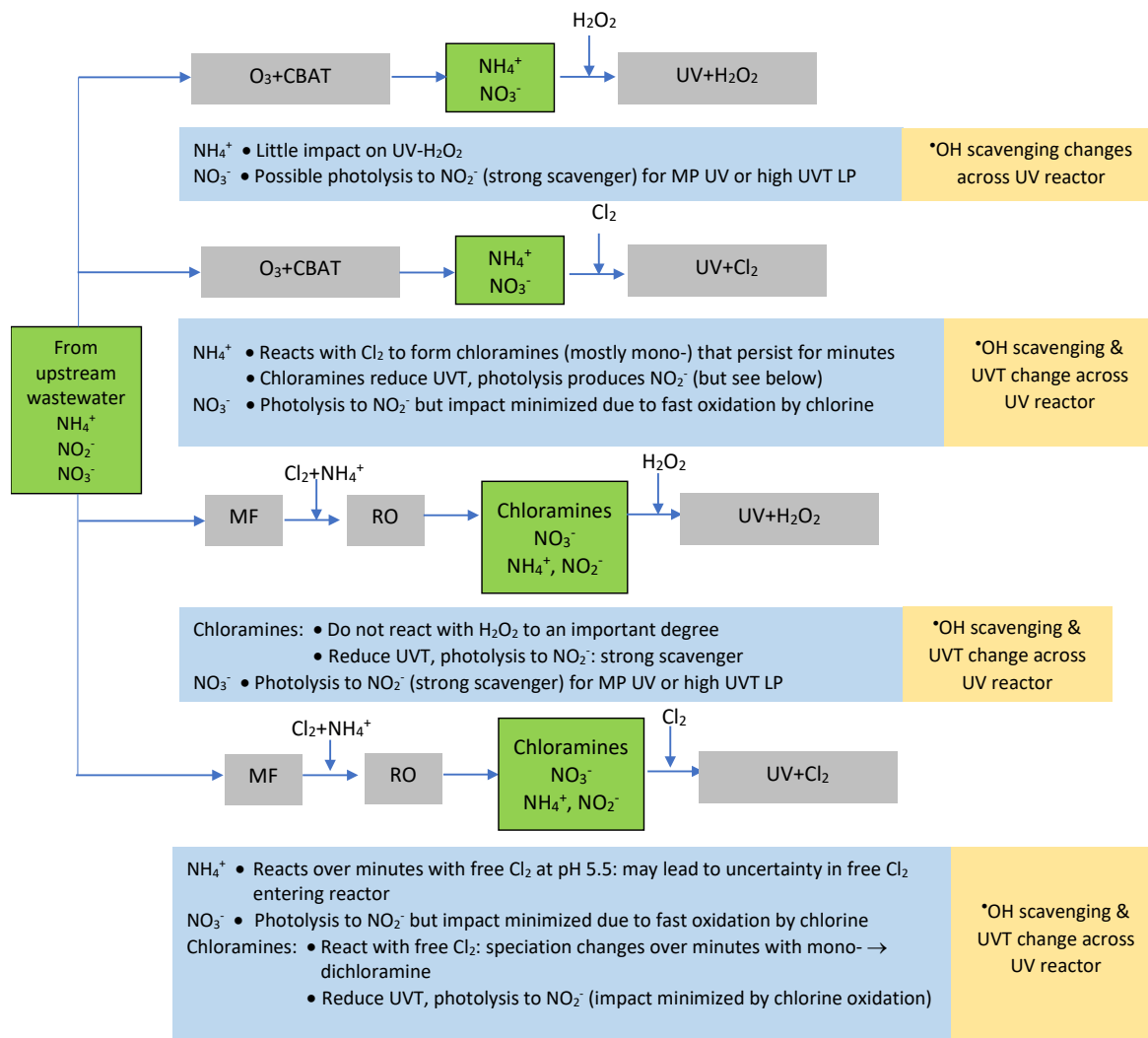
Nitrogen species have multiple important effects on UV-Cl₂ and UV-H₂O₂ system efficiency; design requirements necessitate careful consideration.

UV-AOP is typically placed in the treatment train to minimize the radical scavengers in the feed water (e.g., post RO or post-ozone/biologically active carbon). A wide variety of organic and inorganic species can exert a scavenging demand or otherwise impact UV-AOP treatment. **Radical scavengers include organic matter, inorganic carbon (carbonate and bicarbonate), nitrite, chloramines, the oxidants themselves (chlorine or H₂O₂), bromide, and others.** A discussion of several key constituents follows.

3.1 Nitrogen Species: Ammonia, Chloramines, Nitrate, and Nitrite

Where water is not fully nitrified, ammonia concentrations in treated municipal secondary effluent are often in the range of 20 to >40 mg/L as nitrogen (N). During conventional wastewater treatment, some of the ammonia may be converted to nitrite or nitrate depending on whether nitrification/denitrification processes are employed. The resulting effluent that could serve as the source for potable water reuse may, therefore, contain a range of ammonia, nitrate, and nitrite. A summary of the role of nitrogen-containing species is illustrated on Figure 3-1. More detail on this complex topic is provided in Appendix A.

Hydrogen peroxide added in a UV-H₂O₂ system is relatively inert with respect to nitrate, ammonia, and even chloramines (the half-life of the reaction between H₂O₂ and chloramines at typical concentrations and conditions would be in the order of many hours to days (Wang et al., 2020). A major impact of these nitrogen species, particularly chloramines, would, however, be due to their potentially high UV absorbance and corresponding reduction of UVT. Further, as shown on Figure 3-2, it is possible that, under some conditions, a major fraction of the photons can be absorbed unproductively by nitrogen-containing species instead of by the oxidants (H₂O₂ or chlorine), thereby requiring the application of higher UV doses or oxidant concentrations to achieve the desired treatment level. The impact of these species on the UVT must, therefore, be considered during design.



CBAT = carbon-based advanced treatment (i.e., ozone-biologically active filtration)

NH_4^+ = Ammonia; NO_3^- = nitrate; NO_2^- = nitrite

Figure 3-1. Summary of the Roles of Nitrogen-Containing Species in Potable Reuse Applications of UV-AOP.

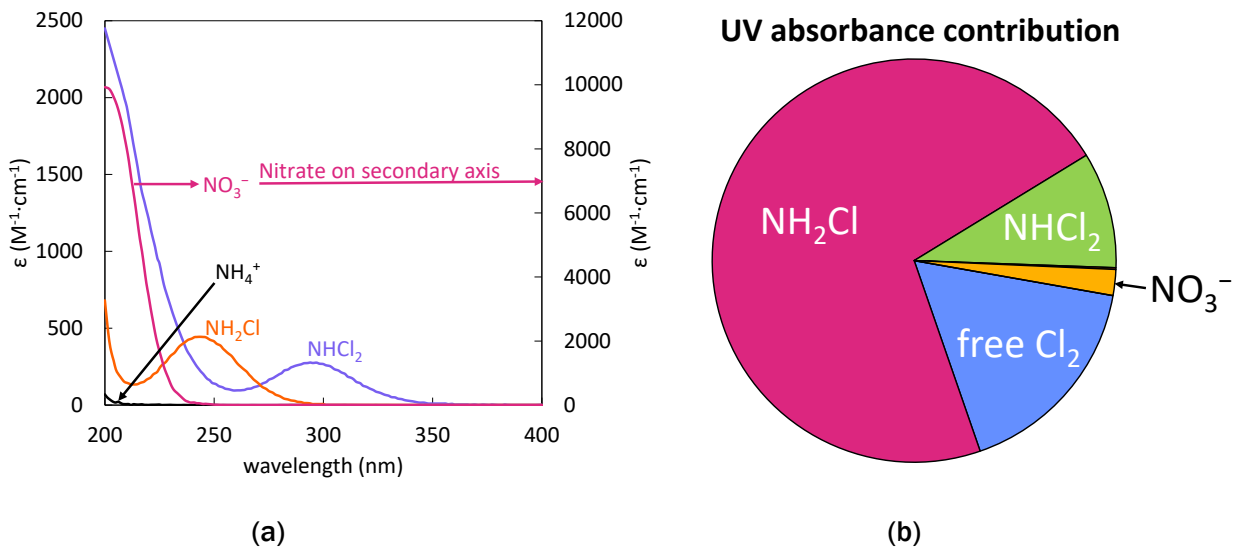


Figure 3-2. Impact of Nitrogen Species on UV Absorption Spectra for (a) Ammonia, Nitrate, Monochloramine, and Dichloramine. (b) Example of Relative Contribution to 254 nm Photon Absorption in a Fictive RO Permeate Containing 5 mg/L Free Chlorine, 3 mg/L Monochloramine, 4 mg/L Dichloramine, and 1.5 mg/L as N Nitrate.

The second major impact of the nitrogen species is due to radical scavenging. The ability of the $\cdot\text{OH}$ or RCS to destroy the contaminants of interest can be modeled as a first-order kinetics equation:

$$\frac{d[1,4\text{-dioxane}]}{dt} = -k[\cdot\text{OH}][1,4\text{-dioxane}] \quad \text{Equation (3.1)}$$

where k is the bimolecular reaction rate coefficient, and $[\cdot\text{OH}]$ and $[1,4\text{-dioxane}]$ are the concentrations of the radicals and contaminant, respectively. The reaction rate coefficients between $\cdot\text{OH}$ and the various species are shown in Table 3-1, along with their illustrative contributions to $\cdot\text{OH}$ scavenging for a fictive water, and are discussed in detail in Appendix A, Chapter A2.1. Under some conditions, these compounds can exert a significant demand.

Table 3-1. OH Radical Scavenging of Nitrogen Species Post-RO (pH 5.5)

Species	Concentration	$k_{\cdot\text{OH}}$ ($\text{M}^{-1}\text{s}^{-1}$)	Contribution to $\cdot\text{OH}$ scavenging	Reference
Free chlorine	3 mg/L as Cl_2	2.0×10^9 HOCl, 8.8×10^9 OCl	71%	Buxton and Subhani, 1972 Anastasio and Matthew, 2006
Monochloramine	2 mg/L as Cl_2	1.0×10^9	23%	Anastasio and Matthew, 2006
Dichloramine	1.5 mg/L as Cl_2	6.2×10^8	6%	Anastasio and Matthew, 2006
Nitrate	0.8 mg/L as N	4.0×10^5 ^b	< 1%	Yin et al. 2020 ^b
Nitrite	Variable ^a	1.1×10^{10}	Variable ^a	Yin et al. 2020

$\text{M}^{-1}\text{s}^{-1}$ = per molar per second

a. Nitrite is likely to be present only in some systems with UV- H_2O_2 , since free chlorine quickly converts nitrite to nitrate

b. This reaction rate coefficient is reported in a secondary source from an ambiguous primary source, but evidence suggests that the rate is negligible.

When nitrate and chloramines are photolyzed in the UV reactor they can produce nitrite (Kwon et al. 2020). Nitrite is a strong $\cdot\text{OH}$ scavenger (Table 3-1). If a UV reactor design were to be

based on the $\cdot\text{OH}$ scavenging capacity of the water *as it enters* the UV reactor, and if nitrate and/or chloramines are present, there will be an *underestimation* of the actual radical scavenging *inside* the reactor due to the formation of nitrite. Note that this phenomenon is likely to only be important for UV- H_2O_2 , since the free chlorine in a UV- Cl_2 AOP would react very quickly with any nitrite that is formed to oxidize it back to nitrate. Note also that nitrate photolysis to nitrite is generally associated only with MP UV, since nitrate photolysis is strongest in the 200 to 230 nm range. However, in waters with a very high UVT (e.g., >98%) and high nitrate, there is the potential for considerable nitrite formation even when using LPHO lamps. In contrast, photolysis of chloramines can occur with both LP and MP systems. When sizing UV- H_2O_2 systems with nitrate or nitrite, the designer should work with the UV manufacturer(s) to account for the presence and formation of nitrite from both nitrate and chloramine photolysis. An analysis of the potential economic impact of nitrite on operations and maintenance (O&M) costs is included in Chapter 5.

For UV- Cl_2 systems, the effect of nitrogen species is even more complicated because, unlike H_2O_2 , free chlorine is reactive with some of the species. In particular, the role of chloramines is critical.

If ammonia is present in the water, at neutral pH it will react almost instantaneously with chlorine (with good mixing) to form chloramines—monochloramine and dichloramine. At pH 5-6, the kinetics are slower; ammonia and free chlorine can co-exist for tens of seconds. This is critical. It means that the ammonia in the RO permeate can continue to consume free chlorine as the water travels from the chlorine injection point to the UV reactor, so if free chlorine is measured near the injection point, the free chlorine entering the reactor may be *overestimated*. Or, if a free chlorine sample line has a 2-minute travel time to the free chlorine monitor, *less* free chlorine may be registered than what is going into the reactor if the travel time to the reactor is much lower.

The stoichiometric ratio of free chlorine required to convert ammonia to chloramines is approximately 1:1 molar, or 5 Cl:1 N mass ratio. The stoichiometric amount of free chlorine required to destroy chloramines is approximately 0.5:1 on a molar basis (depending on the chloramine species), or 2.6 mg- Cl_2 /L:1 mg/L as N. Therefore, the amount of chlorine required to drive this reaction to convert ammonia through chloramines and all the way to nitrogen and nitrate (i.e., breakpoint chlorination) is \sim 1.5:1 molar, or 7.6 Cl: 1 N mass ratio.

An important factor in this process to note is that the reaction between free chlorine and chloramines to destroy the chloramines is *not instantaneous*. It can take many minutes, depending on the pH, temperature, and concentrations involved. This is illustrated on Figure 3-3, which shows a model prediction of the chlorine speciation between RO permeate and a UV reactor positioned up to 3.5 minutes downstream of chlorine application. In a UV- Cl_2 AOP, it is likely that the free chlorine would be added only some seconds or a minute or two upstream of the UV reactor. This means that if ammonia is initially present in the water or if chloramines are present, by the time the water reaches the UV reactor there is likely to be some mixture of chloramines and free chlorine present. As explained earlier, chloramines, while necessary in many applications, can pose a challenge with regard to UVT and $\cdot\text{OH}$ scavenging.

Their presence must, therefore, be carefully considered during the design stage through reactor modelling or pilot-scale testing.

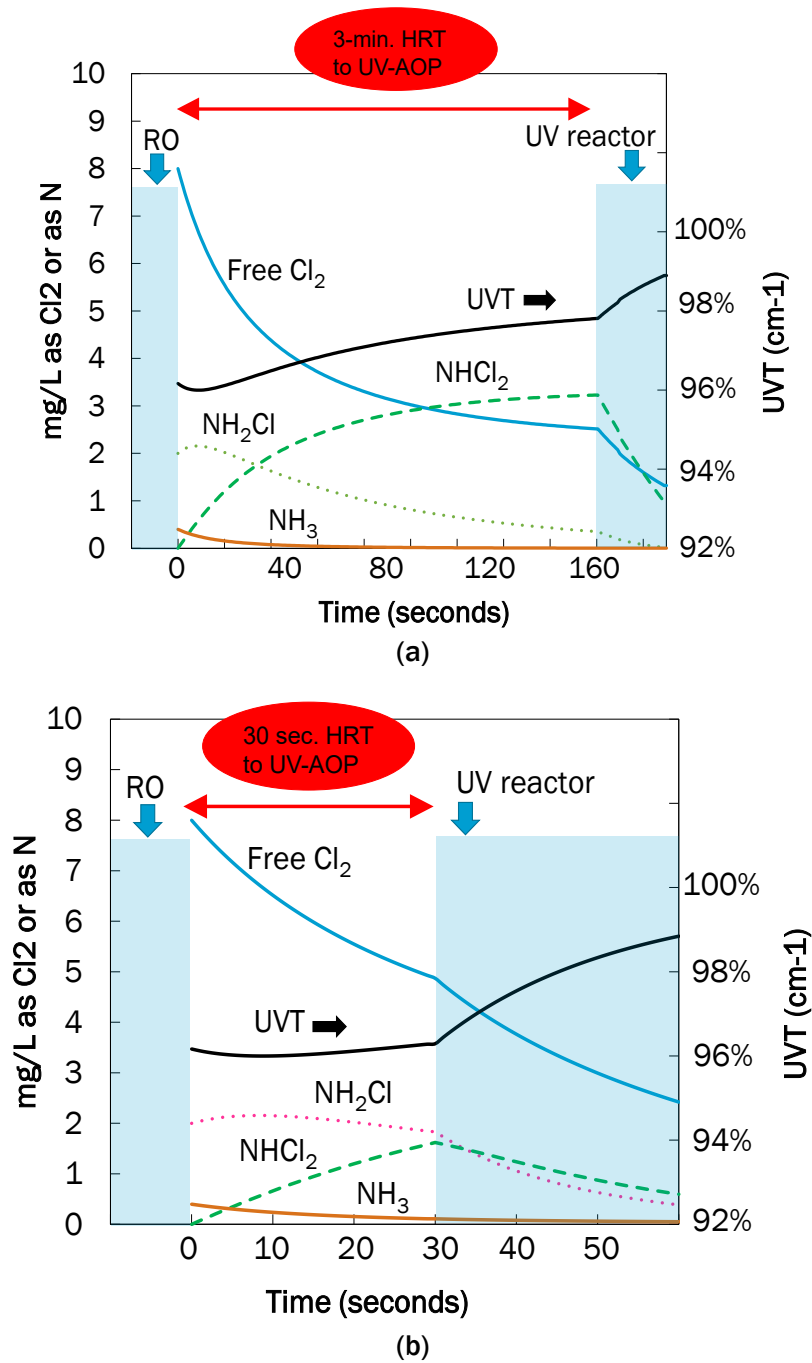


Figure 3-3. Example of the Fate and Impact of Chloramines in a Post-RO UV-Cl₂ Treatment Process at pH 5.5. with (a) a 3-minute hydraulic retention time (HRT) versus (b) a 30-second HRT.

More discussion of the role of nitrogen species in UV-Cl₂ is provided in Appendix A.

3.2 pH

The effect of pH is different depending on whether UV light is being produced only at 254 nm (LPHO lamp) or over the range from 200 to 400 nm (MP lamp), and when considering UV-Cl₂ or UV-H₂O₂.

UV-Cl₂ AOP. Chlorine exists predominantly as hypochlorous acid (HOCl) below pH 7.5, and hypochlorite ion (OCl⁻) above (Figure 3-4). When using an LP lamp emitting at 254 nm, the quantum yield of radical formation is higher for HOCl photolysis (i.e., more radicals are produced with HOCl than with OCl⁻), and there is also less scavenging of the •OH by HOCl than by OCl⁻. That is, HOCl, the predominant species at lower pH, scavenges less, making more radicals available for treatment. Both of these factors lead to there being *more net availability of •OH (and other radicals) at lower pH than at higher pH* (Bulman et al., 2019). In other words, for an LPHO UV system, all other factors being equal, the UV-Cl₂ process will be more efficient than the UV-H₂O₂ process at lower pH.

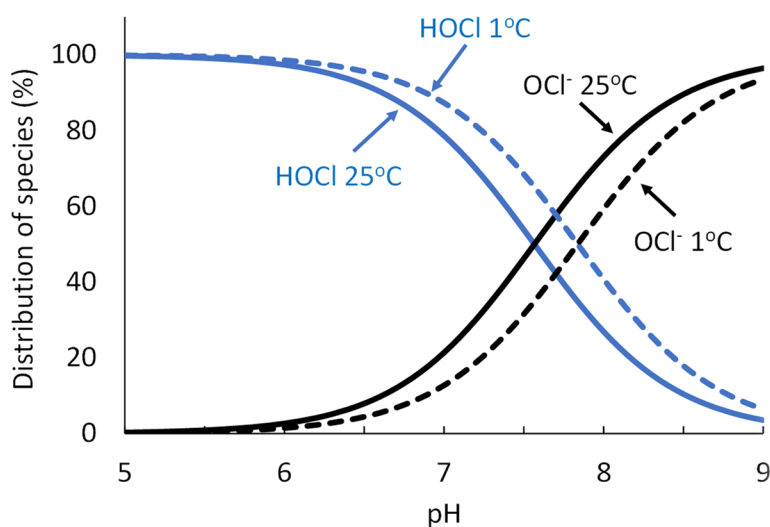


Figure 3-4. Relative Proportions of HOCl and OCl⁻ as a Function of pH.

For an MP system emitting wavelengths higher than 254 nm, the situation is more complicated (e.g., Wang et al. 2019, Wu et al. 2017). Overall, it can be theorized that for an MP UV system, there is lower •OH formation at higher pH values but potentially more RCS formation. The net impact of pH on overall AOP performance, therefore, depends on whether the target contaminants are reactive with RCS or not.

These concepts are discussed in detail in Chapter A2.7 of Appendix A.

UV-H₂O₂ AOP. Unlike chlorine, the form of H₂O₂ does not change over the pH range experienced in practice, and therefore its fundamental photochemistry remains the same. In other words, there is no immediate and direct impact of pH on UV-H₂O₂ performance under typical conditions. Note that if pH were to increase significantly above neutral (e.g., to >8), treatment efficacy may decrease due to a shift of bicarbonate to carbonate which is a stronger •OH scavenger. However, if the increase in pH is accomplished using a decarbonator prior to the AOP, the net effect may be an overall decrease in •OH scavenging. Whether the increase in pH from a decarbonator leads to an increase or decrease in •OH scavenging can be predicted mathematically by calculating the contribution to scavenging by the (bi)carbonate species.

During laboratory measurements of scavenging capacity, particularly for RO permeate, the water can quickly absorb carbon dioxide from the atmosphere prior to testing, which leads to water that is no longer representative of full-scale conditions. Care should be taken to eliminate this phenomenon, such as by keeping the samples sealed.

3.3 Alkalinity

Bicarbonate (HCO₃⁻) and carbonate (CO₃²⁻) ions are radical scavengers. When these species react with hydroxyl radicals or the chlorine atom, a carbonate radical (CO₃•) is formed (Fang et al., 2014). This formation is reportedly more significant in UV-Cl₂ systems than with UV-H₂O₂ because bicarbonate reacts faster with the chlorine atom than with •OH (Guo et al., 2018).

In short, elevated alkalinity affects scavenging. In RO permeate, alkalinity ranges from 5 to 20 mg/L as calcium carbonate (CaCO₃). At this level, the impact of alkalinity is minimal. At higher levels, the designer should consider reduction strategies with adjustments to upstream processes.

3.4 Chloride and Bromide

Both chloride and bromide can react with •OH and Cl• and serve as primary radical scavengers. However, the product of this scavenging may be secondary radicals (including other RCS and radical bromide species) that can also destroy contaminants (Yin et al., 2018; Guo et al., 2020; Yang et al., 2020; Grebel et al., 2010). Evidence so far suggests, however, that the overall impact of chloride and bromide on either scavenging primary radicals or forming secondary radicals is likely to be negligible under most normal conditions, such that the presence of chloride and bromide has little impact on overall AOP effectiveness.

While chloride and bromide are likely to have little impact on UV AOP performance, the presence of elevated bromide can result in the formation of bromate in UV-Cl₂ systems. As discussed in Appendix A, chlorine reacts with bromide to form free bromine (HOBr and OBr⁻), and free bromine can undergo UV-photolysis to form bromate. In contrast, hydrogen peroxide (H₂O₂) does *not* react with bromide and, therefore does not create bromine and (subsequently) bromate.

This issue became important for the Terminal Island Water Reclamation Facility in Los Angeles where initial pilot testing of UV-Cl₂ AOP treated effluent from the wastewater treatment plant, which contained moderately low bromide levels in the range of 100 micrograms per liter (µg/L).

Following commissioning of the full-scale UV-Cl₂ system, however, suspected infiltration of seawater to the water reuse plant supply line from the wastewater facility increased bromide to more than 3,000 µg/L which, upon UV-Cl₂ treatment of the RO permeate, led to bromate formation up to 30 µg/L, well above the maximum concentration limit for drinking water (10 µg/L). This problem was solved by retrofitting the plant to include ammonia injection immediately following RO and before chlorine application. The presence of ammonia in water prevents the formation of bromate because it reacts very quickly with free bromine to form bromamines. Addition of ~0.3 mg/L as N ammonia limited the formation of bromate. Refer to Chapter 2.11 of Appendix A for more information.

3.5 Organic Matter

Since organic matter generally consists of a mixture of many different species whose composition can change over time in a source, the impact of organic matter on UV-AOP performance (as measured by bulk parameters such as TOC) is difficult to determine with precision. Measurement of TOC may provide general information on the presence of organic material, but as a bulk measure it provides little information on the *nature* of the organic material. For this reason, elevated TOC may not directly lead to higher scavenging, although there is typically a direct relationship. In general, the following aspects of organic matter should be considered:

- **Radical scavenging demand.** Organic carbon will exert a scavenging demand. In a typical RO permeate the contribution of organic matter to scavenging is likely to be very small compared to other species in the water (e.g., bicarbonate and chloramines). In an ozone-CBAT (carbon-based advanced treatment) system, however, the concentration of organic matter will be much higher, and both its concentration and its character will likely have an important effect on UV-AOP performance.
- **UVT.** Organic matter can effectively absorb photons at the wavelengths produced by LP and MP UV systems. The impact of organic matter on the UVT of the water should, therefore, be considered in the design stage. It is likely, however, that in RO permeate, the contribution of organic matter to UV absorbance is small compared to absorbance due to other species, such as chloramines.

CHAPTER 4

Design Considerations for UV-AOP Systems

A designer must consider numerous factors, including treatment goals, system sizing, UV and oxidant dosing, and monitoring strategy in the design of a UV-AOP system. Some considerations are universal (i.e., common to both UV-H₂O₂ and UV-Cl₂) and others are oxidant specific. The following sections describe the elements that go into UV-AOP system design, with emphasis on design elements specific to UV-Cl₂ systems.

4.1 Setting Design Criteria

The designer sets the treatment *target* for the UV-AOP system as a function of the *objective*. In broad terms, UV-AOP is designed to accomplish either *chemical* contaminant removal alone, or *both* microbial inactivation and chemical contaminant removal. In general, chemical contaminant treatment requires a higher level of UV energy compared to UV disinfection, plus the addition of an oxidant. More UV energy is required to break the bonds of a chemical contaminant than is required to inactivate microorganisms, hence chemical contaminant treatment drives system sizing. This comes with a caveat, however, in that if the UV system has assigned, through its validation report, a large safety factor for microorganism inactivation (termed “validation factor” in UVDGM 2006), and the system requires a relatively low reduction of a chemical contaminant, there can be instances where the UV dose required for 6-log virus inactivation credit becomes the driving operational consideration; however, this is the exception rather than the rule.

Whatever the treatment targets, a range of water quality, flow, and operational questions must be considered in developing the design. Recommended considerations for developing design criteria are summarized in Table 4-1.

Table 4-1. Considerations for Developing Design Criteria.

Recommendations	Rationale
Consider variations in flow and system operations	If seasonal and diurnal variations in flow must be accommodated, they should be fully defined, and the anticipated range of operation provided to the UV manufacturers so they can select the optimal size and number of reactors for the application.
Establish a robust source water quality dataset	<p>To characterize the full range of regulated and unregulated target contaminants to capture data on all potential drivers for system sizing.</p> <p>If possible, collect at least 1 year of monthly data on the advanced treatment system's source water(s) to capture variations in chemical concentrations. A limited dataset may result in oversizing the system to account for uncertainties. For example, if an unusual spike in a particular contaminant (e.g., NDMA) is captured, the system may be sized for a high concentration without knowledge that the spike was only a transitory, unusual event. Conversely, missed high-concentration periods may result in undersizing of the system.</p> <p>This dataset, and the impact of upstream treatment (both removal of contaminants and any addition, such as an increase in NDMA concentration due to formation), should be incorporated into development of feed water quality design criteria. If UV-AOP is part of a treatment train, modeling of the upstream processes (e.g., RO removal) will be needed to develop these data.</p>
Include both treatment targets and background water quality	Make sure that meeting the treatment goal(s) is tied to a reasonably conservative background water quality dataset that reflects the range of potential water quality. Background scavengers and UV absorbers (e.g., chloramines) that have a significant impact on process efficiency must be considered.
Capture the potential variation in upstream process performance	Consider the potential variation in treatment efficacy of the upstream water purification processes in defining the feed water quality to the UV-AOP system. This is particularly important where multiple source waters and/or changes in source water contributions occur.
Know which general system size range (UV dose and oxidant concentration) should be operating	While system sizing comes from the UV manufacturers, the designer must still have a general understanding of proper system sizing to verify that the manufacturer has developed an appropriate proposal. The proposed UV dose and electrical energy per order (or E_{EO} , described in more detail in section 4.10) should be consistent with other operating UV-AOP facilities and obviously should be sufficient to accomplish the treatment targets. Data from existing UV-AOP facilities with similar source waters and treatment targets, peer-reviewed literature, and data from pilot testing can all be used to verify adequate system sizing.

Common Treatment Targets in Potable Reuse

For microbial treatment, inactivation of Cryptosporidium, Giardia, and virus are common targets. The UVDGM (USEPA 2006) and the Innovative Approaches to UV Disinfection (USEPA 2020) provide the required UV dose targets as a function of log inactivation desired. For example, the Innovative Approaches document states that the required UV dose for accomplishing 6-log inactivation of virus is 276 mJ/cm². The UVDGM details calculation procedures to account for uncertainties associated with the validation of the UV unit. It is common for state regulators to reference this document and require that its practices be followed in dosing, operation, and installation. Gaining regulatory credit for disinfection, even in cases where a higher UV dose is being applied for UV-AOP treatment of chemical contaminants than would be for a disinfection-only application, is a key step in many projects.

In California, the SWRCB requires that an oxidation step be part of the treatment train for indirect potable reuse using groundwater injection as the discharge location. This oxidation step must accomplish broad treatment of several chemical compounds or demonstrate a minimum **0.5-log removal of 1,4-dioxane**. When using UV-AOP, most practitioners have elected to take the latter approach.

If **NDMA is a target contaminant** and has been detected in secondary effluent of the plant that will supply water to an advanced treatment facility, the amount of NDMA treatment required may dictate the UV-AOP system size (but not the oxidant dose). For example, if 150 nanograms per liter (ng/L) of NDMA is present in the advanced treatment plant influent and RO is expected to reduce the concentration of NDMA by, for example, 33%, then 100 ng/L may enter the UV-AOP system. In California, **10 ng/L** is the Notification Level for NDMA that utilities must meet. In this scenario, a 1-log removal of NDMA requirement, in addition to a 1,4-dioxane log removal requirement, may be stipulated to reduce NDMA from 100 ng/L to 10 ng/L.

As potable reuse regulations are varied and evolving in many areas, so too are treatment requirements. The designer should carefully consider current local and state treatment requirements.

4.2 Flow Rate and Redundancy

The process water flow rate is clearly of great importance. The optimum number of treatment trains (i.e., parallel flows carried within one or more pipes or channels) is determined by factors such as available footprint, whether the system is pressurized or unpressurized, availability and capacity of UV-AOP reactors, and desired redundancy. In drinking water and potable reuse systems, N+1 (full train) redundancy is generally considered the standard configuration. With this configuration, operators may perform maintenance on one train while treating plant flow through the remaining trains or operate in the event of a breakdown of one of the trains. In-vessel redundancy, in the form of a standby bank of UV lamps, is an option that designers may consider to reduce capital cost. In this configuration, the system activates a separate standby bank of lamps that is internal to the operating reactor in the event of a problem (e.g., loss of a ballast or lamp in another bank). This option allows continued operation, but a shutdown or overall plant diversion would be required until UV-AOP operation had been restored.

N+1 redundancy is the standard configuration for drinking water and potable reuse systems. But in-vessel redundancy, in the form of a standby bank of UV lamps, is an option that designers and regulators may consider to reduce overall capital cost, if acceptable to regulators.

4.3 Oxidant Dosing Design

This section addresses oxidant dosing for UV-Cl₂ projects. Hydrogen peroxide dosing requires additional considerations that are not addressed herein.

Today’s water treatment plants typically use multiple chlorine feed pumps at different points in the treatment process. As the UV-Cl₂ AOP uses the same types of chlorine dosing pumps, a designer may procure the same type of pumps with which a plant is familiar or that are being used in other areas of the plant. The pump should receive a signal from the plant SCADA or the UV-AOP system PLC and modulate chlorine flow to accomplish target concentrations. Designers should use a duty/standby pump configuration.

The designer should dose chlorine at an appropriate location upstream of a mixing device. Because the UV-AOP process requires a target concentration of *free* chlorine, two options exist for dosing location:

Option 1: Far upstream, such that the hydraulic retention time (HRT) is sufficient to allow the chlorine/chloramine reactions to proceed to breakpoint (this will often not be practical)

Option 2: Relatively close upstream relative to the UV-AOP system, such that only a limited reduction in free chlorine (due to chlorine/chloramine reactions and/or reaction with free ammonia) occurs prior to UV-AOP

If the designer elects to allow reaction time to allow breakpoint chlorination, at low pH a designer may need to build up to 30 minutes of HRT upstream of UV-AOP to accomplish Option 1. Implications include the cost of piping/storage to accomplish that HRT, unknown time to breakpoint, and increased cost of dosed hypochlorite (i.e., dose high enough to overcome all the demand associated with chloramines). UVT will be higher using Option 1 owing to the reduction of chloramines, which would lead to a reduction in UV-AOP system sizing. Generally, designers have selected Option 2, which minimizes plant footprint, chemistry uncertainty, and oxidant cost. Figure 4-1 illustrates the impact of ammonia on free chlorine and chloramine formation and consumption.

Table 4-2 includes additional recommended design considerations for sodium hypochlorite injection ahead of the UV system.

Table 4-2. Sodium Hypochlorite Injection Best Practices.

Injection method	Quill to assist in mixing
Mixing	Inline static mixer or wafer-type mixer
Pump control	Dose pacing relative to flow rate and concentration requirement (from plant SCADA or UV-AOP system PLC)
Oxidant concentration control	UV PLC controls target oxidant (i.e., free chlorine) concentration

4.4. Source Water Characterization

The feed to the UV-AOP is the product of upstream treatment of the source water, so as the designer defines the upstream treatment processes (s)he must also consider the impact of these processes on UV-AOP design and operation.

Potable reuse projects often draw water supply from multiple sources. For example, increasingly, multiple sources of water, in addition to secondary effluent from a wastewater reclamation facility, are being collected and treated to augment water supplies. This can include multiple reclaimed wastewaters, and/or a combination of reclaimed wastewater and stormwater. This can create a complex range of water quality scenarios to characterize before developing a basis of design. Stormwater runoff is periodic. Different wastewater treatment plants (or even two halves of a parallel train plant) will receive input water from differing percentages of residential and industrial sources. Treatment processes in a single wastewater treatment plant (WWTP) may be different. In drinking water applications, multiple wells with different background water qualities and contaminant concentrations can have varying combinations of water quality, each with its own challenges and design criteria.

Critical design parameters for UV-AOP are summarized in Table 4-3. The roles of various water quality parameters are discussed in detail in Chapters 3 and 4.5.

Table 4-3. Feed Water Quality Parameters Important to UV-Cl₂ System Sizing.

Parameter	Significance
UV absorbance at 254 nm/UVT	Efficacy of UV light transmittance through the water column
Water Temperature	Impact on water chemistry, UV lamp output, and reaction kinetics
pH	Chlorine and carbonate chemical speciation
Ammonia	Oxidant demand, formation of chloramines
Chloramine	Oxidant consumer, UV light absorption, radical scavenging
Alkalinity	Radical scavenging
Nitrate	Impact on UVT (MP), formation of nitrite in reactor
Nitrite	Radical scavenging
Total Organic Carbon	Radical scavenging, disinfection by-product (DBP) precursor
Bromide	DBP precursor for UV-Cl ₂ systems
Iron	Lamp sleeve fouling
Manganese	Lamp sleeve fouling
Calcium	Lamp sleeve fouling
Hardness	Lamp sleeve fouling

Whether it is one source or many, the combined source water to the advanced treatment plant must be carefully characterized to understand the full variability of both the flow and the water quality the process train will treat. It is also important to keep in mind that UV-AOP typically occurs at or toward the end of the treatment train where water quality is highest. The “source water” to the UV-AOP is the product of upstream treatment, so as upstream treatment processes are defined, consideration must be given to the impact of the product water quality on UV-AOP design and operation. For example, changing the RO membrane to a membrane

that has a lower nitrate rejection profile requires the designer to evaluate the potential impact on the UV-AOP system’s performance and question whether design changes are needed.

4.5 Understanding the Dynamic Chemistry of the UV-Cl₂ Process Is Essential to Good Design

The UV-Cl₂ process chemistry is complex and highly dynamic, particularly if there is significant nitrate, nitrite, chloramines, and/or ammonia in the system. Considering what chemistry changes will occur through the process train has a critical impact on system performance; therefore, chlorine chemistry must be carefully considered through the process train and should influence the selection and placement of chemical injection points, required chemical addition, chlorine and other monitors (see Chapter 4.10 for detailed discussion on monitoring), and system sizing. Challenges posed by chlorine/chloramine chemistry that cannot be resolved in a cost-effective manner may preclude the use of UV-Cl₂ altogether. Table 4-4 summarizes the chlorine chemistry through the UV–AOP process and related considerations for system design. A more detailed explanation of the impact of ammonia and other nitrogen species on UV-AOP is provided in Appendix A.

Table 4-4. Chlorine Chemistry through the UV-Cl₂ Process.

Location In the Process	Chlorine Chemistry	Design Considerations
Sodium hypochlorite is injected into the pipe	<ul style="list-style-type: none"> • If ammonia is present in the water, the ammonia and free chlorine will react to form chloramines. This reaction is complete within tens of seconds under good mixing, but poor mixing can allow chlorine and ammonia to co-exist in a pipe for some distance, and potentially into the reactor itself. • This results in an increase in combined chlorine above that which may already be present (e.g., for RO biofouling control) and will reduce the UVT and contribute to radical scavenging. Also, the chloramines will increase free chlorine demand prior to and through the UV reactor. • If nitrite is present in the RO permeate, it will exert an immediate free-chlorine demand. 	<ul style="list-style-type: none"> • Chlorine and any combined chlorine (chloramines) present will begin reacting toward the breakpoint. This process is not instantaneous. It can take many minutes, depending on the pH and concentrations involved, so travel time to the reactor must be carefully considered. • If free chlorine is measured near the injection point, the free chlorine entering the reactor may be overestimated. Therefore, sampling must be done relatively close to the reactor inlet, being careful to match HRT between sample lines and process lines (to match the reaction time between the monitor line and the process line, with the goal of accurately measuring free chlorine entering the UV-AOP reactor). • A high concentration of ammonia may preclude UV-Cl₂ due to its demand to form monochloramine. In practice, designers of the UV-Cl₂ AOP should target <i>residual</i> ammonia concentrations below ~0.25 mg/L as N to limit the performance and economic impacts of ammonia/chloramines unless there is concern with residual free chlorine impacting an upstream RO membrane process (and thus a higher residual might be warranted). • While increasing HRT following chlorine injection to allow the system to reach

Location In the Process	Chlorine Chemistry	Design Considerations
		<p>breakpoint is one option, the preferred option is to place the chlorine injection point to minimize HRT prior to UV-AOP while achieving good mixing.^a This minimizes consumption of free chlorine and reduces system footprint and cost.</p> <ul style="list-style-type: none"> • If the concentration of chloramine entering and exiting the RO system is insufficient (or if the system does not use chloramines for fouling control), the designer should consider adding ammonia upstream of the UV system for bromate control in high-bromide waters. • Nitrite in RO permeate can be minimized by improved upstream denitrification or optimized free chlorine dosing/mixing when forming chloramines for membrane fouling control. With good complete mixing, free chlorine should react preferentially with nitrite to convert it to nitrate over reaction with ammonia to form chloramines. Incomplete mixing can allow a fraction of the flow to remain unchlorinated, which would allow nitrite to persist for some distance downstream.
The chlorinated water enters the UV reactor	<ul style="list-style-type: none"> • The chlorinated water undergoes transformations in the UV reactor. • Due to the relatively high absorption of UV light by chlorine species and their subsequent degradation, at the high UV doses applied for UV-Cl₂ treatment significant degradation of total chlorine through the UV-AOP system can be expected. This, in turn, results in a dynamic UVT as water progresses through the UV system. 	<ul style="list-style-type: none"> • Chloramines absorb UV light and decrease UVT. While this may initially reduce the efficiency of the UV-Cl₂ process, the UVT will increase through the reactor as chlorine species are photolyzed in the UV-AOP chamber.

a. *In some cases, while reaching breakpoint may be impractical, increased HRT reduces the monochloramine concentration at the reactor, thereby increasing the UVT entering the UV-AOP system and increasing the efficiency of that process. This efficiency gain is, however, at the expense of the infrastructure required to achieve the HRT and would also require a higher hypochlorite dose. That is, if HRT is increased, there is less monochloramine (a benefit), but also less free chlorine to drive the AOP (a negative; requires increase in dosed sodium hypochlorite concentration to reach the target free-chlorine concentration). Chemical/kinetic modeling may be required to understand the various impacts and to evaluate the economic trade-offs. In practice, minimizing the HRT between chlorine injection and the UV-AOP system has proven effective.*

A designer must also understand and address this dynamic chemistry in the monitoring strategy. For example, if the water stream for measuring UVT in the online monitor is diverted from the process stream *after* the addition of sodium hypochlorite, the chlorine reactions observed in the process stream will also take place *in the sample line*. Ideally, the HRT in the sample line matches the HRT in the process water line between the sample point and the

entrance of the UV reactor. In practice, matching HRT is challenging, given a fixed sample line size and process flow rates that vary with time. Special considerations for locating chlorine injection and monitoring points are discussed in Chapter 4.11.

Illustrating the Dynamic Chemistry of the UV-Cl₂ Process: The Impact of Varying HRT

Consider the progression of monochloramine, dichloramine, free chlorine, ammonia, and UVT as water progresses through RO and into the UV-AOP system in two HRT scenarios with an initially dosed concentration of sodium hypochlorite of 8 mg/L as Cl₂ (Figure 4-1). Following the addition of sodium hypochlorite, the concentration of chloramine begins to decline as reactions with sodium hypochlorite start. This converts monochloramine to dichloramine, which increases the UVT. Free chlorine declines to a reduced concentration (~2.5 mg/L as Cl₂ on Figure 4-1a, and ~5.5 mg/L on Figure 4-1b) entering UV-AOP. Within the reactor, UV light further degrades chloramines and free chlorine through photolysis and oxidation, which results in an increase in UVT as the water passes through the UV-AOP system. Note that the influent free chlorine concentration should be high enough that water exiting the UV-AOP system contains some residual free chlorine. If this is not the case, photolysis of monochloramine can result in the accumulation of nitrite, which impacts treatment efficiency through the increase in •OH scavenging (as discussed in Section 3-1). A significant difference between the two cases is the concentration of hypochlorite arriving at the UV reactor. This difference clearly impacts the operational cost of the system and is arguably too high in the short HRT case (Figure 4-1b). With the short HRT, the initially dosed sodium hypochlorite concentration should be reduced to accomplish a lower free chlorine concentration entering the UV-AOP system. This is due to the fact that high free chlorine concentrations may damage the UV reactor. UV manufacturers generally limit the concentration of free chlorine in the UV-AOP system to 5 mg/L due to chlorine's high corrosivity and the potential for damage to the UV reactor interior. Note also that this upper limit on concentration of free chlorine in the reactor limits the flexibility of the UV-Cl₂ process in general in that, in the event of a target concentration increase or change in water quality, operators are limited in their ability to increase oxidant concentration to increase treatment. In contrast, with a UV-H₂O₂ system, there is more flexibility to increase H₂O₂ concentration to increase treatment in the event of a change in treatment requirements.

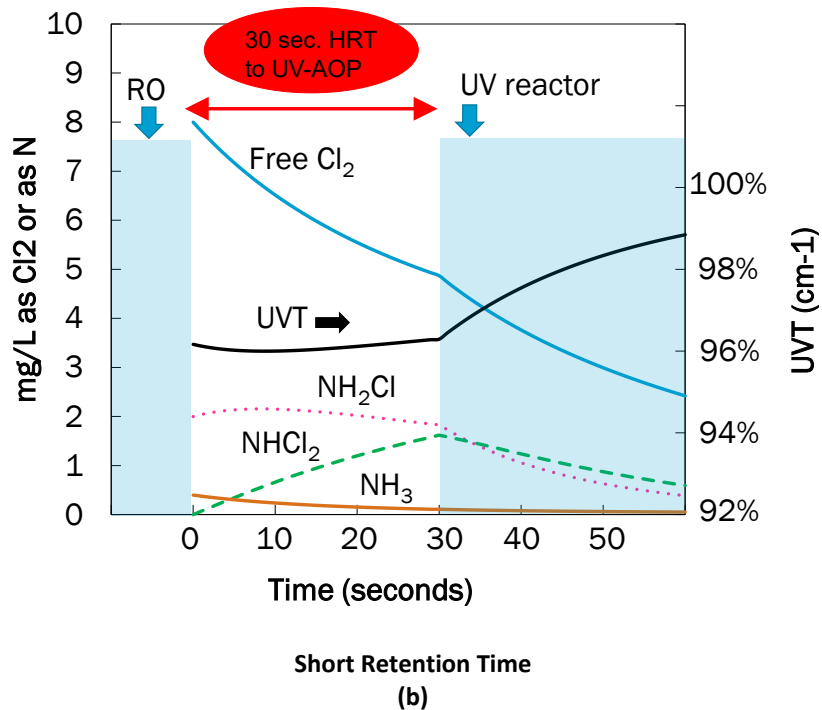
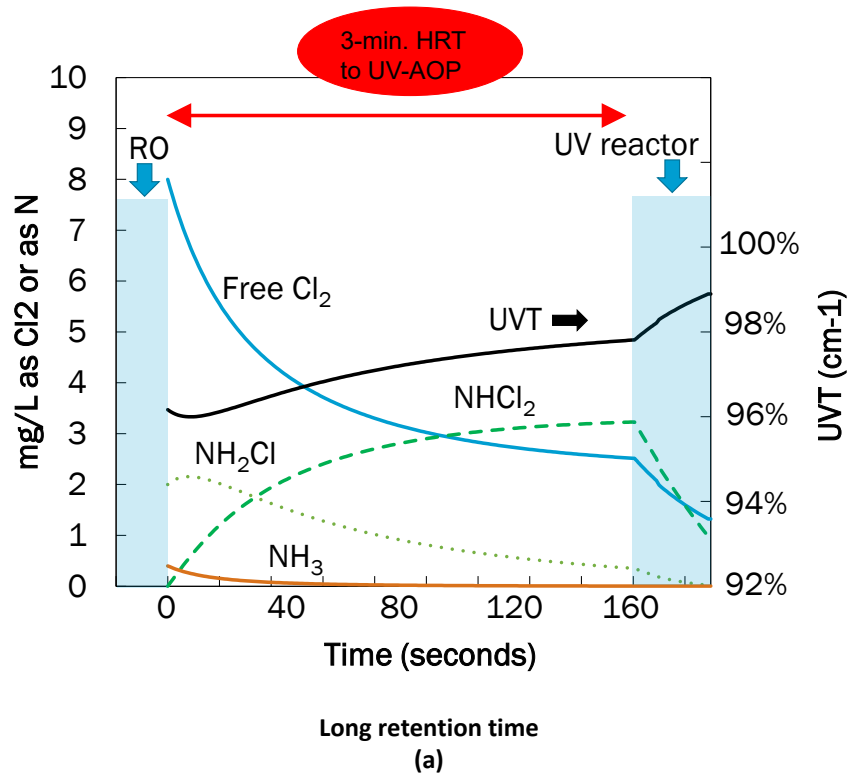


Figure 4-1. Travel Distance to the UV Reactor Can Affect the Required Free Chlorine Dose (results from modeling shown under typical conditions—for general illustration only)

4.6 Water Quality Considerations

Source water quality has a strong impact on the efficiency, practicality, and cost of UV-AOP systems. Chapter 5 presents an economic analysis of various water quality factors related to

UV-Cl₂ and UV-H₂O₂ selection. Chapter 6 presents a decision tree that organizes the evaluation process and guides the user through oxidant selection. As stated, a number of water quality parameters have a significant impact on UV-Cl₂ system design and operational requirements. The following summary of considerations described above are recommended when evaluating the appropriateness of UV-Cl₂ for a given application and developing design criteria and details:

- **Optimal pH**

- pH is a critical factor in evaluating the efficacy of treatment in UV-Cl₂ systems. As discussed in Section 3.2, lower pH drives the speciation of free chlorine toward hypochlorous acid (and away from the hypochlorite ion), with hypochlorous acid being more efficient than hypochlorite at producing [•]OH at 254 nm which is characteristic of LPHO UV reactors. An MP system can partially counteract this phenomenon since the higher wavelengths from an MP lamp (shown previously on Figure 1-2) cause OCl⁻ to generate [•]OH and reactive chlorine species, potentially allowing an MP system to be more effective at higher pH than LPHO. Overall, though, low pH is generally preferred for both LPHO and MP systems.
- A general rule of thumb is that low pH (5.0 to 5.5) is generally considered optimal for UV-Cl₂. The use of MP UV light, with its polychromatic light spectrum, may allow for a higher pH range while maintaining effective treatment, although this topic remains an outstanding research need. All potable reuse UV-Cl₂ systems installed to date are LPHO systems treating low-pH water. MP UV-Cl₂ *has* been used successfully to remove contaminants in a groundwater drinking water plant with a pH of 7.2 to 7.5 (Region of Waterloo, Canada).

- **If ammonia is present**

- In systems that do not fully nitrify/denitrify, a higher concentration of ammonia (and nitrite) can be expected. Excess ammonia rapidly combines with chlorine to form (additional) chloramines; in UV-Cl₂ applications this has multiple impacts.
- To maintain a free chlorine residual through the UV-AOP system, sodium hypochlorite must be added in sufficient quantity to overcome the ammonia demand.
- The goal of chlorine dosing is to apply enough chlorine to react with the ambient ammonia and to provide sufficient excess free chlorine within the UV reactor to accomplish the AOP treatment.
- Overcoming ammonia demand will only be practical (and economical) at relatively low ammonia concentrations. Any added sodium hypochlorite, of course, has an associated cost. Therefore, in the overall cost analysis of the UV-Cl₂ AOP, ammonia concentration entering the UV-AOP must be considered. For additional information on the cost implications of the presence of ammonia, please refer to the economic factors discussion in Chapter 5.
- Organic matter will also consume free chlorine; therefore, the final chlorine dose required to achieve the desired free chlorine concentration at the UV reactor should be determined through chlorine demand tests using the actual water, where possible.
- Significant trihalomethane (THM) formation with the UV-Cl₂ process has not been noted in the literature, but this potential issue should be considered, especially in non-RO-based treatment. DBP formation in UV-Cl₂ applications is discussed in Appendices A and E.

- **If nitrite is present**
 - Nitrite by itself is not a major concern for UV-Cl₂ systems. Nitrite may exert a small chlorine demand that will slightly impact the economic analysis. While nitrite is fundamentally a very strong hydroxyl radical scavenger, free chlorine will oxidize any nitrite to nitrate prior to the UV reactor (assuming free chlorine is well mixed in the water stream. If not, nitrite can strongly scavenge the •OH).
 - The economic impacts of nitrite on a UV-H₂O₂ system are potentially significant. Nitrite concentrations in excess of 1 mg/L as N may exert a scavenging demand so significant that oxidation treatment targets may be impossible to achieve. A practical maximum for the nitrite concentration into the UV reactor is ~0.1 mg/L as N, although that too will exert a high radical demand.
 - Nitrite is regulated in drinking water at a maximum concentration of 1 mg/L as N in the United States and Canada, and 0.1 mg/L as N in parts of Europe.
- **If chloramines are present**
 - Chloramines will exert a free chlorine demand that will lead to a difference between the free chlorine dose applied and the amount entering the UV reactor. The magnitude of this demand is a function of pH, temperature, concentrations of the species involved, and other factors, and must be accounted for in design and operations (Section 3.1).
 - Both mono- and dichloramines may exist. Personnel at the Orange County Water District report approximately 60% monochloramine and 40% dichloramine in RO permeate. The evolution of the mono- vs. dichloramines over time as the water travels from the RO process to the UV-Cl₂ process must be considered, since monochloramine impairs UV-chlorine AOP performance to a greater extent than dichloramine due to greater UV absorbance (at 254 nm) and greater hydroxyl radical scavenging. This phenomenon must be considered through modelling and/or pilot-scale testing.
 - Chloramines absorb UV light. This reduction in UVT will require an increase in the size of the UV-AOP system to meet the treatment goal, which comes with a corresponding increase in operating costs to accomplish treatment targets associated with UV-AOP.
 - Chloramines impose additional scavenging demand which, in turn, increases the requirements of energy and oxidant to accomplish treatment targets associated with UV oxidation.
- **If bromide is present >~25 µg/L**
 - In a UV-Cl₂ system, bromide can react with free chlorine and form bromate. Early experience suggests that a practical rule of thumb of a bromide concentration of <25 µg/L in RO effluent would likely preclude formation of bromate above 10 µg/L without other mitigation efforts. Note that the presence of chloramines in the UV-AOP system will limit the formation of bromate (see Appendix A). Note also that the upper limit for allowable bromide entering the UV-AOP system may be higher depending on the specific location and water quality. Additional research on the topic of bromate formation in UV-Cl₂ is included in the list of future research needs.
 - If there is higher bromide in the UV-AOP influent, and chloramines are not used for biofouling control in upstream membranes, the addition of a low dose of ammonia may be needed to prevent bromate formation in the UV-Cl₂ process (see Section 3.2 for further discussion of this issue). The Terminal Island Water Reclamation Plant has used

addition of ~0.3 mg/L as N ammonia along with chlorine upstream of the UV-Cl₂ process to limit bromate formation to ≤6 µg/L.

- **Organic matter is a scavenger and should be evaluated if present in significant concentrations (>0.5 mg/L)**
 - Organic matter can be a significant radical scavenger. While TOC and scavenging are not always directly related, a designer should include the concentration of TOC in design criteria.
 - For non-RO-based potable reuse and drinking water systems, TOC may be present at elevated levels (>~0.5 mg/L) and should be evaluated when sizing the UV-AOP system. The UV manufacturer may require water samples for analysis to quantify scavenging to provide a performance guarantee. Scavenging demand is discussed in more detail in Section 4.8.
 - With respect to disinfection byproduct (DBP) formation, especially in non-RO treatment scenarios, literature information on the direct formation of haloacetic acids and trihalomethanes during the UV-Cl₂ process is limited. Initial studies have indicated that on the short timescale of UV-Cl₂ treatment, haloacetic acid and trihalomethane formation is not significantly increased (see Chapter A3.3 of Appendix A for details). However, given the limited data in this field to date, the potential for chlorinated DBP formation should be considered in UV-Cl₂ applications, and advances in the available peer-reviewed literature should be consulted.

4.7 Selection of UV Dose and Oxidant Dose Impact Both Efficacy and Cost Considerations

The designer should engage with the UV manufacturer about the optimum ratio of UV energy vs. oxidant concentration early in the design phase. Water quality data will aid in system sizing. The relationship between UV dose and oxidant is determined through UV reactor modelling or full-scale reactor testing in similar water. Section 7.1 discusses the advantages/disadvantages of pilot testing in the design phase, but in short, small-scale piloting does not generally provide useful information related to sizing given the differences in efficiency, timescale, mixing, and path length between a pilot-scale system and a full-scale system. The balance of increasing UV energy vs. increasing oxidant concentration (including any quenching requirement) within constraints of effectiveness depends on the local electricity vs. chemical costs. In much of North America, where energy tends to be relatively cheap, it is common to preferentially operate at a higher UV energy while minimizing the amount of chemical needed to achieve the desired level of treatment (as H₂O₂ and sodium hypochlorite are relatively expensive). The relationship between UV lamp power and oxidant concentration needed to achieve the treatment goal for a particular UV-AOP system is determined using proprietary models maintained by the manufacturers. This relationship between lamp power and oxidant concentration depends on the reactor efficiency, target contaminant, and water properties.

As mentioned above, there may be scenarios where adding higher concentrations of oxidant to increase treatment is desired (e.g., a change in treatment requirement); however, three considerations limit this potential:

- Due to corrosion considerations, the concentration of free chlorine entering the UV system in a UV-Cl₂ system is sometimes limited to 5 mg/L as Cl₂. **Free** chlorine is corrosive at high concentrations. Free chlorine in a UV-Cl₂ AOP system at doses of 8 to 10 mg/L as Cl₂ can cause corrosion of both metallic and non-metallic (e.g., gaskets) components in the UV reactor. A facility using UV-Cl₂ AOP to treat trichloroethylene-contaminated groundwater encountered accelerated corrosion of welded joints, suspected to be due to high chlorine concentrations (~8 mg/L). Reducing the chlorine concentration to ~2 mg/L in that application reduced corrosion. This cap on free chlorine concentration limits the ability of an operator/designer to increase free chlorine concentration to increase treatment. This limit in flexibility with UV-Cl₂ AOP may be a reason, in some treatment scenarios, to prefer UV-H₂O₂. The oxidant itself is a radical scavenger. Therefore, **adding oxidant at a concentration above some optimum level will actually reduce treatment performance**. The reason is that AOP reactor conditions need to be such that the added oxidant forms more •OH and RCS through photolysis than it is consuming through radical scavenging. As the oxidant concentration increases, the scavenging effect increases proportionally, but the radical formation increases less than proportionally. This effect is more commonly observed in UV-H₂O₂ systems; the corrosion consideration noted above in UV-Cl₂ systems that limits the concentration of free chlorine in the UV-AOP system reduces the likelihood of this effect as the maximum concentration is capped.
- The oxidant absorbs UV light and reduces UVT. Because the oxidant itself absorbs UV light, one impact of increasing oxidant is to reduce UVT. Reduced UVT leads to reduced treatment efficacy.

Typical design free chlorine doses are on the order of 1.0 to 2.5 mg/L as Cl₂ for installed potable reuse systems, but higher doses can be used if needed. Typical target H₂O₂ doses in installed potable reuse systems range from 3 to 6 mg/L.

Design engineers should also use best practices for sodium hypochlorite feed system design. While chemical feed system detailed design is outside the scope of this Guidance Manual, designers should consult treatment plant design resources like *Water Treatment Plant Design* (AWWA and ASCE 2012; *Water Quality and Treatment* (AWWA 2011) and *Chlorine and Alternative Disinfectants* (White 2010). It is also important for designers to discuss with UV manufacturers whether the concentrations of oxidants being proposed fall within the manufacturer's range of experience and system warranty range. Further, all common-sense factors associated with acquiring and storing chemicals must be considered. For example, decay should be considered in chemical storage sizing. Both hydrogen peroxide and chlorine decay with time. Hypochlorite solutions will decay to form chlorate and perchlorate over a timeframe on the order of weeks to months depending on bulk chemical concentration and temperature. Typical practice for sodium hypochlorite storage is generally to provide for 21 to 30 days at average rates of chemical consumption. This helps to control chlorate and perchlorate in the hypochlorite solution to acceptably low levels and will not add to any chlorate that may be formed by the UV photolysis of chlorine (more details are provided in Chapter A3.8 of Appendix A). While the USEPA has not currently set a limit on chlorate, other organizations, such as the

World Health Organization and Health Canada, recommend limits in drinking water on the order of 0.7 mg/L to 1.0 mg/L as Cl₂, respectively.

Hydrogen peroxide is comparatively stable, but best practice is still generally to size storage for 30 to 40 days at average flow to manage footprint requirements and minimize losses to decay. Hydrogen peroxide should be sheltered from heat and UV light to minimize decomposition.

4.8 Hydroxyl Radical Scavenging Demand

A standard method for quantifying scavenging, at the time of this Guidance Manual's publication, does not exist. Further, there are no known commercial labs that measure scavenging. Some UV manufacturers measure scavenging using proprietary methods. In practice, the inability to determine scavenging by an objective third party and by a commonly accepted method is a key industry gap. Development of online scavenging monitoring would be a valuable addition to the suite of online monitors for UV-AOP; therefore, the development of scavenging measurement techniques is identified as a research need in this Guidance Manual.

As discussed, UV-AOP systems generate radicals within the UV reactor. These short-lived species react with oxidizable contaminants in the water; however, numerous compounds compete with the target contaminant for radicals. The oxidant itself is also a scavenger.

The number of radical scavengers in a water to be treated is a critical design parameter, since it dictates the oxidant and UV doses that must be applied to generate sufficient radicals to destroy the target contaminants. The relationship between the radical scavenging of the water and the AOP system design can be modelled. However, given the high level of effort and computational fluid dynamics and analytical chemistry expertise required to accurately model performance, and that geometry data is proprietary, models that link UV dose, scavenging, and treatment performance are maintained by UV-AOP manufacturers.

Scavenging can be quantified in the laboratory as a bulk parameter (see Chapter A2.1 of Appendix A for details). As noted, there is currently no common, industry-accepted, method for quantifying scavenging.

Scavenging can change with time as water quality changes; therefore, end users should plan to measure scavenging periodically (e.g., bi-annually) to identify changes.

One approach to indirectly capture scavenging in a design specification, in the absence of a specific scavenging value as determined by an independent third party, is to define bulk parameters that impact scavenging. As discussed in Chapter 3, alkalinity, chloride, nitrite, TOC, and chloramine concentration are examples of water quality parameters that affect scavenging. A UV-AOP system designer may specify values for these and other parameters, as surrogates for scavenging, for UV-AOP manufacturers to consider in their design. However, this is an imperfect method as the bulk scavenging measurement includes contributions from a variety of constituents, some of which are not captured by discrete measurements of specific parameters.

Pro Tip

How the scavenging demand measurement is used for sizing input and operation is a function of the manufacturer, but at present, most estimate a single worst-case value. Some use this value as a discrete numerical input into controls calculations, while others use it in a more empirical fashion to assist in sizing and to determine threshold operational values of UV dose and oxidant. If the scavenging demand term is an input into the control system, it should be periodically re-measured to ensure that the value is correct or conservative. Changes in the scavenging demand can lead to changes in the UV-AOP system's performance.

4.9 Fouling Potential

In a typical UV system, UV lamps within protective natural or synthetic quartz sleeves are submerged in the water stream. Constituents dissolved or suspended in water can accumulate on external surfaces, including the lamp sleeves, monitoring windows of UV intensity sensors, and other wetted components of UV reactors. These foulants can absorb UV light and impair the ability of the UV-AOP system to treat target contaminants. The issue of fouling for UV systems in general is covered extensively in Sections 2.5.1.4 and 3.4.4.2 of the UVDGM (USEPA 2006). This Guidance Manual focuses on the issues specific to the UV-Cl₂ AOP with regard to the water quality expected in potable reuse applications.

In general, the rate of fouling can be expected to increase with increasing calcium, alkalinity, hardness, iron, and manganese. pH, natural organic matter, and TOC potential can also impact the rate of fouling. **A key take-away is that in the absence of a fouling study, with water that is representative of the water that will be treated at full scale, fouling is difficult to predict.**

Water entities building green-field reuse facilities will not have access to representative water. Even pilot-scale facilities may not accurately simulate full-scale water given differences in membranes, long-term biological activity in biofilters, and operational practices. For this reason, designers rely on predicted water quality and precedent associated with upstream processes to determine whether fouling is anticipated to be an issue. Fouling guidance for the two primary potable reuse treatment trains follows:

- **RO-based pretreatment.** For reuse plants that will use RO, the low concentration of dissolved constituents, low hardness, and acidic pH leads to low fouling potential. Users of UV-AOP following RO report low rates of external sleeve fouling. For this reason, most designers consider sleeve cleaning systems unnecessary in RO permeate applications. Fouling factors (a discounting factor used in UV system sizing to account for a future, fouled-sleeve state of operation) typically range from ~0.92 to 0.95, depending on water quality and designer preference.
- **Ozone/biofiltration pre-treatment.** Ozone/biofiltration pre-treatment systems are not as effective as RO systems at reducing dissolved organic and inorganic constituents, including iron, manganese, and calcium. As mentioned above, fouling is difficult to predict. Designers of treatment trains without RO should consider conducting a UV sleeve fouling study using representative water (i.e., water produced from an identical source water and treated with identical upstream processes). Such a study is, of course, expensive and time consuming and may not accurately represent water quality, and therefore fouling potential, at full-scale. For this reason, specification of a sleeve-cleaning system to mitigate sleeve fouling is

recommended as a simpler and more cost-effective approach. Fouling factors with ozone/biofiltration pretreatment typically range from ~0.85 to 0.90.

UV-AOP system design should account for both lamp aging and lamp sleeve fouling, similar to drinking water systems.

4.10 Critical Control Point Monitoring

In designing UV-AOP for potable reuse applications, the designer should consider the requirements for critical control point (CCP) monitoring for permit compliance early in the process. CCPs are integrally related to the UV-AOP system’s available control strategy, the on-line monitoring strategy, and the permit for operation eventually issued by the regulating entity. Water Research Foundation Report 13-03, *Critical Control Point Assessment to Quantify Robustness and Reliability of Multiple Treatment Barriers of a DPR Scheme*, presents recommendations regarding CCP monitoring of the overall water reuse advanced facility (Walker et al., 2016). While this WRF report included a section on UV-H₂O₂ and not specifically UV-Cl₂, there are parallels to operating a UV-Cl₂ system. Table 4-5 describes the primary CCPs that can be used to maintain sufficient oxidant concentration and applied electrical energy. These recommendations have been adapted and expanded for operating UV-AOP systems today.

Table 4-5. UV-AOP Alert and Alarm Level Summary.

Monitoring Parameter	Alert Level	Critical Failure Level	Notes
Hydrogen peroxide (or free chlorine) (1-minute moving average)	25% less than target dose	50% less than target dose level	This same approach can be used if sodium hypochlorite is used instead of hydrogen peroxide.
Electrical energy dose (EED)(measured EED to target EED) or UV dose	Less than 105% of target dose	Less than 100% of target dose	This control approach considers UVT, UV intensity, flow, and power. Control algorithms are contained in proprietary manufacturer control systems.
UV lamp failure	Greater than 10% of lamps	Greater than 15% of lamps	This figure may be adjusted for each reactor at an individual site for an appropriate number of lamps.

Source: Walker et al. 2016

There are generally three CCP approaches currently taken for controlling the *UV energy* applied by a UV-AOP system to accomplish treatment objectives:

- **Control by Minimum Electrical Energy Dose (EED).** EED measures the power used by the lamps in the UV system and normalizes it by flow rate. EED is calculated as power delivered by lamps / flow rate and has units of kilowatt hour per volume (kWh/volume). This metric is derived from the figure of merit described by Bolton et al. 2001 (IUPAC, Pure and Applied Chemistry 73, 627–637) in which the authors presented the concept of electrical energy per order (E_{EO}). E_{EO} describes the amount of energy required to reduce the concentration of a contaminant by one order of magnitude (1-log) in a given volume. It is described as “a direct link to the electric- or solar-energy efficiency (lower values mean higher efficiency) of an advanced oxidation technology.” EED, as a component of EEO (E_{EO} = EED/log reduction)

measures energy per volume (kWh/unit volume). Controlling to a minimum EED requires that the UV-AOP system always delivers a minimum energy per flow.

- Coupled with a minimum oxidant concentration, this CCP would maintain a UV dose that meets treatment objectives at all times. In this approach, energy input to the water from the UV-AOP system changes when flow rate changes, i.e., the system “flow paces.” However, this metric does *not* respond to changes in UVT. If the EED was determined at a lower UVT, and the system operates at a higher UVT, the system will generally be applying more power than is necessary to accomplish treatment.
- **Control by Minimum UV Dose.** UV dose, as discussed in Chapter 1.2.2, is a metric calculated within the UV system’s PLC based on equations derived from third-party validation testing. In this CCP approach, the UV-AOP system must deliver a minimum UV dose. This approach is more adaptive than the EED approach in that it responds to changes in UVT. It results in lower energy use than the EED monitoring control approach. The permit for one of the case studies presented in Chapter 8, Terminal Island in Los Angeles, lists UV dose as one of its CCPs.
- **Control by Calculated Achieved Log Reduction.** A third approach for monitoring the amount of UV energy applied to the water is the calculation of log reduction achieved by the UV-AOP given the combination of UV dose, flow rate, UVT, oxidant concentration, and other water quality parameters. The metric of “achieved log reduction” has been proposed in lieu of EED or UV dose with proper regulatory approval and site demonstration. At the time of this publication, at least one site had received an operating permit in California to operate based on a target log reduction calculation via an algorithm residing in the UV-AOP system PLC.

Each of these CCPs relies on accurate real-time monitoring. For example, a flow meter is used to measure flow rate entering the UV-AOP system. Flow rate is a critical input to each of the three control approaches.

Typical CCPs, in permits written for UV-AOP systems using one of the above approaches, include:

- Minimum EED, UV dose, or target log reduction as computed by the UV system’s PLC
- Minimum oxidant concentration (free chlorine or hydrogen peroxide) present in the influent of the UV system as computed by the UV system PLC and as confirmed by pump speed thresholds, flow rate of oxidant, or as measured by an oxidant monitoring device (e.g., a monitor for free chlorine)
- Maximum pH in UV-AOP influent
- Minimum UVT in UV-AOP influent

Real-time monitoring of the parameters themselves or as inputs to a PLC-based computation is possible and is being implemented in today’s UV-AOP systems. The next section will address the monitoring requirements for a UV-AOP system.

4.11 Monitoring of UV-AOP Systems

The *objectives* of the UV-AOP system at a particular facility (i.e., what the system was designed to accomplish) drive permit requirements. Subsequently, *permit* requirements drive the real-time *monitoring* requirements. An operating water treatment facility monitors numerous parameters, but only a fraction are the critical parameters related to the permit. A designer must carefully consider the monitoring strategy and, when considering the oxidant used by the UV-AOP system, should consider the differences between the monitoring strategies for UV-Cl₂ and UV-H₂O₂.

There are two parameters critical to all UV-AOP systems: UVT and flow rate. Monitoring considerations for each are described below.

- **UVT.** The importance of UVT as a design parameter was discussed in Chapter 2.2. UVT is monitored in virtually all UV disinfection and UV-AOP applications that use the calculated dose approach. UVT can fluctuate in a water stream for a variety of reasons. For example, in a UV-AOP application, UVT is a function of the upstream treatment process, the concentration of the oxidant present, and in the case of UV-Cl₂ in a chloramine-containing water, the HRT between the chlorine dosing point and the UV-AOP system (i.e., the kinetics of free chlorine-chloramine chemistry, see Chapter 4.5 for details).

When designing the UVT monitoring strategy, a designer should consider:

- Location of UVT sampling point relative to oxidant dosing point: The addition of oxidant will change the UVT of the water. Installed UV-AOP systems have taken one of two approaches: monitor prior to the addition of oxidant or monitor immediately prior to the UV-AOP system. In the former, a predictive algorithm in the UV-AOP PLC calculates the change in UVT associated with the oxidant addition and the change in UVT associated with chlorine-chloramine reactions to determine the UVT *at the entrance UV-AOP system*. In the latter approach, UVT monitoring occurs at the actual entrance to the UV-AOP system but is subject to inaccuracies due to sample line to process line HRT differences (more on this topic below). Note that a regulator may want to see the UVT entering the UV reactor monitored for regulatory purposes given that oxidant concentration is often a CCP.
- Train considerations: UVT can be measured upstream of all trains in a common header or at each individual reactor.
- Whether to implement a UVT monitor following the UV-AOP system: Post-treatment monitoring can capture the change in UVT change across the UV reactor. Some UV dose monitoring algorithms use both as inputs to the equation.
- Redundancy: Analyzers can be installed as duty + standby or duty only, and in the event of a UVT monitor failure, the system defaults to a minimum UVT.
- High UVT ($\leq 97\% \text{ cm}^{-1}$) may warrant selection of a UVT analyzer with a longer path length: RO permeate with low or no chloramine (e.g., $<1 \text{ mg/L}$ as Cl₂), will often have UVT values of $>98\% \text{ cm}^{-1}$. This very high UVT is more accurately measured with a UVT monitor employing a longer pathlength than the standard 1 cm. Consult with the UVT

monitor manufacturer for their recommendation. Commercially available UVT monitors offer options of 2 cm, 5 cm, and greater.

- **Changing UVT within the UV reactor:** In UV-Cl₂ applications where chloramines are formed prior to water entering the UV-AOP system, the UVT will increase as water travels through the UV reactor. UV photolysis process breaks down UV-absorbing compounds. For example, monochloramine absorbs UV light and is broken down as it progresses through the UV-AOP system. The breakdown of chloramines, particularly monochloramine, results in a reduction of UV-absorbing compounds and a higher UVT. The absorbance of UV light by free chlorine also results in a decrease in concentration of free chlorine through the UV system. Finally, ongoing breakpoint reactions also result in a reduction in chloramines and higher UVT as a function of time. In an RO-based application using UV-Cl₂, an increase in UVT from 96% cm⁻¹ to 98% cm⁻¹ from the influent of the UV reactor to the effluent would be considered typical. While an increase in UVT through a UV-H₂O₂ system would also occur due to the photolysis of chloramines, it would not be expected to be as large because the absorbance/decomposition of H₂O₂ is not as significant as free chlorine. The increase in UVT is non-linear with distance through the reactor (Figure 4-2).
- As UVT increases due to photolysis of chloramine and chlorine, the delivered UV dose increases as well (i.e., less light is absorbed as it travels through the water from the lamp to the target). That is, the UV dose delivered by a lamp near the effluent of the UV-AOP system is greater than the UV dose delivered by a lamp near the influent of the UV-AOP system (assuming equivalent lamp output). The changing UVT should be considered in UV dose monitoring algorithms that use equations for UV dose and/or log inactivation derived from third-party validations and be used to calculate UV dose. Typically, these equations use measured UVT to calculate UV intensity from a new lamp/lamps at 100% lamp power in a term known as “S₀”. If UVT is a function of location in the reactor as it would be in potable reuse applications using chloramine for membrane fouling control, then S₀ is also a function of location in the reactor. Clearly, this complicates dose calculations. Monitoring UVT at each lamp or lamp bank is difficult and impractical. Designers may consider using a second UVT monitor at the effluent of the UV-AOP reactor, and then using an assumption of UVT change through the system either linearly or non-linearly, to calculate S₀. This calculation is then applied in the UV-AOP system control logic.

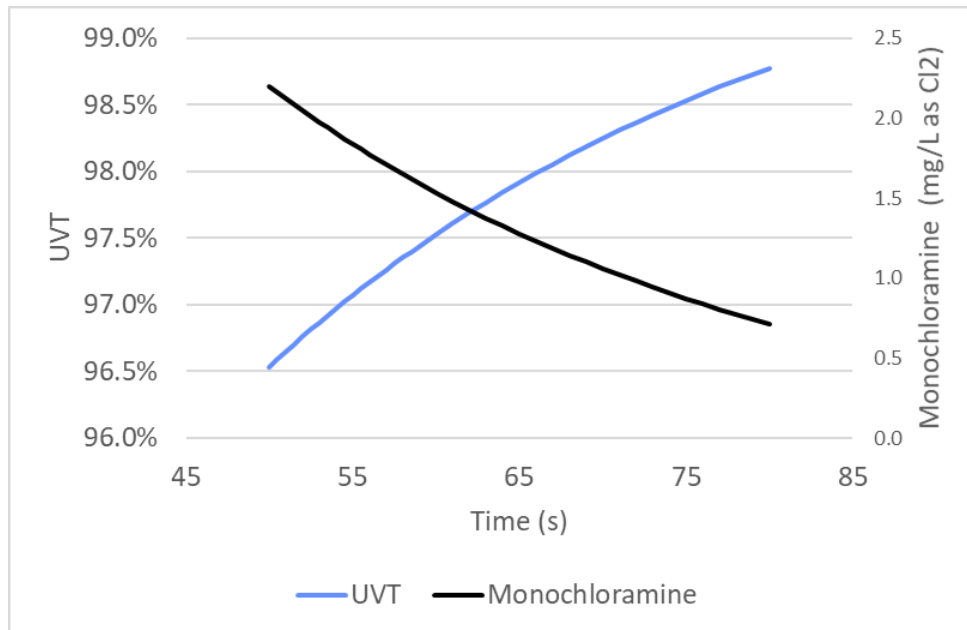


Figure 4-2. Hypothetical Change in UVT and Monochloramine through a UV-AOP Reactor.

- **Flow Rate.** The flow rate through each UV train is a critical input to UV dose and achieved log reduction approaches. The designer should apply sound engineering practices to flow meter installation, such as straight pipe upstream to ensure measurement accuracy.

The following parameters are often monitored in real time in UV-Cl₂ systems:

- **Free chlorine.** Monitoring free chlorine online is challenging because of the interaction between free chlorine and chloramines (i.e., the changing concentrations of each with time) and the potential for interference of chloramines on the free chlorine measurement.

When designing a free chlorine monitoring strategy, a designer should consider:

- Location of free chlorine sampling point relative to oxidant dosing point: As discussed above, there are two philosophies related to the dosing of sodium hypochlorite upstream of the UV-AOP reactor. The first approach would allow the chlorine-chloramine reaction to complete (i.e., reach breakpoint) and the second is to dose sodium hypochlorite relatively close upstream of the UV-AOP system to minimize the progress of chlorine chloramine reactions. If the latter approach is selected, the chlorine-chloramine reactions will still be taking place where the monitoring sample line draws water from the process pipe, and the dynamic nature of the ongoing reaction may impact the measurement derived from the online monitor. This leads to the second important consideration:
- The HRT of the sample line relative to the HRT of the process piping (between the sample point and the UV-AOP reactor): Sample line HRT, is of course, a function of the length, size/diameter, and flow rate through the sample line, just as it is in the process pipe. Best practice would suggest that the chlorine analyzer be located in a nearby panel, relatively close to the UV reactor and the process piping. The analyzer requires a sample line to transfer water from the process pipe to the monitor. Chlorine-chloramine

reactions will take place while the sample travels to the monitor, just as it would as it travels between the sample point in the process pipe to the UV-AOP reactor; therefore, it is best practice to attempt to match the HRT of the sample line with the HRT from the sample point to the reactor. This is difficult to do in practice given a fixed sample line size and varying process flow rates, but the designer should attempt to match as closely as possible to obtain an accurate free chlorine measurement. Figure 4-3 illustrates this concept. Note that measurement of UVT following the addition of the oxidant will also be affected by this sample line versus process line HRT phenomenon.

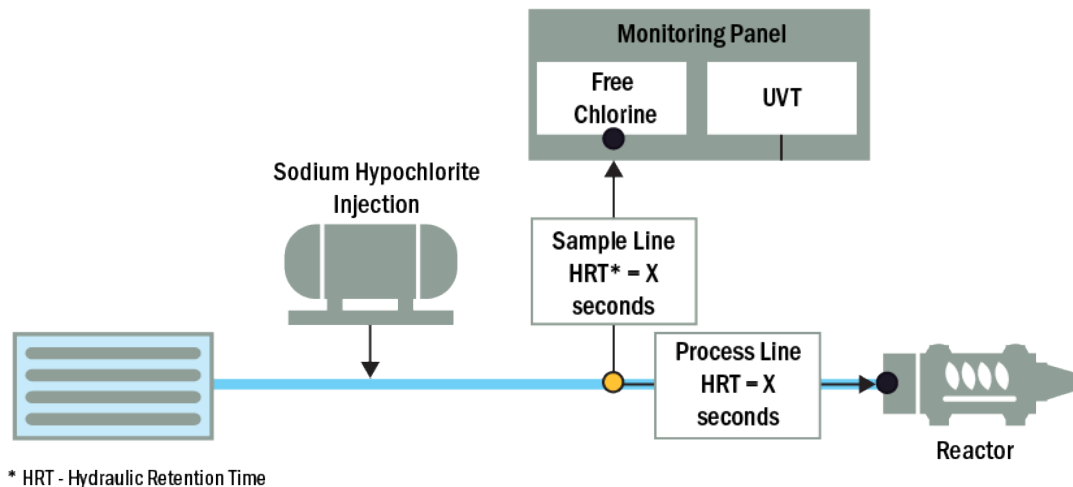


Figure 4-3. Sample Line Design.

- Handling of the free chlorine measurement in the UV-AOP PLC: As with the UVT measurement described previously, installed UV-AOP systems have taken one of two approaches: monitoring free chlorine prior to the addition of sodium hypochlorite or monitoring free chlorine immediately prior to the UV-AOP system (downstream of sodium hypochlorite addition). Again, if the former, a predictive algorithm in the UV-AOP PLC calculates the change in free chlorine associated with the oxidant addition and the change in free chlorine associated with chlorine-chloramine reactions to determine the UVT at the entrance UV-AOP system.

This may require several monitors including ammonia, monochloramine, total chlorine, and pH to understand the complete reaction progression. In the latter approach, free chlorine monitoring occurs immediately prior to the UV-AOP system but is subject to inaccuracies due to the sample line vs. process line HRT differences described above.

- Train considerations: measurement of free chlorine in a multi-train system containing chlorine and chloramine may require a free chlorine monitor at the entrance to each UV-AOP reactor.
- Deciding whether to implement a free chlorine monitor *following* the UV-AOP system: Free chlorine photolyzes as it passes through the UV-AOP system. In applications that require a residual disinfectant, the designer may target a post UV-AOP chlorine concentration to confirm free chlorine is present through the entire reactor (or to

determine the upstream trim concentration required). Further, maintaining above-zero free chlorine concentrations in the UV-AOP system prevents the formation of nitrite and its associated •OH radical scavenging potential (by oxidizing nitrite formed from monochloramine photolysis back to nitrate); downstream monitoring allows confirmation that this is occurring.

- Selection of the type of online free chlorine analyzer: Two types of analyzers can be used for free chlorine monitoring: colorimetric and amperometric. Table 4-6 summarizes the major differences between the two approaches and provides method recommendations.

Table 4-6 Chlorine Analyzer Comparison.

	Colorimetric	Amperometric
Design Considerations	<ul style="list-style-type: none"> • Online analyzer monitors free chlorine with minimal interference from chloramines. Provides periodic measurements at defined frequency (e.g., 3 minutes). • Requires reagents (routine reagent replacement and waste stream management) • Handheld colorimetric device for measuring free chlorine in the presence of chloramines is prone to interference 	<ul style="list-style-type: none"> • Requires regular calibration. Most accurate over a limited range of concentrations near the calibration point. • Chloramines can cause interference with free chlorine measurement • Reagentless • No interference issues with total chlorine monitoring
Measurement time	<ul style="list-style-type: none"> • 3 minutes 	<ul style="list-style-type: none"> • 5 minutes
Use	<ul style="list-style-type: none"> • Monitoring free and total chlorine 	<ul style="list-style-type: none"> • Suggested for total chlorine measurement only

Total Chlorine

Both free and total chlorine are often monitored in the UV-Cl₂ system, though selecting which monitors are warranted is specific to water quality. In the presence of high amounts of ammonia, free and total chlorine analyzers may be useful in monitoring the breakpoint chlorination chemistry. The UV-AOP manufacturer may request total chlorine monitoring in the monitoring strategy as an input to the control system.

Total chlorine accounts for the free and combined chlorine and can therefore be used to determine the full spectrum of chlorine speciation. If ammonia is present or dosed upstream for bromate control, total chlorine and monochloramine should both be monitored upstream to understand the available chlorine for reaction (free).

If a trim is desired in the treated, stabilized water—if ammonia is present, it should also be measured downstream of the UV reactor, as should monochloramine, to determine additional dosing requirements (trim) if there is a target monochloramine residual.

pH

The designer may consider pH monitoring both upstream and downstream of oxidant dosing. The pH should be monitored in the upstream process-treated effluent to ensure it falls within the specified ranges to meet design and warranty requirements. It can also be used to optimize

pH control in upstream processes. However, because pH might change as a function of the addition of hypochlorite, a designer may elect to also monitor pH downstream of the chlorine injection point to confirm it is still in the proper range ahead of the reactor, and to inform chemical speciation. In most cases, monitoring of pH immediately upstream of the UV-AOP system (and following sodium hypochlorite dosing) will suffice to satisfy both objectives.

Ammonia and Monochloramine

Ammonia may be monitored if liquid ammonia is dosed upstream of the system for bromate control or if a high amount is present in the influent stream. The amount of ammonia, monochloramine, and total chlorine may be useful in calculating the free chlorine residual. Further, the UV-AOP manufacturer may request ammonia/monochloramine monitoring prior to sodium hypochlorite injection to estimate free chlorine demand at the dosing point.

UV Intensity

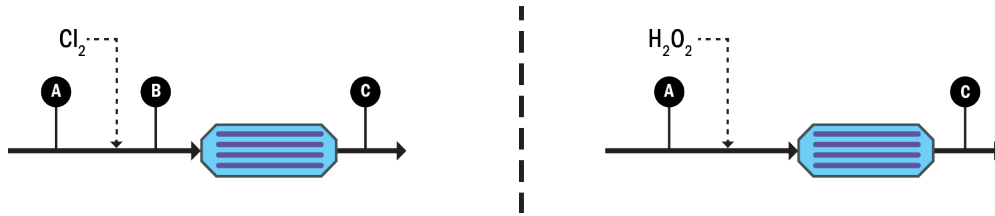
UV intensity sensors are typically located within quartz sleeves inside or on the wall of a UV chamber. These sensors detect emitted UV light. UV intensity sensors are used to confirm UV light output and provide input to UV dose calculation algorithms.

A Note Regarding H₂O₂ Analyzers

Though H₂O₂ analyzers exist in the marketplace they are not commonly used in UV-H₂O₂ applications. Field experience to date suggests that they are prone to inaccuracies at the low levels at which they are required to monitor in an AOP application. Typically, a peroxide monitor is not required for determining the H₂O₂ dose, which is commonly determined from a well-calibrated chemical pump. Feed rate and resulting H₂O₂ concentration is a simple linear relationship to pump speed.

Comparing the Monitoring Requirements for UV/Cl₂ Versus UV/H₂O₂

Figure 4-4 presents monitoring locations typically employed to provide input to the UV PLC for operation and to monitor CCPs for both UV-Cl₂ and UV- H₂O₂. Table 4-7 describes how various analyzers can be used at the different locations (before chlorine addition, after chlorine addition, after AOP treatment). Not all of the monitors identified for each location in Figure 4-4 may be required. Different manufacturers request different monitoring packages and water quality, and related monitoring requirements vary from site-to-site. However, whatever the particular system requirements, the number of monitors required for UV-Cl₂ is significantly greater than that required for UV-H₂O₂. Table 4-4 further describes the options, respective functions, and potential locations of various monitors that can be used for UV-Cl₂. The optimal design of the monitoring system depends on a cost/benefit analysis for the specific plant, the proposed CCP strategy, and regulatory requirements.



Monitoring Point	UV-Cl ₂	UV-H ₂ O ₂
A	Flow Rate, Ammonia/ Monochloramine, UVT, Total Chlorine	Flow Rate, UVT ^a
B	pH, Free Chlorine	--
C	UVT, Free Chlorine, Total Chlorine	UVT

a. If nitrite scavenging is a concern the manufacturer may request additional monitoring

Figure 4-4. Monitoring Locations and Monitor Options for UV-Cl₂ (left) and UV-H₂O₂ (right).

Table 4-7. Summary of UV-AOP System Monitoring Requirements and Options.

Monitor	Location Relative to Reactor	Required/ Optional	Function	Considerations for Positioning
UVT	Upstream	Required	<ul style="list-style-type: none"> Monitors UVT for UV dose pacing and confirmation of operation in the validated and/or design range Confirms that UVT is in the permitted range 	<ul style="list-style-type: none"> Locate upstream or downstream of oxidant injection based on manufacturer recommendation.
UVT	Downstream	Optional	<ul style="list-style-type: none"> Use together with the influent UVT monitor, to calculate the UVT at various locations in the reactor 	<ul style="list-style-type: none"> Locate downstream of the UV reactor prior to post-treatment water conditioning If downstream of RO, consider analyzer path length required for accurate measurement of very high UVT
pH	Upstream of UV reactor,	Required	<ul style="list-style-type: none"> Confirms effluent of upstream process is in correct pH range 	<ul style="list-style-type: none"> Sample downstream of chlorine addition to confirm pH influent to the UV vessel Locate upstream or downstream of oxidant dosing point depending on regulatory requirements and manufacturer control strategy
Free chlorine	Upstream	Required	<ul style="list-style-type: none"> Monitors free chlorine in the reactor feed to confirm adequate dosing 	<ul style="list-style-type: none"> Locate sample port far enough downstream of oxidant injection to allow good mixing

Monitor	Location Relative to Reactor	Required/Optional	Function	Considerations for Positioning
Free chlorine	Downstream	Recommended	<ul style="list-style-type: none"> Confirm presence of free chlorine through the reactor 	<ul style="list-style-type: none"> Locate sample port near the reactor outlet
Total chlorine	Upstream	Optional	<ul style="list-style-type: none"> Quantify concentration of all chlorine species in the feed water (free and combined chlorine) 	<ul style="list-style-type: none"> Co-locate with free chlorine sampler
Total chlorine	Downstream	Optional	<ul style="list-style-type: none"> Measures free and combined chlorine 	<ul style="list-style-type: none"> Co-locate with free chlorine sampler
Mono-chloramine	Upstream	Optional	<ul style="list-style-type: none"> Helps confirm chlorine chemistry operating range (where the system is with respect to the breakpoint curve) to inform operational setpoints 	<ul style="list-style-type: none"> Note that ammonia and monochloramine are monitored by the same instrument
Mono-chloramine	Downstream	Optional	<ul style="list-style-type: none"> Confirms chlorine speciation when a treated effluent residual is desired; used with total chlorine monitor 	<ul style="list-style-type: none"> Locate in single analyzer panel with total chlorine analyzer and position near the reactor outlet
Ammonia	Upstream	Optional	<ul style="list-style-type: none"> Used in the prediction of the required dosing of sodium hypochlorite to overcome ammonia demand Also used to predict formation of chloramines 	<ul style="list-style-type: none"> Upstream of oxidant injection Note that ammonia and monochloramine are monitored by the same instrument

Other monitoring considerations include:

- Calibration checks.** These are typically required on all online analyzers, which are another consideration for UV-Cl₂ systems. Interviews with utility personnel at facilities where UV-Cl₂ is used indicated that maintenance on the additional monitors for UV-Cl₂ did not significantly impact overall maintenance efforts at the facility; however, it is important to note that significantly more monitoring is required, and that the monitoring approach is much more dynamic and complex than a UV-H₂O₂ system.

CHAPTER 5

Economic Analysis of UV-Cl₂ vs. UV-H₂O₂

Under certain water quality conditions, UV-Cl₂ appears to offer an efficiency and cost advantage over UV-H₂O₂ for the treatment chemical contaminants, particularly in systems employing RO pretreatment. Based on research performed as part of this project, the use of UV-Cl₂ has the potential to lead to lower equipment, energy, and oxidant requirements, and in turn, lower operational costs for UV-Cl₂ relative to UV-H₂O₂ assuming the water quality conditions are suitable.

To determine the most cost-effective approach in a particular application and location, the designer should perform a life-cycle cost comparison of the two alternatives. Up-to-date, local cost information is very important for this analysis, as regional oxidant costs (associated with longer delivery distances or regional demand pressures) may significantly impact the life cycle cost comparison. Other factors that impact the cost comparison include whether quenching of residual H₂O₂ is required. This chapter will explore the cost differences between using chlorine (in the form of added bulk sodium hypochlorite) versus H₂O₂ as the oxidant to perform UV-AOP.

5.1 Capital Cost Comparison in an RO-Based Application

The purchase price of a particular UV-AOP system varies project to project, is bid dependent, and is a function of the specification requirements regarding guarantees, on-site time, scope, and redundancy. For this reason, this Guidance Manual discusses only the general trends associated with purchase price of UV-AOP systems.

In general, LPHO systems have a higher purchase price than MP systems. This is because LPHO systems, using relatively lower wattage lamps, require more lamps to accomplish the specified treatment. Efficiency differences notwithstanding, the initial capital purchase price of MP systems is generally lower than LPHO systems.

In the sizing analysis returned by manufacturers as part of this project, manufacturers did not provide sizing with significantly lower numbers of lamps in their designs for UV-Cl₂ vs. UV-H₂O₂; however, the operating power anticipated was consistently less for UV-Cl₂ vs. UV-H₂O₂. The results of this comparison suggest that UV-AOP manufacturers may anticipate slightly smaller equipment requirements, and therefore the subsequent O&M cost reductions related to equipment (e.g., lamp replacement costs, discussed below), with UV-Cl₂ vs. UV-H₂O₂. Given the relatively early nature of predictive sizing tools for UV-Cl₂ applications and the small number of operating and proven systems, the efficiency advantages for UV-Cl₂ in low-pH, RO-based, installations may not yet translate into smaller (i.e., lower kilowatt capacity and lower lamp count) systems for UV-Cl₂ relative to UV-H₂O₂ in a particular application. This may change as manufacturers refine their predictive tools.

As noted in Chapter 4.11, UV-Cl₂ systems generally require a larger number of online analyzers to monitor a larger number of operational parameters critical to performance than UV-H₂O₂ systems. The additional capital cost of these additional monitors for UV-Cl₂ systems relative to

UV-H₂O₂ systems is on the order of several tens-of-thousands of dollars, up to potentially one hundred thousand dollars. Therefore, the additional costs of these monitors would proportionally impact the overall capital cost of small systems more heavily than large systems.

5.2 Operation and Maintenance Cost Comparison in an RO-Based Application

As has been described previously, a common application of UV-AOP is as a final treatment barrier in RO-pretreated applications in potable reuse. The use of RO results in a high UVT, low •OH scavenging demand, and low pH product water that flows to UV-AOP.

In a small-scale pilot study conducted at the Orange County Water District's Groundwater Replenishment System (reported in Kwon et al. 2020), the authors observed, at an equivalent concentration of oxidant, that the E_{EO} for removal of 1,4-dioxane with UV-Cl₂ was approximately 40% lower than that for UV-H₂O₂. If this lower E_{EO} is reflected in the full-scale application, it would result in a corresponding 40% reduction in required power to accomplish identical treatment of 1,4-dioxane. Several factors were cited as leading to this result:

- A higher primary radical generation rate for hypochlorite (HOCl, predominant at the observed pH) versus H₂O₂
- A decrease in the •OH scavenging demand in the UV-Cl₂ process relative to UV-H₂O₂ due to chlorine oxidation of 30 to 120 µg/L of nitrite to nitrate
- The in-situ formation of nitrite in the UV-H₂O₂ process resulting from the photodecomposition of monochloramines (leading to relatively lower efficiency)

A study at full scale has observed similar phenomenon (Dowdell et al. 2016).

At this point in the technology's evolution, however, and as mentioned above, these observed/potential efficiency advantages have not yet translated into significantly smaller UV-AOP equipment designs by manufacturers.

To facilitate a comparison, several manufacturers of UV-AOP equipment provided sizing and O&M information for different scenarios for an RO/UV-AOP potable reuse scenario. Selected solutions included various models of UV equipment based on both LPHO and MP lamps. This information was incorporated into a cost estimation model and used to predict annual O&M. Three facility flow rates for hypothetical facilities treating RO permeate were sized: 2 million gallons per day (mgd), 12 mgd, and 100 mgd. Each targeted NDMA and 1,4-dioxane reduction as a primary objective. Table 5-1 summarizes the design criteria and assumptions used in the exercise.

Table 5-1. Conditions for Full Advanced Treatment Scenario with UV-Cl₂ and UV-H₂O₂.

Parameter	Value	Units
Design Flow Rate	2, 12, 100	mgd
Average Flow Rate (for O&M)	1.5, 10, 80	mgd
Design UVT	96% cm ⁻¹	--
Average condition UVT	98% cm ⁻¹	--
Cost of Electricity	\$0.12	Per kWh
Cost of H ₂ O ₂ (50%)	\$4.50	Per gallon
Cost of Sodium Hypochlorite (12.5%)	\$1.50	Per gallon
Ammonia at UV-AOP Inlet	0.1	mg/L as N
Nitrite at UV-AOP Inlet	0.1	mg/L as N
Log Reduction Target 1	0.5	1,4-dioxane
Log Reduction Target 2	1.2	NDMA
Fouling Factor	0.95	--
Lamp Types	LPHO or MP	--
End of Lamp Life	Per manufacturer	hours
Method of Quenching Residual Hydrogen Peroxide	Sodium hypochlorite (liquid)	--

The results of annual cost calculations are presented on Figure 5-1 for the 12-mgd system using LPHO lamps. The core annual cost of operation, not including quenching of residual H₂O₂, is shown to be approximately 15% lower for UV-Cl₂ than UV-H₂O₂ using the cost assumptions in Table 5-1. If the facility requires quenching of H₂O₂, and if one assumes that sodium hypochlorite is used for this quenching, the economics heavily favor UV-Cl₂. In that scenario, the annual O&M cost of UV-Cl₂ is 46% lower than that for UV-H₂O₂. The costs of quenching are discussed in further detail below. Note that the reference to “hypo dose” in the figure refers to the concentration of sodium hypochlorite added at the dosing point being sufficient to overcome chlorine demand, which leads to a resultant stated free chlorine concentration in the UV-AOP system. Note also that the O&M cost associated with “sensors” refers to the periodic replacement of UV intensity sensors within the UV-AOP system (versus any external monitors for parameters such as pH or free chlorine). Finally, the cost analysis for UV-Cl₂ assumes that the residual free chlorine concentration exiting the UV-AOP system does not require quenching before discharge to the environment (e.g., groundwater injection).

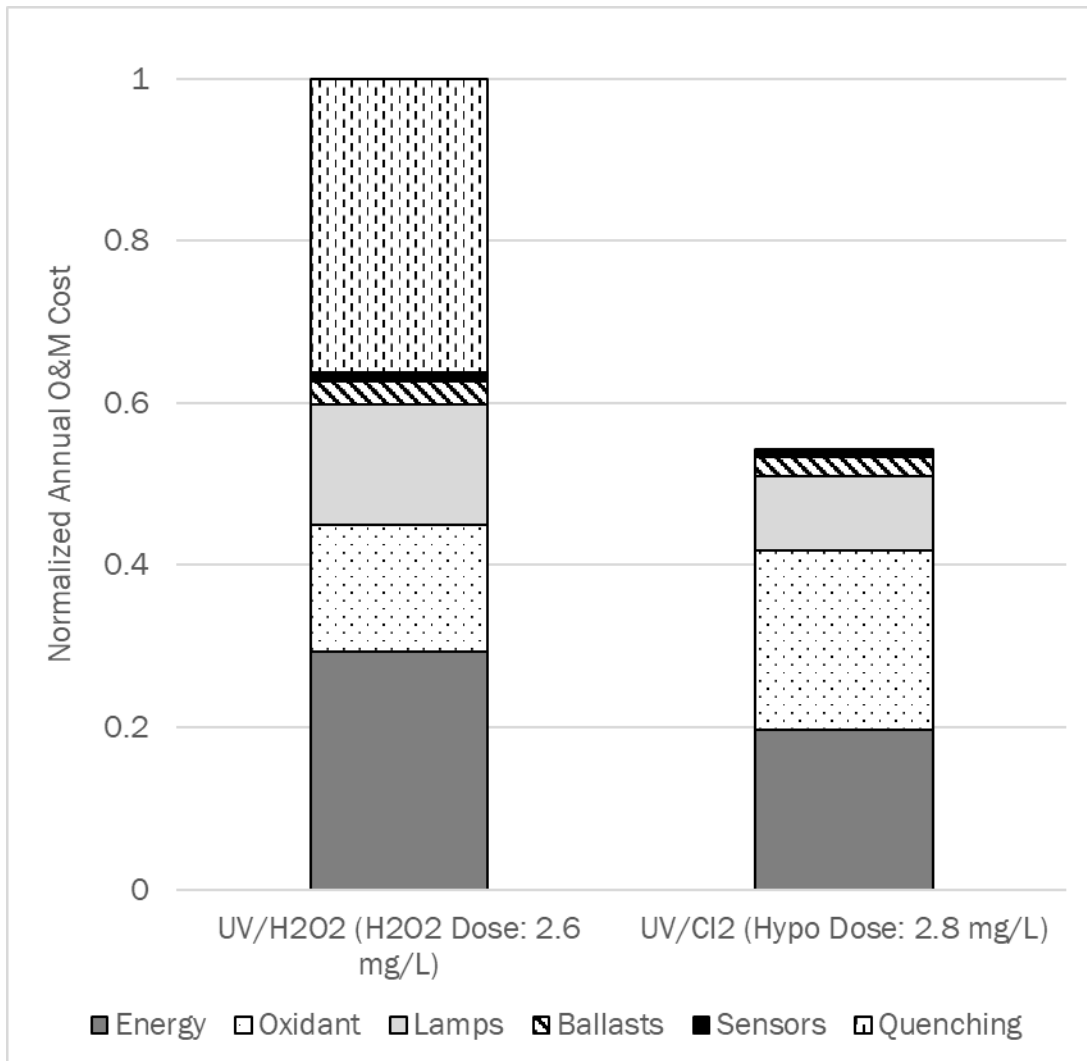


Figure 5-1. Comparison of Annual O&M Costs for UV-Cl₂ and UV-H₂O₂ for a 12-mgd FAT Installation with Low Ammonia and Nitrite; LPHO lamp-based UV-AOP systems.

The analysis indicates that while the overall cost of operation is lower for UV-Cl₂ relative to UV-H₂O₂, the cost of oxidant (dotted section of the bars) in UV-Cl₂ applications is *higher* than UV-H₂O₂ under the conditions noted despite the chlorine demand being relatively low. That is, in this example, upstream secondary treatment processes would control nitrite and ammonia to relatively low levels. This results in a correspondingly low chlorine demand. If either of these parameters were to increase, the chlorine demand would increase, and the amount of sodium hypochlorite required to accomplish the target free chlorine concentration entering the UV-AOP system would also increase and exacerbate the difference in oxidant cost. Chapter 5.3 further explores this topic.

Plant size does not affect the overall cost comparison conclusions (refer to Figure 5-2 for a normalized O&M cost analysis at three hypothetical plant flow rates). In all cases, UV-Cl₂ offers lower annual O&M costs, especially when considering a requirement to quench H₂O₂. This

analysis assumes that the resulting free chlorine concentration exiting the UV-Cl₂ system is low enough that quenching of residual chlorine is not required.

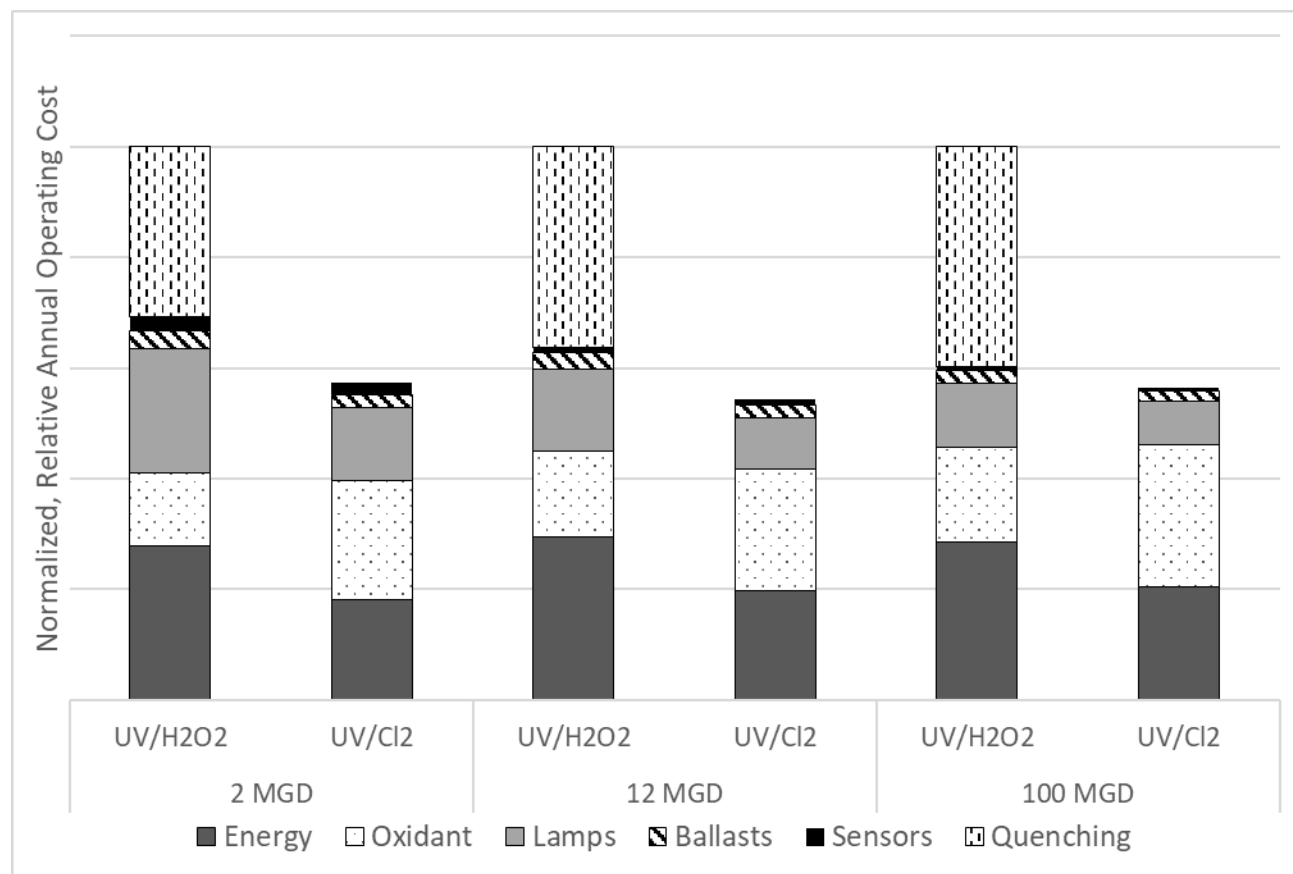


Figure 5-2. Relative Cost Comparison of Annual O&M costs for UV-Cl₂ and UV-H₂O₂ with Low Ammonia and Nitrite; LPHO lamp-based UV-AOP systems at 2, 12 and 100 mgd.

Users of UV-Cl₂ AOP systems should also anticipate a moderately higher labor requirement for operating and maintaining the various monitors required (see Chapter 4.11 for a detailed discussion of monitoring requirements and options).

5.3 Comparison of the Cost of Chlorine vs. Hydrogen Peroxide (Oxidant)

As mentioned above, in the example case, the cost of sodium hypochlorite as the oxidant exceeds that of H₂O₂. The left two bars of Figure 5-3 illustrate this point. Detailed further below, the delivered cost of sodium hypochlorite has increased recently (in 2022) and given the usage requirements for this case results in a higher oxidant cost. This analysis assumed a price of \$1.50/gallon for sodium hypochlorite (Table 5-1). Providers of H₂O₂ report that the base price of H₂O₂ has not significantly increased, delivery costs notwithstanding.

The impact of increasing dosed chlorine concentration added to overcome chlorine demand was explored. Shown also on Figure 5-3 is the oxidant cost as a function of chlorine demand at the point of sodium hypochlorite dosing. At the low chlorine demand conditions used in the

above analysis, the average dosed sodium hypochlorite concentration proposed by the manufacturers was 2.8 mg/L as Cl₂. If this increased to 4 mg/L as Cl₂, to overcome ammonia and/or nitrite demand, for instance, the cost of sodium hypochlorite rises to levels significantly higher than that of H₂O₂.

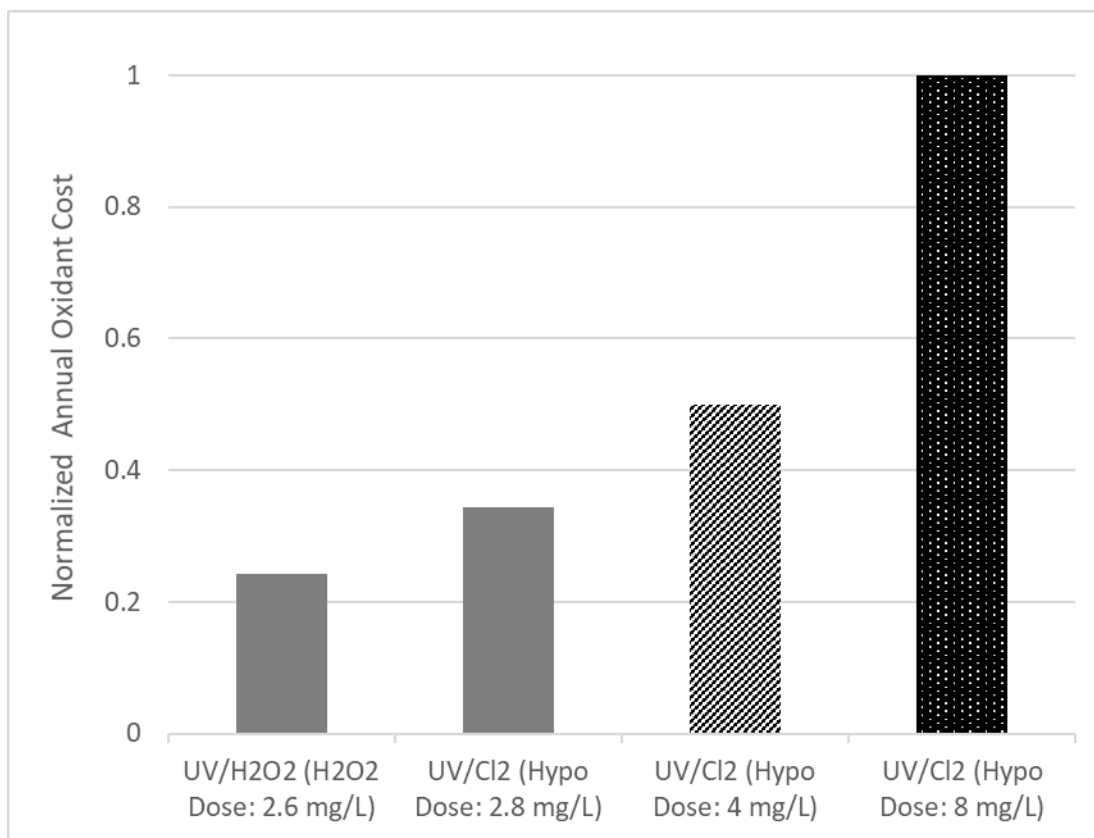


Figure 5-3. Comparison of Annual Oxidant Costs for UV-Cl₂ and UV-H₂O₂ for a 12-mgd FAT Installation; LPHO Lamp-Based UV-AOP Systems.

Figure 5-4 illustrates the overall economic impact of this change. Note that the cost of UV-Cl₂ with chlorine at 8 mg/L as Cl₂ very nearly rises to that of UV-H₂O₂, including the cost of quenching (with bulk hypochlorite). Changes in chlorine *demand*, therefore, have a significant impact on the overall economics of the analysis and can change the overall conclusion regarding which oxidant is most economical for a particular installation. This analysis highlights the importance, in UV-Cl₂ applications, of controlling ammonia and nitrite in UV-AOP influent to maintain low chlorine demand.

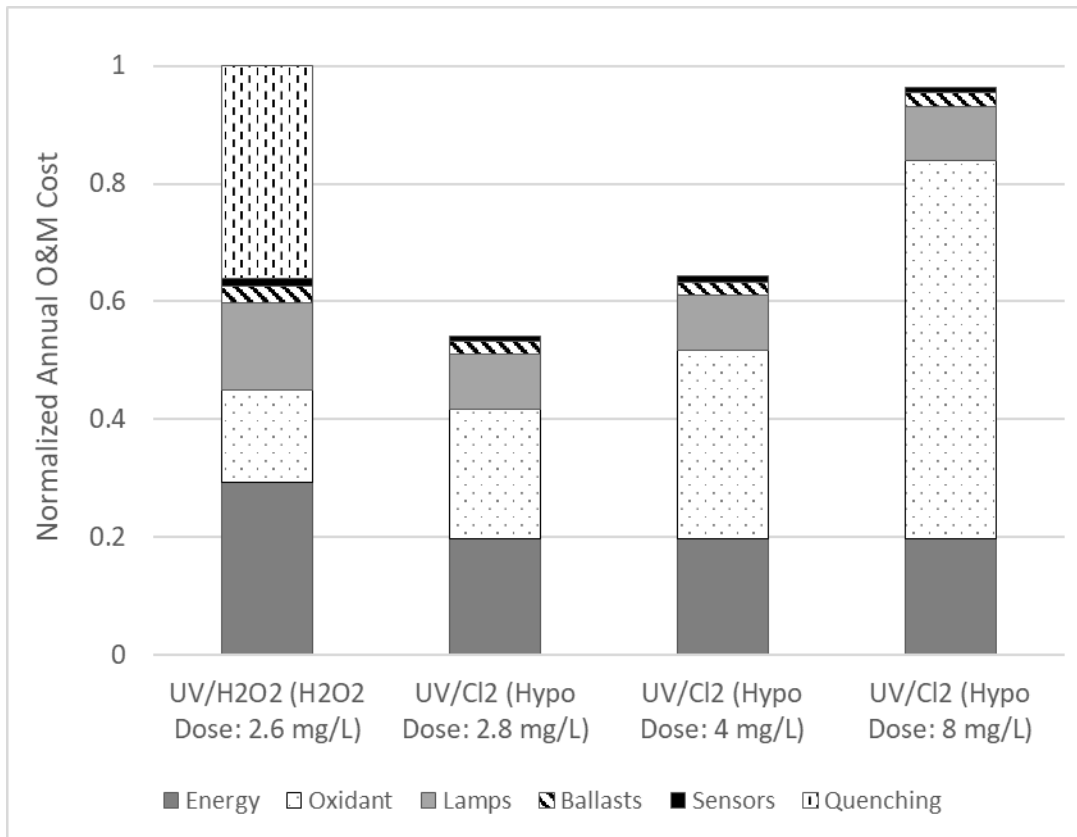


Figure 5-4. Detail of Annual O&M Costs for UV-Cl₂ and UV-H₂O₂ for a 12-mgd FAT Installation; LPHO Lamp-Based UV-AOP Systems in Scenarios of Increased Free Chlorine Demand at the Dosing Point.

5.4 Increases in the Costs of Oxidants Related to Market Forces

The price and availability of plant chemicals has come under significant pressure over the past 20 years, and even more so in the timeframe of 2020-2022. This has led to price increases and, in some locations, shortages. Historically, prior to the recession of 2007-2009, chemical prices increased notably. Henderson et al. (2009) reported a steady increase in prices for general water treatment chemicals and a 19% average increase in the price of sodium hypochlorite from January 2008 to January 2009 alone per one industry survey. This indicates that the drivers for price increases and shortage, including manufacturing capacity limitations, increased demand from outside the U.S., and increased consumption by non-water treatment industries were in place prior to the COVID-19 pandemic. During the pandemic, additional pressures have combined to drive price increases. Figure 5-5 shows a producer price index (PPI) for water treatment compounds. During the 20-month period between September 2020 and April 2022, the water treatment compound PPI increased by more than 43%.

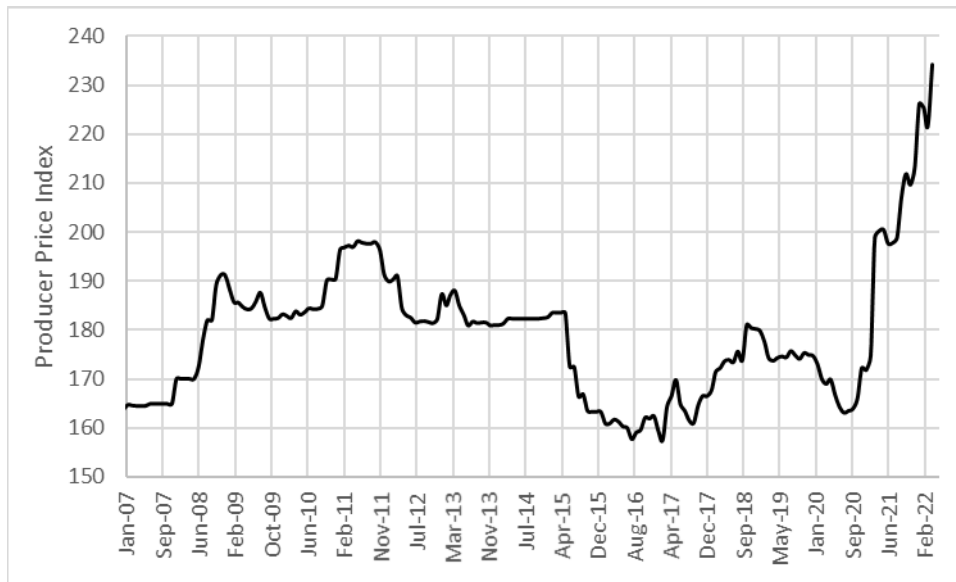


Figure 5-5. PPI for Water Treatment Compounds January 2007 through April 2022
(FRED 2022) Category: WPU06790961.

The PPI is not specific to either peroxide or chlorine; however, market forces arguably have applied greater pressure on chlorine. For example, a fire destroyed a chlorine plant in Louisiana in the summer of 2020 in the aftermath of Hurricane Laura. Factories in Louisiana produce much of the chlorine used in the United States. By rendering this facility inactive, supply was reduced. Further pressure was applied by the fact that chlorine must be transported from the location of manufacture to the user, which, in the case of water treatment, are widely dispersed. Rising fuel prices and staff shortages that impact the trucking industry, therefore, have a direct effect on delivery. The inherent risk of transporting chlorine has also impacted pricing as fewer haulers are willing to accept the risk. Subsequently, the price of chlorine in the form of sodium hypochlorite (and gaseous chlorine) has arguably increased beyond that of some other treatment chemicals, including H₂O₂. This increase is also driving increased interest in onsite hypochlorite generation, which could also be considered for this type of application.

At the time of publication, the range of prices paid for 12.5% bulk sodium hypochlorite, based on conversations with a variety of end users, was \$1.30/gallon (gal) to \$2.10/gal. This range is reported for context, but with the strong caveat that local prices may be higher (or lower) due to a range of factors, including high transportation costs to a particular location or economies of scale related to the size of purchase. Whatever the location, any consideration of UV-Cl₂ AOP should begin with a site-specific price-of-oxidant analysis. Only then can an end user properly and accurately compare the cost of different AOPs.

To illustrate the impact of the cost of 12.5% sodium hypochlorite, consider the comparison plot on Figure 5-6, expanded to show the impact of rising sodium hypochlorite costs. The cost of quenching residual H₂O₂ has been removed for clarity. The base case above considered an average price of \$1.50/gal. If this price is lower (\$1.00/gal), then the advantage of UV-Cl₂ relative to H₂O₂ is amplified. If the price is higher (\$2.00/gal), the annual O&M cost of UV-Cl₂ approaches that of UV-H₂O₂ (quenching not considered). Overall, the price of oxidant has a

relatively smaller impact on the overall comparison than an impact of an increase in required concentration of sodium hypochlorite (Figures 5-3 and 5-4 above). However, high site-specific costs of sodium hypochlorite could reduce or eliminate an O&M cost advantage of UV-Cl₂ relative to UV-H₂O₂.

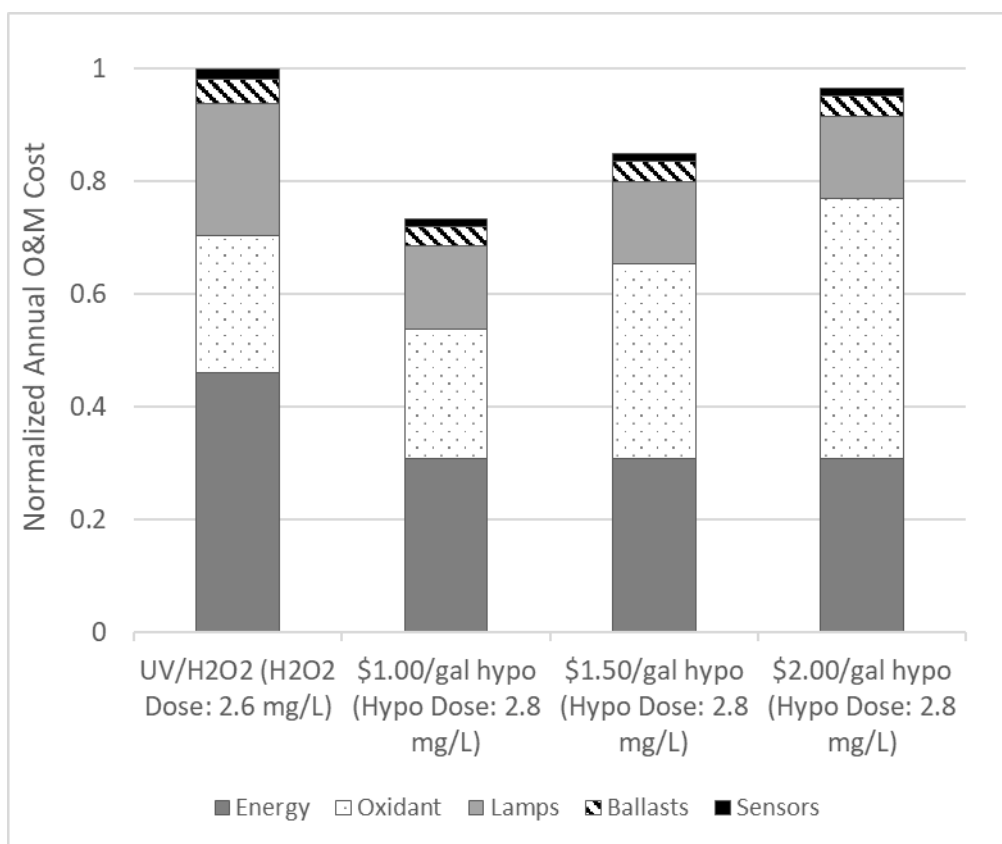


Figure 5-6. Sensitivity Analysis of the Impact of the Price of Chlorine on O&M Costs.

Despite the possible O&M cost advantages presented by UV-Cl₂ in RO-based treatment applications, there are cases (even treating RO permeate) in which UV-H₂O₂ could be a lower O&M cost solution:

- Relatively high ammonia (e.g., >1 mg/L as N)
- Where quenching of residual is not required
- Where pH is relatively higher (e.g., >7.0 as with ozone/biofiltration)

Examining Figure 5-4, the higher sodium hypochlorite dosing scenarios (i.e., 4 mg/L as Cl₂ and 8 mg/L as Cl₂ sodium hypochlorite) would be associated with higher chlorine demand due to ammonia or the location of dosing (Chapter 4.10). In this case, UV-H₂O₂ becomes more cost competitive. It also should be noted that under scenarios of elevated ammonia, operators may find it challenging to achieve the required free chlorine concentration in the UV-AOP system. In these cases, UV-H₂O₂ would likely be preferred.

In cases where quenching of residual H₂O₂ may not be required, as illustrated on Figures 5-4 and 5-6, UV-H₂O₂ may offer a cost-competitive alternative, especially when the additional monitoring burden associated with UV-Cl₂ is considered.

When pH is higher, as described in Chapter 3.2, the relative efficiency of UV-Cl₂ decreases. In these cases, UV-H₂O₂ may be more cost competitive.

5.5 Economic Impacts of Lamp Type Selection

The cost impact of using different lamp types was explored. Figure 5-7 shows results of annual cost calculations for a 12-mgd system using LPHO lamps versus a 12-mgd system using MP lamps and the UV-Cl₂ AOP. This analysis was performed for the conditions listed in Table 5-1, including target reductions of 0.5 and 1.2 for 1,4-dioxane and NDMA, respectively, at conditions of low nitrite and low ammonia and a sodium hypo cost of \$1.50/gal. Results returned from the manufacturers suggest that the UV O&M cost of a LPHO system is lower than that of an MP system. This analysis represents a single, non-guaranteed scenario but is reinforced by industry trends that have seen projects select LPHO systems for UV-Cl₂ applications. Sizing predictions for each project, with project-specific conditions (for example, MP may offer advantages where there are footprint constraints), should be collected and where possible, backed by manufacturer performance guarantees. **Research is needed at pilot and demonstration scale to better demonstrate what treatment benefits MP may offer over LPHO systems and under what conditions (see Chapter A5 Research Needs in Appendix A for details).**

Other conditions that *may* offer advantages when using MP lamps are discussed in the next section.

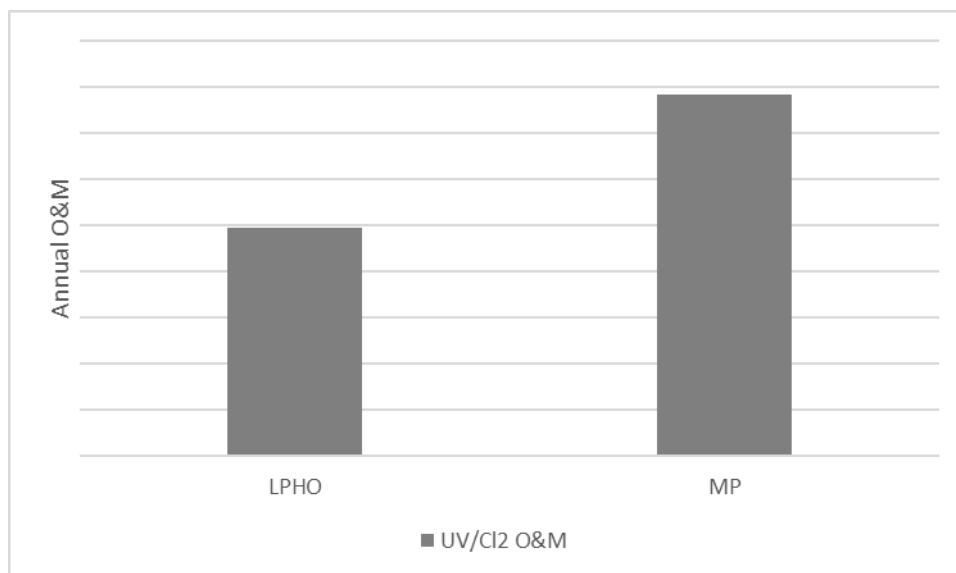


Figure 5-7. Annual O&M Cost of LPHO versus MP Lamp-Based Systems in a 12-mgd FAT Application with Low Ammonia and Nitrite.

5.6 Cost Impact of Alternate Target Contaminants

The sizing analysis of Chapter 5 to this point has considered *both* NDMA and 1,4-dioxane as target contaminants. This has become a common set of design target contaminants in potable reuse in California. NDMA is treated by UV-photolysis, and 1,4-dioxane is treated by UV-oxidation. In this way, the UV-AOP system is delivering two treatment processes simultaneously and acts as a barrier to contaminants that are both photolyzed (e.g., nitrosamines) and oxidized (e.g., 1,4-dioxane, pharmaceuticals and personal care products, solvents, other industrial contaminants); however, this dual action treatment is not always needed.

As NDMA is degraded primarily by UV-photolysis, the presence of NDMA as a target drives the UV dose requirement in the Chapter 5.1 example. If NDMA were *not* a treatment requirement in a particular system, advantages of MP-based systems relative to LPHO-based systems may be more significant. That is, if 1,4-dioxane or another oxidizable contaminant is the *only* target, MP UV systems that make use of wavelengths emitted throughout the UV spectrum, particularly at higher wavelengths (>254 nm) that are preferentially absorbed by the hypochlorite ion (versus hypochlorous acid), may offer efficiency advantages. This effect is potentially amplified at higher pH, where the hypochlorite ion becomes the predominant chlorine species. LPHO, emitting light only at 254 nm, will not realize this advantage. As discussed above, this phenomenon is predicted by theory but has limited supporting evidence from field trials or full-scale installations.

In ozone-carbon-based advanced treatment trains, where pH is expected to be in the neutral range, there is potential that UV-Cl₂ using MP lamps may present a more cost-effective option. Further, outside of potable reuse, e.g., in water treatment for taste and odor contaminants, UV-Cl₂ using MP lamps may provide additional advantages relative to UV-Cl₂ systems using LPHO lamps. In a drinking water application, for example, in which UV light is used as a disinfection method year-round, an MP system equipped with standby lamps that are activated only for the treatment of taste and odor contaminants (e.g., 2-methylisoborneol [MIB] and geosmin) for part of the year may be a cost-effective option to supplement activated carbon for taste and odor treatment. In this scenario, chlorine added as an oxidant, combined with sufficient UV energy, treats MIB and geosmin by oxidation. The addition of chlorine does not present the same challenges as the addition of hydrogen peroxide (e.g., the requirement to quench, the presence of an additional chemical on site, etc.). Certainly, the presence of nitrate (and the potential to convert to nitrite) must be considered in all applications. However, noting that a residual chlorine concentration can oxidize nitrite to nitrate and thereby eliminate nitrite as a by-product of concern, this is not expected to present a significant issue in drinking water applications.

At the time of this Guidance Manual's publication, installed systems in RO-based reuse applications were using LPHO lamps. The potential cost advantages of MP systems in RO or ozone/carbon-based reuse systems, with various contaminant treatment targets, has been included in the list of research needs in this document.

5.7 Costs of Quenching Residual Oxidant

The cost of quenching residual H_2O_2 can add significantly to the annual O&M costs in UV- H_2O_2 applications. In the above examples, the analysis assumed that residual H_2O_2 is quenched with chlorine at a stoichiometric ratio of 2.1:1. In drinking water applications, quenching with granular activated carbon GAC is a typical approach. GAC, using either a standard carbon or a catalytic carbon, catalyzes the decomposition of residual H_2O_2 . Sodium bisulfite is also effective, but only at pH <6 due to slow reaction at higher pH.

In some cases, gaseous chlorine vs. liquid chlorine may be used. Gaseous chlorine is generally lower cost but presents site health and safety implications associated with its potential release. As regulations evolve at a federal and state level, gaseous chlorine may be subject to increased risk management planning (RMP), given its potential hazards. The effect of more involved RMP will lead to a greater cost of complying with regulation. Gaseous chlorine may be lower in cost but has the trade-off of higher risk and increased RMP costs. These factors will likely have the effect of driving users to bulk hypochlorite or on-site generation of chlorine. As has been discussed, analyses in this chapter assume bulk, delivered, 12.5% sodium hypochlorite, but a site-specific analysis is imperative to the success of any project.

Dechlorination can also be needed, such as before discharge to a surface water body such as a stream or reservoir. The need for and cost of this additional step in a UV- Cl_2 application should be determined.

Matching quenching chemical to a concentration of H_2O_2 or chlorine presents a control challenge, especially when the dosed concentrations of the oxidant themselves change. If the designer anticipates significant changes to oxidant concentrations or flow rate, a static quenching step such as GAC may offer a more operationally friendly solution.

Note that chemical quenching requires contact time. The designer should consider a requirement for additional contact time in the system. While piping between dosing and the compliance point may offer sufficient time, the designer should consider the required time and build in additional contact time if necessary.

5.8 Cost Impact of Nitrite

The presence of nitrite can have a significant impact on operating cost of the UV-AOP system as a function of the selected oxidant. In this economic section, we will discuss the monetary impact of elevated nitrite in influent water. Nitrite can be elevated in an RO-based treatment train in a treatment process that does not accomplish full nitrification/denitrification, as an example.

As was discussed previously, nitrite significantly impacts UV- H_2O_2 sizing but not UV- Cl_2 sizing. The reason is that chlorine oxidizes nitrite to nitrate quickly (assuming proper mixing). Peroxide does not oxidize nitrite as quickly as chlorine. Therefore, in UV- H_2O_2 situations, nitrite remains and presents a high $\bullet OH$ radical scavenging demand. This requires that additional oxidant and energy be applied to accomplish treatment.

Take the example first presented in Chapter 5.1, but with varying concentrations of nitrite (Figure 5-8). Increasing nitrite *significantly* affects the O&M cost of the UV-H₂O₂ system, even without quenching, but does not significantly affect the O&M cost (i.e., treatment requirements) of the UV-Cl₂ system.

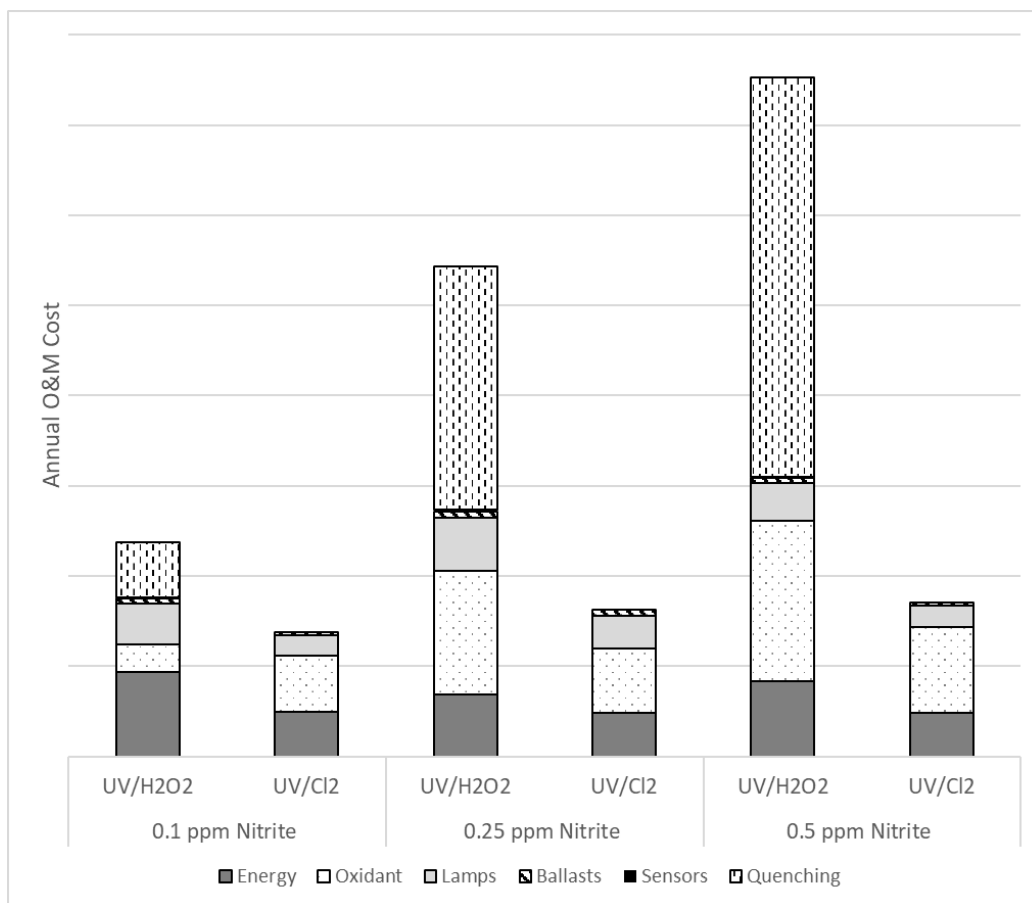


Figure 5-8. Impact of Increasing Nitrite on Annual O&M Cost.

This scenario considers a situation where nitrite is high but ammonia remains relatively low (at 0.1 mg/L as N). In practice, this scenario is unusual, as high nitrite will typically be associated with high ammonia due to incomplete nitrification/denitrification. Therefore, while switching to UV-Cl₂ would be an ideal solution if ammonia is low, the high-nitrite RO-based application is likely to be associated with high ammonia as well. As has been discussed, high ammonia can make it cost ineffective to accomplish the free chlorine concentration required in the UV-AOP system to accomplish oxidation, and also results in considerable monochloramine formation, which reduces UVT. In this case, to use UV-Cl₂, the designer should consider changes to the overall treatment process to control *both* nitrite and ammonia.

5.9 Non-Monetary Considerations

When considering the use of UV-AOP, a designer must consider either the impact of adding another oxidant to the plant's suite of oxidants (in the case of H₂O₂) or, if chlorine is used, the

increase in usage and addition of dosing points/storage locations and the increase in operational complexity introduced by the addition of more monitoring requirements.

CHAPTER 6

Selecting the Right UV-AOP: A User's Decision Tree

Numerous factors impact the decision of which oxidant is most suitable for UV-AOP in a particular treatment application and what upstream and downstream treatment requirements may be needed.

As discussed above, under certain conditions of water quality at the influent to the UV-AOP, an end user may realize savings in operation, maintenance, and potentially initial capital costs by using UV-Cl₂ instead of UV-H₂O₂. The water quality trade-offs, however, are complex to navigate. **A decision tree (Figure 6-1) is provided below to guide the reader through the process of evaluating UV-Cl₂ vs. UV-H₂O₂.** This procedure, along with the economic considerations detailed in Chapter 5, can be used to evaluate the viability and cost of each UV-AOP alternative for a given treatment scenario. The following subsections guide the reader through each decision point (triangle) and describe the decisions, considerations, and potential solutions that apply at each point. It is recommended that both paths be explored in parallel to develop both UV-Cl₂ and UV-H₂O₂ scenarios for comparison. Background information on the impact of water quality and UV-Cl₂ chemistry on treatment requirements and efficacy are provided in Chapters 3 and 4.

As a general note on the decision tree: the presence of monochloramine in UV AOP influent, resulting from the common practice of its addition for controlling membrane fouling, affects *both* UV-Cl₂ and UV-H₂O₂, although in different ways. For both technologies, as has been discussed, monochloramine impacts the UVT and scavenging. High concentrations of ammonia in UV-Cl₂ applications lead to high concentrations of chloramines (Chapter 6.2) and potentially precludes the use of UV-Cl₂. However, the presence of chloramines in the UV-AOP influent will limit the formation of bromate with UV-Cl₂ where bromide is present. The impact of monochloramine on UV-H₂O₂ is related to the formation of nitrite. In the absence of free chlorine (present in UV-Cl₂ applications, by design, but not in UV- H₂O₂), UV photolysis of monochloramine forms nitrite. The designer (working with the UV manufacturer[s]) should therefore account for the formation of nitrite and associated impact on •OH scavenging in the design of a UV-H₂O₂ system. In summary, the reader should note that monochloramine impacts the design of the UV AOP system, but the presence of monochloramine is not specifically included as a decision point in the decision tree.

This decision methodology uses general rules of thumb for evaluating viability and practicality of UV-Cl₂ and UV-H₂O₂. As every case is unique, users are encouraged to use their best judgment and a site-specific economic analysis to verify that the recommended cutoffs are appropriate for their application.

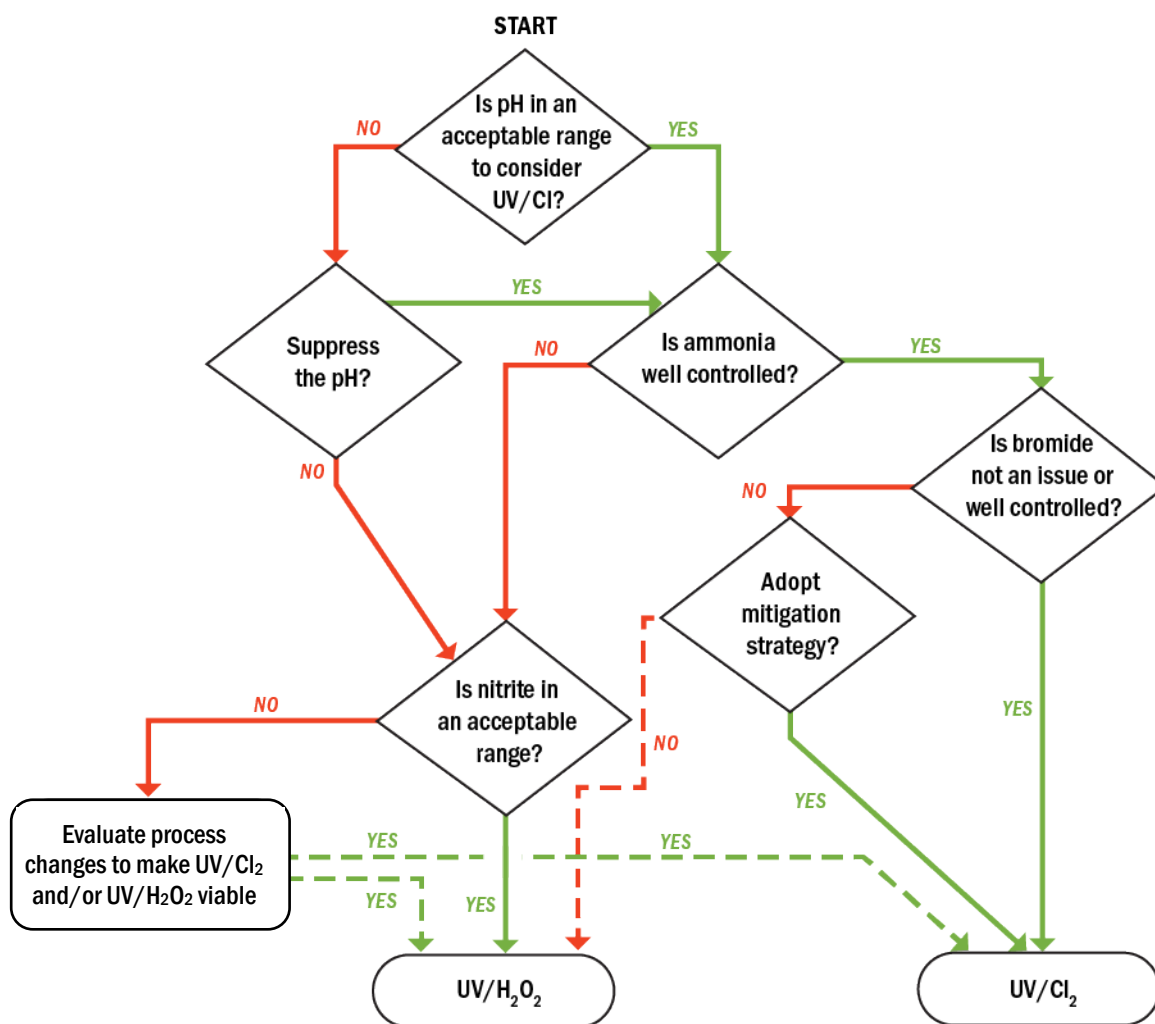


Figure 6-1. UV-Cl₂ vs. UV-H₂O₂ Evaluation Process Decision Tree.

6.1 Is pH in an Acceptable Range to Consider UV-Cl₂?

pH has a strong influence on radical generation with UV-Cl₂. Lower pH drives the speciation of chlorine toward hypochlorous acid (and away from the hypochlorite ion). Hypochlorous acid has a higher absorption coefficient at 254 nm and, in turn, generates •OH more effectively. Hypochlorous acid is also a less effective scavenger of •OH than the hypochlorite ion. Finally, pH impacts the rate of reaction between ammonia and free chlorine in the formation of chloramines (lower pH leads to a slower reaction and therefore a smaller impact on UVT and scavenging).

A general rule of thumb is that at a pH of less than 6, UV-Cl₂ may be more efficient than UV-H₂O₂ (although higher pH may be feasible under site-specific conditions, especially with MP lamps). In all cases, the designer should work with UV manufacturers to evaluate required UV dose and system sizing for the source water quality, including evaluation of background scavenging. The impact and importance of pH is discussed in Chapters 3.2 and 4.6.

The next step(s) in the decision process are:

- **If conditions are favorable for UV-Cl₂, proceed to Chapter 6.2.**
- **If conditions are *not* favorable, consider pH suppression (below).**

Evaluate pH suppression

The pH rule of thumb discussed herein is <6, but the optimal pH for UV-Cl₂ is approximately 5 to 5.5. pH in this range drives a shift in chlorine speciation and makes production of radicals more efficient. It also has the benefit of shifting carbonate speciation to bicarbonate (away from carbonate), thereby reducing scavenging. However, depending on the starting point and background water quality, this could require significant chemical addition to lower the pH and then subsequent to AOP treatment, raise it again. This would add cost and complexity to the process.

- **If the plan is to reduce pH to the favorable range for UV-Cl₂, proceed to Chapter 6.2.**
- **If pH suppression is not practical, proceed to Chapter 6.2 with the understanding that the process will not be optimized, or rule out UV-Cl₂ and proceed to Chapter 6.6.**

6.2 Is Ammonia Well Controlled?

Ammonia combined with added sodium hypochlorite yields chloramines. If ammonia is kept very low, the plant minimizes chlorine demand, the formation of chloramines, and resultant increase in scavenging and decrease in UVT. To maintain a free chlorine residual through the UV-AOP system, sodium hypochlorite must be added in sufficient quantity to overcome the ammonia demand. As a reference, to overcome 1 mg/L as N ammonia, more than 7.6 mg/L as Cl₂ of sodium hypochlorite is required. Clearly the cost implications of this amount of sodium hypochlorite are significant (Figure 5-3). **A rule of thumb for the optimal ammonia concentration for UV/Cl₂ is <~0.2 - 3 mg/L as N.**

Recall the discussion of the location of the dosing point of sodium hypochlorite in Chapter 4.3. In short, Option 1 described a scenario in which sufficient HRT is provided downstream of the dosing point to allow chlorine/chloramine reactions to reach breakpoint and Option 2 described the dosing point as sufficiently close to the reactor to minimize loss of free chlorine due to chlorine/chloramine reactions. If ammonia is >0.2 mg/L as N but other considerations drive the end user toward UV-Cl₂, consider Option 2 as the best option to minimize chloramines formation to the extent possible, and select “yes” for this decision step.

Careful consideration of reaction kinetics (a function of pH) and available contact time relative to the reactor inlet is needed to determine if a practical dosing scenario can be created at full scale when significant ammonia is present. This may not be possible if ammonia exists significantly above 0.2 mg/L as N. For example, there is a big difference between managing 1 mg/L as N excess ammonia versus 30 mg/L as N. This is explored in detail in Chapter 4.5. Careful placement of analyzers is also needed to match the HRT of the UV reactor so the variations in water chemistry can be accurately measured, and the system properly controlled (Chapter 4.11).

If ammonia is elevated, the designer may want to consider upstream process changes to reduce ammonia. Where upstream modifications are not feasible or too costly, UV-H₂O₂ may be the most practical and cost-effective option.

The next step(s) in the decision process are:

- **If ammonia will be kept low through upstream treatment or its demand can be overcome or managed, proceed to Chapter 6.3.**
- **If ammonia is high enough to make UV-Cl₂ impractical, proceed to Chapter 6.6.**

6.3 Is Bromide Not an Issue or Well Controlled?

Free bromine is formed in the UV-Cl₂ process, which can subsequently react to form bromate, potentially above the regulatory limit. Based on limited case study data, the yield of bromate from bromide in the absence of mitigation strategies in UV-Cl₂ is 10 to 30%. Therefore, an influent concentration of bromide above the recommended level of 25 µg/L could approach an exceedance of the maximum contaminant level of 10 µg/L. See Chapter 3.4 of this Guidance Manual and Chapter A2.11 of the UV-Cl₂ Literature Review in Appendix A for more discussion on this topic.

Based on the limited data available, it is recommended that the potential for bromate formation be evaluated at bench or pilot scale where bromide in the UV-AOP feed water is >~25 µg/L. If no bench- or pilot-scale testing data are available, the potential for adding low-dose ammonia or the ability to convert to UV-H₂O₂ in the future should be considered in system design. If bench or pilot testing is done, the considerations outlined in Chapter 7.1 should be evaluated.

The next step(s) in the decision process are:

- **If the bromide concentration is <25 µg/L, proceed to Chapter 6.4.**
- **If the bromide concentration is >25 µg/L, consider ammonia addition to mitigate bromate formation (below).**

To mitigate bromate formation, consider ammonia addition for bromate control. Ammonia blocks the free bromine pathways by reacting with free bromine to form bromamines (Hofmann and Andrews, 2001), thereby short-circuiting bromate formation. The designer should recall, however, that monochloramine is a radical scavenger (Pearce et al. 2022).

A low dose of ammonia (~0.2 mg/L as N), together with the added sodium hypochlorite to form chloramines, has been successfully used to mitigate bromate formation at LA Sanitation District's Terminal Island potable reuse UV-Cl₂ process. The free chlorine dose target at the site, is 2.2 mg/L as Cl₂ (shown in the case study presented in Chapter 8). Pearce et al. (2022) have also demonstrated a substantial decrease in bromate formation in ozone AOP systems with preformed monochloramine. In their study, adding 3 mg/L as Cl₂ monochloramine to a reuse feed water with approximately 400 – 440 µg/L bromide maintained bromate concentrations below the MCL.

While this approach has been demonstrated to be effective, it will affect the UVT and exert a free chlorine demand; therefore, the impact should be considered in UV system sizing where used.

The next step(s) in the decision process are:

- **If you the plan is to control bromate formation, proceed to Chapter 6.5.**
- **If bromate formation cannot be well controlled and rules out UV-Cl₂, proceed to Chapter 6.6.**

6.4 Is Nitrite in an Acceptable Range?

If this point is reached on the decision tree some significant challenges have been identified to using UV-Cl₂, and UV-H₂O₂ may be a better option. The next step is to start evaluating potential barriers and treatment requirements for UV-H₂O₂.

The first critical water quality question is whether there is significant nitrite in the UV-AOP feed water. As discussed in Chapters 3.1 and 5.8, nitrite is an extremely strong radical scavenger and will greatly affect treatment requirements and sizing of a UV-H₂O₂ system. But nitrite is quickly oxidized to nitrate by free chlorine, and so can be managed as part of the free chlorine dosing upstream of a UV-Cl₂ process. **If significant nitrite is present (>0.1 µg/L), the designer should work with the UV manufacturer(s) to identify what level of nitrite is acceptable for a performance guarantee and determine if nitrite removal is required for UV-H₂O₂ to be viable.**

If UV-Cl₂ is not a good option for other reasons (e.g., high ammonia) and UV-H₂O₂ is still a necessary or desired option, but there is too much nitrite to get a performance guarantee or the guaranteed system size would be cost-prohibitive, then an evaluation of upstream process changes to remove the nitrite is needed. The list of process changes or additions in Table 6-1 are well-proven solutions for nitrite reduction.

Table 6.1. Potential Treatment Process Modifications to Address Elevated Ammonia and Nitrite in the Feed Water in Potable Reuse.

Process Change or Addition to Address Nitrite Issues	Considerations
Upgrade the existing treatment process to completely nitrify the source water to the potable water purification system	<ul style="list-style-type: none"> • Significant additional capital and operating expense • Potential partial cost offset if a membrane bioreactor is used (relative to other solutions) because a process is replaced (MF or UF) rather than added
Add ozone upstream of MF/RO.	<ul style="list-style-type: none"> • Significant additional capital and operating expense • May provide other water quality benefits
Add a nitrifying biologically active filter	<ul style="list-style-type: none"> • Significant additional capital and operating expense
Select RO membranes that have high rejection of nitrite	<ul style="list-style-type: none"> • May affect projected removal of other inorganic constituents relative to other membrane choices • May not eliminate the issue depending on the concentration of nitrite that needs to be removed and the ability to get a performance guarantee

Adding or modifying a treatment process usually involves a significant capital expenditure and additional operating costs.

The next step(s) in the decision process are:

- **If nitrite is manageable or not an issue and all other UV-Cl₂ water quality parameters are controllable or not an issue, proceed to Chapter 6.5.**
- **If nitrite is manageable or not an issue and all other UV-Cl₂ water quality parameters cannot be well controlled, proceed to Chapter 6.6.**
- **If neither UV-AOP option seems viable, review options for meeting treatment goals.**

6.5 UV-Cl₂ is Viable

If this point on the decision tree is reached, a viable path forward for using UV-Cl₂ has been determined.

The following next steps are recommended:

- Incorporate consideration of issues identified through this exercise as part of an economic and non-economic analysis. An economic comparison between UV-Cl₂ and UV-H₂O₂ is particularly important if additional treatment requirements (e.g., upstream process changes, dechlorination) have been identified.
- Review Chapter 7 to identify any additional needed process evaluation steps and startup planning.
- Review Chapter 4 to inform design development and monitoring approach.

6.6 UV-H₂O₂ May be a Better Option

If this point on the decision tree is reached, it has been determined that UV-H₂O₂ is a viable option and may be better than UV-Cl₂.

To fully develop the UV-H₂O₂ process requirements, the need for quenching should also be evaluated and included in the economic analysis comparing UV-Cl₂ to UV-H₂O₂ if included. The need for post-treatment H₂O₂ quenching will depend, in part, on the use of treated water as well as local regulatory requirements. Note that in some locations, regulators have required quenching prior to groundwater injection while in other locations they have not. For drinking water applications, where addition of high-dose oxidation or reducing agents isn't feasible, GAC in a parallel configuration with a short empty bed contact time (<10 minutes) is the traditional approach. In potable reuse, chemical quenching may be preferred over GAC due to footprint, cost, or preferences. Reducing agents like sodium bisulfite or sodium thiosulfate can also be used to quench peroxide, but note that the reaction speed and therefore effectiveness can be heavily affected by pH.

6.7 Decision Tree Summary

Using the UV-Cl₂ AOP presents clear advantages relative to UV-H₂O₂ when:

- The pH is ≤6
- Ammonia concentrations are low (<~0.2 - 0.3 mg/L as N)

- Nitrite is relatively high (above ~0.1 mg/L as N)
- Regulations require quenching of residual H₂O₂

The presence of bromide may require a mitigation strategy, but the presence of high bromide does not necessarily, in itself, preclude the use of UV-Cl₂. Quenching of residual H₂O₂ adds significant cost to the UV-H₂O₂ process (Chapter 5), but similarly, a quenching requirement will not, in itself, preclude the use of UV-H₂O₂. In all cases, the designer should conduct a thorough analysis to determine the best choice of oxidant.

Examples of Common UV-AOP Scenarios

Several common potable reuse scenarios have been developed to illustrate the use of the decision process and common outcomes.

Example #1: The governing regulatory body for a municipality planning a potable reuse installation requires that an oxidation step be implemented post-RO for an additional barrier to chemical contaminants and for additional disinfection. The pH is expected to be 5.5 or lower, ammonia and nitrite will be well controlled via full nitrification/denitrification, and bromide is near the detection limit.

Solution #1: This is the most favorable condition for UV-Cl₂. Given that the pH, bromide, and ammonia concentrations are expected to be low, UV-Cl₂ is the preferred solution.

Example #2: An inland reuse facility planning potable reuse has no economical options for brine disposal. For this reason, RO options are not practical, and the plant considers a pre-post-secondary treatment train of ozone/biofiltration/UV-AOP/GAC to be the best solution. The pH of the ozone/biofiltration system effluent is expected to be approximately 7.5.

Solution #2: Because the pH is expected to be relatively high, the plant should consider UV-H₂O₂ to accomplish disinfection and potentially oxidation. The agency will need to evaluate the •OH scavenging potential of the water to determine whether oxidation via UV-H₂O₂ is economical. If not, oxidation could be accomplished with the ozone step. The UV system may be configured as a high-level disinfection system only for accomplishing 4- to 6-log virus/Cryptosporidium/Giardia inactivation, with contaminant removal accomplished in a different way.

Example #3: RO permeate is expected to contain ammonia at 2 mg/L as N and have a pH of <6.0.

Solution #3: In this case, the low pH initially suggests that UV-Cl₂ is the best option; however, significant additional sodium hypochlorite (>14 mg/L as Cl₂) will be required to overcome the chlorine demand presented by the ammonia. The resulting combination of free chlorine with ammonia will form additional chloramines that will enter the UV-AOP system. The cost of the required sodium hypochlorite, combined with the larger UV-AOP system resulting from the increased scavenging and lower UVT, may drive the selection to UV-H₂O₂. UV-H₂O₂ is not significantly impacted by the presence of ammonia.

Example #4: RO permeate is expected to contain nitrite at 1.0 mg/L as N and have a pH of <6.0.

Solution #4: The addition of sodium hypochlorite oxidizes nitrite to nitrate. While nitrite at this level does present a chlorine demand (~5 mg/L as Cl₂), the overall cost equation favors the use of UV-Cl₂. Evaluate the presence of ammonia in this scenario, as often the conditions that lead to high nitrite also lead to high ammonia, which may adversely affect the potential to use UV-Cl₂.

CHAPTER 7

Testing and Startup

This chapter provides considerations and recommendations related to pre-design testing and startup performance testing.

7.1 Considerations for Bench- and Pilot-Testing in the Pre-design Phase

There are many reasons for conducting bench- or pilot-scale testing in the pre-design or design phase. They include use of the pilot facility to convince potential consumers, through demonstration, that a proposed treatment train produces water of sufficient quality to meet aesthetic or regulatory standards, or confirms the ability of selected treatment processes to work together to produce water of sufficient quality. UV-AOP as a treatment step in the bench or pilot system, obviously would play a role in meeting either of these objectives.

However, the performance of a UV-AOP system (i.e., the efficiency of treatment) using chlorine or H₂O₂ differs at pilot scale versus full scale (Wang et. al., 2019). To summarize, first, UV-AOP performance is a function of the path length of UV light inside the UV system. Small-scale pilot systems often do not simulate the path length of a full-scale UV-AOP system. Second, mixing improves with increased flow rate. Small-scale pilot systems typically do not approximate the flow rate of a full-scale system. Inherently, therefore, bench and pilot systems are less efficient than full scale. Finally, UVT changes through a full-scale reactor are challenging to simulate at a bench or pilot scale. For these reasons, generation of performance data at bench or pilot scale for the specific purpose of scale-up should not be considered as a primary objective of the bench or pilot study.

One approach that has been used to generate full-scale sizing information through piloting is to employ a two-step process to determine UV and oxidant dosing. First, bench-scale collimated beam (CB) testing is used to determine the UV dose required to accomplish treatment of contaminants treated primarily by UV-photolysis (e.g., NDMA). This step is performed without oxidant. Once this baseline UV dose is determined, an accompanying oxidant dose required to accomplish treatment of oxidizable contaminants (e.g., 1,4-dioxane) is determined using the previously determined UV dose, using the pilot system. This combination results in threshold levels of operation (e.g., UV dose above some threshold and oxidant concentration above a threshold), which may be codified in the operating permit of the system. The challenge with this approach is that, given the reasons described above, these dose and oxidant thresholds may result in over-treatment and higher-than-required use of energy and oxidant at full scale. Adjustments of the threshold levels determined through piloting and now fixed in the operating permit presents a challenge. Figure 8-2 describes an adjustment made to the Terminal Island Facility's free chlorine setpoint, initially set by piloting and later reduced following demonstration of better-than-anticipated performance at full scale. Therefore, while this presents a possible pathway to using pilot data, effort should be made to build in flexibility in

operating levels, following a demonstration at full-scale start-up to adjust threshold levels if necessary.

Collimated beam testing presents unique challenges for UV-Cl₂ applications. CB tests rely on being able to control the UV dose under homogeneous batch test conditions, but if the water quality is complex (e.g., significant ammonia is present leading to dynamic formation of chloramines) then the chemistry within the water sample would be changing during the experiment (and also in a full-scale flow-through reactor, but likely not in identical ways). The CB, therefore, will not accurately reflect full-scale conditions or treatment results. Given that the CB is used to determine the dose response of a surrogate or contaminant, these issues may propagate through an analysis and result in erroneous conclusions. Similar challenges exist with pilot testing, where chemical travel time, mixing, and changes in UVT through the UV system resulting from chloramines degradation, for example, are difficult, even impossible, to match. Therefore, care should be taken when considering bench- and pilot-tests and when evaluating results for use in scale-up. More research and exploration of lessons learned sizing full-scale systems would aid in use and interpretation of such tests.

7.2 Performance Testing the Installed UV-Cl₂ AOP System

Once the UV-AOP system has been installed, standard procedure dictates that the entity contractually responsible for system performance (e.g., the design build team, the contractor, or the manufacturer) verify treatment. That is, the system's actual performance is measured against specification requirements in a carefully controlled, on-site test.

The performance test should primarily confirm that the system meets the criteria stated in the specification regarding contaminant removal. That is, if the specification required that the UV-AOP system reduce 1,4-dioxane concentrations by 0.5-log (i.e., 68.4%), then the responsible entity should collect a dataset that demonstrates that this target is met by spiking with 1,4-dioxane or some other indicator chemical if necessary and operating the system as designed and collecting influent/effluent pairs. Further discussion of this topic can be found in Chapter 1.2.2 and 7.2.5.

The project design, as well as preliminary communications with the regulator, will have outlined a control strategy (see Chapters 4.10 and 4.11). This strategy includes a definition of how the system operates to meet ongoing performance metrics. For example, if the system is equipped with a PLC that calculates log-reduction of contaminants in real time using site parameters, then performance testing should verify this control strategy. Similarly, if the system will operate using a minimum required UV dose, then the responsible entity should demonstrate that the system can meet this dose threshold.

Preparations for the site performance test begin in the design phase. Conducting an on-site test at an operating water treatment plant presents challenges under the best conditions. Careful early planning will help ensure success. For example, injection points for spiking solutions are one of the most important considerations. Upfront design of tap size and location will avoid costly on-site rework after initial installation but before performance testing.

Table 7-1 presents a checklist of tasks/considerations important for performance test preparation and a brief description of each.

Table 7-1. Checklist for a Successful Performance Test.

Topic	Description	Installation/Design Considerations/Additional Detail
Site preparation	Valved sample ports are needed to inject spiking solutions and UVT modifier and for collecting influent and effluent samples	<ul style="list-style-type: none"> • Install a minimum of two injection ports for injection of spike solutions upstream of mixers. • Include a mixing device (e.g., static mixer) between the injection port and the UV-AOP system. • Install an influent sampling port downstream of the mixers but upstream of the UV-AOP system; ideally far enough upstream that no light penetrates to the sample port (confirming treatment has not started) • Install one sample port downstream for effluent sampling. This port should be located far enough downstream that no UV light travels to the sampling port (so no additional treatment of contaminants is occurring downstream in the pipe).
Conduct steady-state mixing test	Establishes the time required to achieve steady state mixing	<ul style="list-style-type: none"> • Inject SuperHume™, ligno-sulfonic acid (LSA), H₂O₂, or other indicator chemical upstream and monitor downstream every 30 seconds to establish time to steady-state following a change in test conditions.
Choose performance indicator compounds	Identifies compounds to be used as performance indicators	<ul style="list-style-type: none"> • Where possible, it is recommended that the actual compounds targeted be used in the performance testing. That is, if 1,4-dioxane is the target contaminant, then use 1,4-dioxane in performance testing.
Assign cost responsibility for analytical testing	Determines who will pay for laboratory/ analytical costs	<ul style="list-style-type: none"> • A clear decision regarding who pays for the analytical work and who conducts the testing is important, especially when the test matrix is large. The analytical work may fall in the UV-AOP manufacturer's scope or may be paid for by the site owner or the builder/contractor. The testing typically involves both the manufacturer and the builder/contractor.
Identify analytical laboratory partner	Select a state-certified analytical laboratory to analyze the samples	<ul style="list-style-type: none"> • The lab is a partner in the performance test. Identification is a key first step. The regulator should approve of the laboratory selected.
Plan sample handling	The matrix of tests will generate numerous samples – plan for how these will be handled.	<ul style="list-style-type: none"> • With the help of the selected analytical lab, determine when samples will be sent and by what method (e.g., drop off, courier). • Decide on the sample methodology (e.g., headspace or not, size/type of bottles, etc.). • Prepare chain of custody (COC) documentation ahead of the test. • The laboratory should provide guidance on these decisions and may provide sampling kits (coolers, bottles, COCs).

Topic	Description	Installation/Design Considerations/Additional Detail
Calibrate and prepare monitoring instruments	Confirm that online instruments are functioning and properly calibrated (e.g., UVT, ammonia/monochloramine, free chlorine, etc.)	<ul style="list-style-type: none"> To the extent possible, the performance testing team should use the instruments that will be used in the full-scale operation. For example, use the online free chlorine monitor plumbed into the system to monitor, or at least verify, free chlorine values. Getting the monitors operational and properly calibrated can present a planning challenge, so these efforts should start well before test day.
Obtain spike solution injection pumps	Procure, rent, or otherwise identify the pumps for injecting spiking compounds, UVT modifier, etc.	<ul style="list-style-type: none"> For simplicity, a lab-scale peristaltic pump works well. Match the injection rate with the amount of spike solution required.
Order spike solutions	Order spike solutions and reagents well ahead of the testing for sufficient delivery time. Consider cross-border issues with potentially hazardous substances (and recognize that aircraft travel, carrying spiking compounds, etc., may not be an option).	<ul style="list-style-type: none"> Examples of spiking solutions include performance indicator compounds and UVT modifiers. Field test methods for peroxide or chlorine may require reagents.
Confirm the bulk concentration of oxidant prior to testing	Get chemical delivery close to testing time.	<ul style="list-style-type: none"> Sodium hypochlorite degrades relatively rapidly over time. Timely delivery ahead of the performance test, therefore, is critical. Measuring the concentration of sodium hypochlorite in the bulk solution, using titration or a test kit, prior to testing allows proper chemical dosing during the test.
Determine methods to measure key field parameters	Identify which parameters will be monitored on site and determine which field instruments are required.	<ul style="list-style-type: none"> Field equipment for measuring UVT, free chlorine, and H₂O₂ (if applicable) should be identified prior to the tests. A portable field UVT monitor is a helpful instrument for verifying UVT quickly. Field methods for free chlorine that avoid interference issues (from chloramines) include the indophenol method. The DPD method may also be used but may experience interference issues.
Identify key background <i>influent</i> non-target constituents	Plan for sampling and analysis of key influent parameters.	<ul style="list-style-type: none"> Examples of background constituents could include nitrite, bromide, and ammonia. Some will affect performance; others could lead to byproduct formation.
Identify key <i>effluent</i> non-target constituents	Advanced oxidation processes can, in some cases, produce by-products; plan for testing the effluent for these constituents.	<ul style="list-style-type: none"> Make these decisions in conjunction with the regulator of note. Examples of potential by-products are carboxylic acids or low-molecular-weight aldehydes (formaldehyde is one for which to look).
Modify the UVT entering the UV-AOP system	The test matrix should explore performance over a variety of UVTs (including the design value) aside from ambient conditions.	<ul style="list-style-type: none"> For more information, see Chapter 7.2.1. In UV-AOP applications, options for UVT adjustment include SuperHume™, LSA, or chloramines.

Topic	Description	Installation/Design Considerations/Additional Detail
Prepare the UV-AOP system	Confirm that the UV-AOP system is ready to operate on test day.	<ul style="list-style-type: none"> Explore aspects such as control algorithm, check cleanliness of sleeves (e.g., do they need to be cleaned following a fouling event during installation?), and complete general commissioning.
Determine which train(s) will be tested	Decide on whether parallel trains will all be tested or just one of the trains.	<ul style="list-style-type: none"> If multiple trains are identical, then an assumption that all will perform the same is reasonable. However, differences in hydraulics, distribution of oxidant, and inherent (likely small) differences in UV-AOP reactors themselves make the case for testing using all trains (i.e., splitting testing across different reactors).
Determine where the treated water will be sent following performance testing	Treated water from the performance test must be discharged. A regulator may allow the facility to discharge to waste or recirculate to the head of the wastewater treatment plant.	<ul style="list-style-type: none"> Consult the regulator of record to discuss options related to discharging treated water from the performance test. Options are disposal to the head of the WWTP, containerization and subsequent additional batch treatment of product water, or discharge to another location (e.g., a surface water nearby). Note that a permit may be required.
Confirm that the pre-treatment processes are operating normally	Verify that the overall plant is operating as intended.	<ul style="list-style-type: none"> Example processes to check are RO membranes, MF/ultrafiltration, and conventional upstream treatment.
Collect a sample of UV-AOP influent water to confirm quality	Collect a water sample and analyze for key constituents immediately prior to the performance test.	<ul style="list-style-type: none"> This will let you confirm that the water quality is as expected and that matrix values are appropriate. Build any outside laboratory analyses into the schedule.
Decide whether performance at end-of-lamp-life (EOLL) conditions will be simulated	Capping new-lamp output at the anticipated end of lamp life output simulates performance with aged lamps.	<ul style="list-style-type: none"> UV lamps degrade over time. The UV-AOP system is designed by manufacturers to perform over the lifetime of the lamps. To confirm performance at end-of-life, operators via the UV-AOP system controls can artificially limit power level of the lamps output. For example, if a lamp has an end of lamp life of 0.9 (90%), limit lamp output to 90%.
Identify which operating parameters will be recorded during the performance test	Operating parameters such as flow rate, status of the UV-AOP system (lamps operational, power level, HMI-reported performance of UV-dose delivered or log reduction achieved, etc.), and the measurements made by monitoring instruments should be recorded.	<ul style="list-style-type: none"> Some of these parameters may be available through the SCADA system and retrieved following the test, but others may need to be recorded manually. Manual checks of on-line measured parameters should be recorded in field logs. Collection of these data will enable calculation of parameters such as EED and E_{E0} following the testing.

7.2.1 Creating the Performance Test Matrix

Project objectives and the overseeing regulator's requirements will dictate the matrix of tests performed during the performance test. At a minimum, it is important to evaluate the guaranteed operational conditions of UVT, flow, and target performance. The testing team will likely need to suppress UVT in this case. Testing ambient conditions is also useful to verify the anticipated energy and oxidant usage that can be expected during normal operation.

One approach to testing a wide variety of operating conditions over a wide range of potential conditions is to test a comprehensive matrix that includes three scenarios each of flow, UVT, and oxidant concentrations. The EPA's UVDGM takes this approach for UV system disinfection validation. This approach would require a minimum of 3 x 3 x 3 (27 total) tests. While this approach is useful for verifying performance over a wide undetermined range, it is not the approach generally taken for UV-AOP performance tests. Aside from the challenges and costs associated with performing on-site performance verifications, installations have limited range to test a broad range of anticipated operational conditions. Target testing to the anticipated operating conditions is generally sufficient (and less costly).

Options of variables to adjust, over a limited range, include UVT, flow, and oxidant. The performance test should also evaluate the planned operational modes. For example, if the facility plans to operate based on a threshold UV dose/oxidant dose, the matrix should explore performance with this operational control, at anticipated conditions, and should verify accuracy of any predictions.

Table 7-2 is an example of a performance test matrix for a UV-AOP system planning to operate with a dose/oxidant threshold strategy using the example site described in Chapter 6.1. The first tests (1 and 2) are control tests to verify zero contaminant degradation when oxidant or energy, respectively, are zero. The second set of tests (3 through 5) explores performance as a function of flow rate at ambient UVT (expected to be ~98%). Tests 6 through 8 repeat the flow rate tests at a suppressed UVT of 96%. These tests will require that the testing team add a UVT modifier to the water stream. Finally, tests 9 and 10 evaluate performance at lower and higher oxidant concentrations (0.5 and 3.0 parts per million (ppm) free chlorine, respectively). In tests 3 through 8, the UV-AOP system will operate using the prescribed operational control strategy of a target UV dose and a minimum free chlorine concentration of 1.5 mg/L as Cl₂. In this way, results will provide information regarding the system's ability to control effectively. If the system uses another control strategy, e.g., a system that targets, calculates, and maintains a target log reduction of contaminants, then tests within the matrix should be conceptualized to evaluate the effectiveness of that control strategy.

Table 7-2. Example Performance Test Matrix^a.

Test Number	Flow (mgd)	UVT	Free Chlorine Concentration (mg/L)	1,4-dioxane Treatment Target (log reduction)	NDMA Treatment Target (log reduction)	Power Level	Operating Strategy
1	Peak/design (12 mgd)	Ambient	0	0	0	100%	Manual
2	Peak/design (12 mgd)	Ambient	1.5	0	0	0%	Manual
3	Peak/design (12 mgd)	Ambient	1.5	0.5	1.2	95% ^b	UV Dose/oxidant threshold
4	Average (10 mgd)	Ambient	1.5	0.5	1.2	60% ^b	UV Dose/oxidant threshold
5	Minimum (3 mgd)	Ambient	1.5	0.5	1.2	30% ^b	UV Dose/oxidant threshold
6	Peak/design (12 mgd)	96%	1.5	0.5	1.2	100% ^b	UV Dose/oxidant threshold
7	Average (10 mgd)	96%	1.5	0.5	1.2	65% ^b	UV Dose/oxidant threshold
8	Minimum (3 mgd)	96%	1.5	0.5	1.2	35% ^b	UV Dose/oxidant threshold
9	Average (10 mgd)	Ambient	0.5	0.5	1.2	100% ^b	Manual
10	Average (10 mgd)	Ambient	3	0.5	1.2	100% ^b	Manual

a. Conditions: 12 mgd peak flow, 10 mgd average, 0.5-log reduction of 1,4-dioxane, 1.2-log removal of NDMA, 96% design UVT, 98% average UVT, single duty train with one redundant train, UV-Cl₂ process, minimum UV dose, and free chlorine operational strategy.

b. Manufacturer should provide recommended power level for performance.

7.2.2 Steady State/Mixing Test

When the testing team makes changes to the operating conditions during the performance test, a certain amount of time must pass before collecting samples to allow the system to reach steady state. This time is a function of the flow rate and the hydraulic retention time between the influent sampling/spiking ports and the effluent sampling/spiking ports. In general terms, the test consists of injecting an indicator or “tracer” at time zero and evaluating the measurement of that indicator at prescribed intervals in the effluent sampling ports.

As described above, effective indicators include a UVT modifier such as SuperHume™, or the oxidant such as chlorine or peroxide. In all cases, the test team should collect samples at intervals (e.g., 30 seconds) and evaluate the concentration of the indicator at each interval. This will produce a curve of indicator concentration starting at zero and increasing or decreasing to a

steady-state level. The time required to reach steady state should pass prior to collecting samples following a change in test conditions.

7.2.3 Regulatory Involvement

The regulator of record should review the testing plan prior to starting testing. This allows the regulator to comment and approve of the approach and reduces the potential for changes or additions following the testing. Topics on which to agree include the number of tests in the test matrix (and the number of associated replicates), the compounds sampled in the influent and the effluent, disposal of treated water during testing, and review of the operational control strategy.

7.2.4 Adjusting UVT

For a comprehensive, meaningful performance test, the test matrix will include test runs at a lower-than-ambient design UVT. In the example above, the ambient UVT was expected to be approximately 98% cm^{-1} , but the UV-AOP system was designed for a more conservative UVT value of 96% cm^{-1} . This lower UVT accounts for possible future changes in water quality that results from aging membranes, changes to upstream treatment processes, etc. The testing team may consider SuperHume™, LSA (ligno-sulfonic acid), or chloramines for lowering the UVT.

In potable reuse using RO-based pretreatment, designers typically prescribe chloramines in water entering RO to prevent biofouling. Chloramines, particularly monochloramine, are a strong absorber of UV light. For this reason, UVT suppression with chloramines that are already on site and in use, is one option. If the test team plans to use this option, it should coordinate with plant staff to adjust chloramine concentrations accurately and when required. Note that chloramines also present a radical scavenging demand that could affect performance of oxidation processes and should be considered.

UV disinfection validations that evaluate performance over a wide range of conditions often use SuperHume™ or similar UV-absorbing product to reduce UVT. SuperHume is a natural organic matter source that is delivered in a liquid concentrate that is largely inert to UV light and has limited interaction with radical species. It has been used successfully in numerous performance tests.

7.2.5 Indicator Compounds – The Surrogate Question

In some locations, the regulator of note may restrict the injection of the target compound due to toxicity concerns. In these cases, the site may not have a suitable or acceptable means of disposal (e.g., recirculation to the head of the WWTP). In these cases, a non-toxic surrogate compound is more attractive than injecting NDMA or 1,4-dioxane (or other potentially harmful target compound) for the performance test. Examples of inert, non-toxic indicators include caffeine, sucralose, or other pharmaceutical compounds. In the case of caffeine and sucralose, these compounds may be present in wastewater, and injection of these compounds may be unobjectionable. The removal of the indicator compounds can be related to the removal performance of the target compounds by the ratio of reaction rate to the hydroxyl radical.

But alternate compounds present several challenges. Clearly, the reduction of a surrogate will not directly equate to the target compound. That is, if a 1-log reduction of the surrogate is achieved, it is not directly relatable to a 1-log reduction of NDMA or other target compounds. The fundamental photochemical properties of the compounds obviously will differ. A phenomenon known as RED bias (see Chapter A4 of the UV-Cl₂ Review and Section 5.9.1 of the UVDGM (USEPA 2006) for more details) impacts the dose delivered to the compound as a function of the dose-sensitivity of the individual compound. Listed in the research needs associated with UV-AOP is the topic of non-toxic surrogate/indicator compounds.

7.2.6 Performance Test Issues Related to the Dynamic Chemistry of UV-Cl₂

The testing team should give special consideration to the aspects of dynamic chemistry described in previous chapters. For example, in the presence of chloramines, free chlorine concentrations will change as a function of time and may cause interference with testing methods for free chlorine. For these reasons, the methods and timing of sample collection are important. For example, the testing team should quickly analyze field samples for free chlorine, used to confirm on-line monitor results, to prevent significant changes in concentrations due to chlorine/chloramine chemistry and the breakpoint reactions. If free chlorine concentration in the UV-AOP reactor is the target of analysis, analyze samples after the time of travel in the process piping has elapsed. That is, if the time of travel in the process pipe is X seconds at a given flow rate, wait X seconds to perform the field measurement.

As discussed in Chapter 7.1, dynamic chemistry issues also affect collimated beam tests for performance evaluation, by-products studies, generation of dose-response curves, etc. Practitioners use CB device to deliver a known UV dose to a water sample (by way of a “column”), typically to a relatively small sample contained in a petri dish. Collimated beam devices use a lower wattage UV light source, either low-pressure (single wavelength) or medium pressure (multi-wavelength). Lower-wattage lamps deliver lower intensity UV light than full-scale systems, and for this reason the time required to accomplish a UV dose in a CB apparatus is longer than that required for a full-scale UV reactor. Obviously, the dynamic chemistry can lead to changes in the water quality present during that longer treatment time and affect results. Carefully consider these issues when planning the performance test and associated bench tests.

CHAPTER 8

Pulling It All Together

Many key considerations, from operation to design, have been included in this Guidance Manual. Table 8-1 summarizes key considerations and takeaways from this work. Two UV-Cl₂ case studies are presented in Figures 8-1 and 8-2.

Table 8-1. Key Considerations and Takeaways in the Evaluation of the UV-Cl₂ AOP.

Topic	Key Considerations	Recommendations	Chapter Reference(s)
Water Quality Impacts			
pH	Net availability of *OH (and other radicals) is higher at lower pH than at higher pH	Consider UV-Cl ₂ versus UV-H ₂ O ₂ when pH is <6.	3.2 4.4 4.6 6.1
Ammonia	Will combine with free chlorine to form chloramines (which decreases UVT and increases scavenging and sodium hypochlorite costs)	Elevated ammonia will present a chlorine demand so high that achieving target free chlorine concentrations may not be possible or very expensive. Ammonia between 0.3 mg/L and 1 mg/L can drive sodium hypochlorite costs significantly higher than H ₂ O ₂ . For UV-Cl ₂ , adjust upstream treatment to maintain ammonia <0.3 mg/L.	4.4 4.6 6.2 6.4
Alkalinity	Alkalinity > 20 mg/L as CaCO ₃ can impact scavenging	Be sure to fully characterize source water quality to capture the impact of scavenging in system sizing and planned operation.	3.3 4.4
Disinfection By-products	High levels of bromide can result in bromate formation	Carefully review water quality and the potential for the presence of bromide in the source water, including possibility of infiltration of bromide-containing water into the collection system. Maintain bromide <25 µg/L to avoid exceeding the 10 µg/L MCL. If bromide is >25 µg/L, consider bromate formation mitigation strategies.	3.4 4.4 4.6 6.3
	Limited peer-reviewed data suggest that during the limited time that typical post-RO UV-Cl ₂ systems dose relatively higher concentrations of chlorine, DBP concentrations do not increase	Initial studies have indicated that haloacetic acid and trihalomethane formation is not significantly increased. More data is needed for non-RO based systems. However, the impact of UV-AOP on TOC relative to the selected chlorine reaction time may lead to impacts on DBP formation potential; bench- or pilot-scale testing may provide useful supplemental data.	4.6
Nitrite	Nitrite does not significantly impact UV-Cl ₂ systems; >0.1	Consider UV-Cl ₂ as a more cost-effective solution in systems with elevated	4.4

Topic	Key Considerations	Recommendations	Chapter Reference(s)
Water Quality Impacts			
	mg/L as N significantly increases system sizing and O&M costs for UV-H ₂ O ₂ systems and may preclude its practical use	nitrite. <i>However</i> , nitrite often co-occurs with elevated ammonia, which can preclude the use of UV-Cl ₂ . In these cases, additional treatment may be needed to make UV-AOP viable.	4.6 6.4 6.7 5.9
Organic matter	May be present in significant concentrations in non-RO applications (e.g., with ozone-CBAT pretreatment in reuse)	Consider bench-scale testing to determine impact on scavenging, treatment performance, UVT, and DBP formation potential.	3.5 4.4 4.6
Design Features			
Lamp and Oxidant Type	Chlorine absorbs UV light more strongly than H ₂ O ₂ at 254 nm; higher pH will increase speciation to the hypochlorite ion, which absorbs more strongly at higher wavelengths, potentially driving an efficiency advantage for MP lamps vs. LPHO lamps. More research needed on this topic.	At the time of publication, LPHO systems have been, and are being, installed for full-scale UV-Cl ₂ systems. Full-scale demonstration testing of MP-based UV-Cl ₂ AOP is needed to demonstrate MP efficiency advantages at higher pH or in treating oxidizable contaminants (vs. NDMA which is treated by UV-photolysis)	1.2.1 7.1
Monitoring	UV-Cl ₂ systems require a number of monitors to collect data capturing the dynamic nature of the chlorine chemistry	The utility, designer, manufacturer, and regulator must work together to agree upon the appropriate monitoring and control strategies for the facility.	4.5 4.10 4.11 7.1
Sample line HRT vs. process line HRT	Dynamic chemistry (due to chlorine-chloramine and ammonia-free chlorine reactions) proceeds both in the process line and the sample line after sodium hypochlorite is injected	Designer should attempt to match the HRT in the sample line to the HRT in the process line (between the sample point and the UV-AOP system) to ensure that the sample arriving at the monitor is representative of the chemistry of water entering the UV-AOP reactor.	4.5 4.11 7.1
Cost Considerations			
Chemical costs	Oxidant costs for UV-Cl ₂ (i.e., cost of bulk sodium hypochlorite chemical) can be higher than oxidant costs if using H ₂ O ₂ depending on current local chemical costs	Begin the oxidant selection process with a site-specific sodium hypochlorite and H ₂ O ₂ delivered cost evaluation. Couple current, local costs with UV-AOP manufacturer sizing recommendations, to determine the oxidant component of the life-cycle cost.	5
Operating costs	For a post-RO for low nitrite, ammonia, and chloramine scenario, a moderate sodium hypochlorite cost (~\$1.50/gallon), UV-Cl ₂ AOP was estimated to be ~15% lower than UV-H ₂ O ₂ unless	Cost estimates should use local chemical costs in the analysis as this factor has a large effect on long-term operations costs and the benefits of UV-Cl ₂ relative to UV-H ₂ O ₂	5 6.5 6.6

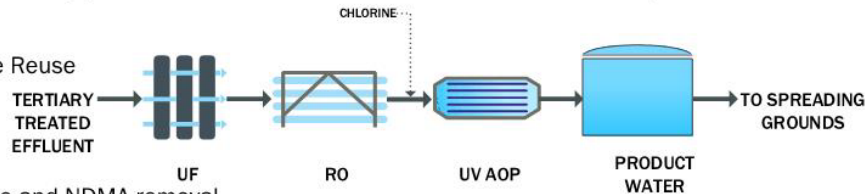
Topic	Key Considerations	Recommendations	Chapter Reference(s)
Water Quality Impacts			
	H ₂ O ₂ quenching is required, in which case UV-Cl ₂ is significantly less costly to operate.	Consider the H ₂ O ₂ quenching requirements for the application, which has a significant impact on operating costs.	
Capital costs	UV-Cl ₂ capital costs were, at the time of publication, equivalent or similar to that of UV-H ₂ O ₂ systems. As manufacturers' predictive models improve and as a more end users install UV-Cl ₂ systems, there will likely be sizing advantages for UV-Cl ₂ under the right conditions.	Request capital cost estimates from manufacturers early in the evaluation process.	5
Testing			
Pre-design testing requirements	Bench- and pilot-scale testing are not expected to provide useful data for scale-up	Bench- and pilot-scale testing has several benefits, but sizing of full-scale UV-AOP systems is generally the responsibility of the manufacturers.	7
Start-up testing requirements	Validate system performance and the intended operational strategy and control while verifying system performance vs. specification	Extensive preparation, starting in the design stage, is required to successfully performance test a UV-AOP system following installation.	7.2

Case Study: Water Replenishment District of Southern California – Albert Robles Center

WRD ARC is one of the first applications of UV/Cl₂ for advanced treatment in the U.S. The WRD ARC Facility produces 14.9 MG of advanced treated water daily.

Application

Indirect Potable Reuse



Goals

- 1,4-Dioxane and NDMA removal
- 6-log virus, *Cryptosporidium*, and *Giardia* inactivation

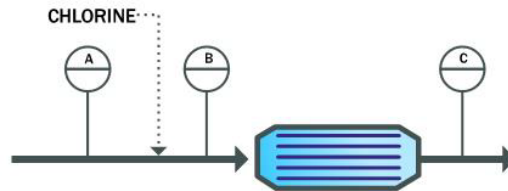
WRD ARC UV AOP Design	
Criteria	Value
UV AOP Influent pH	6.0
Number of UV Trains	2
Capacity per UV Train	7.45 MGD
Reactors per Train	6
Lamps per Train	432
Power Draw per Lamp	0.24 kW
Lamp Type	LPHO
Design UVT	96%
Free Chlorine Concentration	1.5 mg/L
1,4-Dioxane Reduction	0.5 log
NDMA Reduction	1.67 log

Operation

Design: Monitor free chlorine and dose-space chlorine to feed 1.5 mg/L free chlorine to UV system

Current: Operate to threshold UV and chlorine dose. EED leads to adjustment of delivered power-based flow rate

Monitoring Strategy



Point A: UVT, ammonia/monochloramine, pH, flow

Point B: free chlorine, total chlorine

Point C: UVT, free chlorine

Maintenance

- Chlorine analyzers serviced twice daily
- Online monitor calibration checks

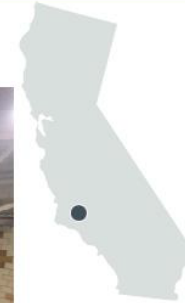
Facility Permit:

NPDES for spreading
DDW for drinking water

Regulatory Requirements

- 15-minute variance on reporting parameters
- <0.1 mg/L total chlorine in discharge for NPDES
- DDW does not currently allow dose pacing for chlorine

CCPs (Operation and Reporting): pH, EED, free chlorine, UVT



Lessons Learned

- Chemical and UV dose thresholds can result in over-dosing and more frequent manual adjustment. WRD is working with regulators to upgrading the control strategy to a UV power and free-chlorine pacing strategy based on a target contaminant treatment objective
- Match analyzer sample line and process line hydraulic retention time for accurate chlorine measurement
- Use UV-resistant piping upstream and downstream of the UV reactor where UV light can penetrate.

Figure 8-1. Water Replenishment District of Southern California UV-Cl₂ Case Study.

Case Study: LA Sanitation - Terminal Island Water Reclamation Plant Advanced Water Purification Facility

The City of Los Angeles TIWRP AWP Facility was constructed in 2002, upgraded in 2011 to increase capacity to 6 MGD and expanded in 2017 to produce 12 MGD of advanced treated water.

Application

Indirect Potable Reuse

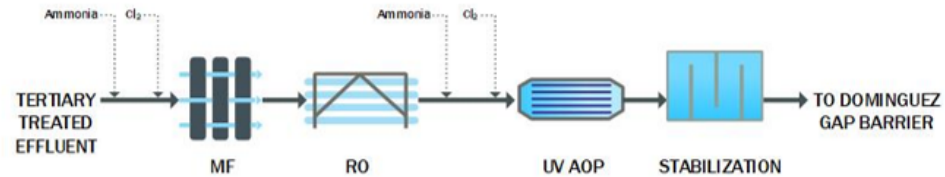
Goals

- 1,4-Dioxane ≥ 0.5 -log removal
- NDMA < 10 ng/L
- 6-log virus, *Cryptosporidium*, and *Giardia* inactivation

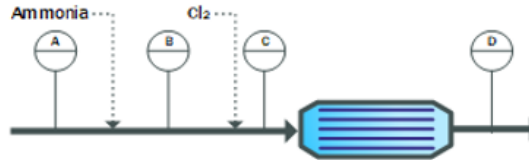
Terminal Island AWP UV AOP Design	
Criteria	Value
UV AOP Influent pH	4-6
Number of UV Trains	1+1
Capacity per UV Train	12 MGD
Lamps per Train	204
Power Draw per Lamp	0.24 kW
Lamp Type	LPHO
Design UVT	96%
Free Chlorine Concentration	1.7 mg/L
1,4-Dioxane	>0.5 log
NDMA Reduction	>0.5 log
UV Dose	920 mJ/cm^2

Operation – UV AOP Influent

- Ammonia dose is controlled with an online monitor.
- Hypochlorite dose controlled by free chlorine in the UV influent.
- UV dose based on flow and UVT, 15-min rolling average to provide process response time.



Monitoring Strategy



Point A: UVT, flow

Point B: Ammonia

Point C: UVT, free Cl, total Cl, pH

Point D: Total chlorine

Maintenance

- Chlorine analyzers serviced twice daily
- Online monitor calibration checks

Facility Permits:

DDW for drinking water

Regulatory Requirements

- 15-minute variance on reporting parameters
- 1.7 mg/L free chlorine residual
- DDW does not currently allow dose pacing for chlorine

CCPs (Operation and Reporting): UV dose, free chlorine, pH, UVT

Lessons Learned

- Ammonium hydroxide dosing was added to the design as a mechanism to control bromate formation. Provide a day tank for ammonia to reduce travel.
- The permit initially required 2 mg/L free chlorine in the UV AOP influent, but TI has since worked with DDW to reduce the limit to 1.7 mg/L.
- Allow a 15-minute rolling average to calculate the parameters before triggering a shutdown response
- Keep analyzer sample points submerged instead of at the top of a pipe to avoid air entrainment.
- Explore wide range of UVT during permitting.
- Replaced total chlorine analyzer with amperometric analyzer for quicker, more stable response.

Figure 8-2. LA Sanitation UV-Cl₂ Case Study.

References

- AWWA and ASCE. 2012. *Water Treatment Plant Design 5th Edition*. McGraw Hill: New York.
- AWWA. 2011. *Water Quality and Treatment 6th Edition*. McGraw Hill: New York.
- Bolton, J. R., Bircher, K. G., Tumas, W. and Tolman, C. A. 2001. "Figures-of-Merit for the Technical Development and Application of Advanced Oxidation Technologies for Both Electric- and Solar-Driven Systems (IUPAC Technical Report)." *Pure Appl. Chem.*, vol. 73, no. 4, pp. 627–637.
- Bukhari, Z., S. Dasgupta, R. Marfil-Vega, and V. Sundaram. 2022. "Optimization of Ozone-BAC Treatment Processes for Potable Reuse Applications." Project 4776. The Water Research Foundation: Denver, CO.
- Bulman, D. M., Mezyk, S. P., and Remucal, C. K. 2019. "The Impact of PH and Irradiation Wavelength on the Production of Reactive Oxidants during Chlorine Photolysis." *Environmental Science & Technology*, 53 (8): 4450–59.
- Collins, J., and J. Bolton. 2016. "Advanced Oxidation Handbook." AWWA: Denver, CO.
- Dowdell, K., G. Wetterau, P. Fu, and A. Royce. 2016. "UV/Chlorine as an Alternative to Hydrogen Peroxide for Advanced Water Treatment Plants." AWWA Potable Reuse Symposium. Long Beach, CA.
- Fang, J., Y. Fu, and C. Shang. 2014. "The Roles of Reactive Species in Micropollutant Degradation in the UV/Free Chlorine System." *Environmental Science & Technology*, 48: 1859–1868. <https://doi.org/10.1021/es4036094>.
- FRED. 2022. *Economic Data*. Federal Reserve Bank of St. Louis. <https://fred.stlouisfed.org/>.
- Festger, A., M. Stefan, A. Royce, and M. Kwon. "Selecting Your UV/AOP: UV/Peroxide, UV/Chloramine, or UV/Chlorine?" *In Proc. 2021 WateReuse Annual Conference (Virtual)*. March 16-25, 2021.
- Feng, Y., D. W. Smith, and J. R. Bolton. 2007. "Photolysis of Aqueous Free Chlorine Species (HOCl and OCl⁻) with 254 Nm Ultraviolet Light." *Journal of Environmental Engineering and Science*, 6: 8.
- Funk, D., J. Hooper, M. Noibi, J. Goldman, R. Oliva, K. B. Schultz, D. Castaneda, C. -H. Huang, and E. Macheck. 2018. "Ozone Biofiltration Direct Potable Reuse Testing at Gwinnett County." The Water Research Foundation: Denver, CO.
- Grebel, J. E., J. J. Pignatello, and W. A. Mitch. 2010. "Effect of Halide Ions and Carbonates on Organic Contaminant Degradation by Hydroxyl Radical-Based Advanced Oxidation Processes in Saline Waters." *Environmental Science & Technology*, 44: 6822-6828.

- Guo, K., Z. Wu, S. Yan, B. Yao, W. Song, Z. Hua, X. Zhang, X. Kong, X. Li, and J. Fang. 2018. "Comparison of the UV/Chlorine and UV/H₂O₂ Processes in the Degradation of PPCPs in Simulated Drinking Water and Wastewater: Kinetics, Radical Mechanism and Energy Requirements." *Water Research*, 147:184-194.
- Guo, K., S. Zheng, X. Zhang, L. Zhao, S. Ji, C. Chen, Z. Wu, D. Wang, and J. Fang. 2020. "Roles of Bromine Radicals and Hydroxyl Radicals in the Degradation of Micropollutants by the UV/Bromine Process." *Environmental Science & Technology*, 54 : 6415–6426.
- Henderson, J. L., R. S. Raucher, S. Weicksel, J. Oxenford, and F. Mangravite. 2009. "Supply of Critical Drinking Water and Wastewater Treatment Chemicals – A White Paper for Understanding Recent Chemical Price Increases and Shortages." Water Research Foundation: Denver, CO.
- Hofmann, R., and R. C. Andrews. 2001. "Ammoniacal Bromamines: A Review of Their Influence on Bromate Formation During Ozonation." *Water Research*, 35 (3): 599-604.
- Kohen, R., and A. Nyska. 2002. "Invited Review: Oxidation of Biological Systems: Oxidative Stress Phenomena, Antioxidants, Redox Reactions, and Methods for Their Quantification." *Toxicologic Pathology*, 30 (6): 620–50. <https://doi.org/10.1080/01926230290166724>.
- Kwon, M., A. Royce, Y. Gong, K. P. Ishida, and M. I. Stefan. 2020. "UV/Chlorine vs. UV/H₂O₂ for Water Reuse at Orange County Water District, CA: A Pilot Study". *Environmental Science: Water Research & Technology*, 6: 2416-2431.
- Sharpless, C. M., and K. G. Linden. 2003. "Experimental and Model Comparisons of Low- and Medium-Pressure Hg Lamps for the Direct and H₂O₂ Assisted UV Photodegradation of N-Nitrosodimethylamine in Simulated Drinking Water." *Environmental Science & Technology*, 37: 1933-1940.
- Stanford, B., E. R. V. Dickenson, E. Wert, and M. Inyang. 2017. "Controlling Trace Organic Compounds Using Alternative, Non-FAT Technology for Potable Water Reuse." *Water Environment and Reuse Foundation: Denver, CO*.
- Pearce, R., S. Hogard, P. Buehlmann, G. Salazar-Benites, C. Wilson, and C. Bott. "Evaluation of Preformed Monochloramine for Bromate Control in Ozonation for Potable Reuse." *Water Research*, 211 (2022): 118049.
- USEPA. 2020. "Innovative Approaches for Validation of Ultraviolet Disinfection Reactors for Drinking Water Systems." EPA/600/R-20/094. USEPA: Washington, D.C.
- USEPA. 2006. "Ultraviolet Disinfection Guidance Manual for the Final Long Term 2 Enhanced Surface Water Treatment Rule." EPA 815-R-06-007. EPA: Washington, D.C.
- Walker, T., S. Khan, C. Robillot, S. Snyder, R. Valerdi, S. Swivedi, and J. Vickers. 2016. "Critical Control Point Assessment to Quantify Robustness and Reliability of Multiple Treatment Barriers of a DPR Scheme." The Water Research Foundation: Denver, CO.

Wang, C., L. Zheng, S. Andrews, and R. Hofmann. 2020. "Monochloramine Formation and Decay in the Presence of H₂O₂ after UV/H₂O₂ Advanced Oxidation." *Journal of Environmental Engineering*, 146 (6): 06020002.

Wang, C., N. Moore, K. Bircher, S. Andrews, and R. Hofmann. 2019. "Full-Scale Comparison of UV-H₂O₂ and UV-Cl₂ Advanced Oxidation: The Degradation of Micropollutant Surrogates and the Formation of Disinfection Byproducts." *Water Research*, 161: 448–58.

White, C. 2010. *Chlorine and Alternative Disinfectants 5th Edition.* John Wiley & Sons: New York, NY.

Wu, Z., K. Guo, J. Fang, X. Yang, H. Xiao, S. Hou, X. Kong, C. Shang, X. Yang, F. Meng, and L. Chen. 2017. "Factors Affecting the Roles of Reactive Species in the Degradation of Micropollutants by the UV/Chlorine Process." *Water Research*, 126: 351-360.

Yang, W., Y. Tang, L. Liu, X. Peng, Y. Zhong, Y. Chen, and Y. Huang. 2020. "Chemical Behaviors and Toxic Effects of Ametryn During the UV/Chlorine Process." *Chemosphere*, 240: 124941.

Yin, R., L. Ling, and C. Shang. 2018. "Wavelength-Dependent Chlorine Photolysis and Subsequent Radical Production Using UV-LEDs as Light Sources." *Water Research*, 142: 452–58.

Appendix A: Current State-of-the-Science of UV-Chlorine AOP

Prepared by:

Abdallatif Abdalrhman¹, Susan Andrews¹, Tianyi Chen¹, Mahshid Farzanesha², Ron Hofmann¹, Nathan Moore¹, Liz Taylor-Edmonds¹, Chengjin Wang¹

¹University of Toronto, Department of Civil & Mineral Engineering

²Univeristy of New South Wales, School of Civil & Environmental Engineering

Contents

Chapter A1: Photochemistry Fundamentals	95
A1.1 An Overview of Advanced Oxidation Processes.....	95
A1.2 How to Make Free Radicals in an AOP.....	96
A1.3 UV-Based AOPs.....	97
A1.4 UV Light	97
A1.5 UV Lamp Emission Spectra	98
A1.6 Going from Producing Photons to Destroying Contaminants.....	100
A1.7 Production of Primary Radicals.....	101
A1.8 Uncertainty and Variability in the Quantum Yields.....	103
A1.9 Propagation of Radicals and Formation of Other Oxidants	104
A1.10 End Reactions and Treatment	105
A1.11 Added Benefits: Direct UV Photolysis and Oxidant Action	107
A1.12 UV-AOP Sizing and Dose Definition	109
A1.12.1 Approaches to UV Equipment Sizing.....	109
A1.12.2 Dose Per Log, EED and EEO.....	110
Chapter A2: Effect of Water Quality	113
A2.1 Radical scavenging.....	113
A2.2 UV Transmittance (UVT)	115
A2.3 Ammonia, Chloramines, Nitrate, and Nitrite	116
A2.3.1 UV-H ₂ O ₂ AOP	117
A2.3.2 UV-Cl ₂ AOPs	120
A2.4 Strategies for Addressing Nitrogen Species.....	122
A2.5 A Note on the Benefits of Chloramine and Nitrate Photolysis.....	123
A2.6 Toxicity Associated with Photolysis of Nitrogen Species	124
A2.7 pH.....	125
A2.8 Chlorine and H ₂ O ₂ Dose.....	126
A2.9 UV Dose (Fluence)	127
A2.10 Inorganic Carbon	128
A2.11 Chloride and Bromide.....	129
A2.12 Organic Matter	129
A2.13 Temperature	130
Chapter A3: Byproducts	133
A3.1 Biostability.....	133
A3.2 Downstream Chlorine Demand	134
A3.3 Impact on Traditional and Novel Organohalide Byproducts.....	135
A3.4 Impact on Downstream DBP Formation Potential.....	138
A3.5 DBPs as Transformation Products of Specific Precursors	139
A3.6 Nitrosamines	139
A3.6.1 Minimizing NDMA Formation	141
A3.7 Other Novel Organic DBPs.....	141

A3.8	Oxyhalides: Bromate, Chlorite, Chlorate, and Perchlorate	142
A3.8.1	Formation Pathways	143
A3.8.2	Factors Affecting Inorganic DBP Formation in the UV/chlorine AOP	144
A3.9	Toxicity Assays	147
Chapter A4:	Disinfection Credit for a UV-AOP	151
Chapter A5:	Research Needs	155
Chapter A6:	References	159

Tables

A1-1	Standard Oxidation Potential of Various Species.....	96
A1-2	Apparent Quantum Yields of Radical Formation at 254 nm in Pure Water.	102
A2-1	•OH scavenging of Nitrogen Species Post-RO (pH 5.5)	119

Figures

A1-1	Lewis Dot Diagram of (a) Hydroxide Ion and (b) Hydroxyl Radical with an Unpaired Electron.....	95
A1-2	UV Terminology.....	97
A1-3	Electromagnetic Spectrum as a Function of Wavelength (m) with Expanded Scale of Ultraviolet Radiation.....	97
A1-4	Typical UV lamp Emission Spectra and H ₂ O ₂ and Chlorine Adsorption Spectra.....	99
A1-5	Free Chlorine Speciation as a Function of pH at 25°C.....	100
A1-6	The UV-AOP System in Summary.....	101
A1-7	General Initiation Equations Showing Primary Radicals Formed.....	102
A1-8	HOCl Quantum Yield of Decomposition Affected by Organic Matter.....	103
A1-9	Examples of Propagation of Radicals.....	104
A1-10	Simple Overview of Chlorine Photolysis and Propagation of Reactive Chlorine Species.....	105
A1-11	Proportion of Hydroxyl Radical Scavengers in UV-H ₂ O ₂ Treatment of River Water.....	106
A1-12	Example of Contaminant Destruction Rate Calculation.....	106
A2-1	Example of Contributions to Hydroxyl Radical Scavenging for a Fictive Water Treated with UV-Chlorine.....	114
A2-2	Summary of the Role of Nitrogen-Containing Species in UV-H ₂ O ₂ and UV-Chlorine AOPs Following Upstream Ozone-CBAT or RO Treatment.....	117
A2-3	(Top) Example of Percent of Photons Absorbed at 254 nm by Various Constituents in a Fictive RO Permeate Containing 5 mg/L Free Chlorine, 3 mg/L Monochloramine, 4 mg/L Dichloramine, and 1.5 mg-N/L Nitrate. (Bottom) Absorption Spectra for Ammonia, Nitrate, Monochloramine, and Dichloramine.....	118
A2-4	Model of the Fate and Impact of Chloramines in a FAT UV-Chlorine Treatment Process (pH 5.5).....	122
A3-1	DBPs Identified in AOP Studies with Modelled Non-Negligible Toxicity and Little Occurrence Data.....	142
A3-2	Oxidation of Bromide by Chlorine.....	145
A3-3	Reaction of Ammonia with Free Bromine and Free Chlorine.....	147

CHAPTER A1

Photochemistry Fundamentals

A1.1 An Overview of Advanced Oxidation Processes

Advanced oxidation processes (AOPs) refer to water treatment that uses *free radicals*. A free radical is a chemical species that has one or more unpaired electrons (Figure A1-1), but a simpler way to consider it is an atom or molecule that is “missing” an electron and is therefore unstable and strongly reactive as it attempts to regain that electron. Such free radicals can be stronger oxidants than traditional chemicals such as chlorine or ozone. Reaction strength is typically illustrated by standard oxidation potentials, shown in Table A1-1 (Armstrong et al., 2015; Glaze 1990).

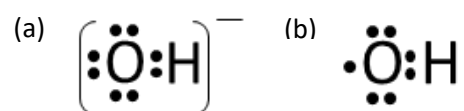


Figure A1-1. Lewis dot diagram of (a) Hydroxide Ion and (b) Hydroxyl Radical with an Unpaired Electron.

One of the most common radicals used for an AOP is the *hydroxyl radical* ($\cdot\text{OH}$). Note that this is different from the hydroxide ion (OH^-) which is a stable ion in water. The hydroxyl radical is extremely reactive and normally persists in water for less than one millionth of a second before reacting to regain its missing electron (Kohen and Nyska, 2002). If that electron is taken from a nearby contaminant, the contaminant may be broken down. This is a key consideration for AOPs compared to adsorptive treatment processes like activated carbon or ion exchange. In adsorption, the contaminant is removed completely from the water intact, but in some cases disposal of the exhausted adsorbent can be challenging if it is classified as a hazardous waste. In contrast, AOPs can alter or even destroy the parent compounds so there is no direct waste stream. A potential downside, however, is that while the parent contaminant may be destroyed, the degree of reaction that occurs during AOPs is usually not enough to completely mineralize the contaminant to simple end products like carbon dioxide (CO_2) and water. Instead, complex organic contaminants tend to be broken down (transformed) into simpler and smaller organic molecules. It has been a research topic for many years to see if the transformation products of AOPs could also exhibit some form of toxicity. More about this is discussed later.

Table A1-1. Standard Oxidation Potential of Various Species
(Data source: Stefan 2018).

Oxidant	Electrochemical Potential (Volts)
•OH	2.80
Cl•	2.43
O	2.42
ClO3•	2.38
Cl2•-	2.13
O3	2.07
H2O2	1.78
KMnO4	1.70
ClO2	1.57
ClO•	1.39
Cl2	1.36
O2	1.23
Br2	1.09
HOCl	0.95
ClO2•	0.94
OCl-	0.94
I2	0.54

A1.2 How to Make Free Radicals in An AOP

One AOP that has been used for municipal water treatment is ozone (O₃) in combination with hydrogen peroxide (H₂O₂), which react quickly together to form •OH. Another common method is to expose H₂O₂ to UV light, whereby the H₂O₂ is broken down into •OH. The UV-chlorine AOP is similar to the UV-H₂O₂ AOP in that UV light causes the decomposition of chlorine into •OH and other radical species. Many other methods exist to perform advanced oxidation, but they are less common at the municipal scale.

AOP treatment methods are expensive compared to common treatment processes such as chlorination. AOPs are therefore typically only used when treatment objectives are extreme: such as for potable reuse treatment, or when water is contaminated with compounds that are resistant to conventional treatment. One of the benefits of AOPs, however, is that they often treat the water through multiple processes. For example, when applying O₃-H₂O₂, it is common to add ozone (alone) first to take advantage of direct molecular reaction of ozone with contaminants, and also to disinfect the water. Then, when H₂O₂ is applied, the remaining ozone is converted into •OH which serves as a “polishing agent” to destroy some of the more recalcitrant contaminants that survived direct ozone attack. Similarly, when using UV-H₂O₂ to treat the water, UV is an excellent disinfectant and can also destroy certain photosensitive contaminants such as n-nitrosodimethylamine (NDMA) while it simultaneously converts the H₂O₂ into •OH to destroy other chemical contaminants. The high cost of AOPs can therefore be partially mitigated by addressing multiple treatment targets simultaneously.

A1.3 UV-Based AOPs

Many chemicals decompose upon exposure to UV light to form radicals—a process called photolysis. Hydrogen peroxide (H₂O₂) is the most commonly used, but chlorine is getting attention particularly for the water reuse market, while chemicals such as peracetic acid, performic acid, persulfate, chloramines, and others are being explored in the research environment. UV alone can generate radicals if applied at short wavelengths in water (185 nm) where the UV reacts with water itself to form the radicals in a process called vacuum UV (VUV). This treatment so far is not yet practical at large scale, but it promises a form of AOP that requires only electricity and no other treatment chemicals to produce radicals.

A note about semantics...

Some may object to the term “UV light” since by strict definition, “light” is visible to the human eye and UV wavelengths are invisible. The correct term is UV **radiation**. It is advisable, however, to avoid the word “radiation” when communicating to the public about water treatment, due to the obvious opportunity for misunderstanding. In this document, we refer to “UV light.”

Figure A1-2. UV Terminology.

A1.4 UV Light

Ultraviolet light is part of the electromagnetic spectrum that extends in the region just beyond violet visible light: hence, *ultraviolet*. It is in the region of the spectrum bounded roughly between 100-400 nm (Figure A1-3).

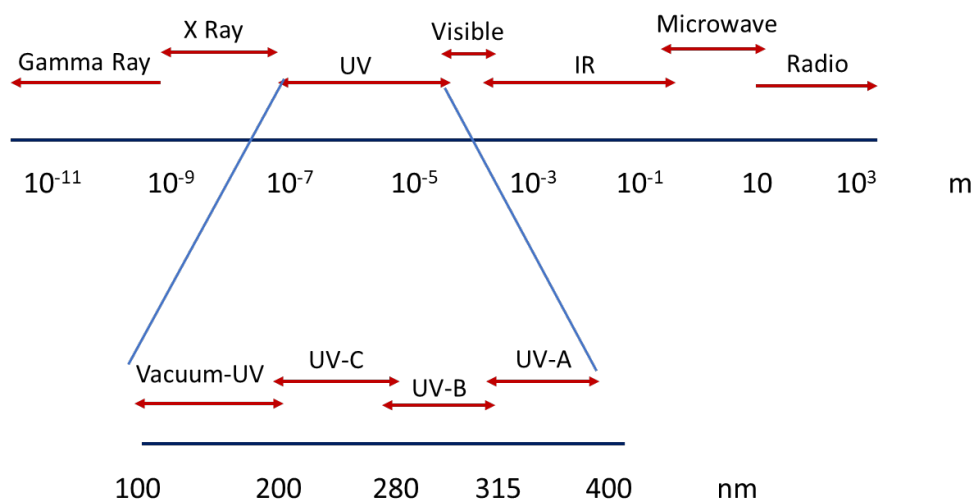


Figure A1-3. Electromagnetic Spectrum as a Function of Wavelength (m) with Expanded Scale of Ultraviolet Radiation; 1 nm = 10⁻⁹ m.

There are several common types of UV lamps used for water treatment: low pressure (LP) lamps, low pressure high output (LPHO), low pressure amalgam, and medium pressure (MP). The details that distinguish these different lamp types can be found elsewhere, but as a very general summary, the three types of low-pressure lamps emit light primarily at 254 nm (they are *monochromatic*), and medium pressure lamps emit light at many wavelengths including

254 nm (they are *polychromatic*). An example of these emission spectra is shown in Figure A1-4. The importance of the different emission wavelengths will be explained later. The three types of LP lamps are generally less powerful than MP lamps, so more lamps are needed to deliver an equal dose. For example, a UV-AOP system might require a LPHO reactor containing 144 lamps to provide the same level of treatment as a MP reactor containing 16 lamps. The MP reactor might therefore be considerably smaller. MP systems might therefore be advantageous where there are footprint constraints. On the other hand, MP systems are typically less energy efficient. Lamp technology evolves continuously so utilities are advised to consult with manufacturers to learn the latest information on lamp power, efficiency, and other related issues.

A1.5 UV Lamp Emission Spectra

Light can be imagined as discrete photons of energy. The principle of a UV-based AOP is that the photons being emitted by the lamp are absorbed by the oxidant (H_2O_2 or chlorine) so that the absorbed energy causes the oxidant to break down to form radicals. If the oxidant is transparent to the photons, the photons will pass straight through the oxidant without causing any chemical change—similar to light passing through a window—and no radicals will be formed. Oxidants that absorb UV light more effectively therefore tend to be preferred for AOPs. The ability of oxidants to absorb photons varies with wavelength, as shown in Figure A1-4. In the figure, it's apparent that H_2O_2 absorbs less light as wavelengths increase, and that at 254 nm, free chlorine absorbs UV light about three times as effectively as H_2O_2 on a per-molar basis.

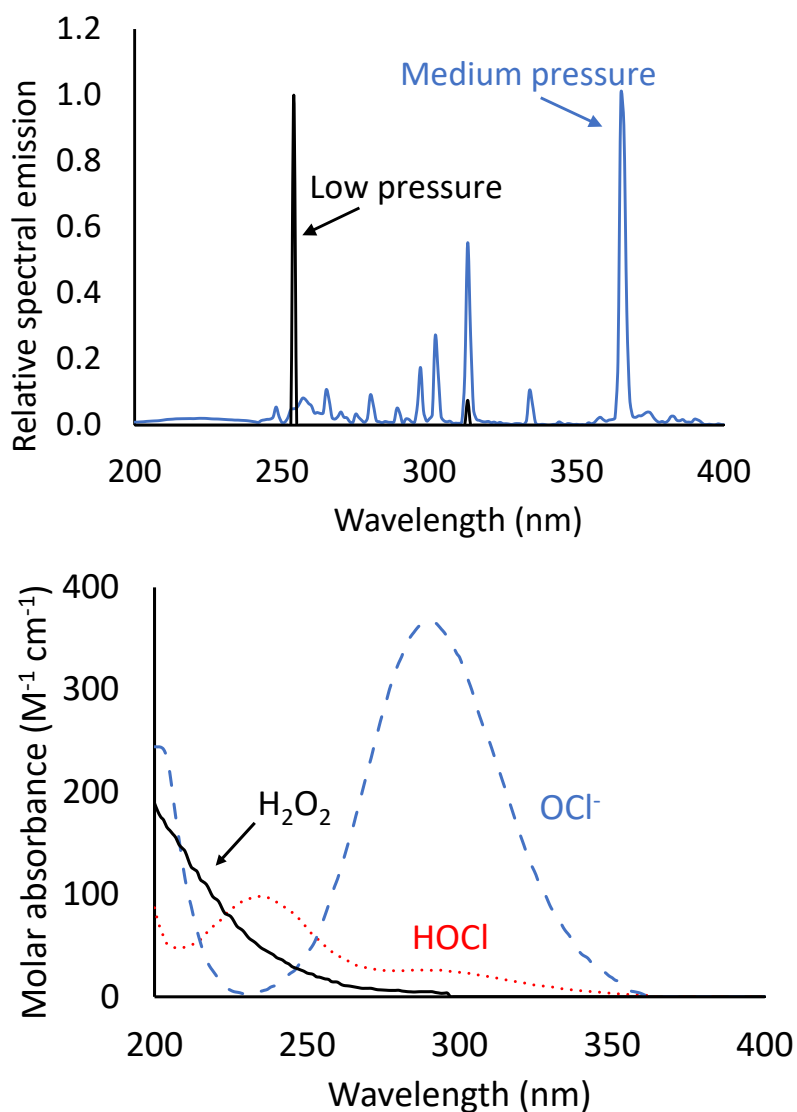


Figure A1-4. Typical UV Amp Emission Spectra (Top) and H₂O₂ and Chlorine Adsorption Spectra (Bottom).

Low pressure and medium pressure lamp emissions are not to scale: medium pressure emission is typically much higher than low pressure.

The absorbance spectrum of H₂O₂ is essentially unaffected by pH within the normal range of treatment, since its pK_a is 11.7 (the pK_a is the pH at which an acid is present in equal concentrations of protonated and unprotonated forms, such as H₂O₂ and HO₂⁻. Hence, virtually all H₂O₂ will be in the H₂O₂ form unless the pH approaches or exceeds 11.7). Just like chlorine, however, the absorbance of H₂O₂ will be slightly affected by temperature. For example, a 2.2% increase in the absorbance of H₂O₂ at 254 nm is observed at 25°C when compared to 1°C (Chu and Anastasio, 2005).

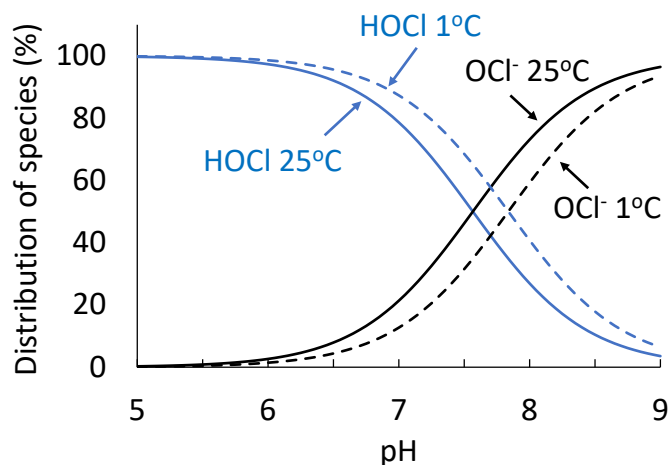


Figure A1-5. Free Chlorine Speciation as a Function of Ph At 25°C

The information presented so far implies that to make a UV-based AOP more efficient and effective, it's best to use an oxidant that most strongly absorbs the photons being emitted from the UV lamp. By examining Figure A1-5, when using a low pressure lamp that emits photons almost entirely at 254 nm, it appears that H_2O_2 is approximately one-third as effective as HOCl in terms of absorbing photons (the 254 nm molar absorption coefficients at room temperature are $\epsilon_{\text{H}_2\text{O}_2} = 19.2 \text{ M}^{-1}\text{cm}^{-1}$ and $\epsilon_{\text{HOCl}} = 59 \text{ M}^{-1}\text{cm}^{-1}$) (Feng et al., 2007). Conversely, if a medium pressure lamp is used, there are many photons being emitted at higher wavelengths that are not absorbed by H_2O_2 . This tends to make medium pressure lamps less energy efficient than LP lamps for UV- H_2O_2 processes (although there are many other factors involved in the overall cost-benefit analysis, as will be explained later). In contrast, at neutral or elevated pH, the higher wavelength photons can be absorbed by OCl^- , which may enhance MP lamp efficiency at high pH for a UV-chlorine AOP.

The theory behind which combinations of oxidants and UV lamps is preferable can be complex. Unfortunately, this is just the beginning. The ability of an oxidant to absorb photons is just one step of several that is needed to ultimately treat the water, as explained in the next section.

A1.6 Going from Producing Photons to Destroying Contaminants

The overall sequence of events that leads to a contaminant being destroyed by free radicals from a UV-based AOP is shown in Figure A1-6. To a chemist, this sequence is referred to as (i) initiation, (ii) propagation, and (iii) termination. In lay terms, the steps include (i) generating what can be called primary radicals (those formed directly from the UV reaction with H_2O_2 or chlorine), then (ii) the subsequent rearrangement of those primary radicals through self-interaction or reaction with other compounds in the water to form a suite of secondary radicals along with any remaining primary radicals, followed by (iii) the reaction of those primary and secondary radicals with the contaminants of interest or other chemicals in the water, whereby the radicals are consumed and the chemicals are destroyed. It's this third step that is the important one from a treatment perspective since this is where the contaminants are destroyed, but the overall efficiency (and cost) is influenced by the first two steps as well. While

the chemistry of this whole sequence is complex, it will be described qualitatively in the next few sections to give the reader a general understanding of which phenomena tend to be important in dictating the effectiveness of UV-chlorine and UV-H₂O₂ treatment. It should be said, however, that while the overall process is understood reasonably well for UV-H₂O₂, much of the fundamental chemistry involved in the UV-chlorine AOP is still unknown. This makes it challenging to predict, without pilot- or full-scale testing, how well a UV-chlorine AOP will perform. This is a running theme throughout this document.

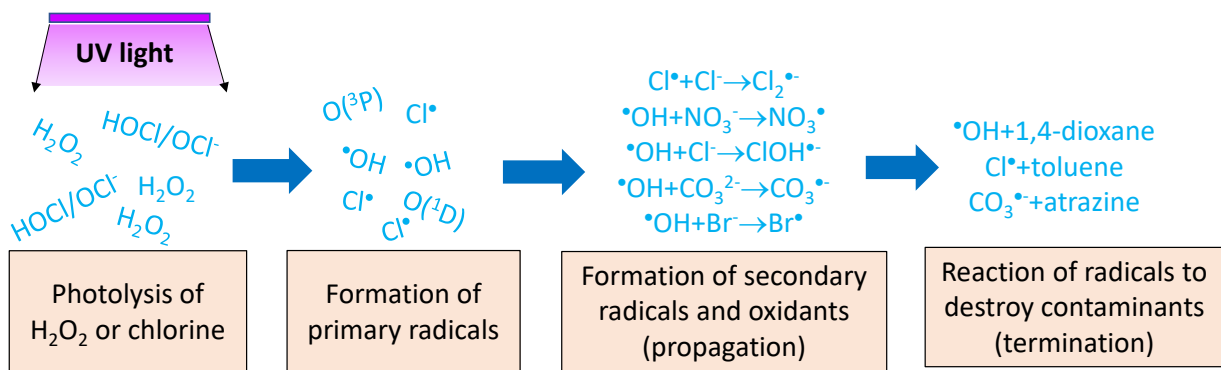


Figure A1-6. The UV-AOP System in Summary.
This sequence all occurs within the UV reactor.

A1.7 Production of Primary Radicals

The first step in the UV-based AOP is to convert the oxidant (H₂O₂ or chlorine) to primary radicals. Sometimes the oxidant is called the *initiator*, since it is this parent compound that helps to initiate to formation of the primary radicals. As explained previously, UV light, if absorbed by the H₂O₂ or chlorine, can cause those compounds to break apart to form radicals, as shown in Figure A1-7 (Yu and Barker 2003; Thomsen et al. 2001). The UV photolysis of both H₂O₂ and HOCl directly yield •OH. Photolysis of OCl⁻ generates O[•] which is the deprotonated form of •OH that exists at elevated pH (pka = 11.7) (Buxton and Subhani 1972; Poskrebyshev et al., 2002). Therefore, all three of H₂O₂, HOCl, and OCl⁻ form hydroxyl radicals upon photolysis, but the UV-chlorine AOP also forms the chlorine atom radical (Cl•). The chlorine atom goes on to form other chlorine-based radicals, generically referred to as *reactive chlorine species* (RCS). The formation of RCS can be considered as an added benefit to UV-chlorine AOP since they can help to destroy contaminants, but as we'll see, it's very difficult to predict the amount of RCS that will be formed. As such, it might be difficult to include the action of these chlorine radicals from a design perspective until the chemistry is better understood. Also, just like the hydroxyl radicals, the high reactivity of RCS means that they are present in the water for only a fraction of a second, and there's therefore no risk of exposure to downstream consumers.

There is an important property in photochemistry called the *quantum yield*. The quantum yield is the ratio of how many molecules are either destroyed or produced per photon absorbed by the parent molecule. For example, in Table A1-2, the quantum yield of H₂O₂ decomposition is shown to be 0.5, meaning that for every photon absorbed by H₂O₂, then mathematically speaking, half of a molecule of H₂O₂ decomposes. An easier way to say this is that it takes 2 photons to be absorbed to destroy one H₂O₂ molecule. The quantum yield of •OH formation, in

turn, is 1.0. This means that for every photon absorbed by H₂O₂, one •OH radical is formed—or, speaking more practically, it takes 2 photons to be absorbed by H₂O₂ to destroy one H₂O₂ molecule, and two •OH radicals are formed in this process.

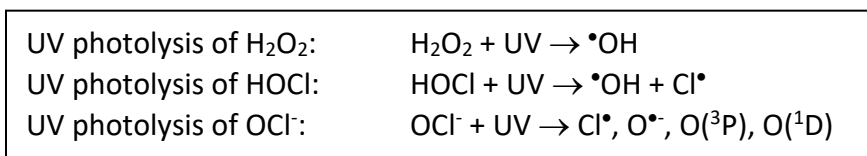


Figure A1-7. General Initiation Equations Showing Primary Radicals Formed.
(stoichiometry not shown).

Table A1-2. Apparent Quantum Yields of Radical Formation at 254 nm in Pure Water.

	Quantum yield of oxidant decomposition	Quantum yield of radical formation
H ₂ O ₂ + UV → •OH	0.5 ¹	•OH: 1.0 ¹
HOCl + UV → •OH + Cl•	1.0-1.64 (apparent) ¹ 0.62 ²	•OH: 0.46 – 1.4 (apparent) ¹ •OH: 0.62 ² •OH: 0.6-1.4 ³ Cl•: TBD
OCl ⁻ + UV → Cl•, O ^{•-} , O(³ P), O(¹ D)	0.84-1.2 ¹ 0.55 ²	Cl• 0.28 ¹ •OH: 0.12-0.61 ¹ •OH: 0.552 ² •OH: 0.133 ³

¹Stefan (2018)

²Chuang et al. (2017)

³Bulman et al. (2019)

The values shown in Table A1-2 for HOCl photolysis and radical formation include apparent quantum yields. The chemistry of HOCl photolysis is not completely understood and likely includes chain reactions of the photolysis products with the HOCl itself, confounding the process. As such, the apparent values are an amalgamation of several independent reactions, and therefore can be impacted by water quality conditions that could affect those reactions. The reader is referred to Chuang et al. (2017) for more information on this topic.

The quantum yields shown in Table A1-2 give us the ability to begin to learn more about the relative competitiveness of UV-H₂O₂ and UV-chlorine AOPs. Recall that if using monochromatic (254 nm) UV lamps, at, say, pH 6.0 where most of the chlorine is in HOCl form, the molar absorbance of H₂O₂ is approximately one-third that of HOCl (Figure A1-4). This means that if we were to compare a UV-H₂O₂ system to a UV-HOCl system where the H₂O₂ and HOCl were at the same (molar) concentrations, HOCl would absorb three times as many photons per second as H₂O₂. Table A1-2 tells us that under these circumstances, the chlorine will decay 6-9 times faster than H₂O₂, since not only is it absorbing 3 times more photons, but each photon is 2 to 3 times more likely to cause the oxidant to decay. However, despite decaying 6-9 times more quickly, the HOCl might only produce 3 times more •OH per second than H₂O₂, since the

quantum yield of $\bullet\text{OH}$ formation for both H_2O_2 and HOCl is 1.0 (actually, for HOCl it is 0.46-1.4, which we'll average to 1.0 for the sake of this argument). This means that overall, UV-chlorine might be approximately 3 times more effective than UV- H_2O_2 at pH 6.0 if the contaminant can only be destroyed by $\bullet\text{OH}$ (and ignoring some other factors that will be explained later). If, however, the contaminant can also be destroyed by RCS, then UV-chlorine might be even better since the photolysis of HOCl will also produce some $\text{Cl}\bullet$, although the amount is hard to estimate from first principles (as noted by the lack of a value for the quantum yield of $\text{Cl}\bullet$ from HOCl in Table A1-2). Another outcome of this thought exercise is that we see that at pH 6.0, much more chlorine decays than H_2O_2 during UV exposure. This is beneficial if quenching of residual oxidant is necessary before releasing the treated water to the customer or to the environment. In general, UV- H_2O_2 processes only result in 5-20% decomposition of the H_2O_2 , whereas much more chlorine can be photolyzed across the UV reactor under typical conditions (often greater than 50%), due to its strong UV absorbance and its higher quantum yield of oxidant decomposition.

A1.8 Uncertainty and Variability in the Quantum Yields

From the previous section, it is obvious that our ability to predict the behavior of a UV-AOP relies on having an accurate knowledge of the quantum yields involved. But as shown in Table A1-2, while the quantum yields for H_2O_2 are well-known, such accurate information is missing in the case of chlorine and the chlorine radicals. Furthermore, the apparent quantum yield for HOCl decomposition when absorbing UV_{254} light, which is reported as 1.0-1.64 in the table, has been shown to be influenced by the presence of organics. The mechanism is proposed to be as shown in Figure A1-8 (Feng et al., 2007; Jin et al., 2011; Örmeci et al., 2005).

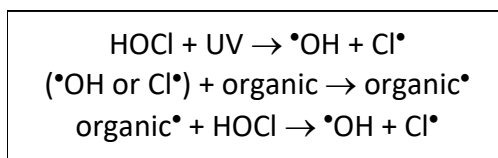


Figure A1-8. HOCl Quantum Yield of Decomposition Affected by Organic Matter.

Here, the radicals that are formed when HOCl undergoes photolysis react with organics that might be in the water, forming an organic radical. This organic radical then reacts with and destroys a molecule of HOCl , releasing more $\bullet\text{OH}$ and $\text{Cl}\bullet$ to begin the cycle again, in a chain reaction. In this way, the HOCl decomposition is accelerated without achieving any net increase in the $\bullet\text{OH}$ and $\text{Cl}\bullet$ available to react with target contaminants. The relevance of this phenomenon from a practical perspective is not clear, and interestingly, this chain reaction does not appear to occur for the photolysis of OCl^- (Feng et al., 2007). Nevertheless, it may account for an observed faster-than-predicted loss of chlorine across UV reactors in real waters containing total organic carbon (TOC) than would be predicted when using the quantum yields in Table A1-2 alone. This underscores the need to do testing to confirm UV-chlorine performance, to supplement the sometimes-poor mathematical models that we have of the process.

It must also be pointed out that the quantum yields illustrated in Table A1-2 are average values. It has been reported that they can vary as a function of both UV wavelength and temperature. The reader is referred to the summary on this topic provided by Stefan (2018) for more detail.

A1.9 Propagation of Radicals and Formation of Other Oxidants

Once primary radicals are formed (described in the previous section), those radicals may be rearranged through reaction with themselves or with other species in the water to form new radicals or other secondary oxidants that can also help to treat the water.

For UV-H₂O₂ treatment, the primary radical that is formed is •OH. While some of the •OH may react immediately with the contaminants of interest, a fraction of it will react with other compounds such as natural organic matter in a way that destroys the •OH and produces no reactive end products (the termination step—described in the next section). A certain amount of •OH, however, may react with species to form secondary reactive compounds that can be helpful in treatment. This is the propagation step.

The propagation of •OH is relatively well-characterized in water treatment. A complete explanation is not provided here, but as an example, the reactions shown in Figure A1-9 are common.

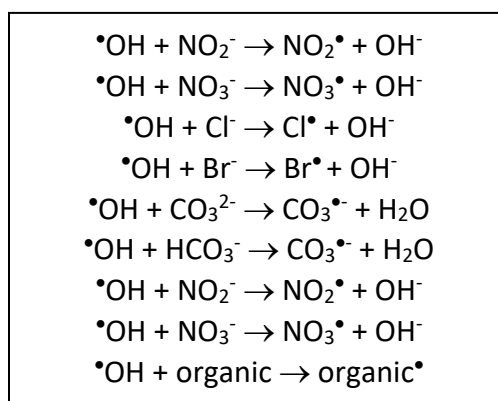


Figure A1-9. Examples of Propagation of Radicals.

As suggested in Figure A1-9, a fraction of the •OH may be converted into secondary radicals through reaction with natural organic matter (NOM), (bi)carbonate, bromide, nitrite, chloride, and other species. From a practical perspective, it is very rare for these secondary radicals to be more useful than the original •OH in treating the water. As such, these reactions can generally be undesirable since they consume •OH. That being said, there is some evidence of partially useful secondary radicals. For example, Mao et al. (2011) reported that secondary radicals such as the carbonate radical were efficient in the degradation of a sunscreen agent, p-aminobenzoic acid (PABA). In contrast, some of the secondary radicals can lead to the formation of undesirable byproducts (Liang et al., 2006 ; Ji et al., 2016; Liu and Zhang, 2014; Zhou et al., 2019). This is described in more detail later.

While the propagation of $\cdot\text{OH}$ is relatively well studied and understood, the same cannot be said of the primary chlorine radical formed by free chlorine photolysis, $\text{Cl}\cdot$. When $\text{Cl}\cdot$ is generated, it reacts with the water itself, chloride (which is always present when the water is chlorinated), and the chlorine, to form an array of possible secondary species, some of which are illustrated in Figure A1-10. These species can react with other natural water constituents, each other, or the contaminants of interest. Our knowledge of this process is incomplete. Ideally, we would be able to use mathematical models to predict the extent to which the $\text{Cl}\cdot$ that is formed by photolysis of chlorine is able to destroy a given contaminant. This would let us estimate how much UV and chlorine is needed under different conditions to destroy the contaminant, leading to cost estimates and comparisons to other potential treatment methods.

But instead, the models that we have are incomplete, and use only estimates for many of the parameters that are needed for the model. There is considerable research underway at present, however, to improve these models, and it is possible that in the near future we will be able to apply these models much more accurately to explore the impact of different treatment conditions on performance.

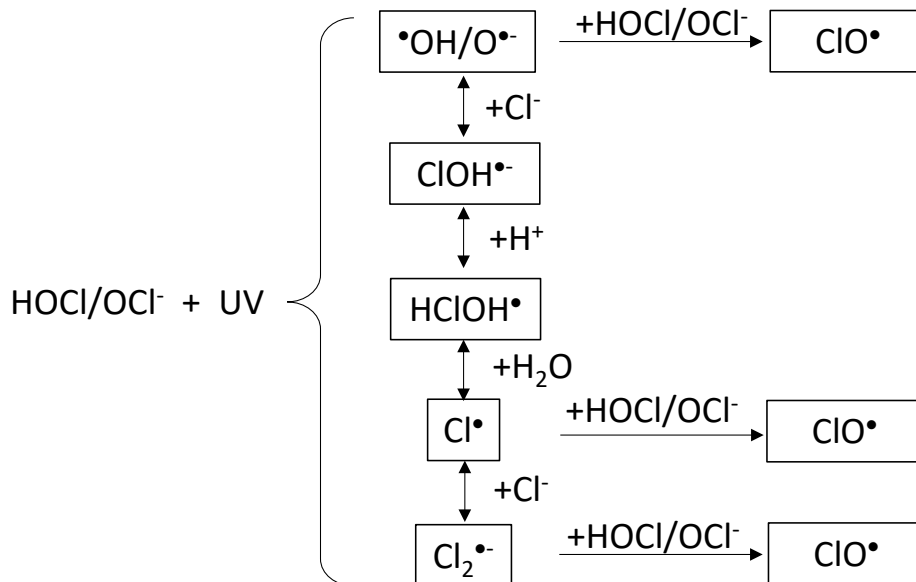


Figure A1-10. Simple Overview of Chlorine Photolysis and Propagation of Reactive Chlorine Species
(adapted from Stefan (2018) with permission from the copyright holders, IWA Publishing).

A1.10 End Reactions and Treatment

The previous section is meant to illustrate that when applying an AOP, there can be a complex series of reactions in addition to the useful step where a radical destroys the target contaminant. For UV- H_2O_2 , these reactions are comparatively well understood, but for UV-chlorine, much of the RCS chemistry is still largely a mystery. At the end of the day, however, both AOP processes result in the formation of a certain amount of radicals that then either react with the target contaminant(s), usually resulting in the destruction of both species, or react with other constituents in the water in a way that eliminates the radical without providing any useful benefit. This latter process is called *radical scavenging* and is analogous to

chlorine demand. Since it is expensive to generate the radicals in the first place, it is usually desirable to try to arrange the treatment in such a way as to minimize the radical scavengers in the water before the AOP is applied. As an example of radical scavenging, Figure A1-11 illustrates that for the river water being considered, organic and inorganic carbon can be important scavengers, but the oxidant itself (H₂O₂ in this case) is also a scavenger. There is therefore a point of diminishing returns in terms of adding more oxidant to render the AOP more powerful. More about the importance of radical scavenging is given later.

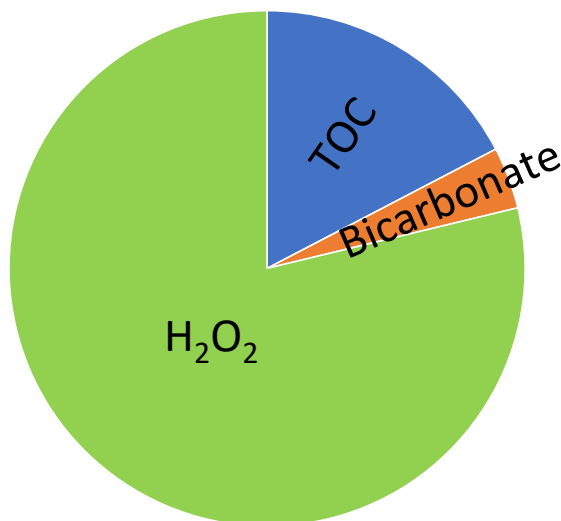


Figure A1-11. Proportion of Hydroxyl Radical Scavengers in UV-H₂O₂ Treatment of River Water.

TOC = 4 mg-C/L, 4 mg/L H₂O₂, 60 mg/L bicarbonate as CaCO₃, pH 7.7.

The ability of the •OH or RCS species to destroy the contaminants of interest is reflected by the bimolecular reaction rate coefficient, *k*. A simplistic illustration of how this works for 1,4-dioxane is given in Figure A1-12.

$$\frac{d[1,4\text{-dioxane}]}{dt} = -k[\bullet\text{OH}][1,4\text{-dioxane}]$$

Figure A1-12. Example of Contaminant Destruction Rate Calculation.

In this equation, the left-hand side indicates how much the concentration of 1,4-dioxane is decreasing per second during treatment where •OH is being generated. This rate is a function of (on the right-hand side of the equation) the current 1,4-dioxane concentration, the amount of •OH in the water, and the reaction rate coefficient, *k*, for the reaction between •OH and 1,4-dioxane. This means that, all other factors being equal, if the *k* value is twice the amount for some other contaminant than it is for 1,4-dioxane, then that other contaminant will be destroyed twice as quickly during AOP treatment. It follows that higher *k* values indicate easier (more cost-effective) treatment for that particular contaminant. A list of *k* values for the reaction of •OH and RCS with many common contaminants is shown in Appendix A. In general,

it has been reported that the compounds that tend to be more reactive with RCS include those that contain electron-donating functional groups (e.g., hydroxyl, amine, alkoxy, alkyl, acyl) (Guo et al., 2017; Gao et al., 2020; Yeom et al., 2021). In contrast, $\bullet\text{OH}$ is able to attack structures with electron-withdrawing groups ($-\text{NO}_2$, $-\text{Cl}$, $-\text{COOH}$) (Yeom et al., 2021).

A1.11 Added Benefits: Direct UV Photolysis and Oxidant Action

In the UV- H_2O_2 and UV-chlorine processes, the UV and the oxidants act, to a certain extent, independently of each other. This is to say that the majority of the UV photons are not absorbed by the oxidants inside a typical UV reactor (Wang et al. 2019), and the oxidants are not completely destroyed by the UV (this is true of H_2O_2 where typically less than 5-20% undergoes photolysis, but it might be possible to achieve more than 50% destruction of chlorine, especially using MP lamps, owing to chlorine's high absorbance at higher UV wavelengths and its high quantum yield of decomposition). This means that a UV-AOP system is a very good UV treatment device. For example, contaminants such as NDMA that are fairly resistant to $\bullet\text{OH}$ reaction but are destroyed by UV, can be eliminated by a UV- H_2O_2 or UV-chlorine system.

This is the rationale behind UV-based AOPs in California's Full Advanced Treatment (FAT) scheme for water reuse treatment. UV-AOP offers a multi-barrier approach given that it can operate through both direct photolysis as well as the formation of free radicals to destroy contaminants. A common question that stems from this is whether a UV-AOP system can be used to claim disinfection credit. This is a more complex issue. First, it should be said that the free radicals such as $\bullet\text{OH}$ and $\text{Cl}\bullet$ are known disinfectants. In fact, $\bullet\text{OH}$ is a dominant disinfectant in natural aqueous environments where it is generated by the reaction of sunlight with various natural constituents (Mattle et al., 2015). There are numerous studies that have demonstrated effective disinfection when generating such radicals deliberately through a variety of means, ranging from applications in ballast water disinfection (Bai et al., 2018), to dental instrument disinfection (Sheng et al., 2014), to the food industry (Hao et al., 2012). In the context of a UV-AOP water treatment process, however, the effect of the UV light itself, and/or the chemical oxidant (chlorine or H_2O_2), is likely to be the main disinfectant in the system. This is because it is thought that the main disinfection mechanism for $\bullet\text{OH}$ and possibly other radicals requires that it first enter into the cell or virus to damage the interior (Watts et al., 1995; Mamane et al., 2007). However, it is postulated that radicals are too reactive with the outer membranes, cell walls, or capsids, to easily penetrate. This has been used as a theory to explain why radical disinfection of bacteria and larger cells is slower than viruses, due to the smaller travel distance across the capsid of a virus (Cho et al., 2005). A study by Mamane et al. (2007) demonstrated that the $\bullet\text{OH}$ component in a UV- H_2O_2 system under typical operating conditions contributed negligibly to the disinfection of bacteria (*E. coli* and *Bacillus subtilis* endospores) and some viruses (T4) but did lead to a measurable reduction in T7 and MS2 virus inactivation. Nevertheless, it can be calculated that the rates of inactivation of such microorganisms as reported by a range of studies, which tend to be in the order of 10^{11} - 10^{14} $\text{M}_{\text{OH}}^{-1}\text{min}^{-1}$, lead to expected inactivations of microorganisms of about 1-log when exposed to UV-AOP conditions for about 20-40 seconds (calculated from data reported by Rattanukul and Oguma, 2017; Mamane et al., 2007; Mattle et al., 2015; and Lankone et al., 2020). During 20-40 seconds of

exposure to the intense UV light of a UV-AOP, the expected log inactivation due to the UV alone would be substantially greater. As such, it is likely sufficient to base predictions of disinfection performance of a UV-AOP system solely on the basis of UV exposure, ignoring the likely small additional role of the radicals. This issue remains, however, poorly explored, and it's possible that under certain specific conditions, or for certain specific organisms, the importance of the radicals might be significant.

When considering the disinfection effectiveness of UV in a UV-AOP reactors, it is first obvious that the UV doses are significantly higher than in traditional UV disinfection systems (e.g., 800 mJ/cm² compared to 40 mJ/cm² for disinfection). Logically, this would imply that a UV-AOP reactor would be much more effective at disinfection than a UV disinfection reactor. However, UV-AOP reactors may be designed to remove no more than 90-99% of a contaminant (1-2 logs). Disinfection UV reactors, however, may require 99.9%-99.9999% inactivation of pathogens (3-6 logs). Studies of UV reactor hydrodynamics and dose distributions can prove that when operating to low log reductions (e.g., 90%), it is sufficient that the average UV dose delivered by the reactor be high enough to destroy the contaminant. The possible presence of minor "low UV dose" flows that short-circuit the reactor are not important. But when treating the water to achieve high log reductions (e.g., 99.99%), it is necessary that the UV reactor have almost no possibility for even a tiny fraction of the flow to achieve anything less than the desired dose—for example, no small stream that short-circuits the reactor quickly through a region that is farthest away from the lamps. Proving the absence of such low-dose streams is the focus of UV reactor validation testing for claiming disinfection credit from regulatory agencies. While it is possible for a UV manufacturer to subject their UV-AOP reactor for disinfection validation testing, this is not necessarily done as a matter of course. While intuitively one can make an educated guess that a UV-AOP reactor must surely also meet common disinfection targets, this remains something of a gray area. More on this topic is provided later.

Just as a UV-AOP system can behave as a strong UV photolysis reactor due to the largely independent behavior of the UV and the oxidants, the oxidants themselves (i.e., H₂O₂ or chlorine) will impact the overall performance of the treatment process. However, the amount of their impact might normally be small. The main reason is that, typically, the oxidant is added only immediately upstream of the UV reactor. As such, there is only very limited reaction time—likely only in the order of seconds to tens of seconds—to cause any chemical change to the water. In the case of UV-H₂O₂, the hydrogen peroxide is generally a very poor direct oxidant. While it has a high standard oxidation potential (1.78 V) (Glaze, 1990), it tends to have very slow reaction kinetics. In the case of free chlorine, there is much more chance for direct oxidation reactions to occur. For example, the interaction between chlorine and chloramines is an important design and operational issue for water reuse treatment using UV-chlorine AOP after RO that has been treated with chloramines for fouling control. The oxidation of iron by chlorine is also practically instantaneous. Possibly of some importance is the reaction between free chlorine and organic matter prior to entering the UV reactor. Preoxidation by free chlorine could lower the subsequent radical scavenging capacity of the organic matter. This is a topic that has not been well reported in the literature, but one can imagine optimizing the UV-chlorine AOP by allowing the chlorine sufficient pre-contact time to reduce the scavenging demand within the reactor. A related issue is the UV transmittance (UVT) of the water. UV

reactor efficiency is strongly influenced by the water's UVT, with even small increases in UVT translating into large improvements in efficiency. Chlorine can attack chromophores in organic matter that block UV light transmission, so again, there may be benefits in studying whether applying chlorine sufficiently upstream of the UV reactor to improve the UVT of the water is desirable. No information on this topic, however, could be identified in the literature, and it remains an area in need of research.

A1.12 UV-AOP Sizing and Dose Definition

Considering that the design water quality parameters are fixed by the designer, the sizing of a UV-AOP system is limited to two variables: the ability to deliver a UV dose (fluence) and the oxidant dose. Manufacturers use proprietary models to determine the optimal UV-AOP sizing and operation of their systems (i.e., applied UV dose and oxidant dose). Differing approaches between manufacturers can make direct comparison of the performance and costs of various UV-AOP systems difficult. One difficulty arises due to the determination of "UV dose," which with respect to a full-scale reactor, is the reduction equivalent dose (RED). Thus, UV dose is specific to the chemical or biological actinometer such that there are many different types of UV doses (e.g., MS2 dose, NDMA dose, H₂O₂ dose, atrazine dose, etc.). Because most practitioners are accustomed to the term "UV dose" as it relates to disinfection, there can be confusion because the same reactor under identical flow conditions can have different delivered UV dose values based upon the target contaminant. For this and other reasons, designers should take care in specifying UV dose targets for design of UV-AOP systems.

A1.12.1 Approaches to UV Equipment Sizing

There are several general approaches used for UV-AOP equipment sizing. The first is development and use of a reactor-specific deterministic model that uses an empirically measured scavenging factor (dependent upon site-specific water quality) to determine combinations of UV and oxidant doses that will meet the treatment objective. The second is a purely empirical approach that leverages a laboratory and pilot-scale data set to determine the minimum UV dose and oxidant concentration required to achieve the treatment objective, coupled with a reactor validation using the target contaminant as the actinometer. In either case, the manufacturer will need water quality data and the treatment objective(s) to size a reactor and develop a cost proposal.

Deterministic modeling using a scavenging factor. Because of the challenges of actinometry at high UV REDs, some manufacturers have developed deterministic models that account for the many factors that must be considered in sizing a UV-AOP reactor. These equations account for the kinetics of photosensitized reactions where UV light is absorbed by an oxidant to form a radical (e.g., •OH), which then reacts with a contaminant. These radicals may also react with scavengers. The details of these models are proprietary, but the ultimate output of the models is a report from the manufacturer on the conditions needed (i.e., UV power and oxidant concentration) to destroy a desired amount of the contaminant under different water quality conditions.

A1.12.2 Dose Per Log, EED and EEO

Because the relationship of log removal of a contaminant as a function of UV dose is linear, Bircher (2011) introduced the dose per log (D_L) concept, which some manufacturers have found useful in the scale-up of bench-scale results to full-scale UV reactors. However, the UV dose calculations for these applications do differ from disinfection applications. In the AOP application, the UV dose required per log removal is calculated based on the absorbance of the oxidant or target contaminant. Thus, D_L is a water quality parameter describing the number of photons needed to be absorbed by the activator chemical (oxidant) to destroy 90 percent of the target contaminant in a site-specific water. It is proportional to the number of photons required to be *absorbed* by the activator and can be used as a relative indicator of how easy it is to achieve the treatment objective for various contaminants in a site-specific water. For example, to degrade a more recalcitrant target contaminant will require a larger number of radicals and will thus have a higher D_L . Anything in the water that interferes with the AOP (e.g., radical scavengers) will lead to a higher D_L .

Because the D_L is solely a property of the water being treated (including the target contaminant and activator chemical), in theory the D_L calculated using a lab- or bench-scale test will be the same as the D_L for a full-scale reactor treating the same water. In this way, D_L is used to scale up. But this relationship can be difficult to accurately simulate with UV- Cl_2 given the potentially dynamic nature of the chlorine chemistry (e.g., when ammonia is present and chloramine formation and destruction changes from the feed point to the entrance to the reactor). This phenomenon is discussed further in a following section.

Another important concept in UV-AOP system characterization is E_{ED} and E_{EO} . These are figures-of-merit that have been developed to reflect the efficiency of a given reactor in terms of the electrical energy in driving the degradation processes (Bolton and Collins, 2016). First is the concept of electrical energy dose (E_{ED}), which is defined as the electrical energy (kWh) consumed per unit volume (e.g., 1 m³ or 1,000 gal) of water treated. A reactor delivers a certain E_{ED} when operating at a given flow rate. E_{ED} is independent of the contaminant treatment or water quality.

Combining E_{ED} with the log reduction of the contaminant undergoing treatment leads to electrical energy per order (E_{EO} ; Bolton et al. 2001). Recommended by the Photochemistry Commission of International Union of Pure and Applied Chemistry (IUPAC), E_{EO} has also been widely used. E_{EO} describes the efficiency of a UV-AOP technology as the amount of electricity needed to be given to the lamps to produce enough radicals to ultimately destroy 90 percent (1-log) of the target contaminant in a unit volume of water. The term is typically expressed in units of kWh/m³-log or kWh/kgal-log. It is notable that E_{EO} is a function of water quality, UV reactor, oxidant concentration, lamp type, and contaminant. It depends on several reactor- and application-specific factors, including the hydraulic and optical design of a reactor, which also affects the AOP efficiency, and thus E_{EO} and power requirements. Importantly, the E_{EO} for a system is also specific to the type and concentration of the oxidant used because different chemicals absorb photons, produce radicals, and scavenge radicals with different efficiencies. Knowing the full-scale E_{EO} for a reactor in a given contaminant treatment scenario leads to full scale sizing (i.e., the amount of energy required at a given oxidant concentration to

accomplish target treatment). In fact, E_{EO} can be calculated as a function of delivered UV dose as described in Stefan (2018).

This text includes a description of the above terms to enable the reader to understand terminology used by UV-AOP manufacturers. Each uses a different approach to scale up. Given uncertainties in accuracy of sizing, the equipment specification should require performance testing following installation and that the manufacturer pay damages (in the form of performance penalties) if the guaranteed, manufacturer-sized, UV system fails to accomplish treatment targets.

CHAPTER A2

Effect of Water Quality

A2.1 Radical Scavenging

The goal of the AOP is to generate radicals (predominantly $\cdot\text{OH}$, but also reactive chlorine species (RCS) and others to a lesser extent), which can then react with and destroy the target contaminants. As discussed previously, the radicals typically react indiscriminately, and many will react with other material in the water instead of the targets, leading to inefficiencies. This is similar to chlorine demand: a high enough chlorine dose must be applied to satisfy the background demand, thereby allowing enough free chlorine residual to persist to accomplish treatment. In a similar way, the AOP dose must be high enough to generate enough radicals such that after accounting for those that are “scavenged” unproductively by other components in the water, the remaining radicals can do the job. The typical radical scavengers that exist in water can include organic matter, inorganic carbon (carbonate and bicarbonate), nitrite, chloramines, the oxidants/initiators themselves (chlorine or H_2O_2), bromide, and others.

Technically, a discussion of this topic should differentiate the scavenging demand that’s exerted on each different radical. In other words, the water might have a certain scavenging demand for $\cdot\text{OH}$ that is different from the scavenging demand for the chlorine atom radical, etc. However, there are no practical methods to differentiate the scavenging demands for the different radicals, and furthermore, the role of radicals other than $\cdot\text{OH}$ is, at present, arguably too difficult to predict to account for in the design of a system. As a result, it is likely practical to consider only $\cdot\text{OH}$ scavenging demand as part of the design and operation of an AOP system.

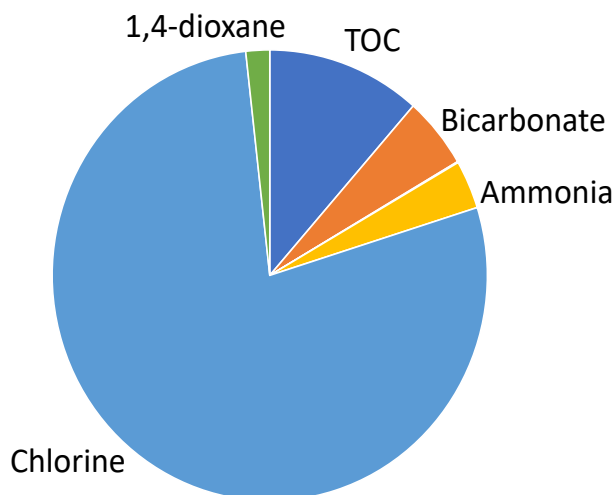
The amount of $\cdot\text{OH}$ scavenging in a water is defined, in practice, as the sum of the products of the various species in the water that react with $\cdot\text{OH}$ when multiplied by their reaction rate coefficients. The unit of measurement is s^{-1} . In other words, pure water containing 0.001M bicarbonate and 1×10^{-6} M TCE ($k_{\text{OH},\text{HCO}_3^-} = 8.5 \times 10^6 \text{ M}^{-1}\text{s}^{-1}$, $k_{\text{OH},\text{TCE}} = 4 \times 10^9 \text{ M}^{-1}\text{s}^{-1}$) would exhibit an $\cdot\text{OH}$ scavenging demand of:

$$\begin{aligned} \cdot\text{OH} \text{ scavenging demand} &= (0.001\text{M})(8.5 \times 10^6 \text{ M}^{-1}\text{s}^{-1}) + (1 \times 10^{-6}\text{M})(4 \times 10^9 \text{ M}^{-1}\text{s}^{-1}) \\ &= 8500 \text{ s}^{-1} + 4000 \text{ s}^{-1} = 12,500 \text{ s}^{-1} \end{aligned}$$

The first term (= 8500 s^{-1}) represents the amount of $\cdot\text{OH}$ scavenged by bicarbonate, and the second term (= 4000 s^{-1}) represents the amount reacted with TCE. In other words, roughly twice as much of the $\cdot\text{OH}$ reacts unproductively with bicarbonate as reacts with TCE under these conditions. If water can be treated prior to the AOP process to remove some of the radical scavengers, there may be cost savings for the AOP.

Taking this concept further, the example in Figure A2-1 shows a fictive water containing various species that consume $\cdot\text{OH}$, along with 1,4-dioxane that is used as an example of a target contaminant. Here, we see that most of the scavenging is due to the 3 mg/L chlorine added as part of the UV-chlorine AOP, whereas the second greatest scavenger is the 2 mg-C/L TOC. Only

2% of the $\cdot\text{OH}$ reacts as desired with the target of 1,4-dioxane. RO permeate might contain much less TOC than in this example, so typically the main scavenger in RO-treated water is the oxidant itself (chlorine or H_2O_2). For water being treated for reuse following an ozone-CBAT process, or for UV-chlorine treatment for drinking water, the TOC is likely to be an important scavenger.



Species	Concentration	k_{OH} ($\text{M}^{-1}\text{s}^{-1}$) or ($\text{C}^{-1}\text{s}^{-1}$)	% reacting with $\cdot\text{OH}$	Reference
TOC	2 mg-C/L	1.3E8	11	Stefan,2018
Bicarbonate	60 mg/L as CaCO_3	8.5E6	5	Buxton et al. 1968
Nitrate	5 mg-N/L	4.0E5 ¹	0	Yin et al. 2020 ¹
Ammonia	1 mg-N/L	9.7E7	3	Yin et al. 2020
Chlorine	3 mg- Cl_2 /L	2E9 (HOCl) 9E9 (OCl ⁻)	78	Buxton and Subhani, 1972 Anastasio and Matthew, 2006
1,4-dioxane	0.1 mg/L	3.1E9	2	Patton et al. 2017

¹This reaction rate coefficient is cited from a secondary source and whose primary source is ambiguous. Evidence suggests nitrate is typically a negligible hydroxyl radical scavenger.

Figure A2-1 Example of Contributions to Hydroxyl Radical Scavenging for a Fictive Water Treated with UV-Chlorine

The amount of radical scavengers in a water to be treated is a critical design parameter, since it dictates the AOP dose that must be applied to generate sufficient radicals to destroy the target contaminants. Unfortunately, the relationship between the radical scavenging of the water and the AOP system design is something that, at present, can only be interpreted by complex UV reactor models that are generally kept confidential by UV equipment manufacturers. In other words, while customers and consultants can understand in a general sense that waters with more scavenging potential are going to be more expensive to treat, the exact details of this relationship can only be provided by manufacturers.

There are two methods to estimate the radical scavenging potential of a water. When most of the radical scavenging is due to known and quantifiable compounds, the scavenging parameter can be calculated theoretically following the examples just given. For example, RO permeate is typically very low in organic matter (< 1mg-C/L), and most of the scavenging will be due to chlorine and chloramines used to prevent RO membrane fouling. These chemicals can all be measured or estimated, and they have well-known reaction rate coefficients with •OH. Care should be taken, however, to consider that most reaction rate coefficients were determined in a laboratory at room temperature. Reaction rates in cold water near freezing may be lower, potentially by 10-20% in one study (Wang et al., 2018a).

For waters where organic matter is likely to be a significant scavenger, the theoretical approach will likely not be accurate. This is because water can contain many different types of organic matter, and each type will react with a different reaction rate coefficient with •OH, often in the order of 10^3 - 10^4 (mg-C/L DOC)⁻¹ s⁻¹ but sometimes extending well outside of that range. As such, the second method to estimate the radical scavenging potential of a water is through direct measurement. At present, however, there is no official protocol to do so, but research methods have been reported in the literature. The reader is directed to Wang et al. (2020a) and Kim et al. (2021) for more information.

It is important to recognize that if water quality is known to vary with time, the radical scavenging potential will also likely vary. As part of the preliminary design process for a new AOP system, the potential variation in this parameter must be considered to ensure that the resulting AOP system can achieve its treatment goals over the range of expected water quality conditions. Unfortunately, there is very little information available about the potential variability in this parameter, especially when influenced by changing organic matter quantity or character. As a single point of reference, the authors of this report have monitored the hydroxyl radical scavenging in Lake Ontario water over the course of a year and found the value to vary by more than twofold between 3 and 8 x 10⁴ s⁻¹. As such, it is difficult to offer advice about the factor of safety that should be included in a design to account for an uncertain amount of radical scavenging. Given the importance of this parameter when sizing an AOP system, efforts should be taken to estimate it as accurately as possible.

A2.2 UV Transmittance (UVT)

UV transmittance is defined as the fraction of light at a specific wavelength that passes through a medium (water in this case) over some specific distance (typically 1 cm). The units of measurement are therefore typically % per cm. A clean water such as an RO permeate may have a UVT at 254 nm (UVT₂₅₄) of greater than 99 % cm⁻¹, whereas the UVT of an untreated wastewater may be below 30 % cm⁻¹. Sometimes the ability of photons to travel through water is expressed by UV absorbance (A), which is related to UVT by:

$$\text{UVT (\% cm}^{-1}\text{)} = 100 \times 10^{-A \text{ (per cm)}}$$

The UVT of a water will profoundly impact the treatment cost of a UV-AOP, since a low UVT implies that photons are being absorbed wastefully. The exact relationship between UVT and reactor design (and therefore treatment cost) is only available in a manufacturer's proprietary

model, at present. To help to ensure that those models are used accurately, however, stakeholders can collect accurate estimates of the UVT of the water to be treated. As with radical scavenging, the UVT can vary with time and it is affected by not only the natural constituents in the water, but also by many treatment chemicals that can be applied. For example, monochloramine that is used as an antifoulant for RO may be present in RO permeate and can contribute significantly to a reduction in the UVT of the water to be treated by UV-AOP. Stakeholders in a UV-AOP design should therefore work towards ensuring that the range of UVT that may occur both naturally in the water and as affected by potential treatment chemicals be considered.

A2.3 Ammonia, Chloramines, Nitrate, and Nitrite

Ammonia concentrations in municipal wastewater are often in the range of 20-40 mg-N/L. During conventional wastewater treatment, some of the ammonia may be converted to nitrite or nitrate depending on whether nitrification/denitrification processes are employed. The resulting effluent that could serve as the source for water reuse treatment may therefore contain a range of ammonia, nitrate, or nitrite.

If reuse treatment were to consist of an ozone-CBAT train followed by UV-AOP, it is likely that ozonation would convert any influent nitrite to nitrate, but otherwise, the removal of the remaining ammonia or nitrate might be inconsistent and difficult to predict across the ozone and BAC processes, with likely a large fraction left to enter the UV-AOP. If reuse treatment were accomplished with a *full advanced treatment* (FAT) process, it is possible that chloramines would be applied to prevent RO fouling. The applied free chlorine for chloramine generation would convert the majority of incoming ammonia to chloramines, while nitrite would theoretically be quickly oxidized to nitrate. However, measurements in a pilot UV-chlorine AOP facility demonstrated that nonideal mixing of chlorine into solution could allow nitrite to escape immediate oxidation (Kwon et al., 2020). Ammonia and nitrite are not completely removed by the RO, with reports of percent removal varying widely among different RO installations. It is therefore possible that both ammonia and nitrite may exist in RO permeate, despite the upstream application of free chlorine to generate chloramines.

In summary, it is expected that when applying UV-AOP to serve for water reuse treatment, there will be a possible influx of nitrate, nitrite, ammonia, and chloramines into the UV reactor. There is also the potential for low concentrations of organic amines to be present in the water that may behave similarly to chloramines, but little is known about this at present. As an additional complication, there is also the potential for nitrate or chloramines to be photolyzed by UV to nitrite *within* the UV reactor. Nitrite is an extremely strong radical scavenger so this can affect treatment.

The effect of ammonia, chloramines, nitrate, and nitrite on UV-AOP treatment is explained in the following sections. Much of the discussion revolves around how quickly the various species react with each other, and with chlorine and H₂O₂, with the speed of these reactions varying with concentrations of the reagents, pH, and temperature. This can be very complex, and an accurate prediction of the effects of the various compounds requires reaction kinetic modelling. It should also be cautioned that nonideal mixing could allow some species to persist despite the

mathematics suggests that they should react immediately (e.g., nitrite as mentioned in the preceding paragraph). A reaction kinetic model is provided in an appendix and is left to the stakeholder to use at their discretion since the model has never been validated under the conditions of low pH and particular ratios of free chlorine and chloramines present in a FAT system. For now, the following discussion draws broad conclusions about these reactions under typical and idealized conditions to illustrate the general trends that can be observed, and to emphasize how important this chemistry is to the performance of a UV-chlorine AOP when these nitrogen species (especially chloramines) are present. The main outcomes of this discussion are illustrated in Figure A2-2.

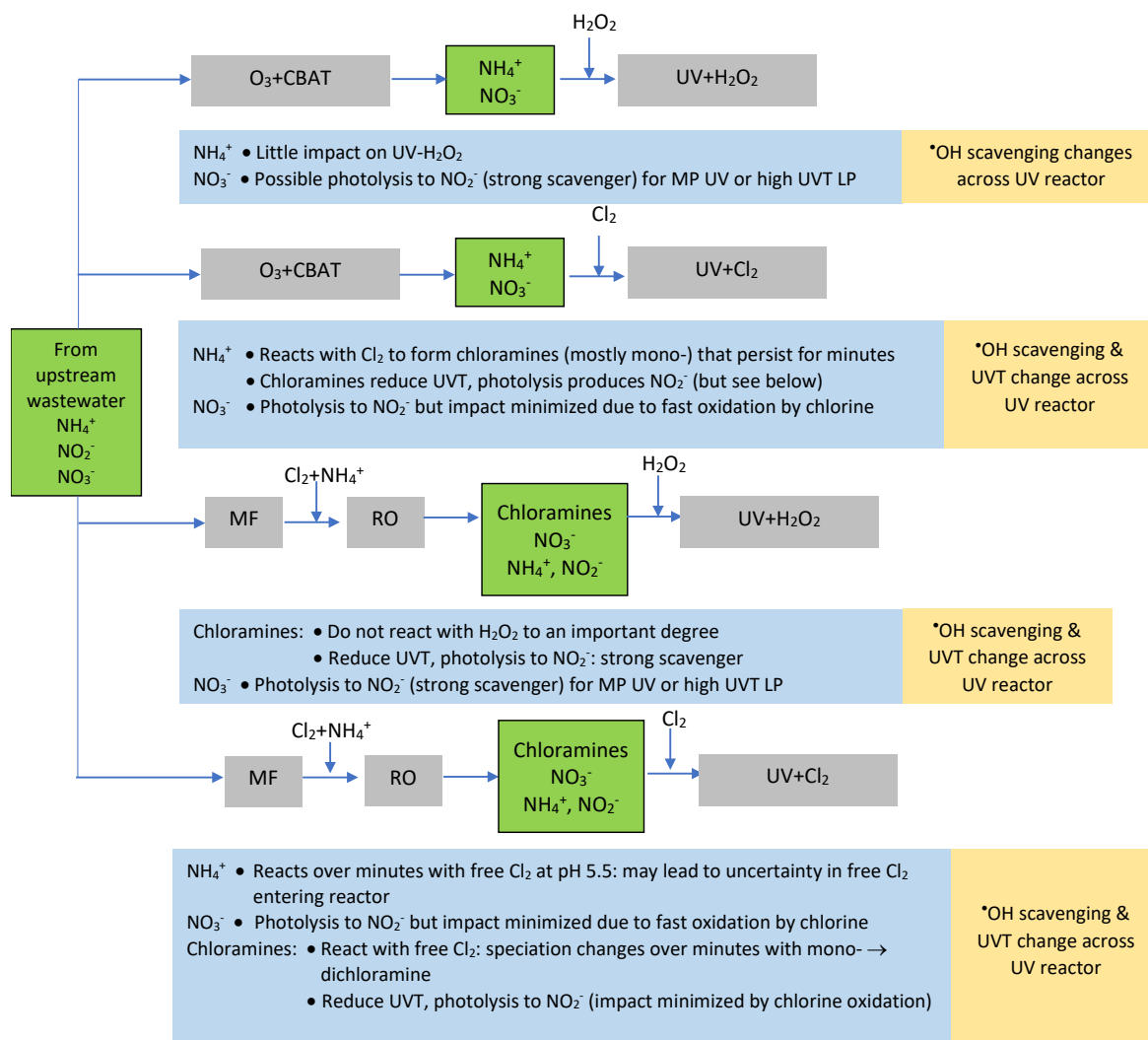


Figure A2-2. Summary of the Role of Nitrogen-Containing Species in UV-H₂O₂ and UV-Chlorine AOPs Following Upstream Ozone-CBAT or RO Treatment.

A2.3.1 UV-H₂O₂ AOP

For a UV-H₂O₂ system, the implications of nitrogen species can include potential reactions with H₂O₂ itself, impacts on UVT, and impacts on radical scavenging. Fortunately, H₂O₂ is relatively inert with respect to nitrate, ammonia, and chloramines (the half-life of the reaction between

H₂O₂ and chloramines at typical concentrations and conditions would be in the order of many hours to days (Wang et al., 2020b)). As such, direct reaction of these species with H₂O₂ can reasonably be discounted. In terms of UVT, ammonia and nitrate will have little or no impact due to their low molar absorptivity at 254 nm, as shown in Figure A2-3, although if nitrate is present at very high concentrations it could interfere with H₂O₂ photolysis in the 230-250 nm range of a MPUV system (compare Figure A1-4 and Figure A2-3). Chloramines, however, can contribute significantly to a reduction in UVT at both 254 nm (for LPUV systems) and over the wider range of wavelengths if using a MPUV system (Figure A2-3). If chloramines are present in the influent to a UV-H₂O₂ system, their effect on UVT must therefore be considered.

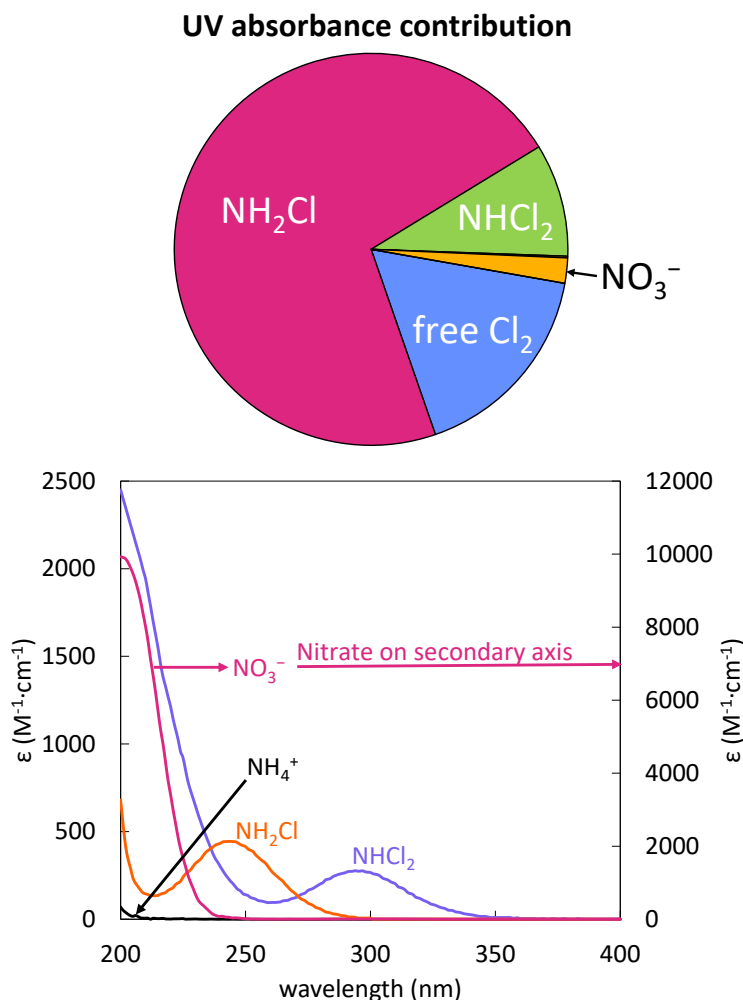


Figure A2-3. (Top) Example of Percent of Photons Absorbed at 254 nm by Various Constituents in a Fictive RO Permeate Containing 5 mg/L Free Chlorine, 3 mg/L Monochloramine, 4 mg/L Dichloramine, and 1.5 mg-N/L Nitrate. (Bottom) Absorption Spectra for Ammonia, Nitrate, Monochloramine, and Dichloramine.

The most significant impact of nitrogen species on UV-H₂O₂ treatment is likely to be radical scavenging. The reaction rate coefficients between [•]OH and the various species are shown in Table A2-1, along with their illustrative percent contributions to [•]OH scavenging. It can be

determined that, under some conditions, a considerable fraction of the overall $\bullet\text{OH}$ scavenging can be due to chloramines, with likely only very minor contributions by nitrate or ammonia.

Table A2-1. $\bullet\text{OH}$ Scavenging of Nitrogen Species Post-RO (pH 5.5).

Species	Concentration	k_{OH} ($\text{M}^{-1}\text{s}^{-1}$)	Contribution to $\bullet\text{OH}$ scavenging	
			UV- Cl_2 system	UV- H_2O_2 system
Hydrogen peroxide	3 mg/L	2.7E7	NA	3%
Free chlorine	5.9 mg/L as Cl_2	2.0E9 HOCl, 8.8E9 OCl^-	68%	NA
Monochloramine	3.9 mg/L as Cl_2	1.0E9	22%	65%
Dichloramine	3.0 mg/L as Cl_2	6.2E8	10%	31%
Nitrate	1.5 mg-N/L	4.0E5 ²	< 1%	<1%
Nitrite	Footnote (1)	1.1E10	Footnote (1)	Footnote (1)
Ammonia (NH_3)	0.1 mg-N/L ³	9.7E7 ²	< 1%	< 1%

¹Nitrite likely to be present only in ozone-CBAT systems with UV- H_2O_2 , since in a FAT system, free chlorine added to form chloramines to prevent RO fouling quickly converts nitrite to nitrate. Nitrite at 0.1 mg-N/L would represent 24%-48% of the overall $\bullet\text{OH}$ scavenging of the water shown above for UV- Cl_2 and UV- H_2O_2 respectively.

²Yin et al. (2020). This reaction rate coefficient is reported in a secondary source from an ambiguous primary source, but evidence suggests that the rate is negligible.

³Reports suggest that $\bullet\text{OH}$ is only reactive with NH_3 and not NH_4^+ , so this estimate that assumes all ammonia in the NH_3 form is likely an over-estimate of the scavenging by ammonia in this water (Huang et al., 2008a).

The design of a UV- H_2O_2 system must therefore carefully consider the potential for these compounds to be present. Furthermore, there is a potential complication for UV- H_2O_2 treatment depending on the circumstances. While it was mentioned earlier that it is unlikely for nitrite to be present in a water reuse stream that arrives for UV-AOP treatment, when nitrate and chloramines are photolyzed in the UV reactor they can produce nitrite. Nitrite is an extraordinarily strong $\bullet\text{OH}$ scavenger (Table A2-1). If a UV reactor design were to be based on the $\bullet\text{OH}$ scavenging capacity of the water *as it enters* the UV reactor, and if nitrate and/or chloramines are present, there will be an *underestimation* of the actual radical scavenging *inside* the reactor due to the formation of nitrite. This phenomenon must be considered via UV reactor modelling during the design phase if there is the potential for nitrite formation in the reactor due to chloramines or nitrate. Note that this phenomenon is likely to only be important for UV- H_2O_2 since the free chlorine and the ClO^\bullet radical in a UV-chlorine AOP would suppress nitrite formation (Stefan, 2021). Nitrate photolysis to nitrite is often thought to be associated only with medium pressure lamps since nitrate photolysis is strongest in the 200-240 nm range, where LP lamps have minimal emission, unlike MP lamps. However, there is little definitive information published on this topic. Medium pressure lamps are often spaced far apart (relatively speaking) in a reactor due to their high intensity, and natural water often contains material that absorbs UV in the 200-240 nm range. As such, the wavelengths associated with MP lamps that would convert nitrate to nitrite may not penetrate far into the water, making nitrite formation inefficient. Furthermore, there is anecdotal information that in waters with a very high UVT at 254 nm such as RO permeate (e.g., >98% cm^{-1}) and with high nitrate, there is the potential for nitrite formation even when using LP lamps. In contrast, photolysis of chloramines to form nitrite can occur with both LP and MP systems.

In summary, for UV- H_2O_2 systems, the impact of nitrogen species is that they can reduce the UVT of the water (primarily due to monochloramine) and increase $\bullet\text{OH}$ scavenging (primarily mono- and dichloramine)—and, importantly, both the UVT and the $\bullet\text{OH}$ scavenging can *change*

within the UV reactor as the nitrogen species are photolyzed. An accurate estimate of the performance of the UV-H₂O₂ AOP during the design stage may therefore need to account for these changes within the reactor through reactor modelling.

A2.3.2 UV-Cl₂ AOPs

For UV-chlorine systems, the effect of nitrogen species is more complicated than for UV-H₂O₂ because unlike H₂O₂, free chlorine is reactive with some of the species. Both the basic chemistry and the practical implications are summarized here.

Role of ammonia. Free chlorine reacts with ammonia very quickly with a maximum rate around pH 8, but the rate decreases dramatically at lower and higher pH values. The observed reaction kinetics between free chlorine and ammonia reported by Weil and Morris (1949) and Huang (2008a) suggest that at pH 8 and with typical concentrations of free chlorine (3 mg-Cl₂/L) and ammonia (0.5 mg-N/L), the reaction half-life is in the order of a tenth of a second. At pH 5, however, the half-life increases to the order of about 2 minutes. Non-ideal mixing may also slow this reaction. Based on this information, it is possible for ammonia in low pH RO permeate to co-exist with free chlorine and enter the UV reactor if the reactor is placed very close to the RO. The implications include the following:

- **UVT:** ammonia has a very low UV absorbance (Figure A2-3Figure 3-2) so its presence at typical concentrations is not expected to interfere with the photolysis of the oxidants or contaminants.
- **Reaction with free chlorine:** At the low pH (≈ 5.5) associated with RO permeate, the reaction between ammonia and free chlorine can take minutes to complete. Ammonia can therefore exert a continuing free chlorine demand downstream of RO. Chlorine and ammonia react with a 1:1 stoichiometric (molar) ratio to form monochloramine. This is a 5.1mg-Cl₂/L: 1 mg-N/L mass ratio. Thus, 1 mg-N/L ammonia will consume 5.1 mg-Cl₂/L within several minutes at pH 5.5, but it reacts over seconds at neutral pH. The need to maintain a target free chlorine residual within the UV reactor must therefore consider this potential free chlorine demand if ammonia is present, and also consider that the reaction may not be effectively instantaneous at low pH. This has implications on the location of water quality sampling, since the free chlorine measured shortly after application may be considerably higher than the free chlorine entering the UV reactor tens of seconds later if ammonia is present.
- **Radical scavenging:** Ammonia is not a strong •OH scavenger. Huang et al. (2008a) report that scavenging is due largely to molecular ammonia (NH₃) and not the NH₄⁺ ammonium ion. Therefore, while the reaction rate coefficient between NH₃ and •OH is reasonably fast ($9.7 \times 10^7 \text{ M}^{-1}\text{s}^{-1}$), given that the pKa of the ammonium ion is 9.3, there is likely to be very little NH₃ in the water under typical conditions (pH 5.5-8). Table A2-1 illustrates that for a fictive RO permeate, ammonia contributes to less than 1% of the •OH scavenging.

Role of chloramines. Chloramines can come from two sources. If ammonia is present in the water arriving at the AOP system, it reacts with free chlorine to form monochloramine within seconds to minutes as described in the previous section. Alternately, chloramines may be applied to control RO membrane fouling, and their rejection by the RO is incomplete (e.g., 0-

50% at some facilities surveyed as part of this project). Recall from the previous section that the stoichiometric ratio of free chlorine required to convert ammonia to monochloramine is 1:1 molar, or 5.1 mg-Cl₂/L : 1 mg-N/L. If free chlorine is added at higher doses than this stoichiometric amount, the monochloramine that is formed will react with that extra free chlorine to produce other chloramine species (mostly dichloramine), but the excess free chlorine will also continue to react with the mono- and dichloramine to eventually destroy much of these species in the process. The ammonia/chloramines are converted to mostly to N₂ with small amounts of NO₃⁻ (e.g., <20% N) (Jafvert and Valentine, 1992; Jeong et al., 2014; Phillip and Diyanamdoglu, 2000). The stoichiometric amount of free chlorine required to destroy chloramines is approximately 0.5:1 molar, or 2.6 mg-Cl₂/L : 1 mg-N/L. Overall, therefore, the amount of chlorine required to drive the reaction to convert ammonia through chloramines and all the way to N₂ and NO₃⁻ is about 1.5:1 molar, or 7.6 mg-Cl₂/L : 1 mg-N/L (i.e., 1:1 molar chlorine to ammonia to initially form the chloramines, and then another 0.5:1 molar chlorine to chloramines to destroy those chloramines: = 1.5:1 total).

This overall process is known as **breakpoint chlorination** and is explained in most water treatment engineering textbooks. The explanation that is given in such textbooks, however, is typically in the context of conventional drinking water or wastewater treatment where the amount of time available for free chlorine to react with ammonia and chloramines is in the order of many minutes to an hour or more. At such time scales, the fact that these reactions require a number of minutes to complete is often ignored: the reaction is described as essentially “instantaneous”, implying that if free chlorine is applied to water containing ammonia and/or chloramines at a concentration exceeding the 1.5:1 (molar) stoichiometric amount, all ammonia and chloramines will be destroyed, leaving only a free chlorine residual. In the context of UV-AOP treatment for reuse, this is misleading. The exact chemistry that exists in the first few dozens of seconds following addition of free chlorine to water containing ammonia and/or chloramines is critical, since this is when the water will likely enter the UV reactor. Importantly, under these conditions, the reaction between free chlorine and chloramines to destroy the chloramines is *not instantaneous*. It can take many minutes, or even many hours, depending on the pH, temperature, and concentrations involved.

This evolution of breakpoint chemistry as a function of time is illustrated in Figure A2-4 and is based on the breakpoint chlorination reaction kinetic model provided in a subsequent appendix. Figure A2-4 shows the chlor(am)ine speciation between RO permeate and a UV reactor positioned up to 3 minutes downstream of chlorine application. The RO permeate contains 2 mg-Cl₂/L monochloramine and 0.5 mg-N/L ammonia, and 8 mg-Cl₂/L free chlorine is applied. It can be observed that in the first few dozens of seconds, the ammonia reacts with free chlorine to form monochloramine, but then over the next few minutes the free chlorine continues to react with monochloramine to form dichloramine. When the mixture arrives at the UV reactor and enters, the various chlor(am)ine species undergo photolysis reactions. The implications are as follows:

- **UVT:** Using Figure A2-4 as an example, it can be observed that as the UV reactor is placed farther downstream of the point where free chlorine is added to the RO permeate, the UVT at 254 nm increases. This is because monochloramine is initially present in the water, and it

is very effective at absorbing UV light (Figure A2-3/Figure 3-2). As free chlorine reacts with monochloramine to form dichloramine or other end products, the overall UVT increases (dichloramine is not a very efficient UV absorber). While this is beneficial in terms of better UV reactor performance, it comes at the cost of a lower free chlorine residual—which, in turn, lowers advanced oxidation performance. There is therefore likely to be an optimum distance (time) between the point of free chlorine injection and the UV reactor to maximize performance. Determining this optimum location requires modelling of the breakpoint chlorination chemistry and the UV reactor. Note that this optimum should ideally also reflect the rapid photolysis of the chloramine species within the UV reactor (shown in Figure A2-4). As the chloramines are photolyzed, the UVT increases. If this is not accounted for in the UV reactor model, the model will tend to underpredict performance.

- **Chlorine demand:** The design of the UV-chlorine AOP reactor requires assumptions about the concentration of free chlorine entering the reactor. Ammonia and chloramines exert a chlorine demand that increases with reaction time over the timeframe that will likely be present between the point of chlorine addition and the reactor. This must be accounted for.
- **Radical scavenging:** As illustrated in Table A2-1, the contribution of the chloramines to overall radical scavenging may be large. The design of the UV reactor must therefore consider the speciation of the chloramines that enter the reactor, and potentially also include the expected variation in those concentrations across the UV reactor as the chloramines are destroyed through photolysis.

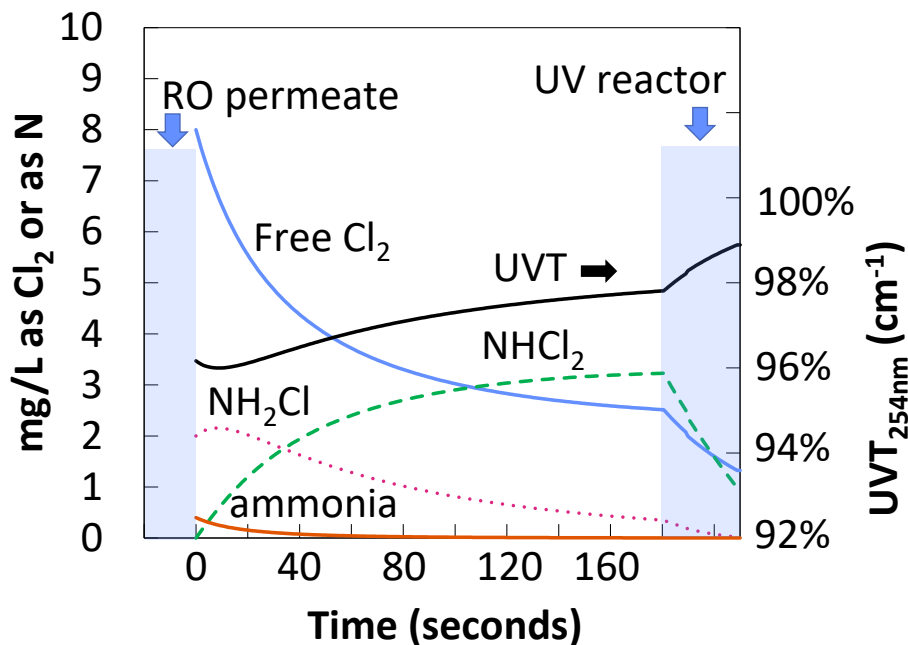


Figure A2-4. Model of the Fate and Impact of Chloramines in a FAT UV-Chlorine Treatment Process (pH 5.5).

A2.4 Strategies for Addressing Nitrogen Species

From the preceding discussion, it's obvious that nitrogen species complicate the design and operation of a UV-AOP system. For a UV-H₂O₂ system the complicating effects are likely to be

limited to the change in chloramine concentrations across the UV reactor as the chloramines undergo photolysis. This has the effect of changing the UVT and radical scavenging characteristics of the water within the UV reactor, which in turn affect overall AOP performance. UV equipment manufacturers should account for this in their design. At present, there are no known systems whereby online and continuous measurements of chloramines in the influent to the UV reactor are made to control UV AOP dosing in real time. Instead, manufacturers likely account for the worst-case impact of chloramines on system performance and adjust operational setpoints accordingly.

For UV-chlorine systems the implications are more complicated. The performance of the UV-chlorine reactor is a function of not only the UVT and radical scavenging capacity of the water entering the reactor as discussed for UV-H₂O₂ systems, but also the free chlorine concentration. The preceding discussion illustrated that the free chlorine concentration can vary over a timeframe of seconds between the point of free chlorine addition to the RO permeate, and the inlet to the UV reactor. The initial design of the UV reactor as well as the operating strategy therefore needs to accurately reflect the actual free chlorine expected at the reactor. Very good modelling, perhaps coupled with onsite testing, is required to estimate the free chlorine concentration profile of the proposed treatment train. Then, from an operational perspective, free chlorine monitoring must be installed in a way that allows the free chlorine at the reactor entrance to be reported. This implies, for example, that any free chlorine monitors should be placed at the UV reactor itself, to minimize travel time through a sample line to the detector. Any delays within the monitor in measuring chlorine may also introduce error. Delays of more than even a few seconds can lead to errors, as illustrated in Figure A2-4. The same rationale applies to UVT monitors. Again, as illustrated in Figure A2-4, a travel time of several tens of seconds between the entrance to the reactor and the monitor can lead to an overestimate of the UVT in the reactor, and a corresponding overprediction of AOP performance.

The complications associated with these nitrogen-containing species can conceivably be eliminated by eliminating the compounds themselves. For example, ammonia and chloramines can be eliminated by applying enough of a free chlorine dose and allowing enough reaction time (likely in the order of dozens of minutes) to accomplish complete breakpoint chlorination, at which point the remaining free chlorine residual can be directed to the UV reactor. It is likely, however, that the cost associated with storage time to achieve breakpoint chlorination would make this option impractical. The presence of ammonia, nitrate, and nitrite in the RO permeate can be mitigated by better upstream control of nitrification-denitrification. This is a desirable treatment objective anyway, and such improved control would have the added benefit of making the downstream UV-AOP performance more predictable and able to be optimized.

A2.5 A Note on the Benefits of Chloramine and Nitrate Photolysis

While the preceding discussion focuses on the negative impacts of chloramines, nitrate, and nitrite on the performance of UV-H₂O₂ and UV-chlorine AOPs, it is known that direct UV photolysis of these species produces radicals that can destroy contaminants. For example, studies have explored, at bench- or pilot-scale, the ability to directly apply UV to the chloramines that persist in the RO permeate of a FAT process to form radicals to destroy

contaminants (Cao et al., 2022; Mangalgiri et al., 2019). This eliminates the need to apply a separate dose of free chlorine or H₂O₂ to achieve treatment. Similarly, studies have explored the application of UV light to nitrified wastewater effluent to use the ambient high levels of nitrate as initiators to form radicals to destroy contaminants (Vinge et al., 2020). While these strategies are elegant and intriguing, their efficiency relative to more conventional UV-H₂O₂ or UV-chlorine treatment in terms of a wide range of contaminants is either not well established, or reportedly demonstrably lower (Kwon et al., 2020). Furthermore, there is some evidence that the UV photolysis of nitrogen species can increase toxicity, as discussed in the next section. It is proposed that more research is needed on this topic before widespread adoption of these intriguing solutions.

A2.6 Toxicity Associated with Photolysis of Nitrogen Species

Nitrate is photolyzed by UV to produce nitrite and nitrogen radicals such as peroxyxynitrite (OONO⁻), which decompose into nitro- and nitroso-radicals, as well as nitrate and nitrite end products (Mack and Bolton, 1999; Goldstein and Rabani, 2007). During this process, inorganic nitrogen can be incorporated with the organic matter present in the water matrix to form nitrated organic by-products (Thorn and Cox 2012; Martijn et al., 2014; Hofman-Caris et al., 2015; Kolkman et al., 2015). Effluents of MP UV-H₂O₂ AOP drinking water treatment have been shown to induce a genotoxic response in the Ames fluctuation test (TA98 strain) for surface water (Martijn et al., 2014 and 2015; Heringa et al., 2011), where the response was correlated to the concentration of the nitrated organics (Kolkman et al. 2015; Wagner et al., 2012). In contrast to the high UV doses applied for such AOP treatment, when UV disinfection doses (20-70 mJ/cm²) were applied in a study of six full-scale plants treating groundwater, surface water, or riverbank filtrate, no Ames response was detected (Hofman-Caris et al., 2015). At one plant of the six, however, an increase in UV dose to 200 mJ/cm² elicited an Ames test response, which increased proportionally as the UV dose increased to 8,000 mJ/cm².

Nitrate photolysis may be enhanced in the MP emission region due to its absorption spectrum (between 200-240 nm). LP UV and LP UV-H₂O₂ processes were observed by Hofman-Caris et al. (2015) and Ijpelaar et al. (2005) to cause little, if any, mutagenicity formation. However, Semitsoglou-Tsiapou et al. (2018) reported that when their water matrix was spiked with nitrate (50 mg/L) and NOM, low but measurable responses in the Ames test were elicited with LP UV-H₂O₂ at high UV fluences (2000 mJ/cm²). As mentioned earlier, lab-scale tests of the effect of LP vs. MP lamps on nitrogenous byproducts may not be representative of full-scale MP systems where light path lengths are much greater (e.g., 20 cm) than in lab-scale tests (e.g., 1 cm). At longer light path lengths, the water may effectively block photons in the 200-240 nm range, so nitrate photolysis to nitrite may be not as prevalent at full scale than at lab scale. However, at least one of the studies demonstrating MP lamp-induced Ames fluctuation responses was from a full-scale MP system in the Netherlands (Martijn et al., 2014). MP lamp quartz sleeves can be doped to exclude wavelengths of 200-240 nm. Another option to reduce the potential formation of mutagenic compounds is to reduce the nitrate concentration by, for example, ion exchange, or to remove high NOM concentrations or at least the (high molecular weight) aromatic part of the NOM. If mutagenic byproducts are formed due to nitrate photolysis, they have also been shown to be removed by means of activated carbon (Heringa et al., 2011).

A2.7 pH

The effect of pH on UV-AOP performance is different depending on whether UV light is being produced only at 254 nm (low pressure lamp) or over the range from 240-400 nm (medium pressure lamp), and when considering a UV-chlorine or a UV-H₂O₂ process.

UV-chlorine AOP. Chlorine exists predominantly as HOCl below pH 7.5, and OCl⁻ above. When using a LP lamp, both HOCl and OCl⁻ absorb photons approximately equally at 254 nm. However, the quantum yield of radical formation is higher from HOCl photolysis, and there is also less scavenging of the •OH formed by HOCl than by OCl⁻. Both of these factors lead to there being more net production of •OH at lower pH than at higher pH (Bulman et al., 2019). In other words, for a LP UV system, the UV-chlorine process is more efficient at lower pH, with all other factors being equal.

For a MP system, or for potential future UV systems employing LEDs at wavelengths higher than 254 nm, the situation is more complicated. The higher wavelengths in the 280-320 nm range that are emitted by MP lamps, or may be emitted by some LEDs, are very efficient at photolyzing OCl⁻ that is present at neutral and alkaline pH values. One of the products of this photolysis is •OH, but this is quickly scavenged by the OCl⁻ itself, so the amount of •OH present at elevated pH is likely to be lower than at lower pH, even for MP systems (Bulman et al., 2019). However, some of the other products of OCl⁻ photolysis by MP lamps lead to RCS, such as ClO[•], which can be effective in destroying some contaminants (Wang et al., 2019; Gao et al., 2019; Li et al., 2017; Chuang et al., 2017; Wu et al., 2016). The compounds that tend to be reactive with RCS include those that contain electron-donating functional groups (e.g., hydroxyl, amine, alkoxy, alkyl, acyl) (Guo et al., 2017; Gao et al., 2020). While the application of UV-chlorine AOP to target and to destroy a single specific contaminant that is reactive with RCS is likely to be rare, it can occur. For example, MP UV-AOP reactors are used in several drinking water treatment plants in Canada for geosmin (taste and odor) control. Geosmin is quite susceptible to RCS. With a water pH in the 7.5-8.0 range, conventional wisdom might suggest that UV-chlorine would not be competitive with UV-H₂O₂, but full-scale trials suggest that the two forms of AOP are roughly equivalent in terms of their ability to destroy geosmin, despite the high pH (Wang et al., 2015b). Overall, though, UV-AOPs are likely to be applied in many cases for protection against a broad spectrum of contaminants. Since •OH is a far more widely effective reagent than RCS, the design philosophy for such installations would likely have to focus on •OH production by the AOP as the main goal of the process, with RCS formation considered more as an unpredictable added benefit—at least in the short term until more is learned about RCS chemistry.

UV-H₂O₂ AOP. The pKa of hydrogen peroxide is 11.7. This means that, unlike chlorine, the form of H₂O₂ does not change over the pH range experienced in practice and therefore its fundamental photochemistry remains the same. In other words, there is no immediate and direct impact of pH on UV-H₂O₂ performance under typical conditions. However, there can be indirect impacts.

The indirect impacts of pH are applicable to not only UV-H₂O₂, but also UV-chlorine. These include the following:

- Inorganic carbon can be a significant radical scavenger, with carbonate being stronger than bicarbonate ($k = 3.9E8 \text{ M}^{-1}\text{s}^{-1}$ vs. $8.5E6 \text{ M}^{-1}\text{s}^{-1}$; Kwon et al., 2020). Since the pKa of bicarbonate is 10.3, as the pH rises towards that point (e.g., above 8), the concentration of carbonate might become non-negligible, thereby increasing the radical scavenging potential of the water. This phenomenon should be considered and accounted for in any modelling or pilot-/full-scale testing to support the design and optimization of a UV-AOP reactor.
- As pH changes, the characteristics of natural organic matter might change via gains or losses of hydrogen and hydroxyl groups. This, in turn, could theoretically affect its reactivity with $\bullet\text{OH}$ or RCS. No information on this topic could be identified in the literature, but it is one reason why it would be prudent to measure the radical scavenging capacity of the water to be treated over the range of water quality characteristics expected, including the pH range.
- As previously discussed, the performance of a UV-AOP system when chloramines are present (typically after RO) is heavily influenced by the exact chlor(am)ine species entering the reactor. This speciation is a function of pH, and therefore the pH must be considered as part of any modelling that is performed for reactor design.

A2.8 Chlorine and H₂O₂ Dose

In a general sense, an increase in oxidant dose will make the AOP process more effective, but only up to a point (discussed momentarily). The design of an AOP system therefore typically involves an analysis of whether to apply more UV light with a lower amount of oxidant, or less UV light with a higher amount of oxidant to achieve the desired level of treatment. In other words, it depends on the local electricity vs. chemical costs and availability. In North America where energy tends to be relatively cheap, it is common to operate UV reactors at a maximum lamp output, and then to adjust the amount of chemical needed to achieve the desired level of treatment. This is particularly true when using H₂O₂, which tends to be more expensive than chlorine. The exact relationship between UV lamp power and oxidant concentration needed to achieve the treatment goal can, at present, only be determined using sophisticated models that tend to be kept confidential by the UV equipment manufacturers, or through pilot- or full-scale testing. This relationship between lamp power and oxidant concentration depends on the reactor configuration, the hydraulics, and the water properties, so the issue is quite complex.

As mentioned above, the benefit of adding more oxidant occurs only up to a point: adding oxidant at a concentration higher than some optimum will lead to a reduction in treatment performance. The reason is that the oxidant itself is a radical scavenger (see Figure A1-11 and Figure A2-1). As such, AOP reactor conditions need to ensure that the oxidant is forming more $\bullet\text{OH}$ and RCS through photolysis than it is consuming through radical scavenging. As the oxidant concentration increases, the scavenging effect increases proportionally, but the radical formation increases less than proportionally, since the oxidant blocks UV light from penetrating further into the water with the result that radical production drops off significantly in regions of the reactor most distant from the lamps. In practice, the optimum concentrations for chlorine and H₂O₂ may be higher than would be affordable or practical anyway, according to a recently reported model (e.g., >7-10 mg/L Cl₂, or >30 mg/L H₂O₂: Sun, 2021), but these exact calculations are typically performed by manufacturers using proprietary models so available information on this topic is scarce.

For a UV-chlorine process, the scavenging of $\cdot\text{OH}$ by free chlorine tends to be stronger than the scavenging of RCS. This means that if UV-chlorine is used to treat chemicals that are reactive towards RCS, higher chlorine doses may be able to be applied before reaching the point of optimum dose, allowing for a higher overall degree of treatment (Wu et al., 2017; Yin et al., 2018). As mentioned earlier, however, this point of maximum effectiveness might be at too high a chlorine dose to be practical, so this phenomenon may not be relevant.

An additional consideration for selecting the oxidant dose is compatibility with materials, and general chemical handling considerations. For example, one plant using UV-chlorine AOP to treat TCE-contaminated groundwater in the Region of Waterloo, Canada, suspects that initially high chlorine concentrations in the range of 8 mg/L caused accelerated corrosion of welded joints, and possibly to the 315 stainless steel (WRF5050, 2021). Subsequent reduction to chlorine concentrations in the 2 mg/L range leads to more typical corrosion rates. It is important for clients to discuss with UV manufacturers whether the concentrations of oxidants being proposed falls within the manufacturer's range of experience. Furthermore, all common-sense factors associated with acquiring and storing chemicals must be considered. For example, how much of a supply should be acquired and stored onsite? Both hydrogen peroxide and chlorine decay in storage. For example, chlorine in hypochlorite solutions might decay by approximately 10% per month (AWWA, 2022), and it is well-reported that chlorate can be an end product of this decay. One survey detected up to almost 30% chlorate relative to free chlorine in hypochlorite solutions on a per-mass basis under worst-case conditions (i.e., application of 10 mg/L free chlorine would add 3 mg/L chlorate to the water) (Stanford et al., 2011). Given the relatively high chlorine doses applied in a UV-chlorine AOP, and the inevitable formation of chlorate through the UV reactor, care must be taken to ensure that chlorate concentrations are minimized. While the U.S. EPA has not currently set a limit on chlorate, other organizations such as the World Health Organization and Health Canada recommended limits in drinking water in the order of 0.7 mg/L – 1.0 mg/L, respectively (WHO, 2005; Health Canada, 2008). It is possible that if appreciable chlorate is present in the hypochlorite solution, it might not be possible to apply a UV-chlorine AOP without exceeding these levels.

A2.9 UV Dose (Fluence)

When more UV energy is applied to the water to be treated, it is expected that a greater degree of treatment will be achieved with all other factors being equal. There are specific instances, however, where this has not been observed. For example, Jia et al. (2019), under laboratory conditions, observed that the product of the degradation of benzophenone-4 by direct chlorine reaction could react with UV light to re-form the parent compound. In other words, excessive UV doses inhibited the net destruction of the compound. It is expected, however, that such phenomena will remain anomalies, and that higher UV doses are likely to lead to greater treatment in most circumstances.

As discussed in the previous section, the design phase will lead to discussions between the end users and the UV manufacturer about the optimum ratio of UV energy vs. oxidant concentration. This relationship is complex and can be estimated by sophisticated UV reactor modelling or tested using full-scale reactors. Pilot-scale reactors can also assist in determining this relationship, but it is complex and the details of how to ensure similitude between pilot-scale and full-scale reactor efficiency is beyond the scope of this document. In brief, it requires that a similar UV *dose distribution* be applied at pilot-scale as would be expected at full-scale, which typically requires that similar lamp output, lamp spacing, and flow rates be applied, in water of the same physicochemical characteristics.

A final consideration about UV dose is the rate at which the dose is applied. In an AOP, the dose refers to the total number of photons absorbed by the oxidant in the water. That dose can be applied with UV lamps that are emitting relatively few photons per second over many seconds, or a higher rate of photons per second over a shorter time period. Or, perhaps more practically, one could install two “weak” UV reactors in series, instead of one more powerful UV reactor with a shorter overall hydraulic residence time. From a theoretical perspective, it is possible to apply the same total UV dose under these two scenarios and achieve different levels of overall treatment, or different levels of undesirable byproduct formation. From a practical perspective, however, it has been reported that such a difference is likely to be minimal (Stefan, 2018). The reason behind the expectation that no large difference would be observed is that a difference would require considerable amount of radical-radical reactions, and given the low concentrations of radicals in a UV reactor under currently practical conditions, the frequency of such reactions would be low. While this hypothesis is based on sound theory, it is a phenomenon that has not been properly scrutinized and reported in the literature. As such, it arguably remains an open question.

A2.10 Inorganic Carbon

Bicarbonate (HCO_3^-) and carbonate (CO_3^{2-}) are radical scavengers. When these species react with hydroxyl radicals or the chlorine atom, a carbonate radical (CO_3^{\bullet}) is formed (Fang et al., 2014). This formation is reportedly more significant in UV-chlorine systems than with UV- H_2O_2 because bicarbonate reacts faster with the chlorine atom than with $\bullet\text{OH}$ (Guo et al., 2018).

The carbonate radical has been observed to contribute to the destruction of certain contaminants, although this reaction is selective (Liu et al., 2015). As such, it is commonly assumed that under most circumstances the presence of inorganic carbon will have an overall negative effect on treatment performance by scavenging the $\bullet\text{OH}$ and RCS. The rate of scavenging is well known and can be included in the UV manufacturer’s models to report on the impact of inorganic carbon on treatment performance.

From a practical perspective during preliminary testing of UV-AOP performance, particularly for RO permeate scenarios, the inorganic carbon should be carefully considered. RO permeate typically has very low levels of inorganic carbon due to rejection by the membrane. If RO permeate were to be brought to a laboratory for lab-scale UV-AOP testing, it is possible for the water to quickly absorb CO_2 from the atmosphere prior to testing, leading to water in the tests that is no longer representative of full scale.

A2.11 Chloride and Bromide

Both chloride and bromide can react with $\bullet\text{OH}$ and $\text{Cl}\bullet$ to form secondary radicals. In other words, chloride and bromide serve as primary radical scavengers. However, these secondary radicals (including other RCS and radical bromide species—RBS) may sometimes be equally or more reactive with various contaminants than the initial $\bullet\text{OH}$ and $\text{Cl}\bullet$ (Yin et al., 2018; Guo et al., 2020; Yang et al., 2020; Grebel et al., 2010). As such, there may be unique circumstances where treatment of a specific compound may be improved in a UV-chlorine or UV- H_2O_2 AOP by the presence of chloride or bromide. There is not much information available in the literature to be able to make broad generalizations about this issue, but the evidence so far suggests that, for chloride in particular, the concentrations typically present in the water do not significantly affect the treatment performance either positively or negatively. Similarly, bromide concentrations in most waters are sufficiently small that any contribution towards AOP effectiveness are likely to be minor.

There is very little impact of chloride and bromide on UVT at the wavelengths employed by LP and MP UV.

While chloride and bromide are therefore likely to have little impact on UV AOP performance, an important consideration for bromide is the potential impact on brominated DBP formation. This is a consideration, however, only for UV-chlorine systems. This is because chlorine reacts with bromide to form **free bromine** (HOBr and OBr^-) which is exactly analogous to free chlorine (in contrast, H_2O_2 does NOT react with bromide). Just as free chlorine can undergo UV photolysis to form chlorate, free bromine can undergo photolysis to form bromate. Drinking water limits for bromate in the United States are $10\ \mu\text{g}/\text{L}$. This issue became important for the Terminal Island water reuse plant in Los Angeles, where initial pilot testing of UV- Cl_2 AOP was on effluent from the wastewater treatment plant which contained moderately low bromide levels in the range of $100\ \mu\text{g}/\text{L}$. Following commissioning of the full-scale UV- Cl_2 system, however, suspected infiltration of seawater to the water reuse plant supply line from the wastewater facility increased bromide to over $3,000\ \mu\text{g}/\text{L}$, which, upon UV- Cl_2 treatment, led to bromate sometimes in the order of $30\ \mu\text{g}/\text{L}$. This problem had to be solved by a retrofit to include ammonia injection immediately following RO and before chlorine application. Another outcome of free bromine formation is that it can react with organic matter to form brominated DBPs (just like free chlorine reacts with organic matter to form DBPs).

A2.12 Organic Matter

Organic matter reacts with $\bullet\text{OH}$, $\text{Cl}\bullet$, $\text{ClO}\bullet$, and other radicals. While some of these reactions have the capability to produce new and potentially useful radicals, experience suggests that organic matter overwhelmingly serves to inhibit AOP performance by acting as a net radical scavenger.

Since organic matter generally consists of a mixture of many different species whose composition can change over time in a source, the impact of organic matter on UV-AOP performance is difficult to determine with precision. In general, the following aspects of organic matter should be considered:

- **Oxidant demand:** Usually, organic matter exerts a chlorine demand and the consequent need to increase chlorine doses to achieve a desired residual entering the UV reactor must be characterized, typically through bench-scale or pilot-scale demand tests. Reaction between H_2O_2 and most organic matter in the environment or in wastewater streams is typically much slower than with chlorine, so while it might be prudent when planning a UV- H_2O_2 process to confirm H_2O_2 demand in the water to be treated, the expectation is that it will be minimal.
- **UVT:** Organic matter can absorb photons at the wavelengths produced by LP and MP UV systems. The impact of organic matter on the UVT of the water should therefore be considered in the design stage. In particular, the potential for the organic matter to exhibit variability in its impact on UVT over time must be assessed. A complication with this issue is that the oxidant (chlorine or H_2O_2) can react with organic matter to potentially change the UVT prior to the water entering the reactor. No information on the magnitude of this issue has been reported in the literature. Given the low organic matter concentrations in RO permeate, this issue may not be important in a FAT process, but it could be important in an ozone-CBAT reuse train or for conventional drinking water treatment. Given the very strong contribution of organic matter to lowering the UVT in some contexts, and the significant impact of UVT on treatment cost, consideration might be given to improving upstream removal of organic matter prior to AOP, to achieve an overall cost savings.

Another factor related to organic matter that can influence design is when comparing the cost-effectiveness of UV-chlorine versus UV- H_2O_2 . Conventional thinking is that UV-chlorine is only cost-competitive at low pH, such as in RO permeate with a pH of about 5.5. However, as organic matter concentrations in the water to be treated increase (or, indeed, the concentrations of other radical scavengers), the pH where UV-chlorine is competitive with UV- H_2O_2 also increases. The reason is that in water without other radical scavengers like organic matter, most of the radical scavenging is due to the oxidants themselves (chlorine or H_2O_2 , with chlorine being a much stronger scavenger than H_2O_2). In water that has more and more other scavengers, the percent contribution of the oxidants to overall scavenging gets lower. In other words, the presence of other scavengers impairs both UV-chlorine and UV- H_2O_2 processes, but UV- H_2O_2 is impaired more significantly percentagewise. This has the effect that in waters with more organic matter (or other scavengers), UV-chlorine tends to become more cost-competitive relative to UV- H_2O_2 (Watts et al., 2012).

A2.13 Temperature

It can be predicted that the majority of the elementary reactions that involve radicals and target contaminants will accelerate in warmer water. In other words, the AOP is likely to become more effective in warmer water. Unfortunately, it is difficult to confirm this prediction because much of the literature that reports the reaction rates between radicals and contaminants does so solely at room temperature. One experimental study of both UV-chlorine and UV- H_2O_2 AOP to treat geosmin, MIB, sucralose, nitrobenzene, and caffeine, reported improvements in percent removal of the contaminants in the order of 0-20% at 22°C relative to 4°C (Wang et al., 2018a). However, the speciation of free chlorine varies with temperature (see Figure A1-5), with the (normally) less-preferred OCl^- increasing relative to HOCl by as much as

about 12% when temperature warms from 4°C to 22°C. This may partially offset the faster radical-contaminant reaction kinetics in warmer water. Overall, very little literature exists to predict the impact of temperature on UV-AOP performance, suggesting that bench- or pilot-scale studies are warranted for locations where water temperature is widely variable.

CHAPTER A3

Byproducts

Using reactive chemicals to treat water can lead to undesirable byproducts. The drinking water industry uses the term *disinfection byproducts* (DBPs) to describe these compounds. While UV-AOPs aren't primarily applied to disinfect, the fundamental chemistry is the same, so we choose to continue to use the term "DBP" here.

There are several general mechanisms of formation, and types DBPs, that can be formed by UV-advanced oxidation. The AOP can lead to changes in the characteristics of organic matter in the water to enhance the biological activity downstream and to increase downstream chlorine demand. AOP reaction with organic matter can make that organic matter more or less reactive to chlorine that may be applied downstream in a way that alters subsequent chlorination DBPs. Advanced oxidation can react with specific contaminants or general organic matter to form transformation products that, rather than being rendered non-toxic, could potentially maintain or enhance toxic properties. Finally, UV-AOPs can react to form traditional DBPs, such as trihalomethanes.

A3.1 Biostability

Waters being treated by UV-AOP normally contain organic matter. In the case of wastewater, this organic matter is often referred to as *effluent organic matter* (EfOM), whereas the organic matter in drinking water sources is typically referred to as *natural organic matter* (NOM) since it comes from (at least partially) natural sources in the watershed. In either case, it is known that strong oxidants will break large organic molecules down into smaller, more oxygenated compounds. These smaller compounds, such as carboxylic acids and aldehydes, are often more bioassimilable than the parent EfOM or NOM. For example, the initial widespread introduction of ozone for drinking water disinfection in North America in the 1990s was sometimes accompanied by problems with maintaining a chlorine residual in the distribution system (Cipparone et al., 1997; Jadas-Hécart et al., 1991). It was soon discovered that ozone was creating "food," or *bioassimilable organic matter* (BOM) for microorganisms in the distribution system, which led to more biofilm in the pipes, which in turn, exerted a chlorine demand. The solution was often to install biologically active carbon (BAC) filters after ozone, to consume the BOM in the plant before it entered the distribution system.

UV-AOPs can be expected to behave similarly to ozone in terms of the formation of BOM, although the extent is not well reported. The oxidation of the organic matter can be due to the free radicals, or due to the oxidant itself (H_2O_2 or chlorine). Research on the structural changes to NOM upon UV-AOP treatment suggest that the products have lower molecular weight and lower aromaticity, and are therefore more hydrophilic, which implies more easily biodegraded (Kleiser and Frimmel, 2000; Sarathy et al., 2011; Sarathy and Mohseni, 2007; Sarathy and Mohseni, 2010; Wang et al., 2017). Conceivably, a UV-AOP could be applied at such a high dose that the organics would be oxidized completely to CO_2 , in which case all potential concern with biodegradation would be eliminated. In practice, however, UV-AOP doses are nowhere near

high enough to mineralize the organics in this way. In other words, UV-AOPs do not appreciably change the total organic carbon (TOC) of the water (Pisarenko et al. 2013; Ike et al., 2019).

Very limited research on natural and synthetic waters at bench- and pilot-scale has shown that UV-H₂O₂ treatment under some conditions can increase the amount of BOM in the water by about 30% to 500% (Metz et al. 2011; Bazri et al., 2012). No similar studies focusing on UV-chlorine AOP have been located, although since the hydroxyl radical is a key reagent in both processes, it might be expected that the results would be similar. While this limited research demonstrates the potential to form BOM when applying UV-AOPs under controlled conditions, there is no known information that suggests that UV-AOPs at full-scale have actually led to biostability problems in distribution systems. This remains an area in need of investigation. Since UV-AOPs would typically be used as one of the final steps in a treatment train, its potential effect on the biostability of the water is arguably an important consideration if the potential for problems related to BOM formation exists. Such potential would likely be highest if using UV-AOP to treat water from high TOC sources, such as wastewaters from an ozone-CBAT train. In contrast, the TOC in reverse osmosis permeate is typically well below 1 mg-C/L, and biostability is likely not a problem for UV-AOP treated water in that context.

A3.2 Downstream Chlorine Demand

Changes to the organic matter due to UV-AOP treatment can lead those organics to exhibit different reactivities to oxidants that might be applied downstream. One example of this phenomenon is Cornwall, Canada, which installed one of the first municipal UV-H₂O₂ systems to treat drinking water from a river source for taste and odor control. This is an MP UV system that delivers a UV dose of approximately 600 mJ/cm² along with typically 2-4 mg/L H₂O₂. The TOC of the water is in the order of 1.5 mg-C/L. Most of the year, the UV reactor operates in a disinfection mode, but the AOP mode is activated in the late summer when taste and odor events are expected due to algal activity. When the AOP is activated, the city experiences an immediate increase in their 24-hour chlorine demand by about 0.8 mg/L. While the city uses free chlorine to quench the residual H₂O₂ from the AOP system, the change in chlorine demand is independent of the slight stoichiometric excess chlorine that's applied for quenching. In other words, it is almost certainly due to a change in the characteristics of the TOC that make it more reactive to chlorine that is applied for secondary disinfection. As a result, the city now expects that it needs to boost its secondary chlorination dose when activating the AOP, to ensure that it can maintain the regulatory requirement for a secondary disinfectant at all points in the distribution system. A similar increase in chlorine demand of Ohio River water was observed for a UV-H₂O₂ treatment system supplying water to Cincinnati (Dotson et al., 2010). A UV dose of 1,000 mJ/cm² combined with 10 mg/L H₂O₂ led to an approximate tripling of the 24-hour chlorine demand.

While the need to maintain a downstream disinfectant residual may be less critical in water reuse applications, this is an example of how it is important to consider all possible side effects of a new treatment process.

A3.3 Impact on Traditional and Novel Organohalide Byproducts

Organohalides is a term that describes organic compounds that contain chlorine, bromine, or iodine atoms. This includes the commonly regulated trihalomethanes (THMs) and haloacetic acids (HAAs), as well as many of the emerging DBPs that are not often regulated but are routinely monitored by the research community, such as haloacetonitriles (HANs), haloketones (HKs), and haloacetamides (HAMs). Organohalides are normally formed when free chlorine is applied as a treatment chemical, and the free chlorine reacts with and merges with an organic molecule, thus forming an *organochlorine* species. Alternatively, the free chlorine can react with bromide that might be in the water, converting the bromide into free bromine (HOBr and OBr⁻: analogous to free chlorine). The free bromine may then react with an organic molecule to form an *organobromine* species. A similar mechanism can also theoretically convert ambient iodide into *organoiodine* species, but the more prevalent mechanism for organoiodine formation requires chloramines to be present instead of free chlorine, since free chlorine quickly reacts with iodide/free iodine to oxidize it completely to iodate, which is essentially inert. When all three of chlorine, bromide, and iodide are in the water, different types of organics containing any combination of these three *halogen* atoms can form: thus, organohalides in general.

The UV-H₂O₂ AOP is not reported to produce organohalides in practice. The reason is that UV-H₂O₂ itself does not contain any chlorine, bromide, or iodide. In theory, there are some chemical reaction pathways whereby the •OH that is produced by UV-H₂O₂ can react with ambient chloride, bromide, or iodide, to form free chlorine, bromine, or iodine, which may then react with organics to form organohalides, but evidence on the significance of this pathway is missing, other than the indirect evidence that conventional DBPs are generally not observed following UV-H₂O₂.

For UV-chlorine, the situation is very different. To begin with, chlorine would normally be added upstream of the UV reactor, and often at doses that are higher than might be typical in drinking water disinfection (e.g., 2-5 mg/L). This might suggest the risk of higher DBP concentrations than would be typical of drinking water, but it must be remembered that the chlorine may be added only several seconds, or tens of seconds, ahead of the UV reactor. Once in the UV reactor, the chlorine will likely undergo a significant amount of immediate photolysis and destruction—possibly much greater than 50%. Therefore, while the initial dose might be higher than in conventional drinking water treatment, the reaction time of that dose is very brief. On the other hand, inside the UV reactor, the chlorine is undergoing photolysis to form an array of different reactive chlorine species whose chemistry is poorly understood. There is evidence, though, that some of the RCS can lead to transfer of the chlorine atom onto organic molecules, thereby directly forming organohalide byproducts (Guo et al., 2017; Xiang et al., 2016).

Overall, information on the direct formation of organohalide DBPs during the UV-chlorine process is sparse. One study performed full-scale UV-chlorine treatment at the Cornwall, Canada, water treatment plant, using an MP UV reactor, with chlorine doses ranging from 2 to 10 mg/L and the pH adjusted between 6.5 and 8.5 (Wang et al., 2015a). The TOC of the water was 1.5 mg-C/L. Under these conditions, there was no observed THM formation over the

estimated 30-60 seconds of time between the point of chlorine addition and sampling immediately downstream of the UV reactor, whereas HAAs increased slightly by approximately 5 µg/L. Similarly, haloacetone and chloropicrin formation was negligible, but two haloacetone nitriles (dichloro- and bromochloro-) were formed at low levels (up to 3 µg/L) across the UV-chlorine system. The researchers also measured adsorbable organohalides (AOX), which is an estimate of the total amount of all organohalide species in the water (i.e., THMs and HAAs are a subset of AOX). The Cornwall plant practiced prechlorination at the intake (approximately 0.5 mg/L), so the incoming AOX at the UV reactor was already approximately 80 µg-Cl/L. Nevertheless, there was no observed subsequent increase in AOX across the UV reactor. In contrast to these results, the researchers also conducted similar bench-scale UV-chlorine tests but on a different water with a higher TOC (3.5 mg/L) and that had not been prechlorinated. In this scenario, there was still no observed THM formation due to UV-chlorine AOP treatment, but approximately 13 µg/L HAAs were formed, and 5 µg/L of haloacetone nitriles. AOX formation across the UV-chlorine AOP was 70 µg-Cl/L, whereas AOX formation over a similar reaction time due to chlorine alone at the same dose was only 15 µg-Cl/L, implying that the photolysis of chlorine enhanced AOX relative to chlorine alone.

Similar results were reported in another full-scale UV-chlorine trial performed in Peel Region, Canada (Wang et al., 2019). The MP system was operated with 5-10 mg/L chlorine at pH 6.5 and 8.0, in water with a TOC of 2.2 mg-C/L that had been prechlorinated with less than 1 mg/L. There was no observed THM formation across the UV-chlorine AOP, whereas HAA formation increased by 6 µg/L relative to a similar chlorine dose and reaction time in the absence of UV. No other organohalide formation was detected, apart from, again, bromochloro- and dichloroacetone nitrile, which increased by approximately 6 µg/L. The formation of haloacetone nitriles from UV-chlorine treatment was also observed in a bench-scale study wherein UV-chlorine treatment was used to destroy chlortoluron (a herbicide) in otherwise pure water (Guo et al., 2016) confirming that some organic precursors can react under UV-chlorine AOP to form these DBPs. A very interesting observation in the study by Wang et al. (2019) was that UV-chlorine tended to enhance AOX formation only at pH 6.5, and not at pH 8.0. The data from this study suggested that the advanced oxidation reactions at pH 6.5 were dominated by •OH reaction, while advanced oxidation at pH 8.0 was dominated by RCS. If true, this implies that the increase in AOX precursors was due to the role of •OH rather than RCS, which might go some way in partially allaying fears that the RCS from UV-chlorine treatment might create unusual or large amounts of DBPs.

Another study employing a bench-top collimated beam apparatus for UV-chlorine treatment of Colorado River water (pH 7.5, 10 mg/L Cl₂) reported no increase in THM formation relative to a dark chlorination control (Pisarenko et al., 2013). However, an approximately 20 µg/L increase in HAA levels was observed due to UV-chlorine. In contrast, total organohalide concentrations (similar to AOX) were observed to be 30 µg-Cl/L lower for UV-chlorine treatment when compared to dark chlorination. In this study, the collimated beam apparatus used relatively low power lamps, requiring that the water samples be exposed to UV light for 2 hours to run the tests. As such, direct chlorine reaction time was not similar to what would occur at full-scale, where the chlorine would typically be present for only a matter of seconds.

A study by Hua et al. (2021) applied LP UV-chlorine treatment (14 mg/L Cl₂) to secondary wastewater effluent, and reported increased formation of THMs, HAAs, chloral hydrate, haloacetamides, trichloronitromethane, and haloacetamides by 90 – 508% relative to a chlorinated dark control. The researchers also aimed to predict the relevance of these DBP trends on toxicity. This was done by using a “calculated toxicity” method that combines information about measured DBPs in a mixture with their published potency data in the CHO comet assay. The CHO comet assay measures DNA damage and cytotoxicity (Wagner and Plewa, 2017). Potency values are based on dose-response curves of a DBP and are reported as the concentration that impacts 50% of the cells in the assay (EC₅₀). The measured DBP in a sample is divided by the EC₅₀ to provide an estimate of the impact on toxicity, where a value of 1 is indicative of a toxic concentration. The DBP toxicity scores for each DBP are summed and represent the calculated toxicity index. In Hua et al.’s study, the potency data of individual DBPs in the CHO comet assay were predicted to exhibit a two-fold increase in reactivity for UV-chlorine treated samples relative to a dark chlorination control. However, when the samples were actually tested for genotoxic reactivity using the SOS/*umu* test, the 20-minute dark chlorination, UV, and UV-chlorine treatments decreased the genotoxicity by 30%, 39% and 76%, respectively. The addition of 1 mg/L bromide to the UV-chlorine process increased the formation of brominated DBPs and the overall calculated cytotoxicity and genotoxicity of the DBPs, but the measured acute toxicity and genotoxicity of the wastewater decreased by 7% and 100%, respectively. When considering calculated or predicted toxicities, it is important to note that these calculations are based on the few DBPs for which published potency data exist, which represents a small portion of the formed DBPs. For example, in this particular study, the genotoxicity scores were all in the 0.001-0.004 range, compared to a value of 1 that reflects a DBP mixture at the EC₅₀ level. At such small values, there can easily be a 2-4-fold difference when scores are empirically compared. Bioassay results are arguably superior to calculated toxicity indexes as they reflect the reactivity of all of the formed DBPs, as well as the destruction of toxic organic compounds, for different treatments.

The studies reported above all focused on UV-AOPs. The action of UV alone to form DBPs has been studied, and in a general sense, very little evidence of direct DBP formation has been observed. One exception is the application of MP-UV in waters containing nitrate. Nitrate is a strong absorber of UV at wavelengths below 250 nm, and its photolysis leads to nitrite radicals (Sharpless et al., 2003). It is believed that these nitrite radicals can cause chemical reactions with organic precursors that can lead to several organohalide DBPs when the water is subsequently chlorinated. MP UV at doses as low as 40 mJ/cm² in water containing 10 mg-N/L of nitrate was observed to lead to formation of 4-8 µg/L of chloropicrin, 1-2 µg/L of chloral hydrate, and higher UV doses (>100 mJ/cm²) were found to increase 1,1,1-trichloropropanone by 1-2 µg/L (Reckhow et al., 2010). As mentioned earlier in this report, however, these experiments used short path lengths which permitted significant penetration of low wavelength (200-240 nm) photons into the water to generate nitrite radicals, whereas in practice, the longer pathlengths associated with MP reactors might lead to relatively inefficient penetration of these photons into the water column.

In all of these cases discussed above, however, the amount of DBPs formed could be argued to be quite small compared to normal drinking water DBPs. Furthermore, it appears that if the water has already been prechlorinated, the organics might be less reactive to chlorine during the UV-chlorine AOP such that additional organohalide formation is small during the very short reaction times available. For raw (unchlorinated) water, however, the organics might be reactive enough to form DBPs across the UV reactor. The work suggests that haloacetonitriles might be among the fastest DBPs to form and therefore most likely to form within the tens of seconds that high concentrations of chlorine are present before becoming photolysed, with HAAs being able to form to some extent in under a minute, but no THM formation has been observed. The presence of haloacetonitriles, however, is noteworthy due to reports that these compounds may be more toxic than the more traditional regulated DBPs, such as THMs and HAAs (U.S. EPA, 2006; Health Canada, 2017; Muellner et al., 2007; Plewa et al., 2008).

A3.4 Impact on Downstream DBP Formation Potential

A UV-AOP may be followed by a secondary disinfectant to provide residual disinfection in a distribution system network. The AOP might therefore alter the characteristics of the organic precursors in such a way as to enhance or to diminish the DBPs that might be formed downstream.

Work by Liu et al. (2002) suggested that when applying LP and MP UV alone (i.e., no oxidant for advanced oxidation) at doses less than 1,000 mJ/cm² to synthetic water containing Suwannee River natural organic matter, no impact on subsequent chlorination THM or HAA formation potential was observed, while doses of 500 mJ/cm² formed some aldehydes and carboxylic acids that can adversely affect biostability. Much higher UV doses of 6,360 mJ/cm² resulted in observed decreases in THM and HAA formation potential in the order of 15-45%, presumably due to the photolysis of precursors.

Studies that have focused on the impact of UV-AOP on subsequent chlorination DBP formation have noticed a variety of effects that are likely to be site-specific. Dotson et al., (2010) demonstrated that when applying both LP and MP UV-H₂O₂ treatment to Ohio River water at high doses (1,000 mJ/cm² and 10 mg/L H₂O₂), the 24-hour THM yield could increase by 150% compared to chlorination alone, however there was no discernable impact on HAA or AOX formation. Sarathy and Mohseni (2010) reported that UV-H₂O₂ treatment of a surface water at fluences < 1000 mJ/cm² resulted in negligible changes to THM formation potential, and up to approximately a 30% reduction in HAA formation potential. In a full-scale analysis of a UV-H₂O₂ system being used to destroy geosmin at a plant treating water from the St. Lawrence River, the 24-hour THM formation potential was found to either increase or decrease by approximately 20%-30% in the UV-H₂O₂ treated water compared to a chlorination-only control in samples collected over the space of a year, suggesting that the impact is a function of the organic matter characteristics, which can vary from season to season (Pantin and Hofmann, 2008).

Studies that have explored the impact of UV-chlorine AOP have shown similar variability on the formation potential of downstream chlorination DBPs. One study performed UV-Cl₂ AOP experiments on two surface waters with a UV fluence of approximately 1800 mJ/cm² and

conducted subsequent formation potential (FP) tests by applying a chlorine dose of 6.5 mg/L over 24 hours to estimate maximum DBP formation (Wang et al., 2015a). In this work, they noted THM and HAA-FP increases of 20-110%, haloacetonitrile-FP increases of 110-260 %, and AOX-FP increases of 30-60%. These results were compared to UV-H₂O₂ AOP treatment at equimolar doses, and no significant difference was found between the two treatments, implying that both UV-H₂O₂ and UV-chlorine were exhibiting similar impacts on downstream chlorination DBP formation under the conditions tested. This also implies that impact on DBP precursors was governed by •OH and not by RCS in these experiments.

A3.5 DBPs as Transformation Products of Specific Precursors

When oxidizing or disinfecting drinking water from groundwater or surface sources, the organic DBP precursors are generally assumed to be primarily the natural organic matter in the water. This is because the concentration of specific organic compounds, such as pesticide contaminants or pharmaceuticals, is hopefully so low that it would not contribute meaningfully to DBP formation. For water reuse, however, there is some concern that the loading of such microcontaminants in the wastewater could conceivably be high enough, and subsequent removal across the wastewater treatment potentially low enough, that there may be a risk that AOP treatment could cause non-trivial formation of DBPs from specific contaminant parent compounds.

Huang et al., (2017) exposed dodecylbenzyltrimethylammonium chloride (DDBAC) to UV-chlorine treatment in ultrapure water at pH 8, and detected the formation of dichloropropanol, trichloropropanol, and chloral hydrate. Sun et al. (2019) applied both UV-chlorine and UV-H₂O₂ to carbamazepine and atrazine solutions to investigate their relative changes in DBP formation and toxicities. UV-chlorine degradation of carbamazepine, which is reactive to both •OH and RCS, was shown to have similar DBP formation and genotoxicity changes compared to UV-H₂O₂ treatment, as well as decreased cytotoxicity when compared to UV-H₂O₂ treatment. UV-chlorine degradation of atrazine, which is reactive to •OH and inert to RCS, showed slightly increased DBP formation, but decreased cytotoxicity and genotoxicity when compared to UV-H₂O₂ treatment.

Wang et al. (2018b) gathered data on a large number of different micropollutants treated by UV-H₂O₂ AOP and found that •OH has a high probability (> 80%) of generating transformation products that are toxic. Toxicity tests with microorganisms also showed that the resultant transformation products had a 51% chance of being more toxic than its parent pollutant. The presence of these toxic products was more prominent at lower UV fluences than higher fluences, indicating that these compounds can mineralize given enough treatment.

A3.6 Nitrosamines

N-nitrosodimethylamine (NDMA) is a DBP that has been identified as a particularly potent carcinogen and is part of a wider class of compounds called nitrosamines. The World Health Organization recommends a drinking water standard for NDMA of 100 ng/L (WHO, 2017). There is no current U.S. EPA limit, but NDMA in drinking water is regulated at 10 ng/L in Massachusetts and has a notification level of 10 ng/L in California (California State Water Resources Control Board, 2017; MassDEP, 2020). In Ontario, Canada, NDMA in drinking water is

regulated at 9 ng/L (Health Canada, 2020). NDMA can be formed when amine precursors, sometimes from anthropogenic sources, react with either ozone or (most commonly) chloramines (Gerrity et al., 2015). Free chlorine is not a direct reagent to form NDMA. NDMA can be destroyed directly by UV light. This is one of the principal reasons behind the use of UV (instead of ozone, for example) for advanced oxidation in a full advanced treatment (FAT) scenario: the UV itself can destroy NDMA, whereas the free radicals, which are relatively inert against NDMA, can destroy a large spectrum of other potential contaminants. NDMA is not necessarily a common concern across many jurisdictions, and therefore the need for targeting NDMA during water reuse treatment, or the importance of direct UV photolysis during water reuse treatment, is potentially site-specific.

While the UV light in a UV-AOP process can destroy NDMA, other elements in water reuse treatment trains can cause NDMA to form during UV-AOP and can also promote NDMA formation downstream of the AOP treatment. As such, there is a complex interplay of NDMA destruction and formation that can occur.

In a microfiltration + reverse osmosis + UV-AOP treatment train, chloramines at concentrations in the 1.5 to 3.0 mg-Cl₂/L range can be applied to control fouling of the MF and RO membranes. Chloramines are poorly rejected by RO (up to ≈50%) (McCurry et al., 2017) and NDMA organic amine precursors are not completely removed (e.g., 90% removal) (Roback et al., 2021). In contrast, RO provides very good rejection of ammonium ion and bicarbonate. The RO permeate therefore may contain some NDMA precursors, is at low pH (<6) and with very low ammonia, and potentially contains in the order of 2 mg/L of chloramines (Szcuka et al., 2020). When free chlorine is then added to the RO permeate, there is a very high chlorine-to-ammonia/chloramine ratio, and it is at a low pH. These conditions favor the reaction of the free chlorine with the pre-existing chloramines to form dichloramine. Dichloramine is the main form of chlorine that reacts with precursors to form NDMA. While the UV-AOP process may destroy some of the NDMA precursors (Roback et al., 2020) enough can survive to react with dichloramine to form NDMA. This reaction can take hours, but in a UV+H₂O₂ system, the residual H₂O₂ reacts slowly with dichloramine and the dichloramine can persist long enough for this to occur downstream of the AOP system (McCurry et al., 2017; Sgroi et al., 2015). This formation has been called NDMA “rebound” since NDMA is observed to form downstream of the UV reactor, despite pre-existing NDMA having been destroyed by the UV. Roback et al. (2019) reported that following UV-H₂O₂ and restabilization using lime to a pH of 8.5, NDMA rebound was observed at a rate of approximately 0.7 ng/L/hr for up to 12 hours. McCurry et al. (2017) reported that raising the pH to 8.5 as soon as possible after UV-AOP would tend to reduce subsequent NDMA formation compared to allowing the reaction to proceed at pH <6, due to the shift in chloramine equilibrium from di- to monochloramine at higher pH, since it is the dichloramine that is the main driver in NDMA formation. There is evidence by Szcuka et al. (2020) that NDMA formation can also occur within a UV reactor through direct photolysis of monochloramine to form NDMA. Their preliminary work in this area suggests that there is a minimum UV dose (300-500 mJ/cm² under the conditions tested) below which the net formation of NDMA across the UV reactor outweighs NDMA destruction through photolysis, but that at higher and arguably more realistic doses (>800 mJ/cm²), the formation is less than the destruction.

For ozone-CBAT treatment trains, the issue of NDMA is likely less significant, since there is less likelihood for dichloramine to exist in the train since pH is typically kept neutral or higher, so even if chloramines are applied (and they generally are not), dichloramine concentrations would be low. Moreover, Zhang et al. (2019) reported that ozonation is effective at reducing NDMA precursors when followed by biologically active filtration.

A3.6.1 Minimizing NDMA Formation

Methods to minimize NDMA rebound are focused on identifying conditions that reduce the presence of dichloramine in the water following RO. One reported method is to ensure an adequate excess of free chlorine to quickly eliminate residual dichloramine (Trussell, 2022). Alternately, since dichloramine is less favored at higher pH, Roback et al. (2021) explored methods at pilot-scale to raise the pH from 5.5 to 7.0 immediately following RO, as opposed to pH adjustment only downstream of the AOP. They reported that this actually led to more NDMA formation when applying UV-chlorine (by about 5 ng/L), presumably due to the weaker UV-chlorine performance at higher pH in terms of destroying NDMA precursors. Raising the pH to 8.5 immediately prior to the UV reactor led to greater NDMA concentrations downstream of UV-H₂O₂ due to less direct UV destruction of NDMA at the higher pH, since its quantum yield of photolysis decreases with pH (Lee et al., 2020). As such, pH adjustment prior to UV-AOP did not provide clear benefits. In principle, however, it is likely advantageous to raise the pH as soon as possible after AOP, to shift the chloramine equilibrium from dichloramine to monochloramine (McCurry et al., 2017). Another issue is that the quantum yield of NDMA may vary based on the type of UV lamp used. For example, Sakai et al. (2012) used a 254 nm LP mercury lamp, a 222 nm KrCl Excimer lamp, and a 230 to 270 nm MP mercury lamp for investigating the degradation of NDMA during UV irradiation experiments at neutral pH and 25 °C. They reported the quantum yield of NDMA for the three light sources to be 0.28, 0.4, and 0.44 mol Einstein⁻¹, respectively, indicating the quantum yield for a 230 to 270 nm MP lamp to be 1.5 times higher when compared to that of a 254 nm LP mercury lamp.

Furst et al. (2018) demonstrated a promising method to reduce NDMA formation through the sequence of chemical addition. In RO permeate containing chloramines, there is a benefit to applying free chlorine in two smaller doses, 30 seconds apart. This tends to reduce the chlorine:ammonia/chloramine ratio at the local point of chlorine application, minimizing dichloramine formation and therefore downstream NDMA concentrations by about 50%. Furthermore, when initially forming chloramines upstream of the MF+RO membranes, they recommend striving for conditions that would minimize high chlorine:ammonia ratios. This means that if the water is fully nitrified, chlorine can be added first. This might help to destroy NDMA precursors and also gives time for the chlorine to diffuse into the flow. Then, when ammonia is added downstream, the region of ammonia application will result in a very low localized chlorine:ammonia ratio, thereby minimizing dichloramine formation. The authors note, however, that while this strategy might minimize NDMA formation potential, it might tend to promote halogenated DBP formation.

A3.7 Other Novel Organic DBPs

A study in the United Kingdom by the Water Research Centre attempted to prioritize potential DBPs of concern for AOP systems (DWI, 2018). A list of all DBPs that had been named in the

literature as being associated with AOPs was compiled (78 were identified). From that list, they removed DBPs for which drinking water standards already exist or for which information is already available discounting their toxicological relevance, as well as compounds that are unlikely to form under relevant treatment conditions. A further 13 DBPs were identified that are known to be toxic, but for which no regulatory standards exist, and therefore presumably sufficient data already exists to establish an operational limit if there is sufficient desire to do so. The remaining list included 9 DBPs (Figure A3-1) which were predicted by ToxTree (toxicity prediction software) to exhibit more than “low” oral toxicity, but for which no additional toxicological data was available, nor operational data about their occurrence in practice. As such, these 9 compounds were considered by this report to be the highest priority for more study in terms of their occurrence, and their likely toxicological relevance. That being said, it must be cautioned that the original list of 78 compounds was obtained from (primarily) lab-scale studies that perhaps somewhat arbitrarily dictated which compounds would be monitored for. There is no compelling reason why these 9 particular compounds would be more likely to present major risks than a wide range of other hypothetical compounds that simply had not been actively searched for in previous AOP studies.

2-hydroxy-5-nitrobenzoic acid
2-methoxy-4,7-dinitrophenol
2-nitrohydroquinone
3,5-dinitrosalicylic acid
4-hydroxy-3-nitrobenzoic acid
4-nitrobenzene-sulfonic acid
4-nitrocatechol
4-nitrophthalic acid
5-nitrovanilin

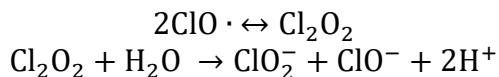
Figure A3-1. DBPs Identified in AOP Studies with Modelled Non-Negligible Toxicity and Little Occurrence Data.

A3.8 Oxyhalides: Bromate, Chlorite, Chlorate, and Perchlorate

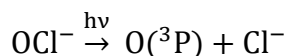
Halogen anions (chloride and bromide) can undergo oxidation to form oxyhalide byproducts, including chlorite (ClO_2^-), chlorate (ClO_3^-), perchlorate (ClO_4^-), and bromate (BrO_3^-). These inorganic DBPs have been reported to have various potential health risks (Feng et al., 2010; WHO, 2005; Yang et al., 2019). In the United States, bromate and chlorite in drinking water are limited by maximum contaminant levels (MCLs) of 10 $\mu\text{g}/\text{L}$ and 1.0 mg/L , respectively (EPA, 2021). The World Health Organization recommends maximum drinking water chlorate and perchlorate concentrations of 0.7 mg/L and 0.07 mg/L , respectively (WHO, 2017). Chlorate, bromate, and perchlorate may also exist as impurities in the sodium hypochlorite solution used for UV-AOPs, especially if the NaOCl solution has been stored for an extended time or under some specific conditions (Asami et al., 2009; Stanford et al., 2011; Wang et al., 2015a). Chlorate, in particular, can be present at elevated concentrations in hypochlorite solutions, so when adding high concentrations of hypochlorite as part of a UV-chlorine AOP, or when quenching H_2O_2 using hypochlorite, the potential contamination of the treated water with chlorate from the hypochlorite solution should be considered. The American Water Works Association has an online tool to help to estimate such formation of oxyanions in free chlorine solutions (AWWA, 2022).

A3.8.1 Formation Pathways

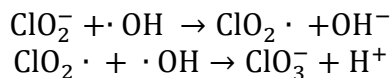
In the UV-chlorine process at 254 nm, reactive chlorine species such as Cl^\bullet , Cl_2^\bullet , and ClO^\bullet will form from the photolysis of free chlorine (Stefan, 2018; Fang et al., 2014; Wu et al., 2017). Chlorite forms through the dimerization of ClO^\bullet and the hydrolysis reaction of Cl_2O_2 (Buxton and Subhani, 1972):



For UV irradiance at 365 nm, atomic oxygen ($\text{O}(^3\text{P})$) will form from the photolysis of hypochlorite (Buxton and Subhani, 1972):



and $\text{O}(^3\text{P})$ can bond with OCl^- to form ClO_2^- . The chlorite formed by hypochlorite photolysis or through dimerization of ClO^\bullet will be quickly oxidized by other oxidative compounds to form chlorate (Buxton and Subhani, 1972). Thus, chlorite is an intermediate and usually little or no chlorite residual is detected after the UV-chlorine process (Feng et al., 2010; Wang et al., 2015a). While Cl^\bullet , ClO^\bullet , and ozone can oxidize chlorite and contribute to chlorate formation (Alfassi et al., 1988; Chuang et al., 2017; Zhao et al., 2021), $^\bullet\text{OH}$ is the most dominant oxidative species responsible for the oxidation of chlorite to ClO_3^- through two steps with ClO_2^\bullet as an intermediate (Zhao et al., 2021):



In addition to this two-step oxidation by $^\bullet\text{OH}$, chlorate can also form by the reaction between $\text{O}(^3\text{P})$ and chlorite under near-UV irradiation (Buxton and Subhani, 1972).

The kinetics of chlorate formation in the UV-chlorine process has not been thoroughly studied. Nevertheless, the total chlorate formation in UV-chlorine treatment as a mass ratio of chlorate formed to free chlorine consumed has been reported to range in the order 2-20% (i.e., the complete photolysis of 3 mg/L free chlorine can form up to 0.6 mg/L chlorate) (Buxton and Subhani, 1972; Feng et al., 2010; Wang et al., 2019, 2015a).

While chlorate is a common end product of the oxidation of free chlorine in a UV-AOP and may be present at concentrations of regulatory concern, perchlorate may also be formed (Kang et al., 2009), but typically at a very low level. The perchlorate yield from chlorine photolysis was reported to be less than 0.01% by mass (Rao et al., 2012).

When bromide is present in water, bromate may form during the UV-chlorine process. Bromide first reacts with chlorine to form free bromine (HOBr and OBr^-) (Kumar and Margerum, 1987). This free bromine, together with the original free chlorine, may then both undergo photolysis to form $^\bullet\text{OH}$, reactive chlorine species (RCS), and also reactive bromine species (RBS) (e.g, Br^\bullet , BrO^\bullet) (Cheng et al., 2018; Fang et al., 2017; Westerhoff et al., 1998). Similar to chlorite

formation, bromite (BrO_2^-) will form through BrO^\bullet dimerization and hydrolysis (Westerhoff et al., 1998):



Bromite will then be oxidized by BrO^\bullet and $^\bullet\text{OH}$ to form bromate (BrO_3^-) with BrO_2^\bullet as an intermediate, similar to the two-step oxidation reactions in chlorate formation. Bromate can also form by BrO_2^\bullet dimerization and reaction with $^\bullet\text{OH}$ (Buxton and Dainton, 1968). Low levels of ozone may also form during the UV-chlorine process, especially from UV-B radiation (wavelengths over 300 nm) (Bulman et al., 2019). The ozonation of bromide may partly contribute to bromate formation in a UV-chlorine process. In addition, bromate may also form by the direct reaction between bromine and chlorine (HOBr and HOCl), but this reaction is much slower (Huang et al., 2008b) compared to bromate formation through the other pathways.

A3.8.2 Factors Affecting Inorganic DBP Formation in the UV/Chlorine AOP

Chlorate. Chlorate formation relies on ClO^\bullet dimerization, so factors that affect the ClO^\bullet concentration will influence the amount of chlorate formed. ClO^\bullet comes primarily from Cl^\bullet or $^\bullet\text{OH}$ reaction with OCl^- (Wu et al., 2017). This means that conditions that favor OCl^- will tend to lead to more chlorate. These conditions include higher pH (free chlorine becomes predominantly OCl^- as the pH rises above its pK_a of about 7.3), a higher chlorine dose, and a higher UV fluence rate that leads to higher ClO^\bullet concentrations. In a full-scale UV-chlorine test, when pH increased from 6.5 to 8.0, the amount of chlorate formed doubled (Wang et al., 2019), and nearly twice the amount of chlorate was measured when chlorine dose increased from 5 to 10 mg/L as Cl_2 . In this study, the highest chlorate concentration among all the conditions tested was 1.1 mg/L, which occurred at pH 8.0, 10 mg/L as Cl_2 chlorine dose, and 100% UV ballast level for a UV reactor that had sixteen 12.3 kW medium pressure lamps. Another study used different types of UV sources, with the highest chlorate formation observed when using UV-B (300 nm) compared to when using UV-A (350 nm) or UV-C (254 nm). It has also been shown that chlorate formation is closely associated with chlorine photolysis; once all the chlorine is photolyzed, chlorate formation stops (Rao et al., 2012).

Methods to actively decrease chlorate formation during UV-chlorine treatment have not been explicitly studied. As such, the most effective method at present is likely to be to minimize the chlorine dose required to achieve the treatment goal. Also, as indicated earlier, a major contributor to chlorate in the final treated water could be the hypochlorite solution used to supply the chlorine. This is a factor that should be carefully considered.

Bromate. The most important contributor to bromate formation is bromide. In many natural waters, bromide concentrations may be in the order of less than 100 $\mu\text{g/L}$ (Amy et al., 1993), but levels can become elevated due to factors such as saltwater intrusion or bromide-containing pesticide contamination. Very little information is reported in the literature on the amount of bromate expected to be formed due to realistic UV-chlorine AOP doses given typical amounts of bromide in the water. Wang et al. (2015a) detected up to 2 $\mu\text{g/L}$ of bromate formation when using UV-chlorine to treat water containing approximately 30 $\mu\text{g/L}$ bromide

with UV doses in the order of 1800 mJ/cm² and chlorine up to 10 mg/L. Huang et al. (2008b) reported 10-20 µg/L of bromate formation with similar UV doses, 5 mg/L chlorine, and 50-80 µg/L bromide. It is theoretically possible to convert all ambient bromide to bromate if a large enough oxidant dose is applied. As such, any bromide concentration above 6.3 µg/L could yield more than the 10 µg/L bromate U.S. drinking water regulatory limit upon complete oxidation.

Bromate formation by UV-chlorine treatment is pH dependent, but the trend with pH is conflicting in previous studies and therefore difficult to predict. This is because two major steps must occur to yield bromate: first, the ambient bromide must be oxidized by free chlorine to form free bromine, and then the free bromine must undergo photolysis and radical reactions to form bromate. The first step is much faster at low pH, with the rate coefficient of the reaction between Br⁻ and HOCl over 17,000 times higher than that for bromide reacting with OCl⁻ (1550 vs 0.09 M⁻¹s⁻¹) (Kumar and Margerum, 1987). This is illustrated in Figure A3-2 which suggests that at pH 5, >95% of the ambient 20 µg/L bromide is oxidized by 5 mg/L of chlorine within half of a minute, whereas at pH 9, it can take almost 10 minutes. This information suggests that bromate formation is accelerated at lower pH.

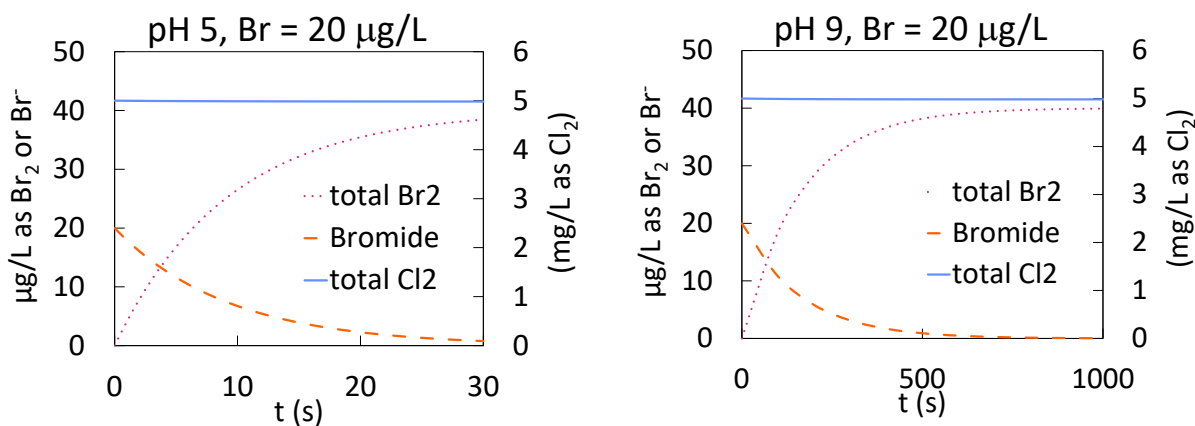


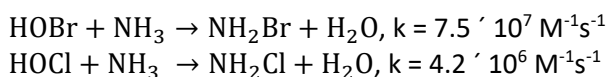
Figure A3-2 Oxidation of Bromide by Chlorine.

Once free bromine is formed, however, the situation becomes more complex. For a monochromatic UV source at 254 nm, the concentrations of reactive bromine species (RBS) that can react to form bromate decrease at higher pH due to OBr⁻ having a lower absorption coefficient than HOBr at 254 nm (Guo et al., 2020). However, for a polychromatic UV source, OBr⁻ has a much higher molar absorption coefficient at the longer wavelengths than HOBr (especially at 300-350 nm). As such, more RBS will form through photolysis at high pH, driving the bromate formation reaction (Guo et al., 2020). Furthermore, pH can also affect the rate of radical reactions. OBr⁻ tends to react faster with radicals than HOBr, which contributes to more bromate formation at higher pH (Von Gunten and Oliveras, 1998). Overall, therefore, there are conditions where low pH might lead to more bromate (when the rate limiting step is governed by free chlorine oxidation of bromide to free bromine), and conditions where high pH may enhance bromate formation (when the rate limiting step involves the photochemical reactions driving free bromine to bromate). While chemical reaction models have been proposed to

attempt to account for much of this complex chemistry (e.g., Yang et al., 2019; Fang et al., 2017), there are no reports whereby these models have been validated, and with the results interpreted from a practical perspective to offer guidance on the influence of pH under typical conditions. Instead, several empirical studies have reported the influence of pH on bromate formation during UV-chlorine treatment under a limited set of experimental conditions. Wang et al. (2015a) reported that when pH decreased from 8.5 to 6.5, the amount of bromate formed increased from 0.1 to 2 µg/L with a 10 mg/L chlorine dose and approximately 10-30 µg/L of bromide in full-scale and pilot-scale UV-chlorine processes with a UV fluence of 1800 mJ/cm² (Wang et al., 2015a). Similarly, Huang et al. (2008b) reported that bromate formed in a UV-chlorine process increased from 8 to 12 µg/L when pH decreased from 11 to 7.9 with a chlorine dose of 4.5 mg/L and 85 µg/L of initial bromide concentration. In contrast, Fang et al. (2017) reported that more bromate was formed at pH 9 than at pH 6 under conditions of a very high bromide concentration of 2 mg/L, and 5 mg/L of chlorine, and when using a medium pressure UV lamp. This contrasting pH effect could be due a very rapid formation of free bromine due to the high initial bromide (2 mg/L). Here, the rate limiting step might be subsequent photolysis and radical reaction of the free bromine, which as mentioned earlier can be favored at high pH when using a medium pressure lamp.

Bromate formation in natural water is predicted to decrease in the presence of radical scavengers such as (NOM). Such scavengers may consume some RBS that are the intermediate species for bromate, leading to a reduction in bromate formation (Fang et al., 2017; Huang et al., 2008b).

Minimizing bromate formation in a UV-chlorine process can be complicated. An interesting case study is the Terminal Island Water Reclamation Plant serving Los Angeles. During initial planning and design of the facility, the bromide concentration in the wastewater to be treated was measured to be minimal, but after construction and commissioning of the plant it was suspected that sewers delivering the wastewater to the plant, which travelled under a harbor, were allowing some saltwater intrusion, and elevating the bromide to almost 4000 µg/L. The RO at the plant reduced this bromide to an average of about 90 µg/L that would enter the UV-chlorine system. The system oxidized this bromide to produce bromate levels approaching 30 µg/L. The plant is under a mandate to produce water that meets drinking water standards with a bromate limit of 10 µg/L, and therefore remedial action was required. The solution was to apply 0.3 mg-N/L ammonia immediately after the RO and before free chlorine application. This reduced bromate formation to less than approximately 6 µg/L. Recall that bromate formation requires the ambient bromide to first be oxidized to free bromine by the free chlorine. Ammonia reacts very quickly with free bromine to form bromamines in a reaction that is analogous to the reaction with free chlorine to form chloramines (Hofmann and Andrews, 2001; Jafvert and Valentine, 1992).



Bromamine effectively sequesters the bromine, removing it from the bromate formation pathway. The downside of this strategy is that the ammonia will also react with free chlorine to

form chloramines, which not only reduces the amount of free chlorine available to drive the AOP, but also lowers the UVT. There is therefore a delicate balance between adding enough ammonia to block bromate formation without consuming too much free chlorine and lowering UVT. The reaction rate coefficients between ammonia and free bromine vs. free chlorine shown in the preceding equations suggest that the ammonia will tend to react approximately 20 times faster with free bromine than free chlorine, so it is possible to favor the bromate inhibition action without creating a high free chlorine demand. This is illustrated in Figure A3-3, which predicts the fate of 0.3 mg-N/L of ammonia reacting in a mixture of 3 mg/L Cl_2 and 100 $\mu\text{g/L}$ bromide at pH 6. As suggested in the previous Figure A3-2, it takes several dozens of seconds for the free chlorine to oxidize most of the bromide to free bromine. In that time, some of the ammonia reacts with free chlorine to consume approximately half of the free chlorine, converting it to monochloramine. However, any free bromine that is formed due to chlorine oxidation is almost instantaneously converted to monobromamine, such that almost no free bromine (free Br_2) accumulates except for at the first few seconds of the reaction. From Figure A3-3, it can be suggested that as long as the ammonia/bromide/chlorine mixture has reacted for at least approximately 10 seconds, the majority of the bromide will have been safely sequestered as monobromamine (NH_2Br) and the mixture can enter the UV reactor in a way that minimizes bromate formation. However, Figure A3-3 also suggests that it would be beneficial to avoid long upstream reaction times because the free chlorine continues to be removed as it converts to monochloramine over tens of seconds, which would make the AOP less effective.

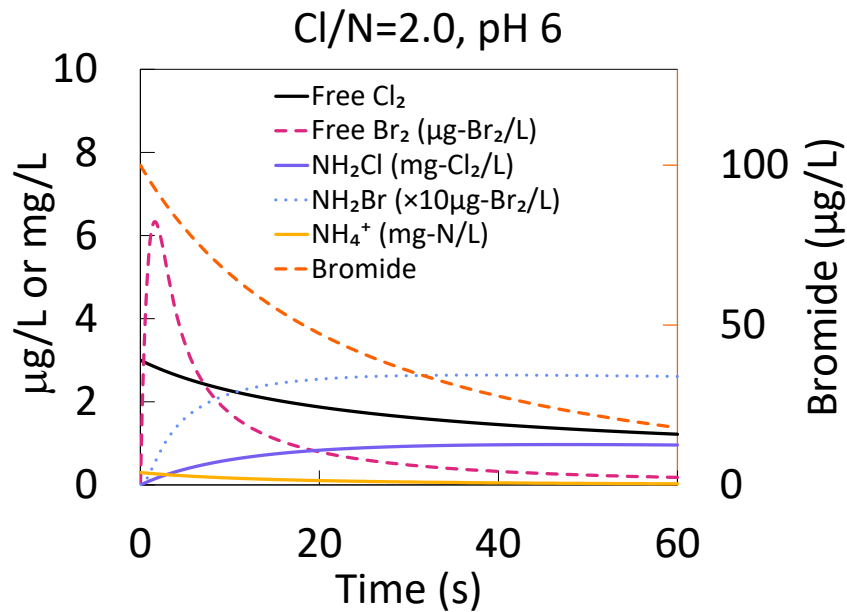


Figure A3-3 Reaction of Ammonia with Free Bromine and Free Chlorine.

A3.9 Toxicity Assays

While UV-chlorine treatment may create certain by-products, it is difficult to assess their relevance. An increasingly common research tool is the toxicity assay, whereby the cumulative toxic effect of a mixture of DBPs in one sample can be compared to a reference sample (such as

normal tap water), without knowing the exact and complete composition of the DBPs in the samples (Sun et al. 2019; Zeng et al. 2015; Escher et al. 2013; Neale and Escher 2019). In fact, this is becoming increasingly recognized as an important tool. The United States Science Advisory Panel for *Monitoring Strategies for Constituents of Emerging Concern (CECs) in Recycled Water* (convened by the (California) State Water Resources Control Board) recently made recommendations for use of bioanalytical screening tools (Drewes et al. 2018). These recommendations were made because it is impossible to capture all possible new compounds that may be entering the market, nor can the existing monitoring framework for recycled water adequately address their transformation products. The Panel recommended that the estrogen receptor alpha (ER- α) and the aryl hydrocarbon receptor (AhR) bioassays be used to respectively assess estrogenic and dioxin-like biological activities in recycled water. A distinction needs to be made for these two assays: they are meant to observe the potential *destruction* of such contaminants that might be present in the feed water across the AOP. They are not likely to be relevant in terms of identifying toxins that might be *produced* (i.e., DBPs) in the AOP reactor, and which might exhibit toxic properties that are different from estrogens and dioxins.

Although there are many bioanalytical tools that can be used to assess DBPs, cell-based *in vitro* bioassays are often favored because they provide high throughput, sensitive, risk-scaled measurements (where a sample with higher toxic potency triggers a greater bioassay response), without harming whole organisms (Neale et al. 2012; Escher and Leusch 2012). Specifically, these bioassays use quantifiable endpoints, such as the induction of an adaptive stress response pathway, or general cell viability, to measure the cumulative effects of all chemicals in a mixture that exhibit the same mode of toxic action (MOA) (Jia et al. 2015). The three major MOA classes are: specific toxicity (receptor-mediated events), non-specific toxicity (cytotoxicity), and reactive toxicity (Escher and Leusch 2012). Reactive toxicity, encompassing genotoxicity (DNA damage) and adaptive stress response pathways, is of particular relevance to DBP formation because DBPs, which are generally electrophilic, react with hard nucleophiles such as DNA (causing direct DNA damage), or soft nucleophiles such as proteins and peptides (activate oxidative stress response pathways or causing indirect DNA damage) (Lin and Hollenberg 2001; Van Welie et al. 1992; Enoch and Cronin 2010; Enoch et al. 2011).

At present, there are few reported applications of bioanalytical tools in the study of UV-chlorine AOPs. Huang et al. (2017) and Li et al. (2016) both reported that UV-chlorine was observed to reduce the cytotoxicity and estrogenicity of specific micropollutants, and Sun et al. (2019) reported that UV-chlorine led to 22-27% less overall cytotoxicity and genotoxicity than UV-H₂O₂ after post-chlorination. In another study, transformation products during UV-chlorine processes were more cytotoxic to *Raphidocelis subcapitata* algae, than UV-H₂O₂ (91% vs. 42% cell inhibition) when treating 17 β -estradiol and 17 α -ethinylestradiol at environmental concentrations (Chaves et al., 2020).

Huang et al. (2017) applied the Microtox assay to LP UV-chlorine-treated ultrapure water containing DDBAC (a biocide) and found early formation of toxic by-products, which were mineralized under extended treatment. This trend in cytotoxicity is similar to what has been found following UV-H₂O₂ treatment, whereby an increase in acute toxicity may be observed at

intermediate AOP doses, followed by a reduction in toxicity at higher doses (Shemer and Linden, 2007; Olmez-Hanci et al., 2015; Rozas et al., 2016).

Only a handful of reports are reported on the effects of UV-chlorine advanced oxidation on reactive toxicity for real water samples (i.e., non-spiked waters with compounds of interest). Reclaimed Ohio river water (pre-treated with GAC) was exposed to LP or MP UV, in the absence and presence of chlorine (as AOP) and tested in the CHO comet assay for genotoxicity and cytotoxicity (Plewa et al., 2012). The LP UV-chlorine water had similar responses to that of chlorinated water, while MP UV-chlorine produced the least reactive water matrix in the comet assay (50% less than LP UV-chlorine treated waters).

Hua et al. (2021) applied chlorine and LP-UV/chlorine to secondary wastewater effluent. The acute toxicity of the wastewater to *Vibrio fischeri* and genotoxicity determined by the SOS/*umu* test decreased by 19% and 76%, respectively, after the 20 min UV-chlorine treatment. The addition of 1 mg/L bromide to the UV-chlorine process dramatically increased the formation of brominated DBPs and the overall calculated cytotoxicity and genotoxicity of DBPs. However, when tested in the bioassays, the acute toxicity and genotoxicity of the wastewater decreased by 7% and 100%, respectively, when bromide was added to the UV-chlorine treatment.

Several studies have shown that reactive toxicity can increase as a result of other UV-based AOPs. For example, Jia et al. (2015) observed an increase in the genotoxicity and mutagenicity of secondary wastewater treatment plant effluent following both UV-H₂O₂ and UV-O₃ treatment, indicating the formation of reactive transformation products. Reactive toxicity changes during UV-H₂O₂ appear to be influenced by the production of certain mutagenic N-containing organic compounds from the photolysis of nitrate (circa 200-240 nm) which can occur from MP UV exposure, but not from LP UV exposure (Lekkerkerker-Teunissen et al. 2013; Hofman-Caris et al. 2015). Pre-treated surface waters treated with MP UV-H₂O₂ elicited positive responses in the Ames TA98 test (frame shift mutation strain), however the Ames II test (mixture of strains) and the comet assay showed no mutagenic activity. Interestingly, GAC post treatment effectively reduced the TA98 activities to control levels for all location sites. While MP UV AOPs may lead to the formation of genotoxic by-products, the transformation products can be removed by subsequent GAC filtration. This significance of UV lamp type (and dose) and nitrate on reactive toxicity may also apply to UV-chlorine advanced oxidation.

CHAPTER A4

Disinfection Credit for a UV-AOP

One of the advantages of using a UV-AOP system for water reuse treatment is that it provides multiple barriers in one treatment unit: the UV light can destroy photosensitive chemical contaminants, the radicals can destroy a wide spectrum of chemicals, and the system can also provide disinfection against pathogens that might have escaped upstream treatment. The disinfection performance, however, is difficult to quantify and to monitor.

UV disinfection reactors are inherently complex, and fundamental to this complexity is the concept of the [UV dose distribution](#). As water passes through a UV reactor, some elements of water pass more quickly through the reactor than others, or closer to the UV lamps than others. Since the UV dose received by a pathogen is a function of intensity of the light (i.e., the distance from the lamp) and the amount of time exposed to the UV, there is therefore a range of doses applied to a total flow of water, and to the pathogens in that flow. A pathogen that receives a high dose may be inactivated, but a pathogen that passes through the reactor in a low dose pathway may survive. Since it's not possible to equip a reactor with enough sensors to monitor the UV dose supplied to every conceivable flow pathway, UV disinfection reactors are generally [validated](#) by a third-party to gain regulatory approval. This validation process typically involves spiking microorganisms into a UV reactor under controlled conditions to ensure that sufficient inactivation is achieved by that reactor. It is beyond the scope of this document to discuss UV reactor validation in detail, but the reader is referred to the U.S. EPA's guidance on this topic (EPA, 2006; EPA, 2020).

There is no industry consensus about the degree to which a UV-AOP reactor for water reuse treatment might be required to provide disinfection. In California, for example, there is currently a proposal to establish uniform direct potable reuse standards that require 10/11/16-log reduction of *Giardia*, *Cryptosporidium*, and viruses respectively, with the UV-AOP component given credit for 6-log inactivation of each of the three organisms, and the RO/membrane processes required to provide the remaining log reduction (Waterboards, 2021). Demonstrating 6-log inactivation of an organism in a UV reactor is at the boundary of what is possible. To demonstrate 6-log inactivation (99.9999%), a microorganism must be delivered into the inflow at a high enough concentration that allows for 6-logs of inactivation across the reactor but with enough survivors to be quantifiable in the reactor effluent to allow determination of the log reduction achieved. In practice, it is often not possible to inject a high enough concentration of organisms to achieve this—or, if the organisms can be generated to a high enough concentration and injected, the resulting flow may be so concentrated with the solution containing the microorganisms that the UVT is necessarily unrealistically too low for the validation testing.

At present, some regulators have been granting 6-log inactivation credit provided that the reactor demonstrate some target level of chemical destruction, such as 1.2-log NDMA destruction, requiring a UV_{254} fluence of approximately 1200 mJ/cm^2 (Sharpless et al., 2003), on

the assumption that the UV dose required to achieve that chemical destruction is conservatively high enough to assuredly achieve 6-log pathogen inactivation (e.g., 6-log adenovirus reduction may require a UV dose in the order of 276 mJ/cm²). Unfortunately, this approach is not strictly valid. The presence of a UV dose distribution dictates that one cannot directly extrapolate from the measured destruction of one chemical or organism to the predicted destruction of another, without considering a number of complicating factors. This is the basis of the [RED bias](#) phenomenon discussed in the U.S. EPA’s UV disinfection guidance manual (EPA, 2006).

An emerging method to solve this problem with UV-AOP disinfection credit is to use what is currently called the “combined variable approach” for validation (EPA, 2020). It is beyond the scope of this document to discuss the details of this approach, but in brief, the following equation is used to govern the process:

$$\log(I) = 10^A \times UVA^{B \times UVA} \times \left(\frac{\frac{S}{S_0}}{Q \times D_L} \right)^{C + D \times UVA + E \times UVA^2}$$

where log(I) is the log inactivation of a microorganism whose dose-per-log is D_L (this is the UV dose required to achieve 1 log of inactivation under ideal laboratory conditions), UVA is the UV absorbance of the water, Q is the flow rate, and S/S₀ is the fraction of the UV lamp intensity relative to maximum (S₀). The coefficients A, B, C, D, and E are determined by finding the best fit for the data generated during the reactor validation test.

To use this approach, the reactor validation test uses a microorganism of a known dose/response, and its log inactivation is recorded under a variety of conditions of UV absorbance (UVA), flow (Q), and lamp power (S/S₀). A regression is then performed to determine the values of A, B, C, D, and E in the equation, which are assumed to be fixed for that model of UV reactor (this is a point of debate in the UV industry: how certain are we that these values are fixed?). Once these coefficients are known, the equation can be used to predict the log inactivation of any other microorganism. In other words, it is possible to perform a validation test using a convenient and safe organism such as MS-2 bacteriophage to determine the values for A-E, and once these are known, the model can predict the inactivation of a regulated organism such as adenovirus for a given flow (Q), lamp power (S/S₀), and UVA, by inputting adenovirus’ dose-per-log (D_L) from the literature into the equation. While this is an elegant solution, there is some debate in the UV community about whether this approach should be permitted because it can lead to extrapolating disinfection performance to conditions beyond those that have been tested. At present, there is some consensus that the equation should be generated using at least two challenge organisms to cross-check the accuracy of the equation by ensuring that the values of coefficients A-E are similar for each organism, and also to avoid using the equation to predict performance outside of the conditions used in the validation tests. Nevertheless, it remains a practical solution with great promise, and arguably an improvement over the status quo whereby a fixed disinfection credit is given automatically on the basis of observed chemical destruction (e.g., NDMA).

A final point about disinfection validation testing for UV-AOP reactors is how to include the role of the oxidant in disinfection. For example, a UV-chlorine reactor will achieve considerable disinfection by the action of the chlorine alone, and a UV-H₂O₂ system might achieve some moderate amount of disinfection directly from the H₂O₂. The radicals produced by the AOP will also contribute to disinfection, although the literature is unclear about the significance of this. At present, there is no framework to guide the industry in how to deal with this complicating factor. A conservative and practical approach might be to deliberately ignore the added disinfection provided by the chemical oxidants and the radical species, and to validate the reactor solely on the basis of UV disinfection. To do this, the reactor would be validated in the absence of the chemical, using only UV light. The water would need to have its absorbance adjusted (increased) by adding a non-disinfecting chemical such as lignosulfonate to simulate the predicted absorbance when the maximum dose of oxidant is present. For example, when validating a LPHO UV-H₂O₂ AOP reactor which may use up to 10 mg/L H₂O₂, it can be calculated that the absorbance at 254 nm due to H₂O₂ would be as much as 0.0056 cm⁻¹ ($\epsilon_{\text{H}_2\text{O}_2} = 19.2 \text{ M}^{-1}\text{cm}^{-1}$). A corresponding amount of lignosulfonate would be added to the water to simulate the inhibiting effect of H₂O₂ on transmission of the UV light through the reactor. In this way, the observed log reduction of the target organism would reflect only the action of UV light in water with the same absorbance as if H₂O₂ were present. In normal operation, it can be expected that the actual log reduction would be even higher, given the added role of the chemical oxidants and the radicals. This approach is purely hypothetical at this point and should be scrutinized by the engineering and research community before being implemented.

CHAPTER A5

Research Needs

The following is a description of some of the key issues related to UV-chlorine advanced oxidation that remain poorly understood.

Fundamental Chemistry

- **RCS.** The chemistry of reactive chlorine species remains uncertain. For example, the primary quantum yields of chlorine photolysis are not well established. Without a much better understanding of RCS formation and reaction with target contaminants, it will likely not be possible to design UV AOP reactors to take advantage of RCS reactions with confidence. One of the benefits of UV-chlorine over UV-H₂O₂ is the formation of not only ·OH, but RCS. If RCS concentrations cannot be predicted, and/or practical methods devised to monitor their presence either directly or indirectly as an operational tool, the role of RCS may have to be ignored. In turn, this leads to overly conservative and less efficient UV-chlorine system design and operation.
- **Temperature.** The effect of temperature on the relevant AOP reactions is largely unreported. Most reaction kinetic models are based on experiments conducted at room temperature. One preliminary study showed a reduction in contaminant destruction in the order of 20% as water cooled from 20°C to near freezing. This may be relevant in some contexts.
- **Organic amines.** It is known that chloramines significantly affect UV-chlorine AOP performance through several mechanisms. Organic amines are known to behave similarly to chloramines in many respects, and their relevance, especially in water reuse in terms of maintaining a free chlorine residual, or affecting UVT or radical scavenging, has not been reported.
- **Chloramine modeling.** The presence of chloramines in RO permeate followed by application of free chlorine leads to reactions that take place over several dozens of seconds that can significantly affect the performance of the UV-chlorine AOP. Models such as the one reported in this study to predict the speciation of the chlor(am)ine species over this timeframe have not been sufficiently validated in terms of their accuracy for this purpose. The models should be validated accordingly, and over the full range of expected operating conditions including pH and temperature.
- **Alternative UV-AOPs.** Some studies have reported the use of UV-chloramines or UV-nitrate as AOPs. While these are elegant and intriguing solutions—using chemicals that are already in the water to initiate the AOP—peer-reviewed articles to date on this subject are not comprehensive enough to allow consultants to adequately evaluate cost vs. performance, or potential negative side effects.

UV Reactor Modeling

- Availability of reactor models to third parties. At present, the ability to predict UV-AOP performance is largely limited to manufacturers and a very few consultants. As a result, customers and their (non-expert) consultants are not able to easily explore AOP treatment alternatives over a wide range of conditions as they work to optimize their designs (for example, sensitivity analyses of UVT, pH control, temperature, lamp output, flow rates, etc.). They must rely instead on trusting the manufacturers to give them accurate information. However, there is a wealth of information in the literature on models for UV disinfection reactors (i.e., computational fluid dynamic models), so there's reason to be optimistic that AOP reactor models can be developed for the general consulting community. In particular, it can be argued that it is easier to build a hydraulic and light irradiance model for an AOP reactor than for a disinfection reactor, since disinfection is usually applied to achieve a high log reduction of a target (e.g., 4 log virus), compared to a low log reduction of a chemical in an AOP reactor (e.g., 0.5-log 1,4-dioxane)—in turn, this makes the AOP model less sensitive to small inaccuracies in the fluence distribution (this is a complicated issue, but in general, AOP reactors are governed by the average dose in the reactor, whereas disinfection reactors that must achieve high log reductions are governed by the smallest dose in the dose distribution, and using a model to find the smallest dose is much more difficult than finding the average dose). The challenge, however, is to superimpose the AOP chemical reactions on the hydraulic/irradiance model of the CFD program. Some AOP reaction schemes include over 100 reactions, and the computational requirements to combine 100+ reactions with a CFD model are daunting. It may be possible, however, to use a simplified chemical reaction scheme along with a CFD model to build an AOP reactor model that is sufficiently accurate to allow consultants to make useful estimates of the performance of different AOP reactor configurations and water quality conditions.
- Oxidant (initiator) concentrations vs. UV dose. There is little information in the published literature to guide consultants and their customers on options with respect to UV dose vs. oxidant dose to achieve the desired level of contaminant destruction. This issue is related to the previous one: consultants don't have a tool available to explore such different options with any degree of confidence and must rely on manufacturer information.
- Changes to water quality across a UV reactor. There is little information in the peer-reviewed literature about the magnitude of changes to UVT, radical scavenging capacity, pH, and other general chemical composition, across the UV reactor from entry to exit. It is known that significant changes to such properties can exist due to the photochemical reactions within the reactor. More information on this topic would allow for more accurate UV reactor models.
- UV dosing rate. There is no information in the literature on whether the UV fluence rate (i.e., the lamp power per unit flow) to achieve a certain total fluence matters in practice. It would be instructive if there was authoritative information on whether, for example, it is advantageous to use fewer but more powerful UV reactors, or a larger number of less powerful reactors to achieve a treatment goal.

Radical Scavenging

The performance of a UV-AOP system is proportional to the amount of radical scavengers in the water, including •OH scavengers and RCS scavengers (in the case of UV-chlorine). The amount of these scavengers must therefore be known to accurately and efficiently design a UV-AOP system.

- Standard OH scavenging potential method. At present, methods to measure the hydroxyl scavenging potential of a water have been described only in the scientific literature, and there is no standard method—although the International Ultraviolet Association currently has a task force to propose such a standard. Furthermore, there is no instrument that allows the measurement to be made easily. It requires labor-intensive wet-laboratory techniques.
- RCS scavenging potential method. Ideally, the presence of RCS should be able to be included in the performance predictions for a UV-chlorine system. One of the steps towards this goal would be to measure RCS scavenging capacity of water, similar to the previous point. No such method has been reported, except in a preliminary way in several scientific papers.
- Variability in scavenging potential. Just as chlorine demand can vary hour-to-hour in a water treatment plant, it is conceivable that radical scavenging capacity can also vary with time. The lack of an easy way to measure radical scavenging potential in the past has led to a lack of data on the potential variability of this parameter. If a simple instrument were available to make this measurement, a database on its variability could be constructed. This information would in turn allow UV AOP systems to be designed with more accuracy and less conservatism.

DBPs, Toxicity, and Downstream Effects

- **Transformation products.** There is a considerable amount of scientific literature that reports the transformation products of various parent compounds upon AOP treatment. However, there is arguably no framework with which to use this information. The water industry has recently recognized this problem, with some voices recommending that we move away from accumulating long lists of transformation products (or DBPs) that may be formed during treatment, and instead, try to identify which parameters are most likely to be relevant from a health, regulatory, or operational perspective. Bioassays are being proposed as one possible means to do this. Any research that can help to inform the discussions on this topic would be beneficial.
- **Nitrate photolysis.** There is a common belief that MP reactors are prone to nitrate photolysis at wavelengths in the 200-240 nm range, which in turn leads to nitrite (a powerful hydroxyl scavenger) and potentially toxic nitrogen-containing byproducts. Most of the evidence for this comes from lab-scale experiments with small light path lengths (e.g., 1 cm), compared to full-scale MP reactors with path lengths often > 10 cm. Water is a strong absorber at 200-240 nm, so it is possible that the 200-240 nm photons are unable to penetrate far into the water column, thereby minimizing nitrate photolysis at full scale. This theory has not been explicitly explored in the peer-reviewed literature. Since there are

several theoretical advantages to using polychromatic (MP) lamps for UV-chlorine treatment under certain conditions, more information on nitrate photolysis would be helpful.

- A topic related to the previous one is the potential for nitrate to undergo photolysis at 254 nm. Nitrate's absorption at 254 nm is very weak, but in water with very high UVT (e.g., RO permeate), there is anecdotal evidence that nitrate photolysis to nitrite can be significant, even when using LP systems. More information on this topic is needed.
- Distribution system chlorine demand and BDOC. Experience from several utilities suggests that UV-H₂O₂ can cause a significant and instantaneous increase (40-300%) in chlorine demand in a distribution system, presumably by transforming organic matter. This phenomenon, along with the potential formation of biodegradable organic matter that can also gradually lead to difficulty in maintaining a chlorine residual, is not well understood.
- **Chlorate.** UV-chlorine AOP leads to chlorate formation as a byproduct. The creation of an accurate chlorate formation model would help utilities to anticipate whether to pay close attention to this potential issue. If chlorate formation approaches regulatory limits, methods to actively minimize the formation should be identified.
- **Bromate.** Similar to chlorate, an accurate bromate formation model under UV-chlorine AOP conditions could allow for utilities and their regulators to predict conditions where more active bromate monitoring may be needed.

Regulatory

- If regulators are going to require that UV AOP reactors achieve a certain level of disinfection performance (e.g., 6-log pathogen inactivation for water reuse applications), there needs to be more data to support a method to initially validate this level of performance, and then to continuously monitor the reactor to ensure that performance is maintained. The “innovative approach” method is a promising tool that can potentially be used for this purpose, but it is arguably not well established in the peer reviewed literature or accepted by the wider UV community.

CHAPTER A6

References

- Alfassi, Z. B., R. E. Huie, S. Mosseri, and P. Neta. 1988. "Kinetics of One-Electron Oxidation by the ClO Radical." *International Journal of Radiation Applications and Instrumentation. Part C. Radiation Physics and Chemistry*, 32 (1): 85-88.
- Asami, M., K. Kosaka, and S. Kunikane. 2009. "Bromate, Chlorate, Chlorite and Perchlorate in Sodium Hypochlorite Solution Used in Water Supply." *Journal of Water Supply: Research and Technology—Aqua*, 58 (2): 107-115.
- Amy, G., M. Siddiqui, W. Zhai, J. DeBroux, and W. Odem. 1993. "Nation-Wide Survey of Bromide Ion Concentrations in Drinking Water Sources." *In Proc. 1993 AWWA Annual Conference*, San Antonio, Texas.
- Anastasio, C., and B. M. Matthew. 2006. "A Chemical Probe Technique for the Determination of Reactive Halogen Species in Aqueous Solution: Part 2—Chloride Solutions and Mixed Bromide/Chloride Solutions." *Atmospheric Chemistry and Physics*, 6 (9): 2439-2451.
- Armstrong, D. A., R. E. Huie, W. H. Koppenol, S. V. Lyman, G. Merényi, P. Neta, B. Ruscic, D. M. Stanbury, S. Steenken, and P. Wardman. 2015. "Standard Electrode Potentials Involving Radicals in Aqueous Solution: Inorganic Radicals (IUPAC Technical Report)." *Pure and Applied Chemistry*, 87 (11-12): 1139-1150.
- AWWA. 2022. Hypochlorite Assessment Model. American Water Works Association. <https://engage.awwa.org/PersonifyEbusiness/tools/hypochlorite>. Accessed January 5, 2022.
- Bai, M., Y. Tian, Y. Yu, Q. Zheng, X. Zhang, W. Zheng, and Z. Zhang. 2018. "Application of a Hydroxyl-Radical-Based Disinfection System for Ballast Water." *Chemosphere*, 208: 541-549.
- Bazri, M. M., B. Barbeau, and M. Mohseni. 2012. "Impact of UV/H₂O₂ Advanced Oxidation Treatment on Molecular Weight Distribution of NOM and Biostability of Water." *Water Research*, 46 (16): 5297-5304.
- Bircher, K. 2011. "Using UV Dose Response for Scale Up of UV/AOP Reactors." *IUVA News*. <https://uvsolutionsmag.com/iuva-archive/>.
- Bolton, J., K. G. Bircher, W. Tumas, C. A. Tolman. 2001. "Figures of Merit for the Technical Development and Application of Advanced Oxidation Technologies for Both Electric and Solar Driven Systems." *Pure and Applied Chemistry*, 73 (4): 627-637.
- Bolton, J., and J. Collins. 2016. "Advanced Oxidation Handbook." American Water Works Association.

- Bulman, D. M., S. P. Mezyk, and C. K. Remucal. 2019. "The Impact of pH and Irradiation Wavelength on the Production of Reactive Oxidants during Chlorine Photolysis." *Environmental Science & Technology*, 53 (8): 4450-4459.
- Buxton, G. V., and M. S. Subhani. 1972. "Radiation Chemistry and Photochemistry of Oxychlorine Ions. Part 2.—Photodecomposition of Aqueous Solutions of Hypochlorite Ions." *Journal of the Chemical Society, Faraday Transactions 1: Physical Chemistry in Condensed Phases*, 68: 958-969.
- Buxton, G. V., and F. S. Dainton. 1968. "The Radiolysis of Aqueous Solutions of Oxybromine Compounds; The Spectra and Reactions of BrO and BrO₂." *Proceedings of the Royal Society of London. Series A. Mathematical and Physical Sciences*, 304 (1479): 427-439.
- California State Water Resources Control Board. 2017. "Groundwater Information Sheet N-Nitrosodimethylamine." State Water Resources Control Board, Division of Water Quality. <https://www.waterboards.ca.gov/gama/docs/ndma.pdf>.
- Cao, Z., X. Yu, Y. Zheng, E. Adam, B. Sun, M. Song, A. Wang, J. Han, and J. Zhang. 2022. "Micropollutant Abatement by the UV/Chloramine Process in Potable Water Reuse: A Review." *Journal of Hazardous Materials*, 424: 127341.
- Chaves, F. P., G. Gomes, A. Della-Flora, A. Dallegrave, C. Sirtori, E. M. Saggiaro, and D. M. Bila. 2020. "Comparative Endocrine Disrupting Compound Removal from Real Wastewater by UV/Cl and UV/H₂O₂: Effect of Ph, Estrogenic Activity, Transformation Products and Toxicity." *Science of the Total Environment*, 746: 141041.
- Cheng, S., X. Zhang, X. Yang, C. Shang, W. Song, J. Fang, and Y. Pan. 2018. "The Multiple Role of Bromide Ion in PPCPs Degradation Under UV/Chlorine Treatment." *Environmental Science & Technology*, 52 (4): 1806-1816.
- Cho, M., H. Chung, W. Choi, and J. Yoon. 2005. "Different Inactivation Behaviors of MS-2 Phage and Escherichia Coli in TiO₂ Photocatalytic Disinfection." *Applied and Environmental Microbiology*, 71 (1): 270-275.
- Chu, L., and C. Anastasio. 2005. "Formation of Hydroxyl Radical from the Photolysis of Frozen Hydrogen Peroxide." *The Journal of Physical Chemistry A*, 109 (28): 6264-6271.
- Chuang, Y. H., S. Chen, C. J. Chinn, and W. A. Mitch. 2017. "Comparing the UV/Monochloramine and UV/Free Chlorine Advanced Oxidation Processes (AOPs) to the UV/Hydrogen Peroxide AOP under Scenarios Relevant to Potable Reuse." *Environmental Science & Technology*, 51 (23): 13859-13868.
- Cipparone, L. A., A. C. Diehl, and G. E. Speitel Jr. 1997. "Ozonation and BDOC Removal: Effect on Water Quality." *Journal-American Water Works Association*, 89 (2): 84-97.
- Dotson, A. D., D. Metz, and K. G. Linden. 2010. "UV/H₂O₂ Treatment of Drinking Water Increases Post-Chlorination DBP Formation." *Water Research*, 44 (12): 3703-3713.

Drewes, J. E., P. Anderson, N. Denslow, W. Jakubowski, A. Olivieri, D. Schlenk, and S. Snyder. 2018. "Monitoring Strategies for Constituents of Emerging Concern (CECs) in Recycled Water." Prepared for the California State Water Resources Control Board. http://ftp.sccwrp.org/pub/download/DOCUMENTS/TechnicalReports/1032_CECMonitoringInRecycledWater.pdf.

DWI. 2018. "Potential for Formation of Disinfection By-Products from Advanced Oxidation Processes." DWI 12852.02. wrpclc: Swindon, Wiltshire, UK. <https://cdn.dwi.gov.uk/wp-content/uploads/2020/10/27111341/DWI70-2-317.pdf>.

Enoch, S. J., and M. T. D. Cronin. 2010. "A Review of the Electrophilic Reaction Chemistry Involved in Covalent DNA Binding." *Critical Reviews in Toxicology*, 40 (8): 728-748.

Enoch, S. J., C. M. Ellison, T. W. Schultz, and M. T. D. Cronin. 2011. "A review of the Electrophilic Reaction Chemistry Involved in Covalent Protein Binding Relevant to Toxicity." *Critical Reviews in Toxicology*, 41 (9): 783-802.

EPA. 2006. "Ultraviolet Disinfection Guidance Manual for the Long Term 2-Enhanced Surface Water Treatment Rule." U.S. Environmental Protection Agency. <https://nepis.epa.gov/Exe/ZyPDF.cgi/600006T3.PDF?Dockey=600006T3.PDF>.

EPA 2020. "Innovative Approaches for Validation of Ultraviolet Disinfection Reactors for Drinking Water Systems." EPA/600/R-20/094. U.S. Environmental Protection Agency: Washington, D.C.

EPA. 2021. "National Primary Drinking Water Regulations." U.S. Environmental Protection Agency. <https://www.epa.gov/ground-water-and-drinking-water/national-primary-drinking-water-regulations>.

Escher, B. I., C. van Daele, M. Dutt, J. Y. Tang, and R. Altenburger. 2013. "Most Oxidative Stress Response in Water Samples Comes from Unknown Chemicals: The Need for Effect-Based Water Quality Trigger Values." *Environmental Science & Technology*, 47 (13): 7002-7011.

Escher, B., F. Leusch, H. Chapman, and A. Poulsen. 2012. *Bioanalytical Tools in Water Quality Assessment*. IWA Publishing, London, UK.

Fang, J., Y. Fu, and C. Shang. 2014. "The Roles of Reactive Species in Micropollutant Degradation in the UV/Free Chlorine System." *Environmental Science & Technology*, 48 (3): 1859-1868.

Fang, J., Q. Zhao, C. Fan, C. Shang, Y. Fu, and X. Zhang. 2017. "Bromate Formation from the Oxidation of Bromide in the UV/Chlorine Process with Low Pressure and Medium Pressure UV Lamps." *Chemosphere*, 183: 582-588.

Feng, Y., D. W. Smith, and J. R. Bolton. 2007. "Photolysis of Aqueous Free Chlorine Species (HOCl and OCl) with 254 nm Ultraviolet Light." *Journal of Environmental Engineering and Science*, 6 (3): 277-284.

Feng, Y., D. W. Smith, and J. R. Bolton. 2010. "A Potential New Method for Determination of the Fluence (UV Dose) Delivered in UV Reactors Involving the Photodegradation of Free Chlorine." *Water Environment Research*, 82 (4): 328-334.

Furst, K. E., B. M. Pecson, B. D. Webber, and W. A. Mitch. 2018. "Tradeoffs between Pathogen Inactivation and Disinfection Byproduct Formation during Sequential Chlorine and Chloramine Disinfection for Wastewater Reuse." *Water Research*, 143: 579-588.

Gao, Z. C., Y. L. Lin, B. Xu, Y. Xia, C. Y. Hu, T. Y. Zhang, T. C. Cao, Y. Pan, and N. Y. Gao. 2019. "A Comparison of Dissolved Organic Matter Transformation in Low Pressure Ultraviolet (LPUV) and Ultraviolet Light-Emitting Diode (UV-LED)/Chlorine Processes." *Science of the Total Environment*, 702: 134942.

Gao, Y. Q., N. Y. Gao, J. X. Chen, J. Zhang, and D. Q. Yin. 2020. "Oxidation of β -blocker Atenolol by a Combination of UV Light and Chlorine: Kinetics, Degradation Pathways and Toxicity Assessment." *Separation and Purification Technology*, 231: 115927.

Gerrity, D., A. N. Pisarenko, E. Marti, R. A. Trenholm, F. Geringer, J. Reungoat, and E. Dickenson. 2015. "Nitrosamines in Pilot-Scale and Full-Scale Wastewater Treatment Plants with Ozonation." *Water Research*, 72: 251-261.

Glaze, W. H. 1990. *Chemical Oxidation. Water Quality and Treatment: A Handbook of Community Water Supplies*. 4th ed. New York: McGraw-Hill.

Goldstein, S. and J. Rabani. 2007. "Mechanism of Nitrite Formation by Nitrate Photolysis in Aqueous Solutions: The Role of Peroxynitrite, Nitrogen Dioxide, and Hydroxyl Radical." *Journal of the American Chemical Society*, 129 (34): 10597-10601.

Grebel, J. E., J. J. Pignatello, and W. A. Mitch. 2010. "Effect of Halide Ions and Carbonates on Organic Contaminant Degradation by Hydroxyl Radical-Based Advanced Oxidation Processes in Saline Waters." *Environmental Science & Technology*, 44 (17): 6822-6828.

Guo, Z. B., Y. L. Lin, B. Xu, H. Huang, T. Y. Zhang, F. X. Tian, and N. Y. Gao. 2016. "Degradation of Chlortoluron during UV Irradiation and UV/Chlorine Processes and Formation of Disinfection By-Products in Sequential Chlorination." *Chemical Engineering Journal*, 283: 412-419.

Guo, K., Z. Wu, C. Shang, B. Yao, S. Hou, X. Yang, W. Song, and J. Fang. 2017. "Radical Chemistry and Structural Relationships of PPCP Degradation by UV/Chlorine Treatment in Simulated Drinking Water." *Environmental Science & Technology*, 51 (18) : 10431-10439.

Guo, K., Z. Wu, S. Yan, B. Yao, W. Song, Z. Hua, X. Zhang, X. Kong, X. Li, and J. Fang, J. (2018). "Comparison of the UV/Chlorine and UV/H₂O₂ Processes in the Degradation of PPCPs in Simulated Drinking Water and Wastewater: Kinetics, Radical Mechanism, and Energy Requirements." *Water Research*, 147: 184-194.

Guo, K., S. Zheng, X. Zhang, L. Zhao, S. Ji, C. Chen, Z. Wu, D. Wang, and J. Fang. 2020. "Roles of Bromine Radicals and Hydroxyl Radicals in the Degradation of Micropollutants by the UV/Bromine Process." *Environmental Science & Technology*, 54 (10) : 6415-6426.

Hao, J., S. Qiu, H. Li, T. Chen, H. Liu, and L. Li. 2012. « Roles of Hydroxyl Radicals in Electrolyzed Oxidizing Water (EOW) for the Inactivation of Escherichia Coli.” *International Journal of Food Microbiology*, 155 (3): 99-104.

Health Canada. 2008. “Guidelines for Canadian Drinking Water Quality: Guideline Technical Document — Chlorite and Chlorate.” Water Quality and Health Bureau, Healthy Environments and Consumer Safety Branch, Health Canada: Ottawa, Ontario.

https://publications.gc.ca/collections/collection_2009/sc-hc/H128-1-08-549E.pdf.

Health Canada. 2017. “Guidelines for Canadian Drinking Water Quality—Summary Table.” Water and Air Quality Bureau, Healthy Environments and Consumer Safety Branch, Health Canada: Ottawa, Ontario. https://publications.gc.ca/collections/collection_2017/sc-hc/H129-24-2017-eng.pdf.

Health Canada. 2020. “Guidelines for Canadian Drinking Water Quality—Summary Table.” Water and Air Quality Bureau, Healthy Environments and Consumer Safety Branch, Health Canada: Ottawa, Ontario. https://publications.gc.ca/collections/collection_2020/sc-hc/H129-24-2020-eng.pdf.

Heringa, M. B., D. J. H. Harmsen, E. F. Beerendonk, A. A. Reus, C. A. M. Krul, D. H. Metz, and G. F. Ijpelaar. 2011. “Formation and removal of Genotoxic Activity during UV/H₂O₂–GAC Treatment of Drinking Water.” *Water Research*, 45 (1): 366-374.

Hofman-Caris, R. C., D. J. Harmsen, L. Puijker, K. A. Baken, A. Wols, E. F. Beerendonk, and L. L. Keltjens. 2015. “Influence of Process Conditions and Water Quality on the Formation of Mutagenic Byproducts in UV/H₂O₂ Processes.” *Water Research*, 74: 191-202.

Hofmann, R., and R. C. Andrews. 2001. Ammoniacal Bromamines: A Review of Their Influence on Bromate Formation during Ozonation.” *Water Research*, 35 (3): 599-604.

Hua, Z., D. Li, Z. Wu, D. Wang, Y. Cui, X. Huang, J. Fang, and T. An. 2021. “DBP Formation and Toxicity Alteration during UV/Chlorine Treatment of Wastewater and the Effects of Ammonia and Bromide.” *Water Research*, 188: 116549.

Huang, L., L. Li, W. Dong, Y. Liu, and H. Hou. 2008a. “Removal of Ammonia by OH Radical in Aqueous Phase.” *Environmental Science & Technology*, 42 (21): 8070-8075.

Huang, X., G. Naiyun, and D. Yang. 2008b. “Bromate Ion Formation in Dark Chlorination and Ultraviolet/Chlorination Processes for Bromide-Containing Water.” *Journal of Environmental Sciences*, 20 (2): 246-251.

Huang, N., T. Wang, W. L. Wang, Q. Y. Wu, A. Li, and H. Y. Hu. 2017. “UV/chlorine as an Advanced Oxidation Process for the Degradation of Benzalkonium Chloride: Synergistic Effect, Transformation Products and Toxicity Evaluation.” *Water Research*, 114: 246-253.

Ike, I. A., Y. Lee, Y., and J. Hur. 2019. “Impacts of Advanced Oxidation Processes on Disinfection Byproducts from Dissolved Organic Matter upon Post-Chlor(am)ination: A Critical Review.” *Chemical Engineering Journal*, 375: 121929.

- Ijpelaar, G. F., A. J. Van der Veer, G. J. Medema, and J. C. Kruithof. 2005. By-product Formation during Ultraviolet Disinfection of a Pretreated Surface Water." *Journal of Environmental Engineering and Science*, 4 (S1): S51-S56.
- Jadas-Hecart, A., C. Ventresque, B. Legube, and M. Dore. 1991. Effect of Ozonation on the Chlorine Demand of a Treated Surface Water and Some Macromolecular Compounds." *The Journal of the International Ozone Association*, 13 (2): 147-160.
- Jafvert, C. T., and R. L. Valentine. 1992. Reaction Scheme for the Chlorination of Ammoniacal Water." *Environmental Science & Technology*, 26 (3): 577-586.
- Jeong, G., J. H. Jung, J. H. Lim, Y. S. Won, and J. K. Lee. 2014. A Computational Mechanistic Study of Breakpoint Chlorination for the Removal of Ammonia Nitrogen From Water." *Journal of Chemical Engineering of Japan*, 47 (3): 225-229.
- Ji, Y., D. Kong, J. Lu, H. Jin, F. Kang, X. Yin, and Q. Zhou. 2016. "Cobalt Catalyzed Peroxymonosulfate Oxidation of Tetrabromobisphenol A: Kinetics, Reaction Pathways, and Formation of Brominated By-Products." *Journal of Hazardous Materials*, 313: 229-237.
- Jia, A., B. I. Escher, F. D. Leusch, J. Y. Tang, E. Prochazka, B. Dong, E. M. Snyder, and S. A. Snyder. 2015. In Vitro Bioassays to Evaluate Complex Chemical Mixtures in Recycled Water." *Water Research*, 80: 1-11.
- Jia, X., J. Jin, R. Gao, T. Feng, Y. Huang, Q. Zhou, and A. Li. 2019. "Degradation of Benzophenone-4 in a UV/Chlorine Disinfection Process: Mechanism and Toxicity Evaluation." *Chemosphere*, 222: 494-502.
- Jin, J., M. G. El-Din, and J. R. Bolton. 2011. "Assessment of the UV/chlorine Process as an Advanced Oxidation Process." *Water Research*, 45 (4): 1890-1896.
- Kang, N., T. A. Anderson, B. Rao, B., and W. A. Jackson. 2009. "Characteristics of Perchlorate Formation via Photodissociation of Aqueous Chlorite." *Environmental Chemistry*, 6 (1): 53-59.
- Kim, M. S., C. Lee, and J. H. Kim. 2021. "Occurrence of Unknown Reactive Species in UV/H₂O₂ System Leading to False Interpretation of Hydroxyl Radical Probe Reactions." *Water Research*, 201: 117338.
- Kleiser, G., and F. H. Frimmel. 2000. "Removal of Precursors for Disinfection By-Products (DBPs)—Differences between Ozone-and OH-Radical-Induced Oxidation." *Science of the Total Environment*, 256 (1): 1-9.
- Kohen, R., and A. Nyska. 2002. "Invited Review: Oxidation of Biological Systems: Oxidative Stress Phenomena, Antioxidants, Redox Reactions, and Methods for Their Quantification." *Toxicologic Pathology*, 30 (6): 620-650.
- Kolkman, A., B. J. Martijn, D. Vughs, K. A. Baken, and A. P. van Wezel. 2015. "Tracing Nitrogenous Disinfection Byproducts after Medium Pressure UV Water Treatment by Stable

Isotope Labeling and High-Resolution Mass Spectrometry." *Environmental Science & Technology*, 49 (7): 4458-4465.

Kumar, K., and D. W. Margerum. 1987. "Kinetics and Mechanism of General-Acid-Assisted Oxidation of Bromide by Hypochlorite and Hypochlorous Acid." *Inorganic Chemistry*, 26 (16): 2706-2711.

Kwon, M., A. Royce, Y. Gong, K. P. Ishida, and M. I. Stefan. 2020. "UV/chlorine vs. UV/H₂O₂ for Water Reuse at Orange County Water District, CA: A Pilot Study." *Environmental Science: Water Research & Technology*, 6 (9): 2416-2431.

Lankone, R. S., A. R. Deline, M. Barclay, and D. H. Fairbrother. 2020. "UV-Vis Quantification of Hydroxyl Radical Concentration and Dose Using Principal Component Analysis." *Talanta*, 218: 121148.

Lee, W., Y. Lee, S. Allard, J. Ra, S. Han, and Y. Lee. 2020. "Mechanistic and Kinetic Understanding of the UV254 Photolysis of Chlorine and Bromine Species in Water and Formation of Oxyhalides." *Environmental Science & Technology*, 54 (18): 11546-11555.

Lekkerkerker-Teunissen, K., A. H. Knol, J. G. Derks, M. B. Heringa, C. J. Houtman, C. H. M. Hofman-Caris, E. F. Beerendonk, A. Reus, J. Q. Verberk, and J. C. van Dijk. 2013. "Pilot Plant Results with Three Different Types of UV Lamps for Advanced Oxidation." *Ozone: Science & Engineering*, 35 (1): 38-48.

Li, M., B. Xu, Z. Liungai, H. Y. Hu, C. Chen, J. Qiao, and Y. Lu. 2016. "The Removal of Estrogenic Activity with UV/Chlorine Technology and Identification of Novel Estrogenic Disinfection By-Products." *Journal of Hazardous Materials*, 307: 119-126.

Li, W., T. Jain, K. Ishida, and H. Liu. 2017. "A Mechanistic Understanding of the Degradation of Trace Organic Contaminants by UV/Hydrogen Peroxide, UV/Persulfate and UV/Free Chlorine for Water Reuse." *Environmental Science: Water Research & Technology*, 3 (1): 128-138.

Liang, C., Z. S. Wang, and N. Mohanty. 2006. "Influences of Carbonate and Chloride Ions on Persulfate Oxidation of Trichloroethylene at 20 C." *Science of the Total Environment*, 370 (2-3): 271-277.

Lin, H. L., and P. F. Hollenberg. 2001. "N-nitrosodimethylamine-Mediated Formation of Oxidized and Methylated DNA Bases in a Cytochrome P450 2E1 Expressing Cell Line." *Chemical Research in Toxicology*, 14 (5): 562-566.

Liu, W., S. A. Andrews, J. R. Bolton, K. G. Linden, C. Sharpless, and M. Stefan. 2002. "Comparison of Disinfection Byproduct (DBP) Formation from Different UV Technologies at Bench Scale." *Water Science and Technology: Water Supply*, 2 (5-6): 515-521.

Liu, J., and X. Zhang. 2014. "Comparative Toxicity of New Halophenolic DBPs in Chlorinated Saline Wastewater Effluents Against a Marine Alga: Halophenolic DBPs Are Generally More Toxic Than Haloaliphatic Ones." *Water Research*, 65: 64-72.

- Liu, Y., X. He, X. Duan, Y. Fu, and D. D. Dionysiou. 2015. "Photochemical Degradation of Oxytetracycline: Influence of Ph and Role of Carbonate Radical." *Chemical Engineering Journal*, 276: 13-121.
- Mack, J., and J. R. Bolton. 1999. "Photochemistry of Nitrite and Nitrate in Aqueous Solution: A Review." *Journal of Photochemistry and Photobiology A: Chemistry*, 128 (1-3): 1-13.
- Mamane, H., H. Shemer, and K. G. Linden. 2007. "Inactivation of E. Coli, B. Subtilis Spores, and MS2, T4, and T7 Phage Using UV/H₂O₂ Advanced Oxidation." *Journal of Hazardous Materials*, 146 (3): 479-486.
- Mangalgi, K. P., S. Patton, L. Wu, S. Xu, K. P. Ishida, and H. Liu. 2019. Optimizing Potable Water Reuse Systems: Chloramines Or Hydrogen Peroxide for UV-Based Advanced Oxidation Process?" *Environmental Science & Technology*, 53 (22): 13323-13331.
- Martijn, A. J., M. G. Boersma, J. M. Vervoort, I. M. Rietjens and J.C. Kruithof. 2014. "Formation of Genotoxic Compounds by Medium Pressure Ultraviolet Treatment of Nitrate-Rich Water." *Desalination and Water Treatment*, 52 (34-36): 6275-6281.
- Martijn, B. J., J. C. Kruithof, R. M. Hughes, R. A. Mastan, R. Van Rompay, and J. P. Malley Jr. 2015. "Induced Genotoxicity in Nitrate-Rich Water Treated with Medium-Pressure Ultraviolet Processes." *Journal-American Water Works Association*, 107 (6): E301-E312.
- Mao, L., C. Meng, C. Zeng, C., Y. Ji, X. Yang, and S. Gao. 2011. "The Effect of Nitrate, Bicarbonate and Natural Organic Matter on the Degradation of Sunscreen Agent P-Aminobenzoic Acid by Simulated Solar Irradiation." *Science of the Total Environment*, 409 (24): 5376-5381.
- MassDEP. 2020. Standards and Guidelines for Contaminants in Massachusetts Drinking Waters. Massachusetts Department of Environmental Protection, Drinking Water Program: Boston, MA. <https://www.mass.gov/doc/2020-standards-and-guidelines-for-contaminants-in-massachusetts-drinking-waters/download>.
- Mattle, M. J., D. Vione, and T. Kohn. 2015. "Conceptual model and Experimental Framework to Determine the Contributions of Direct and Indirect Photoreactions to the Solar Disinfection Of MS2, Phix174, and Adenovirus." *Environmental Science & Technology*, 49 (1): 334-342.
- McCurry, D. L., K. P. Ishida, G. L. Oelker, W. A. Mitch. 2017. "Reverse Osmosis Shifts Chloramine Speciation Causing Re-Formation of NDMA during Potable Reuse Of Wastewater." *Environmental Science & Technology*, 51 (15): 8589-8596.
- Metz, D. H., K. Reynolds, M. Meyer, and D. D. Dionysiou. 2011. "The Effect of UV/H₂O₂ Treatment on Biofilm Formation Potential." *Water Research*, 45 (2): 497-508.
- Muellner, M. G., E. D. Wagner, K. McCalla, S. D. Richardson, Y. T. Woo, and M. J. Plewa. 2007. "Haloacetonitriles vs. Regulated Haloacetic Acids: Are Nitrogen-Containing DBPs More Toxic?" *Environmental Science & Technology*, 41 (2): 645-651.

Neale, P. A., A. Antony, M. E. Bartkow, M. J. Farre, A. Heitz, I. Kristiana, J. Y. Tang, and B. I. Escher. 2012. "Bioanalytical Assessment of The Formation Of Disinfection Byproducts in a Drinking Water Treatment Plant." *Environmental Science & Technology*, 46 (18): 10317-10325.

Neale, P. A., and B. I. Escher. 2019. In Vitro Bioassays to Assess Drinking Water Quality." *Current Opinion in Environmental Science & Health*, 7: 1-7.

Olmez-Hanci, T., D. Dursun, E. Aydin, I. Arslan-Alaton, B. Girit, L. Mita, N. Diano, D. G. Mita, and M. Guida. 2015. "S2O8²⁻/UV-C and H₂O₂/UV-C Treatment of Bisphenol A: Assessment of Toxicity, Estrogenic Activity, Degradation Products and Results in Real Water." *Chemosphere*, 119: S115-S123.

Örmeci, B., K. G. Linden, and J. J. Ducoste. 2005. "UV Disinfection of Chlorinated Water: Impact on Chlorine Concentration and UV Dose Delivery." *Journal of Water Supply: Research and Technology—Aqua*, 54 (3): 189-199.

Pantin, S., and R. Hofmann. 2008. "Impact of UV/H₂O₂ on Subsequent Chlorine Stability and DBP Formation." *In Proc. The 13th Canadian National Conference on Drinking Water*, Quebec City, QC.

Patton, S., W. Li, K. D. Couch, S. P. Mezyk, K. P. Ishida, and H. Liu. 2017. "Impact of the Ultraviolet Photolysis of Monochloramine on 1, 4-Dioxane Removal: New Insights into Potable Water Reuse." *Environmental Science & Technology Letters*, 4 (1): 26-30.

Phillip, N., and V. Diyamandoglu. 2000. "Kinetics of Nitrate Formation in Breakpoint Chlorination." *In Proc. The Water Environment Federation*, 2000 (2): 145-152.

Pisarenko, A. N., B. D. Stanford, S. A. Snyder, S. B. Rivera, and A. K. Boal. 2013. "Investigation of the Use of Chlorine Based Advanced Oxidation in Surface Water: Oxidation of Natural Organic Matter and Formation of Disinfection Byproducts." *Journal of Advanced Oxidation Technologies*, 16 (1): 137-150.

Plewa, M. J., M. G. Muellner, S. D. Richardson, F. Fasano, K. M. Buettner, Y. T. Woo, A. B. McKague, and E. D. Wagner. 2008. "Occurrence, Synthesis, and Mammalian Cell Cytotoxicity and Genotoxicity of Haloacetamides: An Emerging Class of Nitrogenous Drinking Water Disinfection Byproducts." *Environmental Science & Technology*, 42 (3): 955-961.

Plewa, M. J., E. D. Wagner, D. H. Metz, R. Kashinkunti, K. J. Jamriska, and M. Meyer. 2012. "Differential Toxicity of Drinking Water Disinfected with Combinations of Ultraviolet Radiation and Chlorine." *Environmental Science & Technology*, 46 (14): 7811-7817.

Poskrebyshev, G. A., P. Neta, and R. E. Huie. 2002. "Temperature Dependence of the Acid Dissociation Constant of the Hydroxyl Radical." *The Journal of Physical Chemistry A*, 106 (47): 11488-11491.

Rao, B., N. Estrada, S. McGee, J. Mangold, B. Gu, and W. A. Jackson. 2012. "Perchlorate Production by Photodecomposition of Aqueous Chlorine Solutions." *Environmental Science & Technology*, 46 (21): 11635-11643.

- Rattanakul, S. and K. Oguma. 2017. "Analysis of Hydroxyl Radicals and Inactivation Mechanisms of Bacteriophage MS2 in Response to a Simultaneous Application of UV and Chlorine." *Environmental Science & Technology*, 51 (1): 455-462.
- Reckhow, D. A., K. G. Linden, J. Kim, H. Shemer, G. Makdissy. 2010. "Effect of UV treatment on DBP Formation." *Journal-American Water Works Association*, 102 (6): 100-113.
- Roback, S. L., K. P. Ishida, and M. H. Plumlee. 2019. "Influence of Reverse Osmosis Membrane Age on Rejection of NDMA Precursors and Formation of NDMA in Finished Water after Full Advanced Treatment for Potable Reuse." *Chemosphere*, 233: 120-131.
- Roback, S. L., H. Kodamatani, T. Fujioka, T., and M. H. Plumlee. 2020. "Validation of a Novel Direct-Injection Chemiluminescence-Based Method for N-Nitrosamine Analysis in Advanced-Treated Recycled Water, Drinking Water, and Wastewater." *Environmental Science: Water Research & Technology*, 6 (4): 1106-1115.
- Roback, S. L., K. P. Ishida, Y. H. Chuang, Z. Zhang, W. A. Mitch, and M. H. Plumlee. 2021. "Pilot UV-AOP Comparison of UV/Hydrogen Peroxide, UV/Free Chlorine, and UV/Monochloramine for the Removal of N-Nitrosodimethylamine (NDMA) and NDMA Precursors." *ACS ES&T Water*, 1 (2): 396-406.
- Rozas, O., C. Vidal, C. Baeza, W. F. Jardim, A. Rossner, and H. D. Mansilla. 2016. "Organic Micropollutants (OMPs) in Natural Waters: Oxidation by UV/H₂O₂ Treatment and Toxicity Assessment." *Water Research*, 98: 109-118.
- Sakai, H., T. Takamatsu, K. Kosaka, N. Kamiko, and S. Takizawa. 2012. "Effects of Wavelength and Water Quality on Photodegradation of N-Nitrosodimethylamine (NDMA)." *Chemosphere*, 89 (6): 702-707.
- Sarathy, S. R., and M. Mohseni. 2007. "The Impact of UV/H₂O₂ Advanced Oxidation on Molecular Size Distribution of Chromophoric Natural Organic Matter." *Environmental Science & Technology*, 41 (24): 8315-8320.
- Sarathy, S., and M. Mohseni. 2010. "Effects of UV/H₂O₂ Advanced Oxidation on Chemical Characteristics and Chlorine Reactivity of Surface Water Natural Organic Matter." *Water Research*, 44 (14): 4087-4096.
- Sarathy, S. R., M. I. Stefan, A. Royce, and M. Mohseni. 2011. "Pilot-Scale UV/H₂O₂ Advanced Oxidation Process for Surface Water Treatment and Downstream Biological Treatment: Effects on Natural Organic Matter Characteristics and DBP Formation Potential." *Environmental Technology*, 32 (15): 1709-1718.
- Semitsoglou-Tsiapou, S., M. R. Templeton, N. J. D. Graham, S. Mandal, L. H. Leal, and J. C. Kruithof. 2018. "Potential Formation of Mutagenicity by Low Pressure- UV/H₂O₂ during the Treatment of Nitrate-Rich Source Waters." *Environmental Science: Water Research & Technology*, 4 (9): 1252-1261.

- Sgroi, M., P. Roccaro, G. L. Oelker, and S. A. Snyder. 2015. "N-nitrosodimethylamine (NDMA) Formation at an Indirect Potable Reuse Facility." *Water Research*, 70: 174-183.
- Sharpless, C. M., D. A. Seibold, and K. G. Linden. 2003. "Nitrate Photosensitized Degradation of Atrazine during UV Water Treatment." *Aquatic Sciences*, 65 (4): 359-366.
- Shemer, H., and K. G. Linden. 2007. "Photolysis, Oxidation and Subsequent Toxicity of a Mixture of Polycyclic Aromatic Hydrocarbons in Natural Waters." *Journal of Photochemistry and Photobiology A: Chemistry*, 187 (2-3): 186-195.
- Sheng, H., K. Nakamura, T. Kanno, K. Sasaki, and Y. Niwano. 2014. "Microbicidal Activity of Artificially Generated Hydroxyl Radicals." *Interface Oral Health Science*, 2014: 203-215. Springer, Tokyo.
- Stanford, B. D., A. N. Pisarenko, S. A. Snyder, and G. Gordon. 2011. "Perchlorate, Bromate, and Chlorate in Hypochlorite Solutions: Guidelines for Utilities." *Journal of American Water Works Association*, 103 (6): 71-83.
- Stefan, M. I. (Ed.) 2018. "Advanced Oxidation Processes for Water Treatment: Fundamentals and Applications." IWA Publishing, London, UK.
- Stefan, M. I. 2021. "UV/AOPs for Water Reuse: From Science to Implementation." *Presented at The 2021 IUVA Asia Workshop*, February 19, 2021.
- Sun, J., D. Kong, E. Aghdam, J. Fang, Q. Wu, J. Liu, Y. Du, X. Yang, and C. Shang. 2019. "The Influence of the UV/Chlorine Advanced Oxidation of Natural Organic Matter for Micropollutant Degradation on the Formation of DBPs and Toxicity During Post-Chlorination." *Chemical Engineering Journal*, 373: 870-879.
- Sun, P. 2021. "The Degradation of Geosmin and 2-Methylisoborneol by UV-Based AOPs: Kinetic Model and Energy-Cost Optimization." *IUVA Asia Workshop*, February 18-19.
- Szczuka, A., N. Huang, J. A. MacDonald, A. Nayak, Z. Zhang, and W. A. Mitch. 2020. "N-nitrosodimethylamine Formation during UV/Hydrogen Peroxide and UV/Chlorine Advanced Oxidation Process Treatment Following Reverse Osmosis for Potable Reuse." *Environmental Science & Technology*, 54 (23): 15465-15475.
- Thomsen, C. L., D. Madsen, J. A. Poulsen, J. Thøgersen, S. K. Jensen, and S. R. Keiding. 2001. "Femtosecond Photolysis of Aqueous HOCl." *The Journal of Chemical Physics*, 115 (20): 9361-9369.
- Thorn, K. A., and L. G. Cox. 2012. "Ultraviolet Irradiation Effects Incorporation of Nitrate and Nitrite Nitrogen into Aquatic Natural Organic Matter." *Journal of Environmental Quality*, 41 (3): 865-881.
- Trussell, B. 2022. Personal Communication, May 10, 2022

- USEPA. 2006. "National Primary Drinking Water Regulations: Stage 2 Disinfectants and Disinfection Byproducts Rule." *Federal Register*, 71 (2): 388.
- Vinge, S. L., S. W. Shaheen, C. M. Sharpless, and K. G. Linden. 2020. "Nitrate with Benefits: Optimizing Radical Production during UV Water Treatment." *Environmental Science: Water Research & Technology*, 6 (4): 1163-1175.
- Von Gunten, U., and Y. Oliveras. 1998. "Advanced Oxidation of Bromide-Containing Waters: Bromate Formation Mechanisms." *Environmental Science & Technology*, 32 (1): 63-70.
- Wagner, E. D., K. M. Hsu, A. Lagunas, W. A. Mitch, and M. J. Plewa. 2012. "Comparative Genotoxicity of Nitrosamine Drinking Water Disinfection Byproducts in Salmonella and Mammalian Cells." *Mutation Research/Genetic Toxicology and Environmental Mutagenesis*, 741 (1-2): 109-115.
- Wagner, E. D., and M. J. Plewa. 2017. "CHO Cell Cytotoxicity and Genotoxicity Analyses of Disinfection By-Products: An Updated Review." *Journal of Environmental Sciences*, 58: 64-76.
- Wang, D., J. R. Bolton, S. A. Andrews, and R. Hofmann. 2015a. "Formation of Disinfection By-Products in the Ultraviolet/Chlorine Advanced Oxidation Process." *Science of the Total Environment*, 518: 49-57.
- Wang, D., J. R. Bolton, S. A. Andrews, and R. Hofmann. 2015b. "UV/Chlorine Control of Drinking Water Taste and Odor at Pilot and Full-Scale." *Chemosphere*, 136: 239-244.
- Wang, X., H. Zhang, Y. Zhang, Q. Shi, J. Wang, J. Yu, and M. Yang. 2017. "New Insights into Trihalomethane and Haloacetic Acid Formation Potentials: Correlation with the Molecular Composition of Natural Organic Matter in Source Water." *Environmental Science & Technology*, 51 (4): 2015-2021.
- Wang, C., Y. Zhu, S. Ebrahimi, and R. Hofmann. 2018a. "Temperature Impact on the Degradation of Geosmin and 2-MIB by the UV/H₂O₂ and the UV/Cl₂ Processes." *In Proc. Ontario's Water Conference & Trade Show. Niagara Falls, ON. May 1, 2018.*
- Wang, W. L., Q. Y. Wu, N. Huang, Z. B. Xu, M. Y. Lee, and H. Y. Hu. 2018b. "Potential Risks from UV/H₂O₂ Oxidation and UV Photocatalysis: A Review of Toxic, Assimilable, and Sensory-Unpleasant Transformation Products." *Water Research*, 141: 109-125.
- Wang, C., N. Moore, K. Bircher, S. Andrews, and R. Hofmann. 2019. "Full-Scale Comparison of UV/H₂O₂ and UV/Cl₂ Advanced Oxidation: The Degradation of Micropollutant Surrogates and the Formation of Disinfection Byproducts." *Water Research*, 161: 448-458.
- Wang, C., E. Rosenfeldt, Y. Li, and R. Hofmann. 2020a. "External Standard Calibration Method to Measure the Hydroxyl Radical Scavenging Capacity of Water Samples." *Environmental Science & Technology*, 54 (3): 1929-1937.

Wang, C., L. Zheng, S. Andrews, and R. Hofmann. 2020b. "Monochloramine Formation and Decay in the Presence of H₂O₂ after UV/H₂O₂ Advanced Oxidation." *Journal of Environmental Engineering*, 146 (6): 06020002.

Waterboards. 2021. *Derivation of Log Removal Values for the Addendum to a Framework for Regulating Direct Potable Reuse, Presenting an Early Draft of the Anticipated Criteria for DPR*. California State Water Resources Control Board.
https://www.waterboards.ca.gov/drinking_water/certlic/drinkingwater/direct_potable_reuse.html.

Watts, M. J., R. Hofmann, and E. J. Rosenfeldt. 2012. "Low-Pressure UV/Cl₂ for Advanced Oxidation of Taste and Odor." *Journal-American Water Works Association*, 104 (1): 58-65.

Watts, R. J., S. Kong, M. P. Orr, G. C. Miller, and B. E. Henry. 1995. "Photocatalytic Inactivation of Coliform Bacteria and Viruses in Secondary Wastewater Effluent." *Water Research*, 29 (1): 95-100.

Weil, I., and J. C. Morris. 1949. "Kinetic Studies on the Chloramines. I. The Rates of Formation of Monochloramine, N-Chlormethylamine and N-Chlordimethylamine." *Journal of the American Chemical Society*, 71 (5): 1664-1671.

Westerhoff, P., R. Song, G. Amy, R. Minear. 1998. "Numerical Kinetic Models for Bromide Oxidation to Bromine and Bromate." *Water Research* 32: 1687–1699.
[https://doi.org/10.1016/S0043-1354\(97\)00287-X](https://doi.org/10.1016/S0043-1354(97)00287-X).

Van Welie, R. T., R. G. van Dijck, N. P. Vermeulen, and N. J. van Sittert. 1992. "Mercapturic Acids, Protein Adducts, and DNA Adducts as Biomarkers of Electrophilic Chemicals." *Critical Reviews in Toxicology*, 22 (5-6): 271-306.

WHO. 2005. "Chlorite and Chlorate in Drinking-water Background document for development of WHO Guidelines for Drinking-water Quality." *World Health Organization*.
https://www.who.int/water_sanitation_health/dwg/chemicals/chlorateandchlorite0505.pdf.

WHO. 2017. "Guidelines for Drinking-water Quality, 4th ed." *World Health Organization*.
<https://www.who.int/publications/i/item/9789241549950>.

The Water Research Foundation. 2021. Survey Conducted as Part of WRF 5050 with Utility Partners. Personal Communications.

Wright, H., M. Heath, T. Brooks, and J. Adams. 2020. "Innovative Approaches for Validation of Ultraviolet Disinfection Reactors for Drinking Water Systems." U.S. Environmental Protection Agency: Washington, DC, EPA/600/R-20/094, 2020.

Wu, Z., J. Fang, Y. Xiang, C. Shang, X. Li, F. Meng, and X. Yang. 2016. "Roles of Reactive Chlorine Species in Trimethoprim Degradation in the UV/Chlorine Process: Kinetics and Transformation Pathways." *Water Research*, 104: 272-282.

- Wu, Z., K. Guo, J. Fang, X. Yang, H. Xiao, S. Hou, X. Kong, C. Shang, X. Yang, F. Meng, and L. Chen. 2017. "Factors Affecting the Roles of Reactive Species in the Degradation of Micropollutants by the UV/Chlorine Process." *Water Research*, 126: 351-360.
- Xiang, Y., J. Fang, and C. Shang. 2016. "Kinetics and Pathways of Ibuprofen Degradation by the UV/Chlorine Advanced Oxidation Process." *Water Research*, 90: 301-308.
- Yang, J., Z. Dong, C. Jiang, C. Wang, and H. Liu. 2019. "An Overview of Bromate Formation in Chemical Oxidation Processes: Occurrence, Mechanism, Influencing Factors, Risk Assessment, and Control Strategies." *Chemosphere*, 237: 124521.
- Yang, W., Y. Tang, L. Liu, X. Peng, Y. Zhong, Y. Chen, and Y. Huang. 2020. "Chemical Behaviors and Toxic Effects of Ametryn during the UV/Chlorine Process." *Chemosphere*, 240: 124941.
- Yeom, Y., J. Han, X. Zhang, C. Shang, T. Zhang, X. Li, X. Duan, and D. D. Dionysiou. 2021. "A Review on the Degradation Efficiency, DBP Formation, and Toxicity Variation in the UV/Chlorine Treatment of Micropollutants." *Chemical Engineering Journal*, 424: 130053.
- Yin, K., Y. Deng, C. Liu, Q. He, Y. Wei, S. Chen, T. Liu, and S. Luo. 2018. "Kinetics, Pathways and Toxicity Evaluation of Neonicotinoid Insecticides Degradation via UV/Chlorine Process." *Chemical Engineering Journal*, 346: 298-306.
- Yin, R., E. R. Blatchley III, and C. Shang. 2020. "UV Photolysis of Mono- and Dichloramine Using UV-LEDs as Radiation Sources: Photodecay Rates and Radical Concentrations." *Environmental Science & Technology*, 54 (13): 8420-8429.
- Yu, X. Y., and J. R. Barker. 2003. "Hydrogen Peroxide Photolysis in Acidic Aqueous Solutions Containing Chloride Ions. I. Chemical Mechanism." *The Journal of Physical Chemistry A*, 107 (9): 1313-1324.
- Zeng, Q., S. H. Zhang, J. Liao, D. Y. Miao, X. Y. Wang, P. Yang, L. J. Yun, A. L. Liu, and W. Q. Lu. 2015. "Evaluation of Genotoxic Effects Caused by Extracts of Chlorinated Drinking Water Using a Combination of Three Different Bioassays." *Journal of Hazardous Materials*, 296: 23-29.
- Zhang, Z., B. Ma, R. M. Hozalski, C. G. Russell, A. N. Evans, K. O. Led, M. Van Dyke, S. Peldszus, P. M. Huck, A. Szczuka, and W. A. Mitch. 2019. "Bench-Scale Column Evaluation of Factors Associated with Changes in N-Nitrosodimethylamine (NDMA) Precursor Concentrations during Drinking Water Biofiltration." *Water Research*, 167: 115103.
- Zhao, J., C. Shang, X. Zhang, X. Yang, and R. Yin. 2021. "The Multiple Roles of Chlorite on the Concentrations of Radicals and Ozone and Formation of Chlorate during UV Photolysis of Free Chlorine." *Water Research*, 190: 116680.
- Zhou, L., C. Yan, M. Sleiman, C. Ferronato, J. M. Chovelon, X. Wang, and C. Richard. 2019. "Sulfate Radical Induced Degradation of B2-Adrenoceptor Agonists Salbutamol and Terbutaline: Implication of Halides, Bicarbonate, and Natural Organic Matter." *Chemical Engineering Journal*, 368: 252-260.

Appendix B: Reaction Rate Coefficients of Microcontaminants with RCS and •OH

Prepared by:

Tianyi Chen, Yifeng Huang, Ron Hofmann

University of Toronto, Department of Civil & Mineral Engineering

Contents

Chapter B1	177
References	182

Tables

B1-1	Reactions with RCS Species	178
B1-2	Reactions with RCS Species Continued	180
B1-3	Reaction with OH Radical	180

CHAPTER B1

Reaction Rate Coefficients of Microcontaminants with RCS and $\bullet\text{OH}$

References given following the tables in this appendix.

Table B1-1. Reactions with RCS Species.

Contaminants	Cl• (M ⁻¹ ·s ⁻¹)	Ref	Cl ₂ •- (M ⁻¹ ·s ⁻¹)	Ref
Chlorobenzene	1.8 × 10 ¹⁰	[1]	(2 ± 4) × 10 ⁵	[1]
Toluene	1.8 × 10 ¹⁰	[1]	(2 ± 4) × 10 ⁵	[1]
Nitrobenzene	Negligible	[2]	-	-
Acetone			1.40 × 10 ³	[3]
Fumaric acid	3.0 × 10 ⁹	[4]		
N,N-diethyl-3-toluamide (DEET)	3.8 × 10 ⁹	[5]		
Caffeine	1.46 × 10 ¹⁰	[5]	(9.28 ± 0.52) × 10 ⁸	[6]
	(3.87 ± 0.35) × 10 ¹⁰	[6]		
1,4-Dioxane	4.38 × 10 ⁶	[7]	3.30 × 10 ⁶	[7]
Atenolol	1.12 × 10 ¹⁰	[8]	9.81 × 10 ⁶	[8]
Metoprolol	(1.71 ± 0.31) × 10 ¹⁰	[6]	(5.07 ± 0.38) × 10 ⁸	[6]
Propranolol			(17.81 ± 0.6) × 10 ⁸	[6]
Trichloroethylene	1.98 × 10 ⁸	[9,10]	1.00 × 10 ⁷	[9,10]
Paracetamol	2.61 × 10 ⁹	[11]	1.32 × 10 ⁶	[11]
	(1.24 ± 0.26) × 10 ¹⁰	[6]		
Acetaminophen	(1.33 ± 0.19) × 10 ¹⁰	[6]	(4.32 ± 0.39) × 10 ⁸	[6]
Aspirin	(0.68 ± 0.14) × 10 ¹⁰	[6]	(0.23 ± 0.04) × 10 ⁸	[6]
Diclofenac	(3.77 ± 0.65) × 10 ¹⁰	[6]	(11.54 ± 0.52) × 10 ⁸	[6]
Ibuprofen	(2.77 ± 0.35) × 10 ¹⁰	[6]	(< 0.05) × 10 ⁸	[6]
Indomethacin			(4.99 ± 0.51) × 10 ⁸	[6]
Naproxen	(2.01 ± 0.15) × 10 ¹⁰	[6]	(6.57 ± 0.43) × 10 ⁸	[6]
Amoxicillin	(1.27 ± 0.08) × 10 ¹⁰	[6]	(4.20 ± 0.07) × 10 ⁸	[6]
Cefotaxime	(2.30 ± 0.12) × 10 ¹⁰	[6]	(4.91 ± 0.16) × 10 ⁸	[6]
Cephalexin	(2.17 ± 0.25) × 10 ¹⁰	[6]	(5.06 ± 0.29) × 10 ⁸	[6]
Cefaclor	(1.59 ± 0.20) × 10 ¹⁰	[6]	(3.68 ± 0.09) × 10 ⁸	[6]
Penicillin G	(1.25 ± 0.09) × 10 ¹⁰	[6]	(3.30 ± 0.30) × 10 ⁸	[6]
Penicillin V	(1.31 ± 0.09) × 10 ¹⁰	[6]	(3.36 ± 0.41) × 10 ⁸	[6]
Ciprofloxacin	(1.39 ± 0.35) × 10 ¹⁰	[6]	(2.19 ± 0.08) × 10 ⁸	[6]
Enrofloxacin	(1.53 ± 0.40) × 10 ¹⁰	[6]	(3.27 ± 0.15) × 10 ⁸	[6]
Flumequine	(0.77 ± 0.23) × 10 ¹⁰	[6]	(0.94 ± 0.07) × 10 ⁸	[6]
Ofloxacin	(1.54 ± 0.25) × 10 ¹⁰	[6]	(3.48 ± 0.39) × 10 ⁸	[6]
Azithromycin	(0.78 ± 0.04) × 10 ¹⁰	[6]	(< 0.05) × 10 ⁸	[6]
Erythromycin	(0.68 ± 0.03) × 10 ¹⁰	[6]	(< 0.05) × 10 ⁸	[6]
Roxithromycin	(0.72 ± 0.07) × 10 ¹⁰	[6]	(< 0.05) × 10 ⁸	[6]
Tylosin			(0.46 ± 0.03) × 10 ⁸	[6]
Dimetridazole	(0.42 ± 0.03) × 10 ¹⁰	[6]	(0.84 ± 0.05) × 10 ⁸	[6]
Metronidazole	(0.31 ± 0.05) × 10 ¹⁰	[6]	(1.24 ± 0.08) × 10 ⁸	[6]
Ornidazole			(0.93 ± 0.05) × 10 ⁸	[6]
Ronidazole			(1.55 ± 0.08) × 10 ⁸	[6]
Sulfanilamide	(3.12 ± 0.40) × 10 ¹⁰	[6]	(4.32 ± 0.12) × 10 ⁸	[6]
Sulfadimethoxine	(4.08 ± 0.24) × 10 ¹⁰	[6]	(4.46 ± 0.50) × 10 ⁸	[6]
Sulfadiazine	(3.35 ± 0.22) × 10 ¹⁰	[6]	(4.27 ± 0.37) × 10 ⁸	[6]
Sulfamethazine	(3.21 ± 0.11) × 10 ¹⁰	[6]	(4.85 ± 0.28) × 10 ⁸	[6]
Sulfamethoxazole	(3.64 ± 0.21) × 10 ¹⁰	[6]	(4.72 ± 0.39) × 10 ⁸	[6]
Sulfathiazole	(3.78 ± 0.49) × 10 ¹⁰	[6]	(5.08 ± 0.36) × 10 ⁸	[6]
Chlortetracycline			(8.50 ± 0.49) × 10 ⁸	[6]
Doxycycline			(11.35 ± 0.69) × 10 ⁸	[6]
Oxytetracycline	(2.36 ± 0.56) × 10 ¹⁰	[6]	(9.36 ± 0.29) × 10 ⁸	[6]
Tetracycline	(1.98 ± 0.42) × 10 ¹⁰	[6]	(11.80 ± 0.79) × 10 ⁸	[6]
Bezafibrate	(1.04 ± 0.09) × 10 ¹⁰	[6]	3.24 × 10 ⁸	[6]
Clofibric acid	(0.55 ± 0.13) × 10 ¹⁰	[6]	1.41 × 10 ⁸	[6]

Table B1-1. Reactions with RCS Species.

Contaminants	Cl• (M ⁻¹ ·s ⁻¹)	Ref	Cl ₂ • ⁻ (M ⁻¹ ·s ⁻¹)	Ref
Gemfibrozil	(2.41 ± 0.17) × 10 ¹⁰	[6]	(2.87 ± 0.12) × 10 ⁸	[6]
Theophylline	(3.98 ± 0.42) × 10 ¹⁰	[6]	(8.78 ± 0.34) × 10 ⁸	[6]
Xanthine	(3.81 ± 0.40) × 10 ¹⁰	[6]	(1.85 ± 0.11) × 10 ⁸	[6]
Cimetidine	(0.43 ± 0.11) × 10 ¹⁰	[6]	(27.78 ± 1.64) × 10 ⁸	[6]
Famotidine	(1.72 ± 0.26) × 10 ¹⁰	[6]	(16.52 ± 0.43) × 10 ⁸	[6]
Carbamazepine	(3.30 ± 0.26) × 10 ¹⁰	[6]	(0.43 ± 0.03) × 10 ⁸	[6]
Clenbuterol			(5.54 ± 0.14) × 10 ⁸	[6]
Iopromide	(2.75 ± 0.39) × 10 ¹⁰	[6]	(20.54 ± 0.96) × 10 ⁸	[6]
Mabuterol			(3.48 ± 0.27) × 10 ⁸	[6]
Mesalazine	(2.75 ± 0.39) × 10 ¹⁰	[6]	(20.54 ± 0.96) × 10 ⁸	[6]
Metformin			(0.21 ± 0.01) × 10 ⁸	[6]
Primidone	(0.62 ± 0.10) × 10 ¹⁰	[6]	(1.58 ± 0.02) × 10 ⁸	[6]
Salbutamol			(3.02 ± 0.20) × 10 ⁸	[6]
Salicylic acid			(2.10 ± 0.22) × 10 ⁸	[6]
Sucralose	(1.11 ± 0.16) × 10 ¹⁰	[6]	(< 0.01) × 10 ⁸	[6]
Terbutaline			(12.05 ± 0.72) × 10 ⁸	[6]
Triclosan	(2.76 ± 0.44) × 10 ¹⁰	[6]	(2.48 ± 0.14) × 10 ⁸	[6]
Trimethoprim	(2.11 ± 0.12) × 10 ¹⁰	[6]	(18.78 ± 0.23) × 10 ⁸	[6]
Venlafaxine			(3.58 ± 0.14) × 10 ⁸	[6]
Dimethyl phthalate	(1.81 ± 0.18) × 10 ¹⁰	[6]	(0.14 ± 0.03) × 10 ⁸	[6]
Diethyl phthalate	(1.97 ± 0.14) × 10 ¹⁰	[6]	(0.11 ± 0.02) × 10 ⁸	[6]
Dibutyl phthalate	(1.96 ± 0.22) × 10 ¹⁰	[6]	(0.11 ± 0.02) × 10 ⁸	[6]
Estrone (E1)	(2.06 ± 0.21) × 10 ¹⁰	[6]	(3.66 ± 0.24) × 10 ⁸	[6]
Estrone (E2)	(2.01 ± 0.30) × 10 ¹⁰	[6]	3.96 × 10 ⁸	[6]
	(0.8 ± 0.02) × 10 ¹⁰	[12]		
Ethinyl estradiol (EE2)	(2.56 ± 0.11) × 10 ¹⁰	[6]	3.96 × 10 ⁸	[6]
	(0.21 ± 0.02) × 10 ¹⁰	[12]		
Bisphenol A	(1.82 ± 0.23) × 10 ¹⁰	[6]	(5.82 ± 0.62) × 10 ⁸	[6]
Methylparaben	(1.52 ± 0.13) × 10 ¹⁰	[6]	(1.61 ± 0.06) × 10 ⁸	[6]
Nonylphenol	(1.00 ± 0.07) × 10 ¹⁰	[6]	3.65 × 10 ⁸	[6]
4-chloroaniline	(2.17 ± 0.14) × 10 ¹⁰	[6]	(5.23 ± 0.23) × 10 ⁸	[6]
4-methylcatechol	(2.49 ± 0.14) × 10 ¹⁰	[6]	(11.84 ± 0.23) × 10 ⁸	[6]
4-nitroanisole			(0.25 ± 0.03) × 10 ⁸	[6]
6-aminopenicillanic	(0.34 ± 0.03) × 10 ¹⁰	[6]	(3.27 ± 0.31) × 10 ⁸	[6]
7-amino-cephalosporanic	(1.14 ± 0.07) × 10 ¹⁰	[6]	(2.29 ± 0.11) × 10 ⁸	[6]
Acetylacetone	(0.29 ± 0.03) × 10 ¹⁰	[6]	(1.42 ± 0.08) × 10 ⁸	[6]
Aniline	(2.74 ± 0.31) × 10 ¹⁰	[6]	(6.79 ± 0.45) × 10 ⁸	[6]
Anisole			(1.62 ± 0.09) × 10 ⁸	[6]
Benzoic acid	(1.35 ± 0.15) × 10 ¹⁰	[6]	(0.02 ± 0.003) × 10 ⁸	[6]
	(1.80 ± 0.3) × 10 ¹⁰	[1]		
Gallic acid	(1.83 ± 0.27) × 10 ¹⁰	[6]	(7.53 ± 0.43) × 10 ⁸	[6]
Imidazole			(1.82 ± 0.17) × 10 ⁸	[6]
Phenol	(1.12 ± 0.09) × 10 ¹⁰	[6]	(2.20 ± 0.12) × 10 ⁸	[6]
Protocatechuic acid			(5.90 ± 0.31) × 10 ⁸	[6]
p-toluidine	(2.73 ± 0.56) × 10 ¹⁰	[6]	(9.47 ± 0.52) × 10 ⁸	[6]
Pyrimidine	(0.05 ± 0.01) × 10 ¹⁰	[6]	(< 0.01) × 10 ⁸	[6]
Pyrocatechol	(2.82 ± 0.33) × 10 ¹⁰	[6]	(5.66 ± 0.41) × 10 ⁸	[6]
1,3,5-trimethoxy-benzene	(1.33 ± 0.08) × 10 ¹⁰	[6]	(26.06 ± 1.72) × 10 ⁸	[6]
	(0.83 ± 0.18) × 10 ¹⁰	[6]	(28.71 ± 2.55) × 10 ⁸	[6]
2,4-dimethoxy-pyrimidine			(0.30 ± 0.02) × 10 ⁸	[6]
4,6-dimethyl pyrimidine			(< 0.05) × 10 ⁸	[6]
Thiazole			(0.39 ± 0.02) × 10 ⁸	[6]

Table B1-2. Reactions with RCS Species Continued.

Contaminants	ClO• (M ⁻¹ ·s ⁻¹)	Ref
Carbamazepine	9.2 × 10 ⁷	[13]
Gemfibrozil	4.16 × 10 ⁸	[13]
Paracetamol	7.74 × 10 ⁶	[11]
Caffeine	1.03 × 10 ⁸	[13]

Table B1-3. Reaction with OH Radical.

Contaminants	OH• (M ⁻¹ ·s ⁻¹)	Ref	Contaminants	OH• (M ⁻¹ ·s ⁻¹)	Ref
Acetone	1.30 × 10 ⁸	[14]	Tylosin	(8.2 ± 0.1) × 10 ⁹	[6]
Benzoic acid	6.0 × 10 ⁹	[8]	Sulfanilamide	8.2 × 10 ⁹	[6]
Fumaric acid	4.7 × 10 ⁹	[8]	Sulfadiazine	(4.5 ± 1.13) × 10 ⁹	[6]
Nitrobenzene	4.7 × 10 ⁹	[8]	Sulfamethazine	(8.3 ± 0.8) × 10 ⁹	[6]
Acetaminophen	1.7 × 10 ⁹	[6]	Sulfathiazole	(7.9 ± 0.4) × 10 ⁹	[6]
Indomethacin	6.7 × 10 ⁹	[6]	Doxycycline	7.74 × 10 ⁹	[6]
Amoxicillin	(6.94 ± 0.44) × 10 ⁹	[6]	Oxytetracycline	6.96 × 10 ⁹	[6]
Cefaclor	(6.00 ± 0.13) × 10 ⁹	[6]	Bezafibrate	(8.0 ± 0.2) × 10 ⁹	[6]
Penicillin G	(7.97 ± 0.11) × 10 ⁹	[6]	Clofibric acid	6.98 × 10 ⁹	[6]
Penicillin V	(8.76 ± 0.28) × 10 ⁹	[6]	Theophylline	8.22 × 10 ⁹	[6]
Enrofloxacin	(7.95 ± 0.23) × 10 ⁹	[6]	Xanthine	5.2 × 10 ⁹	[6]
Ofloxacin	(4.2 ± 0.5) × 10 ⁹	[6]	Cimetidine	6.5 × 10 ⁹	[6]
Iopromide	3.3 × 10 ⁹	[6]	Mesalazine	6.7 × 10 ⁹	[6]
Salicylic acid	17 × 10 ⁹	[6]	Sucralose	1.6 × 10 ⁹	[6]
Trimethoprim	8.5 × 10 ⁹	[13]	Metronidazole	5.09 × 10 ⁹	[13]
	(6.3 ± 0.85) × 10 ⁹	[15,16]		(44 ± 2) × 10 ⁹	[17]
	7 × 10 ⁹	[18]		(17.9 ± 22) × 10 ⁹	[19]
Chloramphenicol	3.575 × 10 ⁹	[13]	Dimetridazole	4.95 × 10 ⁹	[13]
	5.8 × 10 ⁹	[19]		56 × 10 ⁹	[19]
Tinidazole	4.248 × 10 ⁹	[13]	Erythromycin	(3.8 ± 0.76) × 10 ⁹	[15]
	45 × 10 ⁹	[19]		3.33 × 10 ⁹	[15]
Ornidazole	4.39 × 10 ⁹	[13]	Trichloroethylene	2.90 × 10 ⁹	[20]
Cephalexin	(8.5 ± 0.7) × 10 ⁹	[6]	Terbutaline	(6.9 ± 0.4) × 10 ⁹	[6]
Flumequine	6.33 × 10 ⁹	[13]	1,4-Dioxane	3.10 × 10 ⁹	[7]
Nalidixic acid	5.64 × 10 ⁹	[13]	Sulfamethoxazole	(5.5 ± 0.7) × 10 ⁹	[15]
	6.74 × 10 ⁹	[21]		6 × 10 ⁹	[18]
Ciprofloxacin	4.1 × 10 ⁹	[15]	Tetracycline	7.7 × 10 ⁹	[15]
Azithromycin	3.14 × 10 ⁹	[13]	Roxithromycin	5.53 × 10 ⁹	[13]
Famotidine	(14.6 ± 2.5) × 10 ⁹	[6]	Triclosan	4.43 × 10 ⁹	[6]
Diclofenac	(7.5 ± 1.5) × 10 ⁹	[15]	Ibuprofen	(7.4 ± 1.2) × 10 ⁹	[15]
	7.5 × 10 ⁹	[22]		7.2 × 10 ⁹	[13]
Salbutamol	6.18 × 10 ⁹	[13]	Clenbuterol	(6.6 ± 0.89) × 10 ⁹	[16]
	2.62 × 10 ⁹	[23]		9.48 × 10 ⁹	[13]
Naproxen	9.45 × 10 ⁹	[13]	Atenolol	6.84 × 10 ⁹	[13]
	(8.9 ± 0.65) × 10 ⁹	[16]		(7.7 ± 0.55) × 10 ⁹	[16]
	(9.6 ± 0.5) × 10 ⁹	[24]		8 × 10 ⁹	[22]
Ractopamine	10.6 × 10 ⁹	[13]	Metoprolol	8.2 × 10 ⁹	[13]
	3.85 × 10 ⁹	[23]		(7.8 ± 0.8) × 10 ⁹	[16]

Table B1-3. Reaction with OH Radical.

Contaminants	OH• (M ⁻¹ ·s ⁻¹)	Ref	Contaminants	OH• (M ⁻¹ ·s ⁻¹)	Ref
Terbutaline	$(6.87 \pm 0.43) \times 10^9$	[25]	N,N-diethyl-3-toluamide (DEET)	6.7×10^9	[5]
Propranolol	9.65×10^9	[13]	Primidone	6.63×10^9	[13]
	$(7.6 \pm 4.8) \times 10^9$	[16]		7×10^9	[18]
	$(10 \pm 2) \times 10^9$	[26]		6.7×10^9	[15]
Carbamazepine	8.8×10^9	[13]	Caffeine	7.41×10^9	[13]
	$(8.8 \pm 2) \times 10^9$	[15]		6.9×10^9	[15,24]
	9×10^9	[18]		6.4×10^9	[5]
Venlafaxine	8.83×10^9	[13]	Gemfibrozil	7.68×10^9	[13]
	$(8.8 \pm 1.5) \times 10^9$	[16,21]		10×10^9	[16,18,21]
Bisphenol A	8.77×10^9	[13]	Paracetamol	2.66×10^9	[11]
	$(8.8 \pm 3.1) \times 10^9$	[19]		1.7×10^9	[6]
1,4-Dioxane	3.10×10^9	[7]	Trichloroethylene	2.90×10^9	[20]
Dimethyl phthalate	3.2×10^9	[6]	Diethyl phthalate	4.2×10^9	[6]
Dibutyl phthalate	4.7×10^9	[6]	Ethinyl estradiol (EE2)	$(10.3 \pm 0.7) \times 10^9$	[6]
Estrone (E1)	26×10^9	[6]	Methylparaben	5.01×10^9	[6]
Estrone (E2)	14.1×10^9	[6]	Nonylphenol	$(11 \pm 2) \times 10^9$	[6]
6-amino-penicillanic	$(2.4 \pm 0.05) \times 10^9$	[6]	1,3,5-trimethoxybenzene	8.1×10^9	[6]
Acetylacetone	9.9×10^9	[6]	Aniline	17×10^9	[6]
Anisole	5.4×10^9	[6]	Imidazole	5.4×10^9	[6]
Phenol	6.6×10^9	[6]	Pyrimidine	0.16×10^9	[6]
Pyrocatechol	11×10^9	[6]			

References

1. Martire, D. O., J. A. Rosso, S. Bertolotti, G. C. Le Roux, A. M. Braun, and M. C. Gonzalez. 2001. « Kinetic Study of the Reactions of Chlorine Atoms and $\text{Cl}_2\bullet$ -Radical Anions in Aqueous Solutions. II. Toluene, Benzoic Acid, and Chlorobenzene.” *The Journal of Physical Chemistry A*, 105 (22): 5385-5392.
2. Watts, M. J., and K. G. Linden. 2007. “Chlorine Photolysis and Subsequent OH Radical Production during UV Treatment of Chlorinated Water.” *Water Research*, 41 (13): 2871-2878.
3. Hasegawa, K., and P. Neta. 1978. “Rate Constants and Mechanisms of Reaction of Chloride (Cl_2^-) Radicals.” *The Journal of Physical Chemistry*, 82 (8): 854-857.
4. Gilbert, B. C., J. K. Stell, W. J. Peet, and K. J. Radford. 1988. “Generation and Reactions of the Chlorine Atom in Aqueous Solution.” *Journal of the Chemical Society, Faraday Transactions 1: Physical Chemistry in Condensed Phases*, 84 (10): 3319-3330.
5. Sun, P., W. N. Lee, R. Zhang, and C. H. Huang. 2016. « Degradation of DEET and Caffeine under UV/Chlorine and Simulated Sunlight/Chlorine Conditions.” *Environmental Science & Technology*, 50 (24): 13265-13273.
6. Lei, Y., S. Cheng, N. Luo, X. Yang, and T. An. 2019. “Rate Constants and Mechanisms of the Reactions of $\text{Cl}\bullet$ And $\text{Cl}_2\bullet^-$ with Trace Organic Contaminants.” *Environmental Science & Technology*, 53 (19): 11170-11182.
7. Patton, S., W. Li, K. D. Couch, S. P. Mezyk, K. P. Ishida, and H. Liu. 2017. “Impact of the Ultraviolet Photolysis of Monochloramine on 1, 4-Dioxane Removal: New Insights into Potable Water Reuse.” *Environmental Science & Technology Letters*, 4 (1): 26-30.
8. Mangalgi, K. P., S. Patton, L. Wu, S. Xu, K. P. Ishida, and H. Liu. 2019. « Optimizing Potable Water Reuse Systems: Chloramines or Hydrogen Peroxide for UV-Based Advanced Oxidation Process?” *Environmental Science & Technology*, 53 (22): 13323-13331.
9. Li, K., M. I. Stefan, and J. C. Crittenden. 2007. “Trichloroethene Degradation by UV/ H_2O_2 Advanced Oxidation Process: Product Study and Kinetic Modeling.” *Environmental Science & Technology*, 41 (5): 1696-1703.
10. Li, K., M. I. Stefan, and J. C. Crittenden. 2004. “UV Photolysis of Trichloroethylene: Product Study and Kinetic Modeling.” *Environmental Science & Technology*, 38 (24): 6685-6693.
11. Wang, P., L. Bu, Y. Wu, J. Deng, S. Zhou. 2021. “Mechanistic Insights into Paracetamol Transformation in UV/ NH_2Cl Process: Experimental and Theoretical Study.” *Water Research*, 194: 116938.
12. Sun, P., T. Meng, Z. Wang, R. Zhang, H. Yao, Y. Yang, and L. Zhao. 2019. “Degradation of Organic Micropollutants in UV/ NH_2Cl Advanced Oxidation Process.” *Environmental Science & Technology*, 53 (15): 9024-9033.

13. Guo, K., Z. Wu, C. Shang, B. Yao, S. Hou, X. Yang, W. Song, and J. Fang. 2017. "Radical Chemistry and Structural Relationships of PPCP Degradation by UV/Chlorine Treatment in Simulated Drinking Water." *Environmental Science & Technology*, 51 (18): 10431-10439.
14. Wolfenden, B. S., and R. L. Willson. 1982. "Radical-Cations as Reference Chromogens in Kinetic Studies of Ono-Electron Transfer Reactions: Pulse Radiolysis Studies Of 2, 2'-Azinobis-(3-Ethylbenzthiazoline-6-Sulphonate)." *Journal of the Chemical Society, Perkin Transactions*, 2 (7): 805-812.
15. Yang, X., R. C. Flowers, H. S. Weinberg, and P. C. Singer. 2011. "Occurrence and removal of pharmaceuticals and personal care products (PPCPs) in an advanced wastewater reclamation plant." *Water Research*, 45 (16): 5218-5228.
16. Wols, B. A., C. H. M. Hofman-Caris, D. J. H. Harmsen, and E. F. Beerendonk. 2013. "Degradation of 40 Selected Pharmaceuticals by UV/H₂O₂." *Water Research*, 47 (15): 5876-5888.
17. Sánchez-Polo, M., J. Rivera-Utrilla, G. Prados-Joya, M. A. Ferro-García, and I. Bautista-Toledo. 2008. "Removal of Pharmaceutical Compounds, Nitroimidazoles, from Waters by Using the Ozone/Carbon System." *Water Research*, 42 (15): 4163-4171.
18. Merel, S., T. Anumol, M. Park, and S. A. Snyder. 2015. "Application of Surrogates, Indicators, and High-Resolution Mass Spectrometry to Evaluate the Efficacy of UV Processes for Attenuation of Emerging Contaminants in Water." *Journal of Hazardous Materials*, 282: 75-85.
19. Wols, B. A., and C. H. M. Hofman-Caris. 2012. "Review of Photochemical Reaction Constants of Organic Micropollutants Required for UV Advanced Oxidation Processes in Water." *Water Research*, 46 (9): 2815-2827.
20. Getoff, N. 1991. "Radiation-and Photoinduced Degradation of Pollutants in Water. A Comparative Study." *International Journal of Radiation Applications and Instrumentation. Part C. Radiation Physics and Chemistry*, 37 (5-6): 673-680.
21. Abdelmelek, S. B., J. Greaves, K. P. Ishida, W. J. Cooper, and W. Song. 2011. "Removal of Pharmaceutical and Personal Care Products from Reverse Osmosis Retentate Using Advanced Oxidation Processes." *Environmental Science & Technology*, 45 (8): 3665-3671.
22. Wert, E. C., F. L. Rosario-Ortiz, and S. A. Snyder. 2009. "Effect of Ozone Exposure on the Oxidation of Trace Organic Contaminants in Wastewater." *Water Research*, 43 (4): 1005-1014.
23. Lian, L., B. Yao, S. Hou, J. Fang, S. Yan, and W. Song. 2017. "Kinetic Study of Hydroxyl and Sulfate Radical-Mediated Oxidation of Pharmaceuticals in Wastewater Effluents." *Environmental Science & Technology*, 51 (5): 2954-2962.

24. Broséus, R., S. Vincent, K. Aboulfadl, A. Daneshvar, S. Sauvé, B. Barbeau, and M. Prévost. 2009. "Ozone Oxidation of Pharmaceuticals, Endocrine Disruptors and Pesticides during Drinking Water Treatment." *Water Research*, 43 (18): 4707-4717.
25. Yang, W., S. B. Abdelmelek, Z. Zheng, T. An, D. Zhang, and W. Song. 2013. "Photochemical Transformation of Terbutaline (Pharmaceutical) in Simulated Natural Waters: Degradation Kinetics and Mechanisms." *Water Research*, 47 (17): 6558-6565.
26. Benner, J., E. Salhi, T. Ternes, and U. von Gunten. 2008. "Ozonation of Reverse Osmosis Concentrate: Kinetics and Efficiency of Beta Blocker Oxidation." *Water Research*, 42 (12): 3003-3012.

Appendix C: Kinetics Models

Prepared by:

Tianyi Chen, Ron Hofmann

University of Toronto, Department of Civil & Mineral Engineering

Contents

Chapter C1: Kinetic Models	189
C1.1 The Principle of UV AOP Mechanistic Models	189
C1.2 Current Model Review – A General Critical Analysis.....	191
C1.3 Cross-Comparison of the Models	193
C1.3.1 UV/H ₂ O ₂	194
C1.3.2 UV/Chlorine	195
C1.3.3 Breakpoint Chlorination.....	198
 Chapter C2: Models	 201
 Chapter C3: References	 213

Tables

C1-1	Selected Sources of Experimental Data and Models	193
C3-1	UV/H ₂ O ₂ Chemistry	202
C3-2	Chlorine Photolysis Chemistry	203
C3-3	·OH and O ⁻ Reactions.....	204
C3-4	Cl· Reactions	205
C3-5	Cl ₂ · ⁻ Reactions	206
C3-6	ClO _x Reactions.....	207
C3-7	ClOH· ⁻ Reactions	208
C3-8	HO ₂ · and O ₂ · ⁻ Reactions.....	208
C3-9	CO ₃ · ⁻ Reactions	208
C3-10	Equilibrium Reactions.....	209
C3-11	O ₃ and O ₃ · ⁻ Reactions	209
C3-12	Cl ₂ and Cl ₃ · ⁻ Reactions	210
C3-13	Miscellaneous Reactions	210
C3-14	Breakpoint Chlorination	211

Figures

C1-1	A General Process of a Mechanistic UV AOP Kinetic Model	191
C1-2	Model Fit Comparison	195
C1-3	Model Fit Comparison	197
C1-4	Model Fit Comparison	199

CHAPTER C1

Kinetic Models

C1.1 The Principle of UV AOP Mechanistic Models

Many researchers have built kinetic models of UV AOPs to help to predict their performance and to understand the impact of different water quality characteristics. Most of these models have been mechanistic and are built on the principle of oxidant photolysis and subsequent elementary radical reactions. According to the First and Second Law of Photochemistry (Bolton et al., 2015), to calculate the photolysis rate of the oxidant, the number of photons absorbed by the oxidant must be known. This means the energy-based fluence rate (e.g., with a unit of $\text{mW}\cdot\text{cm}^{-2}$) must be converted to the photon-based fluence rate (e.g., with a unit of $\text{Einstein}\cdot\text{cm}^{-2}\cdot\text{s}^{-1}$) (Bolton et al., 2015). Then the portion of light that is absorbed by the oxidant molecules is calculated based on the Beer-Lambert Law (Bolton et al., 2015; Stefan, 2018). Finally, the amount of absorbed photons required to cause the molecule to undergo photolysis is accounted for by the quantum yield. These principles can be expressed as the following general equations (Stefan, 2018):

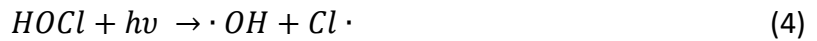
$$E_{p,o} = E_o \frac{\lambda}{hcN_A} \times 1 \times 10^{-9} \quad (1)$$

$$r_B = \frac{E_{p,o}A \varepsilon_B C}{V a} (1 - 10^{-aL}) \Phi \quad (2)$$

In Equation 1, $E_{p,o}$ is the photon-based fluence rate ($\text{Einstein}\cdot\text{m}^{-2}\cdot\text{s}^{-1}$), E_o is the energy-based fluence rate ($\text{W}\cdot\text{m}^{-2}$), λ is the wavelength of light (nm), h is Planck's constant ($\text{J}\cdot\text{s}$), c is the speed of light ($\text{m}\cdot\text{s}^{-1}$), and N_A is the Avogadro constant (mol^{-1}). In Equation 2, r_B is the rate of oxidant photolysis ($\text{mol}\cdot\text{L}^{-1}\cdot\text{s}^{-1}$), V is water volume (L), A is the area exposed to UV light (m^2), ε_B is the molar absorption coefficient ($\text{L}\cdot\text{mol}^{-1}\cdot\text{cm}^{-1}$), a is the total absorption coefficient of water (cm^{-1}), C is the molar concentration of the oxidant ($\text{mol}\cdot\text{L}^{-1}$), L is the light path length (cm^{-1}), and Φ is the quantum yield ($\text{mol}\cdot\text{Einstein}^{-1}$). If the UV source is polychromatic, r_B would become wavelength dependent. The average value of r_B over the wavelength range (from λ_1 to λ_2) of the UV light spectrum is weighted by the incident fluence rate ($E_{p,o}(\lambda)$) within each band (which is usually 1 nm or 5 nm) (Bolton et al., 2015):

$$\bar{r}_B = \frac{\sum_{\lambda_1}^{\lambda_2} E_{p,o}(\lambda) r_B(\lambda)}{\sum_{\lambda_1}^{\lambda_2} E_{p,o}(\lambda)} \quad (3)$$

From Equation 1 and 2, the rate of oxidant photolysis can be obtained, and as radicals are generated during photolysis (Equations 4 to 7) (Bu et al., 2018; Stefan, 2018; Fang et al., 2014; Stefan, 2017; Watts and Linden, 2007), the rate of radical formation can be obtained correspondingly by the stoichiometry.



For example, the rate of Cl and OH formation ($r_{f,Cl}$ and $r_{f,OH}$) can be expressed by the rate of HOCl, OCl, and H₂O₂ photolysis ($r_{p,HOCl}$, r_{p,OCl^-} , and r_{p,H_2O_2}):

$$r_{f,Cl} = r_{p,HOCl} + r_{p,OCl^-} \quad (8)$$

$$r_{f,OH} = 2r_{p,H_2O_2} \quad (9)$$

Next, the radicals formed by oxidant photolysis will quickly react with target pollutants and other compounds in water, such as the oxidant itself, chloride, bicarbonate, and natural organic matter (Crittenden et al., 1999; Fang et al., 2014; Zhang et al., 2019). Therefore, the concentration of radicals and compounds are affected by these reactions. An ordinary differential equation can be built to quantify the rate of concentration change for each compound or radical:

$$\frac{dC_A}{dt} = r_p + \sum_i r_i \quad (10)$$

where dC_A is the derivative of the molar concentration of compound A, dt is the derivative of reaction time, r_p is the rate of C_A formation or consumption by photolysis (if any), and r_i is the rate of formation or consumption of a in the i^{th} reaction, which is expressed as the product of rate constant k_i and the molar concentration of the reactants (i.e., R_1, R_2 ; for most of the cases there are only two reactants in the reaction):

$$r_i = k_i[R_1][R_2] \quad (11)$$

If one compiles all the differential equations, an ordinary differential equation (ODE) set is built accounting for the rate of change of all the compounds in the process. To solve the ODE set, the ODE solvers provided by computing software are often used, such as the 'ode' function in MathWorks.

In addition to constructing and solving the ODE set, input and output processes must also be created. A general process of a simulation by a UV AOP kinetic model is shown in Figure C1-1.

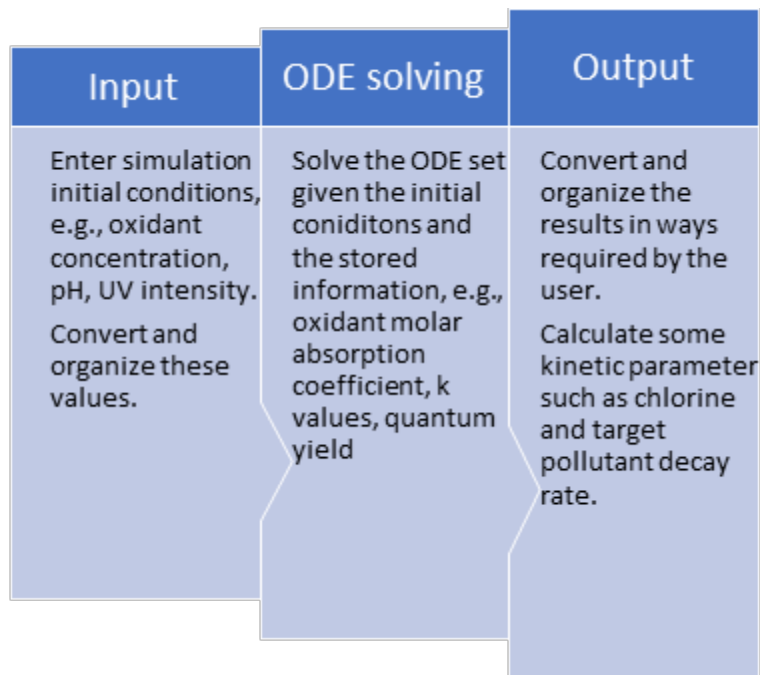


Figure C1-1. A General Process of a Mechanistic UV AOP Kinetic Model

The general model described above is only suitable for a completely mixed batch reactor, which are usually lab-scale batch reactors, such as a quasi-collimated beam reactor (Bolton and Linden, 2003). For larger scale UV reactors, other factors have to be considered, such as the uneven distribution of UV intensity and incomplete mixing, which are beyond of the scope of this model description. There are also some correction factors to account for the dissipation of UV photons for a quasi-collimated beam reactor, such as the divergence factor and reflection factor (Bolton and Linden, 2003). These factors are not discussed here.

C1.2 Current Model Review – A General Critical Analysis

Many research papers have published UV AOP experimental results accompanied by their own mechanistic models (Crittenden et al., 1999; Guo et al., 2018; Kwon et al., 2020; Wu et al., 2017). The models were mostly built for a monochromatic UV source (e.g., low-pressure UV) following the principle above, but different numbers of reactions have been included in such models, ranging from about 20 to 200 (Fang et al., 2014; Guo et al., 2018; Kwon et al., 2020). The extended contents from a relatively simplistic model to a complex one are solely chemical reactions. These reactions are usually the propagation of the radical chain reactions or introducing compounds or radicals (e.g., bromide and chlorite) that were not included in earlier versions of the model (Cheng et al., 2018; Chuang et al., 2017; Zhao et al., 2021). These published models have often attempted to include as many reactions as possible to show accuracy and inclusiveness of the model, but the reported models have not necessarily been tested to demonstrate whether the increase in the number of reactions would increase model accuracy. In contrast, when more reactions are added, there is the risk of violating the “principle of detailed balancing.” This principle holds that both forward and reverse reactions need to consistently be included in a model where reversible reactions exist, otherwise there might (for example) be a numerical “accumulation” of a species as its formation is simulated

without any corresponding decomposition (Stanbury and Harshman, 2019). Only one UV AOP (chloramine) model (Sun et al., 2019) has been identified as having been scrutinized to see if it violates this principle (Stanbury, 2020). It is beyond the scope of this report to test all previous models accordingly.

Sometimes errors (including the violation of detailed balancing) in a model may arise from the reaction rate coefficient (k) used. The k values used in the models mainly come from a range of literature or the National Institute of Standard and Technology (NIST) database (NIST, 2022). Some references are fundamental radical reaction studies using laser flash photolysis or radiolysis technologies (Alfassi et al., 1988; Buxton et al., 1988; Kläning and Wolff, 1985; Neta et al., 1988) and others are environmental studies on related topics (Grebel et al., 2010; Keen et al., 2014). The k values reported in those sources might be inconsistent or only applicable to some certain conditions (e.g., temperature and ionic strength). The k values that were chosen to be used in a model might also be arbitrary or approximate. Occasionally, when some k values are not available from the published literature, the paper authors might assign a k value to the reaction from a similar reaction that has a radical with close reactivity (Fang et al., 2014; Miklos et al., 2019). For example, they might assume that the k value for the $\text{Cl}\cdot + \text{ClO}_2^-$ reaction is the same as that for the $\cdot\text{OH} + \text{ClO}_2^-$ reaction (Chuang et al., 2017). Sometimes, the authors determined the k values themselves by competition kinetics experiments using probe compounds. For example, the k value of $\text{ClO}\cdot$ with natural organic matter (NOM) was determined by competition kinetics experiments with 1,4-dimethoxybenzene, which is a known $\text{ClO}\cdot$ probe compound (Guo et al., 2018, 2017). In some cases, the k values are determined based on the best fit of the simulation results to the experimental results using an optimization algorithm, such as a genetic algorithm (Zhou et al., 2019). As many different k value sources are involved, it is impossible to verify their accuracy. The authors of the models rarely show justification of the choice of a k value, and the possible errors caused by the k values have not been explicitly evaluated. These problems might escalate when more reactions are included in the model.

Furthermore, although many kinetic models have been built to facilitate UV AOP research, most of the models built have not been verified against experimental data—or at least, not against data reported by other independent researchers. It would be useful to develop a universal UV AOP model that is verified against some standard experimental data with known accuracy. Such a model would be a beneficial guide for both academic research and engineering practice. Unfortunately, such a model does not yet exist. For this project, we have compiled most of the latest reported elementary reactions in UV/ H_2O_2 , UV/chlorine, and breakpoint chlorination processes in this Appendix, but the application of these reactions and their k values to build one's own model is at reader's own discretion. In the meantime, some cross-comparisons of the published models with experimental data were conducted in the next section to explore the general accuracy of the models.

C1.3 Cross-Comparison of the Models

While most models in the literature have not been verified against experimental results, several papers published mechanistic models that were in good agreement with their own experimental data under a variety of reaction conditions (Chuang et al., 2017; Crittenden et al., 1999; Fang et al., 2014; Huang, 2008; Shen, 2014; Zhang et al., 2018). Since these models were built, they have not reportedly been used to try to simulate the experimental data from sources other than the paper in which the model was published. This implies that although these models were verified against some experimental data, their validity might be broader. Therefore, we carefully selected several representative experimental data sets from the literature as benchmarks that cover many of the important factors to UV/H₂O₂, UV/chlorine, and breakpoint chlorination (breakpoint chlorination is modelled due to its significant impact on UV/chlorine efficiency. See details in the Breakpoint Chlorination section below). We reconstructed models from different sources in the literature using MATLAB, MathWorks® and tested their capability to simulate the selected experimental datasets. The selection of the experimental data sets considered academic impact (by the number of times cited) and whether the publications covered the effect of important influencing factors (e.g., pH). The selection of the models considered their complexity (by the number of reactions), published year, and how accurately they could predict the data from the paper in which the model was published. The details of the datasets and the models selected are given in Table C1-1.

Table C1-1. Selected Sources of Experimental Data and Models

Experimental data				
	Source	Times cited ^a	Factors covered	Contents
UV/H ₂ O ₂	Crittenden et al., 1999	578	pH, H ₂ O ₂ dose, UV fluence rate, inorganic carbon	Pollutant degradation rate
UV/chlorine	Fang et al., 2014	510	pH, chlorine dose, bicarbonate, TOC	Pollutant degradation rate
Breakpoint chlorination	Chuang et al., 2017	205	pH	Chlorine decay rate
	Wei and Morris 1974	57	pH, ammonia concentration	Free chlorine and chloramine concentration
	Valentine and Jafvert, 1992	411	pH, Cl/N ratio	Free chlorine and chloramine concentration
Models				
	Source	# of reactions ^b	Publication year	
UV/H ₂ O ₂	Crittenden et al., 1999	20	1999	
	Zhang et al., 2018	15	2018	
UV/chlorine	Fang et al., 2014	20	2014	
	Chuang et al., 2017	75	2017	
	Zhao et al., 2021	163	2021	
Breakpoint chlorination	Jafvert and Valentine, 1992	14	1992	
	Huang, 2008	15	2008	

^a Source: Google scholar. Date accessed: 01-27-2022.

^b Some pollutant-specific reactions are not included.

C1.3.1 UV/H₂O₂

A comprehensive dataset for destruction of a contaminant using UV/H₂O₂ is reported by Crittenden et al. (1999), where the degradation of 1,2-dibromo-3-chloropropane (DBCP) was measured over a variety of conditions (Figure C1-2). Two models are used to predict the Crittenden et al. dataset: the one developed by Crittenden et al. themselves to predict the data, and one by Zhang et al. (2018). Generally, both models followed the trends of the experimental data well. Both models are able to simulate the effect of initial H₂O₂ concentration, pH, UV light intensity, and total inorganic carbon concentration on DBCP degradation rate in UV/H₂O₂. The error (the difference between the experimental value and the simulated values) of the simulations by the reconstructed Zhang et al. model is larger than that of Crittenden's model. The model in Crittenden et al., 1999 contains about 20 reactions and it includes H₂O₂ photolysis and ·OH reactions while ignoring the role of chloride. In contrast, Zhang et al. included the reaction of ·OH with chloride, which forms reactive chlorine species such as Cl·, ClOH⁻, and Cl₂⁻. Nevertheless, Zhang's model only has about 15 reactions. Zhang's model might be more accurate in the presence of chloride, but as chloride was not considered in the experimental dataset, its effect was not cross-verified. Although the models are slightly different, both models can predict the effect of influencing factors well, which indicates they both contain the essential reactions in UV/H₂O₂ treatment.

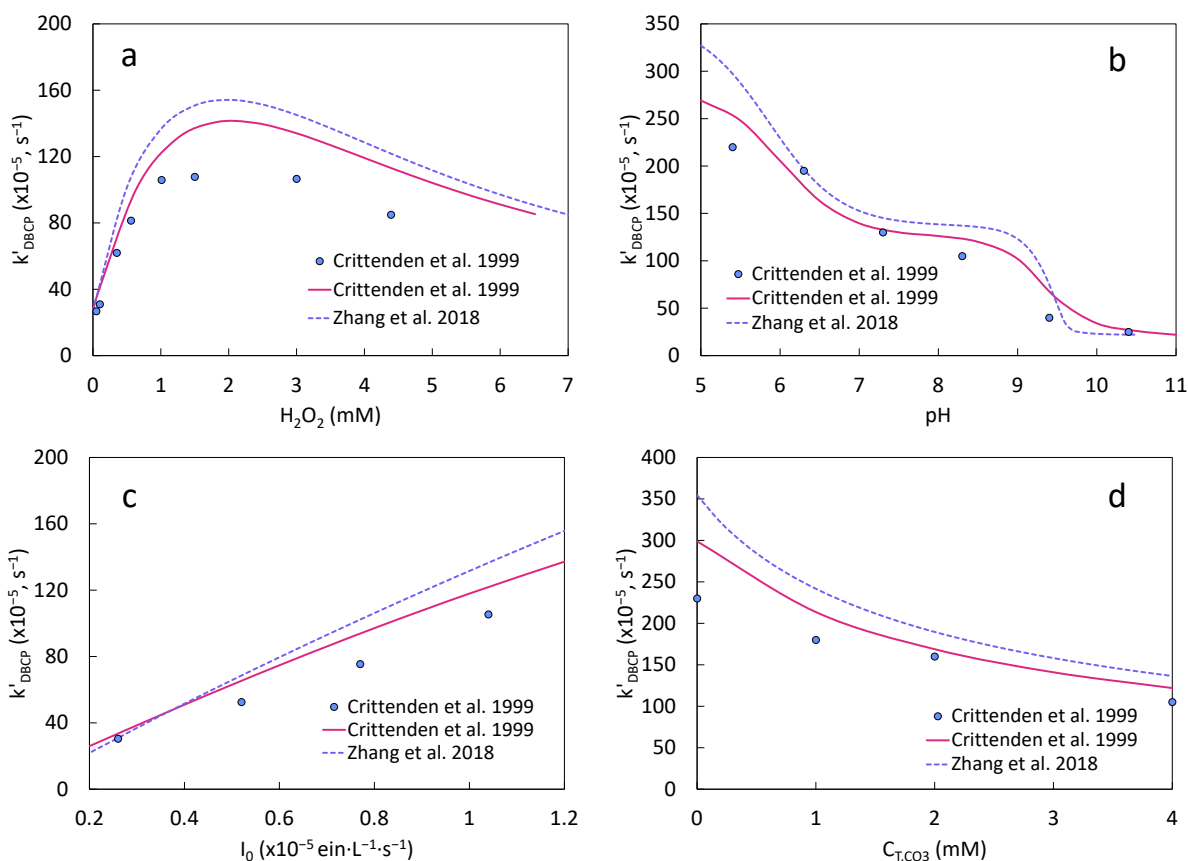


Figure C1-2. Model Fit Comparison.

The experimental data (dots, from Crittenden et al., 1999) and simulation results (lines, from the reconstructed models from Crittenden et al., 1999 and Zhang et al., 2018) of 1,2-dibromo-3-chloropropane (DBCP) pseudo first-order degradation rate (k') by low-pressure UV/ H_2O_2 under the effect of (a) initial H_2O_2 concentration, (b) pH, (c) UV light fluence rate, and (d) total inorganic carbon ($C_{\text{T,CO}_3}$) concentration. Reaction condition: pH 8.4, $[\text{H}_2\text{O}_2]_0 = 1$ mM, $[\text{DBCP}]_0 = 1.83$ μM , $I_0 = 1.04 \times 10^{-6}$ $\text{ein} \cdot \text{L}^{-1} \cdot \text{s}^{-1}$, $C_{\text{T,CO}_3} = 4$ mM, or otherwise indicated in the figure.

C1.3.2 UV/Chlorine

An experimental dataset reporting the UV/chlorine destruction of benzoate along with free chlorine photolysis under different conditions was reported by Fang et al. (2014) and is reproduced in Figure C1-3. Fang et al. developed their own model to describe the experimental data, and their model, along with models reported by Chuang et al. (2017) and Zhao et al. (2021), are used to predict the Fang et al. (2014) data. The predicted benzoate and chlorine destruction are shown under varying conditions of pH, initial concentration, bicarbonate concentration, and TOC.

The three models have different numbers of reactions included and used different key parameters. The model by Fang et al. (2014) has approximately 20 reactions that represent the initial few steps of radical reactions after the photolysis of chlorine. The apparent quantum yields of HOCl and OCl^- at 254 nm and the k value for the reaction of NOM with Cl^\cdot were determined from their own experiments. In comparison, the model by Chuang et al. (2017) has approximately 80 reactions and specifically includes a set of ClO_x -related reactions (reactions involving ClO_2^- , ClO_2^\cdot , and ClO_3^-), which were proven to be crucial to the accuracy of chlorine

decay simulation. The quantum yield of HOCl and OCl⁻ at 254 nm were also determined by their own experiments but with a more delicate experimental design to measure the innate rather than the observed quantum yield. The model by Zhao et al. (2021) contains approximately 160 reactions. Compared to the previous two models, it contains a more comprehensive yet somewhat possibly unimportant set of reactions for most UV/chlorine processes, based on chlorite-related reactions and ozone-related reactions. It is also the only one among the three models that is in compliance with the principle of detailed balance.

While all three models can simulate the general trends in benzoate destruction and chlorine photolysis as a function of the water quality variables explored, arguably none are very accurate. There is also no clear indication that the greater number of reactions in the Zhao et al. (2021) model (≈ 180) leads to any greater accuracy when predicting the independent dataset.

Overall, this analysis suggests that the current mechanistic models reported in the literature may not be reliable predictors of UV-chlorine AOP performance in waters and under conditions that are different from those used to generate the models.

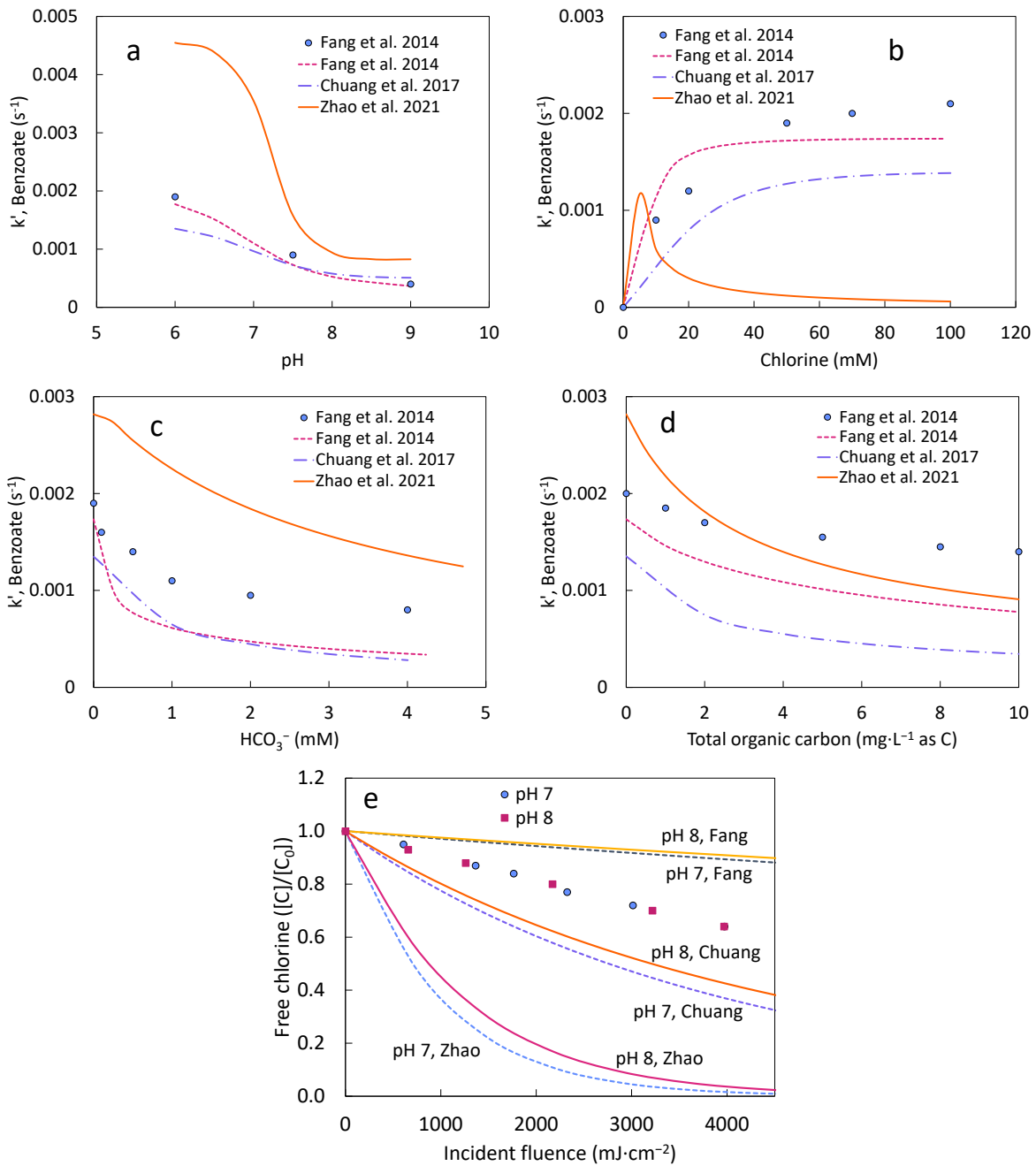


Figure C1-3. Model Fit Comparison.

The experimental data (dots, from Fang et al., 2014 (a-d) and Chuang et al., 2017 (e)) and simulation results (lines, from the reconstructed models from Fang et al., 2014, Chuang et al., 2017, and Zhao et al., 2021) of benzoate pseudo first-order degradation rate (k') by low-pressure UV/chlorine under the effect of (a) pH, (b) initial chlorine concentration, (c) initial bicarbonate concentration, and (d) total organic carbon concentration and (e) free chlorine decay at pH 7 and 8. Reaction conditions: for a-d, pH 6, $[chlorine]_0 = 70 \mu M$, $[benzoate]_0 = 5 \mu M$, $I_0 = 2.52 \times 10^{-7} \text{ ein} \cdot L^{-1} \cdot s^{-1}$, $C_{T,CO_3} = 0 \text{ mM}$, $TOC = 0 \text{ mg} \cdot L^{-1}$ as C; for e, $[chlorine]_0 = 40 \mu M$, $I_0 = 2.55 \times 10^{-7} \text{ ein} \cdot L^{-1} \cdot s^{-1}$, phosphate buffer = 2 mM or otherwise indicated in the figure. The fluence was calculated using a fluence rate of $0.6 \text{ mW} \cdot \text{cm}^{-2}$.

C1.3.3 Breakpoint Chlorination

Breakpoint chlorination can occur in a Full Advanced Treatment (FAT) water reuse process if chloramines are used to prevent RO fouling. As much as 50%-100% of the chloramines may pass through the RO, and then react with free chlorine that is applied for the UV/chlorine process. The breakpoint reactions are not instantaneous, so the chlor(am)ine species may evolve between the point of free chlorine injection and the UV reactor. This evolution can cause errors in the predicted amount of free chlorine entering the reactor, or inaccuracies in predicted UV transmittance due to the strong absorbance from monochloramine compared to free chlorine at 254 nm ($388 \text{ M}^{-1}\text{cm}^{-1}$ vs. $59\text{-}66 \text{ M}^{-1}\text{cm}^{-1}$) (Li and Blatchley III (2009); Stefan et al. (1996)).

Two published models (Jafvert and Valentine, 1992; Huang, 2008) of breakpoint chlorination were reconstructed and verified against published experimental results from Wei and Morris (1974) and Jafvert and Valentine (1992), which are regarded as the classic data that are often used in breakpoint model verification (Huang (2008); Shen (2014)). As the rate of change of free chlorine and monochloramine are likely of greatest importance (described above), only their results are shown. Figure C1-4 shows reactions at different initial ammonia concentration, pH, and Cl/N molar ratios. Figure C1-4a and Figure C1-4b show the concentrations of free chlorine and monochloramine in the reactions that have reached breakpoint (Cl/N=1.8) at pH 7. Figure C1-4c and Figure C1-4d show two Cl/N ratios that are before and after breakpoint has been reached.

Generally, both the reconstructed models from Jafvert and Valentine (1992) and Huang (2008) can predict the experimentally-measured free chlorine and monochloramine concentrations well. Both models overpredicted the free chlorine concentration (Figure C1-4a,b), but the error is relatively small. The reconstructed Huang's model can better predict free chlorine concentration for Cl/N=1.24 and 2.03 at pH 6 (Figure C1-4c,d). This can be attributed to Huang's model having changed the reactions and incorporated more recently reported k values into a previous model by Jafvert (1985). In addition, Huang also extensively validated the model under a variety of conditions. Thus far, Huang's model might be regarded as the best mechanistic model for breakpoint chlorination simulations. However, the verification of Huang's model is against experimental data collected over tens of minutes. In a FAT process, the first tens of seconds is crucial since this is a typical travel time between the point of free chlorine injection and the UV reactor. Experimental data to validate the accuracy of Huang's model in this short timeframe are very limited. Furthermore, the lowest pH validated in Huang (2008) was 6.5, which is likely higher than typical RO permeate (pH 5-6). Therefore, more studies are needed to further verify breakpoint chlorination reaction kinetics under these short timeframes and at low pH.

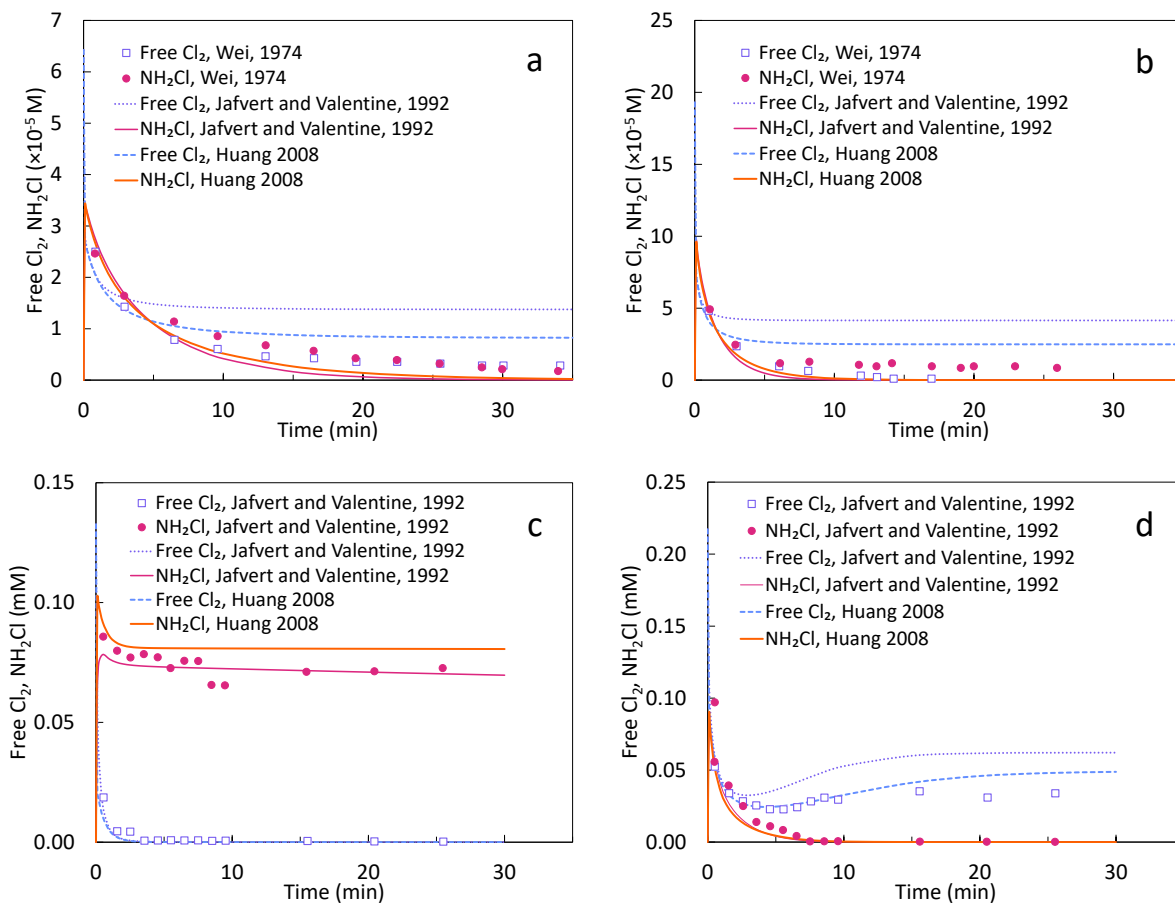


Figure C1-4. Model Fit Comparison.

The experimental data (dots, from Wei and Morris 1974 (a-b) and Jafvert and Valentine, 1992 (c-d)) and simulation results (lines, from the reconstructed models from Jafvert and Valentine, 1992 and Huang 2008) of free chlorine and monochloramine concentration in the reaction of free chlorine with ammonia at initial total ammonia concentration of (a) 0.0357 and (b) 0.107 mM as N and molar Cl/N of (c) 1.24 and (d) 2.03. Reaction conditions: for a-b, pH=7, molar Cl/N=1.8, phosphate buffer=2 mM; for c-d, pH=6, total ammonia concentration=0.107 mM, phosphate buffer=2 mM, or otherwise indicated in the figure.

CHAPTER C2

Models

The most up-to-date reactions for UV/H₂O₂, UV/chlorine, and breakpoint chlorination have been organized in the following tables. Note that the reference shown in the table might not be the origin of the k values. The root source paper can be found in the paper cited in the table. Besides, there are reactions related with bromide, nitrite, and nitrate in UV AOPs. Part of those reactions and associated kinetic parameters can be found in Goldstein and Rabani (2007); Mack and Bolton (1999); Wu et al. (2019); Zhang et al. (2020). To focus on the essential reactions, they are not listed here.

Table C3-1. UV/H₂O₂ Chemistry.
(excerpted from Crittenden et al., 1999; Zhang et al., 2018)

1	$\text{H}_2\text{O}_2 + h\nu \rightarrow 2 \cdot\text{OH}$	$\epsilon(254 \text{ nm})=18 \text{ M}^{-1}\cdot\text{cm}^{-1}$ $\Phi(254 \text{ nm}) = 0.5$
2	$\text{HO}_2^- + h\nu \rightarrow 2 \cdot\text{OH}$	$\epsilon(254 \text{ nm})=228 \text{ M}^{-1}\cdot\text{cm}^{-1}$ $\Phi(254 \text{ nm}) = 0.5$
3	$\text{H}_2\text{O}_2 + \cdot\text{OH} \rightarrow \text{H}_2\text{O} + \text{HO}_2\cdot$	$2.7 \times 10^7 \text{ M}^{-1}\cdot\text{s}^{-1}$
4	$\cdot\text{OH} + \text{HO}_2^- \rightarrow \text{HO}_2\cdot + \text{OH}^-$	$7.5 \times 10^9 \text{ M}^{-1}\cdot\text{s}^{-1}$
5	$\text{H}_2\text{O}_2 + \text{HO}_2\cdot \rightarrow \cdot\text{OH} + \text{H}_2\text{O} + \text{O}_2$	$3 \text{ M}^{-1}\cdot\text{s}^{-1}$
6	$\text{H}_2\text{O}_2 + \text{O}_2^{\cdot-} \rightarrow \cdot\text{OH} + \text{O}_2 + \text{OH}^-$	$0.13 \text{ M}^{-1}\cdot\text{s}^{-1}$
7	$\cdot\text{OH} + \text{CO}_3^{2-} \rightarrow \text{CO}_3^{\cdot-} + \text{OH}^-$	$3.9 \times 10^8 \text{ M}^{-1}\cdot\text{s}^{-1}$
8	$\cdot\text{OH} + \text{HCO}_3^- \rightarrow \text{CO}_3^{\cdot-} + \text{H}_2\text{O}$	$8.5 \times 10^6 \text{ M}^{-1}\cdot\text{s}^{-1}$
9	$\cdot\text{OH} + \text{HPO}_4^{2-} \rightarrow \text{HPO}_4^{\cdot-} + \text{OH}^-$	$1.5 \times 10^5 \text{ M}^{-1}\cdot\text{s}^{-1}$
10	$\cdot\text{OH} + \text{H}_2\text{PO}_4^- \rightarrow \text{HPO}_4^{\cdot-} + \text{H}_2\text{O}$	$2 \times 10^4 \text{ M}^{-1}\cdot\text{s}^{-1}$
11	$\text{H}_2\text{O}_2 + \text{CO}_3^{\cdot-} \rightarrow \text{HCO}_3^- + \text{HO}_2\cdot$	$4.3 \times 10^5 \text{ M}^{-1}\cdot\text{s}^{-1}$
12	$\text{HO}_2^- + \text{CO}_3^{\cdot-} \rightarrow \text{CO}_3^{2-} + \text{HO}_2\cdot$	$3 \times 10^7 \text{ M}^{-1}\cdot\text{s}^{-1}$
13	$\text{H}_2\text{O}_2 + \text{HPO}_4^{\cdot-} \rightarrow \text{H}_2\text{PO}_4^- + \text{HO}_2\cdot$	$2.7 \times 10^7 \text{ M}^{-1}\cdot\text{s}^{-1}$
14	$\cdot\text{OH} + \cdot\text{OH} \rightarrow \text{H}_2\text{O}_2$	$5.5 \times 10^9 \text{ M}^{-1}\cdot\text{s}^{-1}$
15	$\cdot\text{OH} + \text{HO}_2\cdot \rightarrow \text{H}_2\text{O} + \text{O}_2$	$6.6 \times 10^9 \text{ M}^{-1}\cdot\text{s}^{-1}$
16	$\text{HO}_2\cdot + \text{HO}_2\cdot \rightarrow \text{H}_2\text{O}_2 + \text{O}_2$	$8.3 \times 10^5 \text{ M}^{-1}\cdot\text{s}^{-1}$
17	$\text{HO}_2\cdot + \text{O}_2^{\cdot-} \rightarrow \text{HO}_2^- + \text{O}_2$	$9.7 \times 10^7 \text{ M}^{-1}\cdot\text{s}^{-1}$
18	$\cdot\text{OH} + \text{O}_2^{\cdot-} \rightarrow \text{O}_2 + \text{OH}^-$	$7 \times 10^9 \text{ M}^{-1}\cdot\text{s}^{-1}$
19	$\cdot\text{OH} + \text{CO}_3^{\cdot-} \rightarrow \text{Product}$	$3 \times 10^9 \text{ M}^{-1}\cdot\text{s}^{-1}$
20	$\text{CO}_3^{\cdot-} + \text{O}_2^{\cdot-} \rightarrow \text{CO}_3^{2-} + \text{O}_2$	$6 \times 10^8 \text{ M}^{-1}\cdot\text{s}^{-1}$
21	$\text{CO}_3^{\cdot-} + \text{CO}_3^{\cdot-} \rightarrow \text{Product}$	$3 \times 10^7 \text{ M}^{-1}\cdot\text{s}^{-1}$
22	$\cdot\text{OH} + \text{TOC} \rightarrow \text{Product}$	$3 \times 10^8 \text{ M}^{-1}\cdot\text{s}^{-1}$
23	$\text{HCO}_3^- + \text{H}^+ \rightarrow \text{H}_2\text{CO}_3$	$5 \times 10^{10} \text{ M}^{-1}\cdot\text{s}^{-1}$
24	$\text{H}_2\text{CO}_3 \rightarrow \text{H}^+ + \text{HCO}_3^-$	$5 \times 10^5 \text{ s}^{-1}$
25	$\text{CO}_3^{2-} + \text{H}^+ \rightarrow \text{HCO}_3^-$	$5 \times 10^{10} \text{ M}^{-1}\cdot\text{s}^{-1}$
26	$\text{HCO}_3^- \rightarrow \text{CO}_3^{2-} + \text{H}^+$	2.345 s^{-1}
27	$\text{H}_2\text{O}_2 \rightarrow \text{HO}_2^- + \text{H}^+$	0.13 s^{-1}
28	$\text{HO}_2^- + \text{H}^+ \rightarrow \text{H}_2\text{O}_2$	$5 \times 10^{10} \text{ M}^{-1}\cdot\text{s}^{-1}$
29	$\text{H}_3\text{PO}_4 \rightarrow \text{H}_2\text{PO}_4^- + \text{H}^+$	$3.97 \times 10^8 \text{ s}^{-1}$
30	$\text{H}_2\text{PO}_4^- + \text{H}^+ \rightarrow \text{H}_3\text{PO}_4$	$5 \times 10^{10} \text{ M}^{-1}\cdot\text{s}^{-1}$
31	$\text{H}_2\text{PO}_4^- \rightarrow \text{HPO}_4^{2-} + \text{H}^+$	$3.15 \times 10^3 \text{ s}^{-1}$
32	$\text{HPO}_4^{2-} + \text{H}^+ \rightarrow \text{H}_2\text{PO}_4^-$	$5 \times 10^{10} \text{ M}^{-1}\cdot\text{s}^{-1}$
33	$\text{HPO}_4^{2-} \rightarrow \text{PO}_4^{3-} + \text{H}^+$	$2.5 \times 10^{-2} \text{ s}^{-1}$
34	$\text{PO}_4^{3-} + \text{H}^+ \rightarrow \text{HPO}_4^{2-}$	$5 \times 10^{10} \text{ M}^{-1}\cdot\text{s}^{-1}$
35	$\text{Cl}\cdot + \text{NOM} \rightarrow \text{Product}$	$1.56 \times 10^8 \text{ M}^{-1}\cdot\text{s}^{-1}$
36	$\cdot\text{OH} + \text{H}_2\text{O}_2 \rightarrow \text{HO}_2\cdot + \text{H}_2\text{O}$	$2.7 \times 10^7 \text{ M}^{-1}\cdot\text{s}^{-1}$
37	$\cdot\text{OH} + \text{Cl}^- \rightarrow \text{ClOH}^-$	$4.3 \times 10^9 \text{ M}^{-1}\cdot\text{s}^{-1}$
38	$\text{ClOH}^- \rightarrow \cdot\text{OH} + \text{Cl}^-$	$6.1 \times 10^9 \text{ s}^{-1}$
39	$\text{ClOH}^- + \text{Cl}^- \rightarrow \text{Cl}_2^{\cdot-} + \text{H}_2\text{O}$	$1 \times 10^4 \text{ M}^{-1}\cdot\text{s}^{-1}$
40	$\text{ClOH}^- + \text{H}^+ \rightarrow \text{Cl}\cdot + \text{H}_2\text{O}$	$2.1 \times 10^{10} \text{ M}^{-1}\cdot\text{s}^{-1}$
41	$\text{Cl}\cdot + \text{H}_2\text{O}_2 \rightarrow \text{HO}_2\cdot + \text{Cl}^- + \text{H}^+$	$2 \times 10^9 \text{ M}^{-1}\cdot\text{s}^{-1}$
42	$\text{Cl}\cdot + \text{Cl}^- \rightarrow \text{Cl}_2^{\cdot-}$	$8 \times 10^9 \text{ M}^{-1}\cdot\text{s}^{-1}$
43	$\text{Cl}\cdot + \text{H}_2\text{O} \rightarrow \text{ClOH}^- + \text{H}^+$	$2.5 \times 10^5 \text{ s}^{-1}$
44	$\text{Cl}\cdot + \text{HCO}_3^- \rightarrow \text{CO}_3^{\cdot-} + \text{Cl}^- + \text{H}^+$	$2.2 \times 10^8 \text{ M}^{-1}\cdot\text{s}^{-1}$
45	$\text{Cl}\cdot + \text{CO}_3^{2-} \rightarrow \text{CO}_3^{\cdot-} + \text{Cl}^-$	$5 \times 10^8 \text{ M}^{-1}\cdot\text{s}^{-1}$

Table C3-2. Chlorine Photolysis Chemistry.

46	$\text{HOCl} \rightarrow \cdot\text{OH} + \text{Cl}\cdot$	$\epsilon(254 \text{ nm})=59 \text{ M}^{-1}\cdot\text{cm}^{-1}$ $\Phi(254 \text{ nm}) = 1.45$ $\Phi(254 \text{ nm}) = 0.62$	Fang et al., 2014 Fang et al., 2014 Chuang et al., 2017
47	$\text{OCl}^- \rightarrow \text{O}^- + \text{Cl}\cdot$	$\epsilon(254 \text{ nm})=66 \text{ M}^{-1}\cdot\text{cm}^{-1}$ $\Phi(254 \text{ nm}) = 0.97$ $\Phi(254 \text{ nm}) = 0.55$	Fang et al., 2014 Fang et al., 2014 Chuang et al., 2017
48	$\text{OCl}^- \rightarrow \text{O}(3\text{P}) + \text{Cl}^-$	$\Phi(254 \text{ nm}) = 0.074$	Buxton and Subhani, 1972
49	$\text{OCl}^- \rightarrow \text{O}(1\text{D}) + \text{Cl}^-$	$\Phi(254 \text{ nm}) = 0.133$	Buxton and Subhani, 1972

Table C3-3. ·OH and O⁻ Reactions.

50	$\cdot\text{OH} + \text{HOCl} \rightarrow \text{ClO}\cdot + \text{H}_2\text{O}$	$2.0 \times 10^9 \text{ M}^{-1}\cdot\text{s}^{-1}$ $5.00 \times 10^8 \text{ M}^{-1}\cdot\text{s}^{-1}$	Fang et al., 2014 Chuang et al., 2017 Zhao et al., 2021
51	$\cdot\text{OH} + \text{OCl}^- + \rightarrow \text{ClO}\cdot + \text{OH}^-$	$8.8 \times 10^9 \text{ M}^{-1}\cdot\text{s}^{-1}$ $1.85 \times 10^9 \text{ M}^{-1}\cdot\text{s}^{-1}$	Fang et al., 2014 Chuang et al., 2017 Zhao et al., 2021
52	$\cdot\text{OH} + \text{H}_2\text{O}_2 \rightarrow \text{HO}_2\cdot + \text{H}_2\text{O}$	$2.70 \times 10^7 \text{ M}^{-1}\cdot\text{s}^{-1}$ $3.00 \times 10^7 \text{ M}^{-1}\cdot\text{s}^{-1}$	Chuang et al., 2017 Zhao et al., 2021
53	$\cdot\text{OH} + \cdot\text{OH} \rightarrow \text{H}_2\text{O}_2$	$5.50 \times 10^9 \text{ M}^{-1}\cdot\text{s}^{-1}$	Fang et al., 2014 Chuang et al., 2017 Zhao et al., 2021
54	$\cdot\text{OH} + \text{HO}_2\cdot \rightarrow \text{O}_2 + \text{H}_2\text{O}$	$6.60 \times 10^9 \text{ M}^{-1}\cdot\text{s}^{-1}$	Chuang et al., 2017
55	$\cdot\text{OH} + \text{O}_2^- \rightarrow \text{O}_2 + \text{OH}^-$	$7.00 \times 10^9 \text{ M}^{-1}\cdot\text{s}^{-1}$ $1.00 \times 10^{10} \text{ M}^{-1}\cdot\text{s}^{-1}$	Chuang et al., 2017 Zhao et al., 2021
56	$\cdot\text{OH} + \text{HO}_2^- \rightarrow \text{HO}_2\cdot + \text{OH}^-$	$7.50 \times 10^9 \text{ M}^{-1}\cdot\text{s}^{-1}$	Chuang et al., 2017 Zhao et al., 2021
57	$\cdot\text{OH} + \text{OH}^- \rightarrow \text{O}^- + \text{H}_2\text{O}$	$1.3 \times 10^{10} \text{ M}^{-1}\cdot\text{s}^{-1}$ $1.20 \times 10^{10} \text{ M}^{-1}\cdot\text{s}^{-1}$ $1.25 \times 10^{10} \text{ M}^{-1}\cdot\text{s}^{-1}$	Fang et al., 2014 Chuang et al., 2017 Zhao et al., 2021
58	$\cdot\text{OH} + \text{Cl}^- \rightarrow \text{ClOH}^-$	$4.30 \times 10^9 \text{ M}^{-1}\cdot\text{s}^{-1}$	Fang et al., 2014 Chuang et al., 2017 Zhao et al., 2021
59	$\cdot\text{OH} + \text{HPO}_4^{2-} \rightarrow \text{HPO}_4^{\cdot-} + \text{OH}^-$	$1.50 \times 10^5 \text{ M}^{-1}\cdot\text{s}^{-1}$	Chuang et al., 2017
60	$\cdot\text{OH} + \text{H}_2\text{PO}_4^- \rightarrow \text{HPO}_4^{\cdot-} + \text{H}_2\text{O}$	$2.00 \times 10^4 \text{ M}^{-1}\cdot\text{s}^{-1}$	Chuang et al., 2017
61	$\cdot\text{OH} + \text{HCO}_3^- \rightarrow \text{CO}_3^{\cdot-} + \text{H}_2\text{O}$	$8.5 \times 10^6 \text{ M}^{-1}\cdot\text{s}^{-1}$ $8.60 \times 10^6 \text{ M}^{-1}\cdot\text{s}^{-1}$	Fang et al., 2014 Zhao et al., 2021
62	$\cdot\text{OH} + \text{CO}_3^{2-} \rightarrow \text{CO}_3^{\cdot-} + \text{OH}^-$	$3.90 \times 10^8 \text{ M}^{-1}\cdot\text{s}^{-1}$	Zhao et al., 2021
63	$\cdot\text{OH} + \text{H}_2\text{CO}_3 \rightarrow \text{CO}_3^{\cdot-} + \text{H}_2\text{O} + \text{H}^+$	$1.00 \times 10^6 \text{ M}^{-1}\cdot\text{s}^{-1}$	Zhao et al., 2021
64	$\cdot\text{OH} + \text{NOM} \rightarrow \text{Product}$	$3.0 \times 10^8 \text{ M}^{-1}\cdot\text{s}^{-1}$	Fang et al., 2014 Chuang et al., 2017
65	$\cdot\text{OH} + \text{CO}_3^{\cdot-} \rightarrow \text{Product}$	$3.00 \times 10^9 \text{ M}^{-1}\cdot\text{s}^{-1}$	Zhao et al., 2021
66	$\cdot\text{OH} + \text{O}^- \rightarrow \text{HO}_2^-$	$1.00 \times 10^{10} \text{ M}^{-1}\cdot\text{s}^{-1}$	Zhao et al., 2021
67	$\cdot\text{OH} + \text{Cl}^- \rightarrow \text{Cl}\cdot + \text{OH}^-$	$1.10 \times 10^9 \text{ M}^{-1}\cdot\text{s}^{-1}$	Zhao et al., 2021
68	$\cdot\text{OH} + \text{Cl}_2 \rightarrow \text{HOCl} + \text{Cl}\cdot$	$1.00 \times 10^9 \text{ M}^{-1}\cdot\text{s}^{-1}$	Zhao et al., 2021
69			
70	$\text{O}^- + \text{OCl}^- + \text{H}_2\text{O} \rightarrow \text{ClO}\cdot + 2\text{OH}^-$	$2.30 \times 10^8 \text{ M}^{-1}\cdot\text{s}^{-1}$	Zhao et al., 2021
71	$\text{O}^- + \text{H}_2\text{O}_2 \rightarrow \text{H}_2\text{O} + \text{O}_2^{\cdot-}$	$4.00 \times 10^8 \text{ M}^{-1}\cdot\text{s}^{-1}$	Zhao et al., 2021
72	$\text{O}^- + \text{HO}_2^- + \text{H}_2\text{O} \rightarrow \text{HO}_2\cdot + 2\text{OH}^-$	$5.00 \times 10^8 \text{ M}^{-1}\cdot\text{s}^{-1}$	Zhao et al., 2021
73	$\text{O}^- + \text{H}_2\text{O} \rightarrow \cdot\text{OH} + \text{OH}^-$	$1.8 \times 10^6 \text{ s}^{-1}$	Fang et al., 2014 Zhao et al., 2021
74	$\text{O}^- + \text{HPO}_4^{2-} \rightarrow \text{Product}$	$3.50 \times 10^6 \text{ M}^{-1}\cdot\text{s}^{-1}$	Zhao et al., 2021

Table C3-4. Cl· Reactions.

75	$\text{Cl}\cdot + \text{HOCl} \rightarrow \text{ClO}\cdot + \text{H}^+ + \text{Cl}^-$	$3.00 \times 10^9 \text{ M}^{-1}\cdot\text{s}^{-1}$	Fang et al., 2014 Chuang et al., 2017 Zhao et al., 2021
76	$\text{Cl}\cdot + \text{OCl}^- \rightarrow \text{ClO}\cdot + \text{Cl}^-$	$8.2 \times 10^9 \text{ M}^{-1}\cdot\text{s}^{-1}$ $8.30 \times 10^9 \text{ M}^{-1}\cdot\text{s}^{-1}$	Fang et al., 2014 Chuang et al., 2017 Zhao et al., 2021
77	$\text{Cl}\cdot + \text{H}_2\text{O} \rightarrow \text{ClOH}^- + \text{H}^+$	$2.50 \times 10^5 \text{ s}^{-1}$	Chuang et al., 2017 Zhao et al., 2021
78	$\text{Cl}\cdot + \text{OH}^- \rightarrow \text{ClOH}^-$	$1.80 \times 10^{10} \text{ M}^{-1}\cdot\text{s}^{-1}$	Fang et al., 2014 Chuang et al., 2017 Zhao et al., 2021
79	$\text{Cl}\cdot + \text{H}_2\text{O}_2 \rightarrow \text{HO}_2\cdot + \text{Cl}^- + \text{H}^+$	$2.00 \times 10^9 \text{ M}^{-1}\cdot\text{s}^{-1}$	Chuang et al., 2017 Zhao et al., 2021
80	$\text{Cl}\cdot + \text{Cl}^- \rightarrow \text{Cl}_2^-$	$6.5 \times 10^9 \text{ M}^{-1}\cdot\text{s}^{-1}$ $8.00 \times 10^9 \text{ M}^{-1}\cdot\text{s}^{-1}$ $8.50 \times 10^9 \text{ M}^{-1}\cdot\text{s}^{-1}$	Fang et al., 2014 Chuang et al., 2017 Zhao et al., 2021
81	$\text{Cl}\cdot + \text{Cl}\cdot \rightarrow \text{Cl}_2$	$8.80 \times 10^7 \text{ M}^{-1}\cdot\text{s}^{-1}$	Chuang et al., 2017 Zhao et al., 2021
82	$\text{Cl}\cdot + \text{HCO}_3^- \rightarrow \text{CO}_3^- + \text{HCl}$	$2.2 \times 10^8 \text{ M}^{-1}\cdot\text{s}^{-1}$	Fang et al., 2014
83	$\text{Cl}\cdot + \text{CO}_3^{2-} \rightarrow \text{Cl}^- + \text{CO}_3^-$	$5.00 \times 10^8 \text{ M}^{-1}\cdot\text{s}^{-1}$	Zhao et al., 2021
84	$\text{Cl}\cdot + \text{NOM} \rightarrow \text{Product}$	$1.56 \times 10^8 \text{ M}^{-1}\cdot\text{s}^{-1}$	Fang et al., 2014 Chuang et al., 2017 Zhao et al., 2021

Table C3-5. Cl₂⁻ Reactions.

85	$\text{Cl}_2^- \rightarrow \text{Cl}\cdot + \text{Cl}^-$	$1.1 \times 10^5 \text{ s}^{-1}$ $6.00 \times 10^4 \text{ s}^{-1}$ 32 s^{-1}	Fang et al., 2014 Chuang et al., 2017 Zhao et al., 2021
86	$\text{Cl}_2^- + \cdot\text{OH} \rightarrow \text{HOCl} + \text{Cl}^-$	$1.00 \times 10^9 \text{ M}^{-1}\cdot\text{s}^{-1}$	Chuang et al., 2017
87	$\text{Cl}_2^- + \text{Cl}_2^- \rightarrow \text{Cl}_2 + 2\text{Cl}^-$	$9.00 \times 10^8 \text{ M}^{-1}\cdot\text{s}^{-1}$	Chuang et al., 2017 Zhao et al., 2021
88	$\text{Cl}_2^- + \text{Cl}\cdot \rightarrow \text{Cl}_2 + \text{Cl}^-$	$2.10 \times 10^9 \text{ M}^{-1}\cdot\text{s}^{-1}$	Chuang et al., 2017 Zhao et al., 2021
89	$\text{Cl}_2^- + \text{H}_2\text{O}_2 \rightarrow \text{HO}_2\cdot + 2\text{Cl}^- + \text{H}^+$	$1.40 \times 10^5 \text{ M}^{-1}\cdot\text{s}^{-1}$	Chuang et al., 2017 Zhao et al., 2021
90	$\text{Cl}_2^- + \text{HO}_2\cdot \rightarrow 2\text{Cl}^- + \text{H}^+ + \text{O}_2$	$3.00 \times 10^9 \text{ M}^{-1}\cdot\text{s}^{-1}$	Chuang et al., 2017 Zhao et al., 2021
91	$\text{Cl}_2^- + \text{O}_2^- \rightarrow 2\text{Cl}^- + \text{O}_2$	$2.00 \times 10^9 \text{ M}^{-1}\cdot\text{s}^{-1}$	Chuang et al., 2017 Zhao et al., 2021
92	$\text{Cl}_2^- + \text{H}_2\text{O} \rightarrow \text{Cl}^- + \text{HClOH}\cdot$	$1.30 \times 10^3 \text{ s}^{-1}$ $2.34 \times 10^{-2} \text{ s}^{-1}$	Chuang et al., 2017 Zhao et al., 2021
93	$\text{Cl}_2^- + \text{OH}^- \rightarrow \text{ClOH}^- + \text{Cl}^-$	$4.50 \times 10^7 \text{ M}^{-1}\cdot\text{s}^{-1}$	Fang et al., 2014 Chuang et al., 2017 Zhao et al., 2021
94	$\text{Cl}_2^- + \text{HCO}_3^- \rightarrow 2\text{Cl}^- + \text{CO}_3^{2-} + \text{H}^+$	$8.0 \times 10^7 \text{ M}^{-1}\cdot\text{s}^{-1}$	Fang et al., 2014
95	$\text{Cl}_2^- + \text{OCl}^- \rightarrow \text{ClO}\cdot + 2\text{Cl}^-$	$2.90 \times 10^8 \text{ M}^{-1}\cdot\text{s}^{-1}$	Zhao et al., 2021
96	$\text{Cl}_2^- + \cdot\text{OH} \rightarrow \text{HOCl} + \text{Cl}^-$	$1.0 \times 10^9 \text{ M}^{-1}\cdot\text{s}^{-1}$	Zhao et al., 2021
97	$\text{Cl}_2^- + \text{CO}_3^{2-} \rightarrow 2\text{Cl}^- + \text{CO}_3^-$	$1.60 \times 10^8 \text{ M}^{-1}\cdot\text{s}^{-1}$	Zhao et al., 2021
98	$\text{Cl}_2^- + \text{HCO}_3^- \rightarrow 2\text{Cl}^- + \text{CO}_3^- + \text{H}^+$	$8.00 \times 10^7 \text{ M}^{-1}\cdot\text{s}^{-1}$	Zhao et al., 2021

Table C3-6. ClO_x Reactions
(including ClO·, Cl₂O₂, ClO₂·, ClO₂, ClO₂⁻, ClO₃⁻).

99	ClO· + NOM → Product	5.52×10 ⁸ M ⁻¹ .s ⁻¹	Zhao et al., 2021
100	ClO· + ClO· → Cl ₂ O ₂	2.50×10 ⁹ M ⁻¹ .s ⁻¹ 5.00×10 ⁹ M ⁻¹ .s ⁻¹	Chuang et al., 2017 Zhao et al., 2021
101	ClO· + ClO ₂ ⁻ → ClO ₂ · + OCl ⁻	9.40×10 ⁸ M ⁻¹ .s ⁻¹	Chuang et al., 2017 Zhao et al., 2021
102	ClO· + CO ₃ ²⁻ → OCl ⁻ +CO ₃ ⁻	600 M ⁻¹ .s ⁻¹	Zhao et al., 2021
103	ClO· + ·OH → H ⁺ + ClO ₂ ⁻	1.00×10 ⁹ M ⁻¹ .s ⁻¹	Zhao et al., 2021
104	2ClO· + H ₂ O → HOCl + H ⁺ + ClO ₂ ⁻	2.50×10 ⁹ M ⁻¹ .s ⁻¹	Zhao et al., 2021
105	2ClO· + OH ⁻ → OCl ⁻ + H ⁺ + ClO ₂ ⁻	2.50×10 ⁹ M ⁻¹ .s ⁻¹	Zhao et al., 2021
106	Cl ₂ O ₂ + H ₂ O → ClO ₂ ⁻ + HOCl + H ⁺	1.00×10 ⁴ s ⁻¹	Chuang et al., 2017
107	O(3P) + OCl ⁻ → ClO ₂ ⁻	9.40×10 ⁹ M ⁻¹ .s ⁻¹	Zhao et al., 2021
108	·OH + ClO ₂ ⁻ → ClO ₂ · + OH ⁻	7.00×10 ⁹ M ⁻¹ .s ⁻¹	Chuang et al., 2017 Zhao et al., 2021
109	Cl· + ClO ₂ ⁻ → ClO ₂ · + Cl ⁻	7.00×10 ⁹ M ⁻¹ .s ⁻¹ 7.90×10 ⁹ M ⁻¹ .s ⁻¹	Chuang et al., 2017 Zhao et al., 2021
110	Cl ₂ ⁻ + ClO ₂ ⁻ → ClO ₂ · + 2Cl ⁻	1.30×10 ⁸ M ⁻¹ .s ⁻¹	Zhao et al., 2021
111	O ⁻ + ClO ₂ ⁻ + H ₂ O → 2OH ⁻ +ClO ₂ ·	1.95×10 ⁸ M ⁻¹ .s ⁻¹	Zhao et al., 2021
112	O ₂ ⁻ + ClO ₂ ⁻ → Product	40 M ⁻¹ .s ⁻¹	Zhao et al., 2021
113	ClO ₂ ⁻ + HOCl + H ⁺ → Cl ₂ O ₂ + H ₂ O	2.86×10 ⁶ M ⁻¹ .s ⁻¹	Zhao et al., 2021
114	Cl ₂ O ₂ + ClO ₂ ⁻ → Cl ⁻ + 2ClO ₂	8.10×10 ⁵ M ⁻¹ .s ⁻¹	Zhao et al., 2021
115	2HOCl + ClO ₂ ⁻ → ClO ₃ ⁻ + Cl ₂ + H ₂ O	2.10×10 ³ M ⁻¹ .s ⁻¹	Zhao et al., 2021
116	Cl ₂ + ClO ₂ ⁻ → Cl ₂ O ₂ + Cl ⁻	1.61×10 ⁶ M ⁻¹ .s ⁻¹	Zhao et al., 2021
117	CO ₃ ⁻ + ClO ₂ ⁻ → ClO ₂ · + CO ₃ ²⁻	3.40×10 ⁷ M ⁻¹ .s ⁻¹	Zhao et al., 2021
118	·OH + ClO ₂ ⁻ → ClO ₃ ⁻ + H ⁺	4.00×10 ⁹ M ⁻¹ .s ⁻¹	Chuang et al., 2017 Zhao et al., 2021
119	O ⁻ + ClO ₂ · → ClO ₃ ⁻	2.70×10 ⁹ M ⁻¹ .s ⁻¹	Zhao et al., 2021
120	Cl· + ClO ₂ · → Product	4.00×10 ⁹ M ⁻¹ .s ⁻¹	Chuang et al., 2017
121	ClO ₂ · + ClO· + H ₂ O → ClO ₃ ⁻ + HOCl + H ⁺	9.40×10 ⁹ M ⁻¹ .s ⁻¹	Zhao et al., 2021
122	O ₂ ⁻ + ClO ₂ · → ClO ₂ ⁻ +O ₂	3.15×10 ⁹ M ⁻¹ .s ⁻¹	Zhao et al., 2021
123	HO ₂ ⁻ + ClO ₂ · → ClO ₂ ⁻ +HO ₂ ·	9.57×10 ⁴ M ⁻¹ .s ⁻¹	Zhao et al., 2021
124	HO ₂ · + ClO ₂ ⁻ → Product	1.00×10 ⁶ M ⁻¹ .s ⁻¹	Zhao et al., 2021
125	Cl· + ClO ₂ ⁻ → Cl ₂ O ₂	7.80×10 ⁹ M ⁻¹ .s ⁻¹	Zhao et al., 2021
126	Cl ₂ ⁻ + ClO ₂ · → Product	1.00×10 ⁹ M ⁻¹ .s ⁻¹	Zhao et al., 2021
127	O ₃ ⁻ + ClO ₂ ⁻ → ClO ₃ ⁻ +O ₂	1.80×10 ⁵ M ⁻¹ .s ⁻¹	Zhao et al., 2021
128	O(3P) + ClO ₂ ⁻ → ClO ₃ ⁻	1.59×10 ¹⁰ M ⁻¹ .s ⁻¹	Zhao et al., 2021
129	·OH + ClO ₃ ⁻ → Product	1.00×10 ⁶ M ⁻¹ .s ⁻¹	Chuang et al., 2017 Zhao et al., 2021
130	Cl· + ClO ₃ ⁻ → Product	1.00×10 ⁶ M ⁻¹ .s ⁻¹	Chuang et al., 2017
131	O ₂ ⁻ + ClO ₃ ⁻ → Product	0.003 M ⁻¹ .s ⁻¹	Zhao et al., 2021

Table C3-7. ClOH⁻ Reactions.

132	$\text{ClOH}^- \rightarrow \text{Cl}^- + \cdot\text{OH}$	$6.10 \times 10^9 \text{ s}^{-1}$	Fang et al., 2014 Chuang et al., 2017 Zhao et al., 2021
133	$\text{ClOH}^- + \text{H}^+ \rightarrow \text{Cl} \cdot + \text{H}_2\text{O}$	$2.10 \times 10^{10} \text{ M}^{-1} \cdot \text{s}^{-1}$	Fang et al., 2014 Zhao et al., 2021
134	$\text{ClOH}^- + \text{Cl}^- \rightarrow \text{Cl}_2^- + \text{OH}^-$	$1.0 \times 10^5 \text{ M}^{-1} \cdot \text{s}^{-1}$ $1.00 \times 10^4 \text{ M}^{-1} \cdot \text{s}^{-1}$	Fang et al., 2014 Chuang et al., 2017 Zhao et al., 2021
135	$\text{ClOH}^- \rightarrow \text{Cl} \cdot + \text{OH}^-$	23 s^{-1} 15.1 s^{-1}	Fang et al., 2014 Chuang et al., 2017 Zhao et al., 2021
136	$\text{ClOH}^- \rightarrow \text{Cl} \cdot + \text{OH}^-$	15.1 s^{-1}	Zhao et al., 2021

Table C3-8. HO₂[·] and O₂^{·-} Reactions.

137	$\text{HO}_2 \cdot + \text{H}_2\text{O}_2 \rightarrow \text{O}_2 + \cdot\text{OH} + \text{H}_2\text{O}$	$3.00 \text{ M}^{-1} \cdot \text{s}^{-1}$	Chuang et al., 2017 Zhao et al., 2021
138	$\text{HO}_2 \cdot + \text{HO}_2 \cdot \rightarrow \text{O}_2 + \text{H}_2\text{O}_2$	$8.30 \times 10^5 \text{ M}^{-1} \cdot \text{s}^{-1}$ $8.30 \times 10^9 \text{ M}^{-1} \cdot \text{s}^{-1}$	Chuang et al., 2017 Zhao et al., 2021
139	$\text{HO}_2 \cdot + \text{O}_2^- \rightarrow \text{O}_2 + \text{HO}_2^-$	$9.70 \times 10^7 \text{ M}^{-1} \cdot \text{s}^{-1}$	Chuang et al., 2017 Zhao et al., 2021
140	$\text{HO}_2 \cdot + \text{HOCl} \rightarrow \text{Cl} \cdot + \text{H}_2\text{O} + \text{O}_2$	$7.50 \times 10^6 \text{ M}^{-1} \cdot \text{s}^{-1}$	Chuang et al., 2017
141	$\text{O}_2^- + \text{OCl}^- + \text{H}_2\text{O} \rightarrow \text{Cl} \cdot + 2\text{OH}^- + \text{O}_2$	$2.00 \times 10^8 \text{ M}^{-1} \cdot \text{s}^{-1}$	Chuang et al., 2017 Zhao et al., 2021
142	$\text{O}_2^- + \text{H}_2\text{O}_2 \rightarrow \text{O}_2 + \cdot\text{OH} + \text{OH}^-$	$1.30 \times 10^{-1} \text{ M}^{-1} \cdot \text{s}^{-1}$	Chuang et al., 2017 Zhao et al., 2021
143	$\text{O}_2^- + \text{HOCl} \rightarrow \text{Cl} \cdot + \text{OH}^- + \text{O}_2$	$7.50 \times 10^6 \text{ M}^{-1} \cdot \text{s}^{-1}$	Chuang et al., 2017
144	$\text{O}_2^- + \text{CO}_3^- \rightarrow \text{CO}_3^{2-} + \text{O}_2$	$6.00 \times 10^8 \text{ M}^{-1} \cdot \text{s}^{-1}$	Zhao et al., 2021
145	$\text{O}_2^- + \text{Cl}^- \rightarrow \text{Product}$	$140 \text{ M}^{-1} \cdot \text{s}^{-1}$	Zhao et al., 2021

Table C3-9. CO₃^{·-} Reactions

146	$\text{CO}_3^{\cdot-} + \text{H}_2\text{O}_2 \rightarrow \text{HCO}_3^- + \text{HO}_2 \cdot$	$4.30 \times 10^5 \text{ M}^{-1} \cdot \text{s}^{-1}$	Zhao et al., 2021
147	$\text{CO}_3^{\cdot-} + \text{HO}_2^- \rightarrow \text{CO}_3^{2-} + \text{HO}_2 \cdot$	$3.00 \times 10^7 \text{ M}^{-1} \cdot \text{s}^{-1}$	Zhao et al., 2021
148	$\text{CO}_3^{\cdot-} + \text{CO}_3^{\cdot-} \rightarrow \text{Product}$	$3.00 \times 10^7 \text{ M}^{-1} \cdot \text{s}^{-1}$	Zhao et al., 2021
149	$\text{CO}_3^{\cdot-} + \text{OCl}^- \rightarrow \text{ClO} \cdot + \text{CO}_3^{2-}$	$5.70 \times 10^5 \text{ M}^{-1} \cdot \text{s}^{-1}$	Zhao et al., 2021
150	$\text{CO}_3^{\cdot-} + \text{NOM} \rightarrow \text{Product}$	$6.96 \times 10^5 \text{ M}^{-1} \cdot \text{s}^{-1}$	Zhao et al., 2021

Table C3-10. Equilibrium Reactions.

151	$\text{H}_2\text{O}_2 \rightarrow \text{H}^+ + \text{HO}_2^-$	$1.26 \times 10^{-1} \text{ s}^{-1}$ $1.30 \times 10^{-1} \text{ s}^{-1}$	Chuang et al., 2017 Zhao et al., 2021
152	$\text{H}^+ + \text{HO}_2^- \rightarrow \text{H}_2\text{O}_2$	$5.00 \times 10^{10} \text{ M}^{-1} \cdot \text{s}^{-1}$	Chuang et al., 2017 Zhao et al., 2021
153	$\text{HOCl} \rightarrow \text{OCl}^- + \text{H}^+$	$1.41 \times 10^3 \text{ s}^{-1}$ $1.60 \times 10^3 \text{ s}^{-1}$	Chuang et al., 2017 Zhao et al., 2021
154	$\text{OCl}^- + \text{H}^+ \rightarrow \text{HOCl}$	$5.00 \times 10^{10} \text{ M}^{-1} \cdot \text{s}^{-1}$	Chuang et al., 2017 Zhao et al., 2021
155	$\text{H}^+ + \text{Cl}^- \rightarrow \text{HCl}$	$5.00 \times 10^{10} \text{ M}^{-1} \cdot \text{s}^{-1}$	Zhao et al., 2021
156	$\text{HCl} \rightarrow \text{H}^+ + \text{Cl}^-$	$8.60 \times 10^{16} \text{ s}^{-1}$	Zhao et al., 2021
157	$\text{H}^+ + \text{OH}^- \rightarrow \text{H}_2\text{O}$	$1.00 \times 10^{11} \text{ M}^{-1} \cdot \text{s}^{-1}$	Zhao et al., 2021
158	$\text{H}_2\text{O} \rightarrow \text{H}^+ + \text{OH}^-$	$1.00 \times 10^{-3} \text{ s}^{-1}$	Zhao et al., 2021
159	$\text{H}^+ + \text{H}_2\text{PO}_4^- \rightarrow \text{H}_3\text{PO}_4$	$5.00 \times 10^{10} \text{ M}^{-1} \cdot \text{s}^{-1}$	Zhao et al., 2021
160	$\text{H}_3\text{PO}_4 \rightarrow \text{H}^+ + \text{H}_2\text{PO}_4^-$	$3.97 \times 10^8 \text{ s}^{-1}$	Zhao et al., 2021
161	$\text{H}^+ + \text{HPO}_4^{2-} \rightarrow \text{H}_2\text{PO}_4^-$	$5.00 \times 10^{10} \text{ M}^{-1} \cdot \text{s}^{-1}$	Zhao et al., 2021
162	$\text{H}_2\text{PO}_4^- \rightarrow \text{H}^+ + \text{HPO}_4^{2-}$	$3.15 \times 10^3 \text{ s}^{-1}$	Zhao et al., 2021
163	$\text{H}^+ + \text{PO}_4^{3-} \rightarrow \text{HPO}_4^{2-}$	$5.00 \times 10^{10} \text{ M}^{-1} \cdot \text{s}^{-1}$	Zhao et al., 2021
164	$\text{HPO}_4^{2-} \rightarrow \text{H}^+ + \text{PO}_4^{3-}$	$2.50 \times 10^{-2} \text{ s}^{-1}$	Zhao et al., 2021
165	$\text{HCO}_3^- + \text{H}^+ \rightarrow \text{H}_2\text{CO}_3$	$5.00 \times 10^{10} \text{ M}^{-1} \cdot \text{s}^{-1}$	Zhao et al., 2021
166	$\text{H}_2\text{CO}_3 \rightarrow \text{HCO}_3^- + \text{H}^+$	$5.00 \times 10^5 \text{ s}^{-1}$	Zhao et al., 2021
167	$\text{CO}_3^{2-} + \text{H}^+ \rightarrow \text{HCO}_3^-$	$5.00 \times 10^{10} \text{ M}^{-1} \cdot \text{s}^{-1}$	Zhao et al., 2021
168	$\text{HCO}_3^- \rightarrow \text{CO}_3^{2-} + \text{H}^+$	2.50 s^{-1}	Zhao et al., 2021

Table C3-11. O_3 and O_3^- Reactions.

169	$\text{O}(3\text{P}) + \text{O}_2 \rightarrow \text{O}_3$	$4.00 \times 10^9 \text{ M}^{-1} \cdot \text{s}^{-1}$	Zhao et al., 2021
170	$\text{O}_3 \rightarrow \text{O}(3\text{P}) + \text{O}_2$	$4.50 \times 10^{-6} \text{ s}^{-1}$	Zhao et al., 2021
171	$\text{O}_3 + \text{ClO}_2^- \rightarrow \text{O}_3^- + \text{ClO}_2\cdot$	$4.00 \times 10^6 \text{ M}^{-1} \cdot \text{s}^{-1}$	Zhao et al., 2021
172	$\text{O}_3 + \text{ClO}_2^- \rightarrow \text{O}_2 + \text{ClO}_3\cdot$	$1.23 \times 10^3 \text{ M}^{-1} \cdot \text{s}^{-1}$	Zhao et al., 2021
173	$\text{O}_3 + \text{OCl}^- \rightarrow 2\text{O}_2 + \text{Cl}^-$	$1.10 \times 10^2 \text{ M}^{-1} \cdot \text{s}^{-1}$	Zhao et al., 2021
174	$\text{O}_3 + \text{OCl}^- \rightarrow \text{O}_2 + \text{ClO}_2^-$	$30 \text{ M}^{-1} \cdot \text{s}^{-1}$	Zhao et al., 2021
175	$\text{O}_3 + \text{Cl}^- \rightarrow \text{O}_2 + \text{OCl}^-$	$1.60 \times 10^{-3} \text{ M}^{-1} \cdot \text{s}^{-1}$	Zhao et al., 2021
176	$\text{O}_3 + \text{Cl}_2^- \rightarrow \text{Product}$	$9.00 \times 10^7 \text{ M}^{-1} \cdot \text{s}^{-1}$	Zhao et al., 2021
177	$\text{O}_3 + \cdot\text{OH} \rightarrow \text{O}_2 + \text{HO}_2\cdot$	$1.10 \times 10^8 \text{ M}^{-1} \cdot \text{s}^{-1}$	Zhao et al., 2021
178	$\text{O}_3 + \text{OH}^- \rightarrow \text{O}_2 + \text{HO}_2^-$	$14.2 \text{ M}^{-1} \cdot \text{s}^{-1}$	Zhao et al., 2021
179	$\text{O}_3 + \text{H}\cdot \rightarrow \text{O}_2 + \cdot\text{OH}$	$2.20 \times 10^{10} \text{ M}^{-1} \cdot \text{s}^{-1}$	Zhao et al., 2021
180	$\text{O}_3 + \text{HO}_2\cdot \rightarrow \text{O}_2 + \text{H}^+ + \text{O}_3^-$	$1.60 \times 10^9 \text{ M}^{-1} \cdot \text{s}^{-1}$	Zhao et al., 2021
181	$\text{O}_3 + \text{HO}_2^- \rightarrow \text{O}_3^- + \text{HO}_2\cdot$	$5.50 \times 10^6 \text{ M}^{-1} \cdot \text{s}^{-1}$	Zhao et al., 2021
182	$\text{O}_3^- + \cdot\text{OH} \rightarrow \text{O}_2^- + \text{HO}_2\cdot$	$8.50 \times 10^9 \text{ M}^{-1} \cdot \text{s}^{-1}$	Zhao et al., 2021
183	$\text{O}_3^- + \text{H}^+ \rightarrow \text{O}_2 + \cdot\text{OH}$	$5.20 \times 10^{10} \text{ M}^{-1} \cdot \text{s}^{-1}$	Zhao et al., 2021
184	$\text{O}_3^- + \text{ClO}\cdot \rightarrow \text{O}_3 + \text{OCl}^-$	$1.00 \times 10^9 \text{ M}^{-1} \cdot \text{s}^{-1}$	Zhao et al., 2021
185	$\text{O}_3^- \rightarrow \text{O}_2 + \text{O}^-$	$4.28 \times 10^3 \text{ s}^{-1}$	Zhao et al., 2021
186	$\text{O}_3^- + \text{O}_3^- \rightarrow \text{Product}$	$9.00 \times 10^8 \text{ M}^{-1} \cdot \text{s}^{-1}$	Zhao et al., 2021
187	$\text{O}_3^- + \text{O}^- \rightarrow 2\text{O}_2^-$	$7.00 \times 10^8 \text{ M}^{-1} \cdot \text{s}^{-1}$	Zhao et al., 2021
188	$\text{O}_2^- + \text{O}_3 \rightarrow \text{O}_3^- + \text{O}_2$	$1.60 \times 10^9 \text{ M}^{-1} \cdot \text{s}^{-1}$	Zhao et al., 2021

Table C3-12. Cl₂ and Cl₃⁻ Reactions.

188	$\text{Cl}_2 + \text{H}_2\text{O} \rightarrow \text{HOCl} + \text{Cl}^- + \text{H}^+$	15 s^{-1} 0.27 s^{-1}	Chuang et al., 2017 Zhao et al., 2021
189	$\text{Cl}_2 + \text{Cl}^- \rightarrow \text{Cl}_3^-$	$2.00 \times 10^4 \text{ M}^{-1} \cdot \text{s}^{-1}$	Chuang et al., 2017 Zhao et al., 2021
190	$\text{Cl}_2 + \text{H}_2\text{O}_2 \rightarrow 2\text{HCl} + \text{O}_2$	$1.30 \times 10^4 \text{ M}^{-1} \cdot \text{s}^{-1}$	Chuang et al., 2017
191	$\text{Cl}_2 + \text{O}_2^- \rightarrow \text{Cl}_2^- + \text{O}_2$	$1.00 \times 10^9 \text{ M}^{-1} \cdot \text{s}^{-1}$	Chuang et al., 2017 Zhao et al., 2021
192	$\text{Cl}_2 + \text{HO}_2 \cdot \rightarrow \text{Cl}_2^- + \text{H}^+ + \text{O}_2$	$1.00 \times 10^9 \text{ M}^{-1} \cdot \text{s}^{-1}$	Chuang et al., 2017 Zhao et al., 2021
193	$\text{Cl}_3^- \rightarrow \text{Cl}_2 + \text{Cl}^-$	$1.10 \times 10^5 \text{ s}^{-1}$	Chuang et al., 2017 Zhao et al., 2021
194	$\text{Cl}_3^- + \text{HO}_2 \cdot \rightarrow \text{Cl}_2^- + \text{H}^+ + \text{Cl}^- + \text{O}_2$	$1.00 \times 10^9 \text{ M}^{-1} \cdot \text{s}^{-1}$	Chuang et al., 2017 Zhao et al., 2021
195	$\text{Cl}_3^- + \text{O}_2^- \rightarrow \text{Cl}_2^- + \text{Cl}^- + \text{O}_2$	$3.80 \times 10^9 \text{ M}^{-1} \cdot \text{s}^{-1}$	Chuang et al., 2017 Zhao et al., 2021
196	$\text{Cl}_2 + \text{Cl} \cdot \rightarrow \text{Cl}_3 \cdot$	$5.30 \times 10^8 \text{ M}^{-1} \cdot \text{s}^{-1}$	Zhao et al., 2021
197	$\text{Cl}_2 + \text{OH}^- \rightarrow \text{HOCl} + \text{Cl}^-$	$1.00 \times 10^9 \text{ M}^{-1} \cdot \text{s}^{-1}$	Zhao et al., 2021

Table C3-13. Miscellaneous Reactions.

198	$\text{HClOH} \cdot \rightarrow \text{ClOH}^- + \text{H}^+$	$1.00 \times 10^8 \text{ s}^{-1}$	Chuang et al., 2017 Zhao et al., 2021
199	$\text{HClOH} \cdot \rightarrow \text{Cl} \cdot + \text{H}_2\text{O}$	$1.00 \times 10^2 \text{ s}^{-1}$	Zhao et al., 2021
200	$\text{HClOH} \cdot + \text{Cl}^- \rightarrow \text{Cl}_2^- + \text{H}_2\text{O}$	$5.00 \times 10^9 \text{ M}^{-1} \cdot \text{s}^{-1}$	Zhao et al., 2021
201	$\text{HOCl} + \text{H}_2\text{O}_2 \rightarrow \text{H}^+ + \text{Cl}^- + \text{H}_2\text{O} + \text{O}_2$	$1.10 \times 10^4 \text{ M}^{-1} \cdot \text{s}^{-1}$	Chuang et al., 2017 Zhao et al., 2021
202	$\text{OCl}^- + \text{H}_2\text{O}_2 \rightarrow \text{Cl}^- + \text{H}_2\text{O} + \text{O}_2$	$1.70 \times 10^5 \text{ M}^{-1} \cdot \text{s}^{-1}$	Chuang et al., 2017 Zhao et al., 2021
203	$\text{H}_2\text{O}_2 + \text{HPO}_4^{2-} \rightarrow \text{H}_2\text{PO}_4^- + \text{HO}_2 \cdot$	$2.70 \times 10^7 \text{ M}^{-1} \cdot \text{s}^{-1}$	Chuang et al., 2017 Zhao et al., 2021
204	$\text{Cl}^- + \text{HOCl} + \text{H}^+ \rightarrow \text{Cl}_2 + \text{H}_2\text{O}$	$0.182 \text{ M}^{-1} \cdot \text{s}^{-1}$	Zhao et al., 2021
205	$\text{Cl}_2 + \text{H}_2\text{O}_2 \rightarrow \text{O}_2 + 2\text{HCl}$	$1.30 \times 10^4 \text{ M}^{-1} \cdot \text{s}^{-1}$	Zhao et al., 2021

Table C3-14. Breakpoint Chlorination.
(excerpted from Huang (2008)).

#	Reaction	Rate expression (if not the product of k[R1][R2])	k value
206	$\text{HOCl} + \text{NH}_3 \rightarrow \text{NH}_2\text{Cl} + \text{H}_2\text{O}$		$2.04 \times 10^9 \times e^{(-1887/T)} \text{ M}^{-1} \cdot \text{s}^{-1}$
207	$\text{NH}_2\text{Cl} + \text{H}_2\text{O} \rightarrow \text{HOCl} + \text{NH}_3$		$1.38 \times 10^8 e^{(-8800/T)} \text{ s}^{-1}$
208	$\text{HOCl} + \text{NH}_2\text{Cl} \rightarrow \text{NHCl}_2 + \text{H}_2\text{O}$		$3.0 \times 10^5 e^{(-2010/T)} \text{ M}^{-1} \cdot \text{s}^{-1}$
209	$\text{NHCl}_2 + \text{H}_2\text{O} \rightarrow \text{HOCl} + \text{NH}_2\text{Cl}$		$6.5 \times 10^{-7} \text{ s}^{-1}$
210	$\text{NH}_2\text{Cl} + \text{NH}_2\text{Cl} \rightarrow \text{NHCl}_2 + \text{NH}_3$		$(3.78 \times 10^{10} e^{(-2169/T)} / 3600) \times [\text{H}^+] + 1.5 \times 10^{35} (e^{(-22144/T)} / 3600) \times [\text{HCO}_3^-] + (2.95 \times 10^{10} e^{(-4026/T)} / 3600) \times \text{H}_2\text{CO}_3$
211	$\text{NHCl}_2 + \text{NH}_3 \rightarrow \text{NH}_2\text{Cl} + \text{NH}_2\text{Cl}$	$k[\text{NHCl}_2][\text{NH}_3][\text{H}^+]$	$2.67 \times 10^4 \text{ M}^{-1} \cdot \text{s}^{-1}$
212	$\text{NHCl}_2 + \text{H}_2\text{O} \rightarrow \text{NOH} + 2\text{H}^+ + 2\text{Cl}^-$	$k[\text{NHCl}_2][\text{OH}^-]$	$1.67 \times 10^2 \text{ s}^{-1}$
213	$\text{NOH} + \text{NHCl}_2 \rightarrow \text{HOCl} + \text{N}_2 + 2\text{H}^+ + 2\text{Cl}^-$		$2.77 \times 10^4 \text{ M}^{-1} \cdot \text{s}^{-1}$
214	$\text{NOH} + \text{NH}_2\text{Cl} \rightarrow \text{N}_2 + \text{HCl} + \text{H}_2\text{O}$		$8.3 \times 10^3 \text{ M}^{-1} \cdot \text{s}^{-1}$
215	$\text{NH}_2\text{Cl} + \text{NHCl}_2 \rightarrow \text{N}_2 + 3\text{H}^+ + 3\text{Cl}^-$		0
216	$\text{HOCl} + \text{NHCl}_2 \rightarrow \text{NCl}_3 + \text{H}_2\text{O}$		$3.28 \times 10^9 \times [\text{OH}^-] + 9.00 \times 10^4 \times [\text{OCl}^-] + 6.00 \times 10^6 \times [\text{CO}_3^{2-}] \text{ M}^{-1} \cdot \text{s}^{-1}$
217	$\text{NHCl}_2 + \text{NCl}_3 + 2\text{H}_2\text{O} \rightarrow 2\text{HOCl} + \text{N}_2 + 3\text{H}^+ + 3\text{Cl}^-$	$k[\text{NHCl}_2][\text{NCl}_3][\text{OH}^-]$	$5.56 \times 10^{10} \text{ M}^{-1} \cdot \text{s}^{-1}$
218	$\text{NH}_2\text{Cl} + \text{NCl}_3 + \text{H}_2\text{O} \rightarrow \text{HOCl} + \text{N}_2 + 3\text{H}^+ + 3\text{Cl}^-$	$k[\text{NHCl}_2][\text{NCl}_3][\text{OH}^-]$	$1.39 \times 10^9 \text{ M}^{-1} \cdot \text{s}^{-1}$
219	$\text{NHCl}_2 + 2\text{HOCl} + \text{H}_2\text{O} \rightarrow \text{NO}_3^- + 5\text{H}^+ + 4\text{Cl}^-$	$k[\text{NHCl}_2][\text{OCl}^-]$	$2.31 \times 10^2 \text{ M}^{-1} \cdot \text{s}^{-1}$
220	$\text{NCl}_3 + \text{H}_2\text{O} \rightarrow \text{NHCl}_2 + \text{HOCl}$		$1.60 \times 10^{-6} + 8 \times [\text{OH}^-] + 890 \times [\text{OH}^-]^2 + 65 \times [\text{HCO}_3^-] \times [\text{OH}^-] \text{ M}^{-1} \cdot \text{s}^{-1}$

T is the water temperature in Kelvin.

CHAPTER C3

References

- Alfassi, Z. B., R. E. Huie, S. Mosseri, and P. Neta. 1988. "Kinetics of One-Electron Oxidation by the ClO Radical." *International Journal Of Radiation Applications And Instrumentation. Part C. Radiation Physics And Chemistry*, 32 (1): 85-88.
- Bolton, J. R., and K. G. Linden. 2003. "Standardization of Methods for Fluence (UV Dose) Determination in Bench-Scale UV Experiments." *Journal of Environmental Engineering*, 129 (3): 209-215.
- Bolton, J. R., I. Mayor-Smith, and K. G. Linden. 2015. "Rethinking the Concepts of Fluence (UV Dose) and Fluence Rate: The Importance of Photon - Based Units—A Systemic Review." *Photochemistry and Photobiology*, 91 (6): 1252-1262.
- Bu, L., S. Zhou, S. Zhu, Y. Wu, X. Duan, Z. Shi, and D. D. Dionysiou. 2018. "Insight into Carbamazepine Degradation by UV/Monochloramine: Reaction Mechanism, Oxidation Products, and DBPs Formation." *Water Research*, 146: 288-297.
- Buxton, G. V., C. L. Greenstock, W. P. Helman, and A. B. Ross. 1988. "Critical Review of Rate Constants for Reactions of Hydrated Electrons, Hydrogen Atoms and Hydroxyl Radicals ($\cdot\text{OH}/\cdot\text{O}^-$) in Aqueous Solution." *Journal of Physical and Chemical Reference Data*, 17 (2): 513-886.
- Buxton, G. V., and M. S. Subhani. 1972. "Radiation Chemistry and Photochemistry of Oxychlorine Ions. Part 2.—Photodecomposition of Aqueous Solutions of Hypochlorite Ions." *Journal of the Chemical Society, Faraday Transactions 1: Physical Chemistry in Condensed Phases*, 68: 958-969.
- Cheng, S., X. Zhang, X. Yang, C. Shang, W. Song, J. Fang, and Y. Pan. 2018. "The Multiple Role of Bromide Ion in PPCPs Degradation under UV/Chlorine Treatment." *Environmental Science & Technology*, 52 (4): 1806-1816.
- Chuang, Y. H., S. Chen, C. J. Chinn, and W. A. Mitch. 2017. "Comparing the UV/Monochloramine and UV/Free Chlorine Advanced Oxidation Processes (AOPs) to the UV/Hydrogen Peroxide AOP Under Scenarios Relevant to Potable Reuse." *Environmental Science & Technology*, 51 (23): 13859-13868.
- Crittenden, J. C., S. Hu, D. W. Hand, and S.A. Green. 1999. "A Kinetic Model for $\text{H}_2\text{O}_2/\text{UV}$ Process in a Completely Mixed Batch Reactor." *Water Research*, 33 (10): 2315-2328.
- Fang, J., Y. Fu, and C. Shang. 2014. "The Roles of Reactive Species in Micropollutant Degradation in the UV/Free Chlorine System." *Environmental Science & Technology*, 48 (3): 1859-1868.
- Goldstein, S., and J. Rabani. 2007. "Mechanism of Nitrite Formation by Nitrate Photolysis in Aqueous Solutions: The Role of Peroxynitrite, Nitrogen Dioxide, and Hydroxyl Radical." *Journal of the American Chemical Society*, 129 (34): 10597-10601.

- Grebel, J. E., J. J. Pignatello, and W. A. Mitch. 2010. "Effect of Halide Ions and Carbonates on Organic Contaminant Degradation by Hydroxyl Radical-Based Advanced Oxidation Processes in Saline Waters." *Environmental Science & Technology*, 44 (17): 6822-6828.
- Guo, K., Z. Wu, C. Shang, B. Yao, S. Hou, X. Yang, W. Song, and J. Fang. 2017. "Radical Chemistry and Structural Relationships of PPCP Degradation by UV/Chlorine Treatment in Simulated Drinking Water." *Environmental Science & Technology*, 51 (18) : 10431-10439.
- Guo, K., Z. Wu, S. Yan, B. Yao, W. Song, Z. Hua, X. Zhang, X. Kong, X. Li, and J. Fang. 2018. "Comparison of the UV/Chlorine and UV/H₂O₂ Processes in the Degradation of PPCPs in Simulated Drinking Water and Wastewater: Kinetics, Radical Mechanism and Energy Requirements." *Water Research*, 147: 184-194.
- Huang, X. C. 2008. "Reactions between Aqueous Chlorine and Ammonia: A Predictive Model." Northeastern University.
- Keen, O. S., G. McKay, S. P. Mezyk, K. G. Linden, and F. L. Rosario-Ortiz. 2014. "Identifying the Factors that Influence the Reactivity of Effluent Organic Matter with Hydroxyl Radicals." *Water Research*, 50: 408-419.
- Jafvert, C. T. 1985. "A Unified Chlorine-Ammonia Speciation and Fate Model." PhD dissertation, University of Iowa ProQuest Dissertations Publishing, 8527977.
- Kläning, U. K., and T. Wolff. 1985. "Laser Flash Photolysis of HClO, ClO⁻, HBrO, and BrO⁻ in Aqueous Solution. Reactions Of Cl⁻ and Br⁻ Atoms." *Berichte der Bunsengesellschaft für physikalische Chemie*, 89 (3): 243-245.
- Kwon, M., A. Royce, Y. Gong, K. P. Ishida, and M. I. Stefan. 2020. "UV/Chlorine vs. UV/H₂O₂ for Water Reuse at Orange County Water District, CA: A Pilot Study." *Environmental Science: Water Research & Technology*, 6 (9): 2416-2431.
- Li, J., and E. R. Blatchley. 2009. "UV Photodegradation of Inorganic Chloramines." *Environmental Science & Technology*, 43 (1): 60-65.
- Mack, J., and J. R. Bolton. 1999. "Photochemistry of Nitrite and Nitrate in Aqueous Solution: A Review." *Journal of Photochemistry and Photobiology A: Chemistry*, 128 (1-3): 1-13.
- Miklos, D. B., W. L. Wang, K. G. Linden, J. E. Drewes, and U. Hübner. 2019. "Comparison of UV-AOPs (UV/H₂O₂, UV/PDS And UV/Chlorine) for Torc Removal from Municipal Wastewater Effluent and Optical Surrogate Model Evaluation." *Chemical Engineering Journal*, 362: 537-547.
- Neta, P., R. E. Huie, and A. B. Ross. 1988. "Rate Constants for Reactions of Inorganic Radicals in Aqueous Solution." *Journal of Physical and Chemical Reference Data*, 17 (3): 1027-1284.
- NIST. 2022. NDRL/NIST Solution Kinetics Database on the Web. <https://kinetics.nist.gov/solution/>.
- Shen, L. 2014. *Modeling of Chlorination Breakpoint*. University of California, Los Angeles.

- Stanbury, D. M. 2020. "Mechanisms of Advanced Oxidation Processes, the Principle of Detailed Balancing, and Specifics of the UV/Chloramine Process." *Environmental Science & Technology*, 54 (7): 4658-4663.
- Stanbury, D. M., and J. Harshman. 2019. "Large-Scale Models of Radiation Chemistry and the Principle of Detailed Balancing." *The Journal of Physical Chemistry A*, 123 (47): 10240-10245.
- Stefan, M. I. (Ed.). 2018. *Advanced Oxidation Processes for Water Treatment: Fundamentals and Applications*. IWA publishing.
- Stefan, M. I., A. R. Hoy, and J. R. Bolton. 1996. "Kinetics and Mechanism of the Degradation and Mineralization of Acetone in Dilute Aqueous Solution Sensitized by the UV Photolysis of Hydrogen Peroxide." *Environmental Science & Technology*, 30 (7): 2382-2390.
- Sun, P., T. Meng, Z. Wang, R. Zhang, H. Yao, Y. Yang, and L. Zhao. 2019. "Degradation of organic micropollutants in UV/NH₂Cl advanced oxidation process." *Environmental Science & Technology*, 53 (15): 9024-9033.
- Jafvert, C. T., and R. L. Valentine. 1992. "Reaction Scheme for the Chlorination of Ammoniacal Water." *Environmental Science & Technology*, 26 (3): 577-586.
- Watts, M. J., and K. G. Linden. 2007. "Chlorine Photolysis and Subsequent OH Radical Production during UV Treatment of Chlorinated Water." *Water Research*, 41 (13): 2871-2878.
- Wei, I. W., and J. C. Morris, J. C. 1974. "Dynamics of Breakpoint Chlorination. Chemistry of Water Supply, Treatment and Distribution." *Ann Arbor Science Publ.*, Ann Arbor, Michigan.
- Wu, Z., C. Chen, B. Z. Zhu, C. H. Huang, T. An, F. Meng, and J. Fang. 2019. "Reactive Nitrogen Species are Also Involved in the Transformation of Micropollutants by the UV/Monochloramine Process." *Environmental Science & Technology*, 53 (19): 11142-11152.
- Wu, Z., K. Guo, J. Fang, X. Yang, H. Xiao, S. Hou, X. Kong, C. Shang, X. Yang, F. Meng, and L. Chen, L. 2017. "Factors Affecting the Roles of Reactive Species in the Degradation of Micropollutants by the UV/Chlorine Process." *Water Research*, 126: 351-360.
- Zhang, W., S. Zhou, J. Sun, X. Meng, J. Luo, D. Zhou, and J. Crittenden. 2018. "Impact of Chloride Ions on UV/H₂O₂ and UV/Persulfate Advanced Oxidation Processes." *Environmental Science & Technology*, 52 (13): 7380-7389.
- Zhang, X., K. Guo, Y. Wang, Q. Qin, Z. Yuan, J. He, C. Chen, Z. Wu, and J. Fang. 2020. "Roles of Bromine Radicals, HOBr and Br₂ in the Transformation of Flumequine by the UV/Chlorine Process in the Presence of Bromide." *Chemical Engineering Journal*, 400, 125222.
- Zhang, Z., Y. H. Chuang, A. Szczuka, K. P. Ishida, S. Roback, M. H. Plumlee, and W. A. Mitch. 2019. "Pilot-Scale Evaluation Of Oxidant Speciation, 1, 4-Dioxane Degradation and Disinfection Byproduct Formation during UV/Hydrogen Peroxide, UV/Free Chlorine and UV/Chloramines Advanced Oxidation Process Treatment for Potable Reuse." *Water Research*, 164: 114939.

Zhao, J., C. Shang, X. Zhang, X. Yang, and R. Yin. 2021. "The Multiple Roles of Chlorite on the Concentrations of Radicals and Ozone and Formation of Chlorate during UV Photolysis of Free Chlorine." *Water Research*, 190: 116680.

Zhou, S., W. Zhang, J. Sun, S. Zhu, K. Li, X. Meng, J. Luo, Z. Shi, D. Zhou, and J. C. Crittenden. 2019. "Oxidation Mechanisms of the UV/Free Chlorine Process: Kinetic Modeling and Quantitative Structure Activity Relationships." *Environmental Science & Technology*, 53 (8): 4335-4345.

Appendix D: Variation and Removal of OH Radical Scavenging Capacity

Prepared by:

Tianyi Chen and Ron Hofmann

University of Toronto, Department of Civil & Mineral Engineering

Contents

Chapter D1 : Variation and Removal of OH Radical Scavenging Capacity	221
D1.1 Scavenging Capacity of Water Samples	222
D1.2 Method Precision	222
D1.3 Impact of Treatment on Scavenging Capacity	223
D1.4 Contribution of Total (In)organic Carbon to Scavenging Capacity	224
D1.5 TOC Reactivity Towards Hydroxyl Radical (kTOC, OH)	225
D1.6 Conclusions.....	226
D1.7 References.....	227

Tables

D1-1	The Relative Standard Deviation of Scavenging Capacity of the Water Samples	223
------	--	-----

Figures

D1-1	The Measured Scavenging Capacity of Raw and Treated Water Samples from Plant A-F over 5 Months	223
D1-2	Box Plots of the Measured Scavenging Capacity of Raw and Treated Water Samples from Water Plants with Conventional Treatment (Plant A and B) and Membrane Filtration (Plant C and E).....	224
D1-3	The Contribution of Total Organic Carbon (TOC) and Total Inorganic Carbon (TIC) to Total Scavenging Capacity of the Raw and Treatment Water Samples from Plant A-F over 5 Months.	225
D1-4	The Calculated Reactivity of Total Organic Carbon ($K_{toc,OH}$) towards Hydroxyl Radical in Raw and Treated Water Samples from Plant A-F over 5 Months.....	226

CHAPTER D1

Variation and Removal of OH Radical Scavenging Capacity

The hydroxyl radical ($\cdot\text{OH}$) is generated in advanced oxidation processes (AOPs) such as ozonation, UV/ H_2O_2 , and UV/chlorine. This radical is highly reactive and responsible for a wide range of pollutant destruction in an AOP, but it is also subject to competition (scavenging) by non-targeted background material (e.g., natural organic matter, bicarbonate, chloramines). The degree of hydroxyl radical scavenging by a water matrix is related to two factors: the molar concentration of a non-target compound, and its second-order reaction rate constant with hydroxyl radical. The mathematical product of these two factors is called scavenging capacity, also known as scavenging potential, scavenging demand, scavenging factor, or scavenging term (note: currently there is no widely recognized nomenclature to this concept. ‘Scavenging capacity’ will be used in this section arbitrarily). The sum of scavenging capacity of each compound that is reactive to $\cdot\text{OH}$ in a water matrix is the total scavenging capacity of the water. Water scavenging capacity is a useful parameter for the design and operation of an AOP. It helps to determine the decay rate of a target pollutant by affecting the steady-state hydroxyl radical concentration. Ideally, the advanced oxidation “dose” (which is a combination of factors such as oxidant dose, UV light intensity, reactor retention time) would vary with the scavenging capacity to prevent either excessive energy and oxidant input or failure to achieve the treatment goals.

As the concentrations of non-target compounds in water may vary over time, the scavenging capacity of water may also vary. This expected variation should be accounted for in the design and operation of an AOP. In practice, the design and operation of an AOP often relies on the scavenging capacity measurements from only one or a few grab samples, along with conservative safety factors. It is therefore possible that an AOP might be operated at a higher dose (and therefore cost) than actually needed. Furthermore, the process may be unable to adjust the AOP dose to account for fluctuations with time in scavenging capacity.

Different methods have been developed to measure scavenging capacity but they generally require delicate instruments and laborious work (Kwon et al., 2014; Lee and von Gunten, 2010; Rosenfeldt and Linden, 2007; Yang et al., 2016). As a result, the scavenging capacity of water is seldom measured and reported (Hwang et al., 2020; Kwon et al., 2019). Recently, an external calibration method was developed (Wang et al., 2020). It uses methylene blue as a probe to detect hydroxyl radical, UV/ H_2O_2 as a hydroxyl radical source, and isopropyl alcohol as a model hydroxyl radical scavenger. This method measures the rate of methylene blue color decay to reflect the abundance of hydroxyl radical in the test solution, which is controlled by the water scavenging capacity. By preparing a series of standard solutions with known scavenging capacity, which is made from a series of concentrations of isopropyl alcohol, a correlation between the rate of color decay with scavenging capacity is established. Based on this correlation, as long as the rate of color decay is measured under identical conditions (e.g., UV

intensity, reactor setup, H₂O₂ dose) as that for the standard solutions, the scavenging capacity of a sample is determined. This method is relatively fast and simple to conduct. The project team has collaborated with an instrument manufacturer, RealTech, to develop a prototype device based on this method. The reader is also advised that as of the time of writing this document, the International Ultraviolet Association is developing a recommended standard protocol for scavenging capacity measurement.

In this study, the scavenging capacity was monitored over six months at six drinking water treatment plants in Ontario. These plants were selected due to their proximity to the University of Toronto lab. The scavenging capacity for such water is expected to be much higher than would exist in RO permeate from a water reuse plant due to the higher organic matter concentrations, although it may be in the same order of magnitude as might be expected if using advanced oxidation to treat wastewater from an ozone-CBAT process for reuse. The work reported here is preliminary and intended to validate the overall method. Future work will then target RO permeate and other waters more common for reuse.

D1.1 Scavenging Capacity of Water Samples

Water samples at the intake (e.g., raw water) and after major treatment processes were taken biweekly from six water plants running/considering AOP in Ontario for six months. The plants use surface water and ground water as water sources, and the treatment processes include conventional treatment (coagulation, flocculation, media filtration), membrane filtration, granular activated carbon (GAC) filtration, and UV. The scavenging capacity of the collected water was measured by a prototype device provided by RealTech based on the external calibration method, and other common water quality parameters were also measured, including TOC, total inorganic carbon, pH, UV₂₅₄, and nitrite.

The collected water samples were stored at 4 °C and measured within 7 days after they were received, during which time the scavenging capacity was proven to be stable, based on preliminary tests. The samples were brought to room temperature (20 °C) before analysis. Note that scavenging capacity is likely to be a function of temperature, but for the purposes of this study all samples were at 20 °C. The prototype device was calibrated before measurements every time. The R² of the calibration curve was greater than 0.99.

D1.2 Method Precision

The chemistry of the method is as described in Wang et al. (2020), with the UV source and visible wavelength detection performed using the proprietary device from RealTech. The scavenging capacity of the samples were analyzed in triplicate. For the samples analyzed to date, more than two-thirds of the samples have had a relative standard deviation (RSD) of less than 15%, and 98% of the samples have had an RSD of less than 20%. Check standards of known scavenging capacity were used in the middle of the sample analyses, and the recovery rate was always in the 90-110% range. These results show good precision of the method.

D1.3 Impact of Treatment on Scavenging Capacity

For the scavenging capacity results obtained to date, the overall range of the scavenging capacity is $2.1\text{-}7.0 \times 10^4 \text{ s}^{-1}$ and $1.6\text{-}6.2 \times 10^4 \text{ s}^{-1}$ for raw and treated water, respectively, and the overall variation range over the six months of the monitoring for each treated water was 10-20% (as RSD) (Figure D-1; Table D-1). There is no clear trend showing that variation is related with the treatment process. The general removal rate of scavenging capacity from raw to treated water samples is 27-31%.

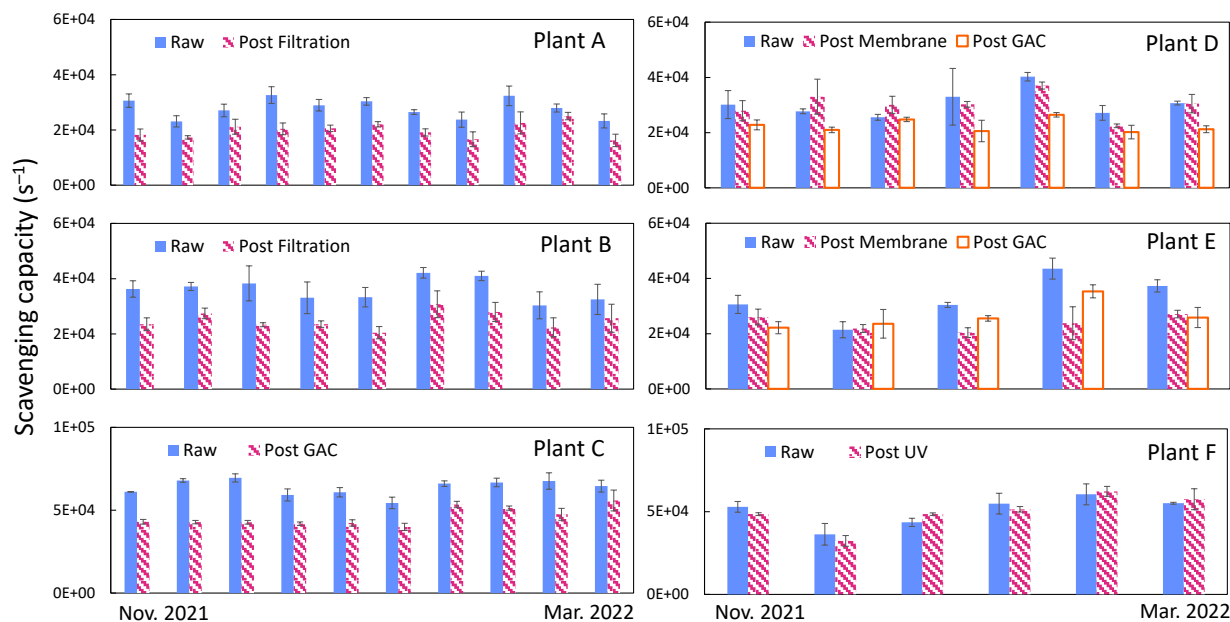


Figure D1-1. The Measured Scavenging Capacity of Raw and Treated Water Samples from Plant A-F over 5 months.

Error bars show the standard deviation of triplicate samples.

Table D1-1. The Relative Standard Deviation of Scavenging Capacity of the Water Samples.

	Raw water	Treated water	Treatment process
Plant A	12%	14%	Conventional
Plant B	11%	13%	Conventional
Plant C	7%	12%	Ultrafiltration + GAC
Plant D	16%	15%;11%	Ultrafiltration; Conventional + GAC
Plant E	25%	12%;19%	Ozone, BAC ¹ , UV, ultrafiltration; Conventional
Plant F	18%	20%	UV

¹ biological activated carbon

The scavenging capacity removal by different treatment processes is compared in Figure D-2. The results show that the conventional treatment process can have a similar removal rate of scavenging capacity as that of membrane treatment (28-31% vs. 27-28%). The variation in the post membrane samples is smaller than that in the raw water samples at Plant E (the relative standard deviation decreased from 25% to 12%), which suggests that the membrane filtration

process may have reduced the variation from raw water and generated a more stable water as a function of time in terms of scavenging capacity. In contrast, the variation in the post GAC samples at Plant C was similar to that of its raw water.

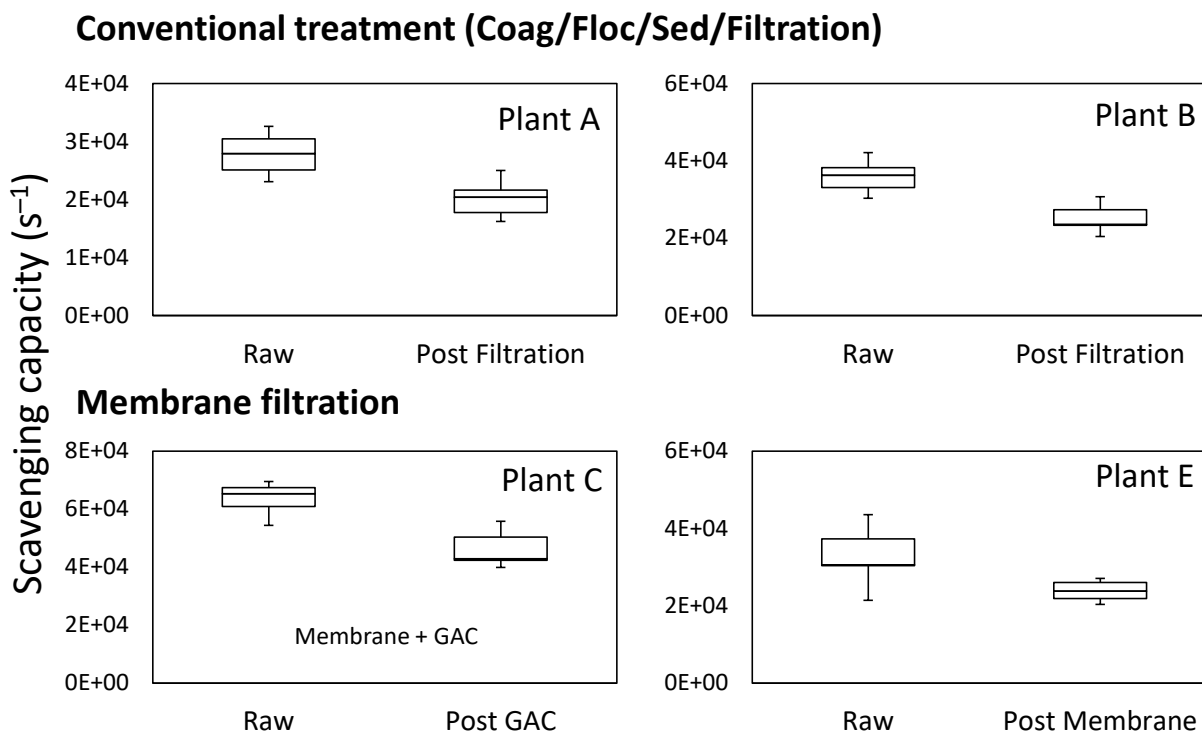


Figure D1-2. Box Plots of the Measured Scavenging Capacity of Raw and Treated Water Samples from Water Plants with Conventional Treatment (Plant A and B) and Membrane Filtration (Plant C and E).

The horizontal lines from top to bottom of each box plot represent maximum, upper quartile, median, lower quartile, and minimum values of the dataset respectively. No outliers were found.

D1.4 Contribution of Total (In)organic Carbon to Scavenging Capacity

The contribution by different non-target compounds in the water samples to the measured scavenging capacity was analyzed. Nitrite concentration was negligible (< 0.01 mg/L as N) in all the water samples. No chlorine or H_2O_2 was detected. Therefore, with other possible contributors excluded, natural organic matter (NOM) and inorganic carbon were the major contributors. NOM and inorganic carbon were measured as TOC and total inorganic carbon (TIC) in the water samples. As the pH of water samples ranged in 7.5-8.8 and the pK_a values for carbonic acid are 6.4 and 10.3 (Sawyer, 2003), the major form of inorganic carbon is bicarbonate. The scavenging capacity by bicarbonate was calculated by the measured TIC concentration and its second-order rate constant with hydroxyl radical ($8.5 \times 10^6 \text{ M}^{-1}\text{s}^{-1}$, Wagner et al., 1986). Then, the contribution by bicarbonate was subtracted from the total scavenging capacity, and the rest was regarded as contribution by TOC. Note that this is unlikely to be strictly correct: other species will contribute slightly to such scavenging capacity (various ions, etc.), but in practice, it is assumed that the majority of the (non-carbonate) scavenging in these water matrices will be due to the TOC.

The contribution of presumed TOC and TIC to the total scavenging capacity of water samples is shown (Figure D-3). The scavenging capacity from bicarbonate was very consistent for each plant, and the treatment process did not significantly alter it. In contrast, the scavenging capacity from TOC was more variable than that from bicarbonate, and the treatment process reduced the scavenging capacity from TOC. Plant F uses ground water as its water source, so the major contributor to the total scavenging capacity was the inorganic carbon, and the TOC contribution was almost negligible. These results showed that the removal of scavenging capacity in water plants mainly relied on the removal of TOC, and the variation in TOC concentrations contributed to the variation in the scavenging capacity. For the water samples collected in this study, only TOC and TIC were found to be the major contributors to the scavenging capacity. However, for other water matrices that might be more complex, such as wastewater effluent, other compounds such as nitrite might also contribute to total scavenging capacity.

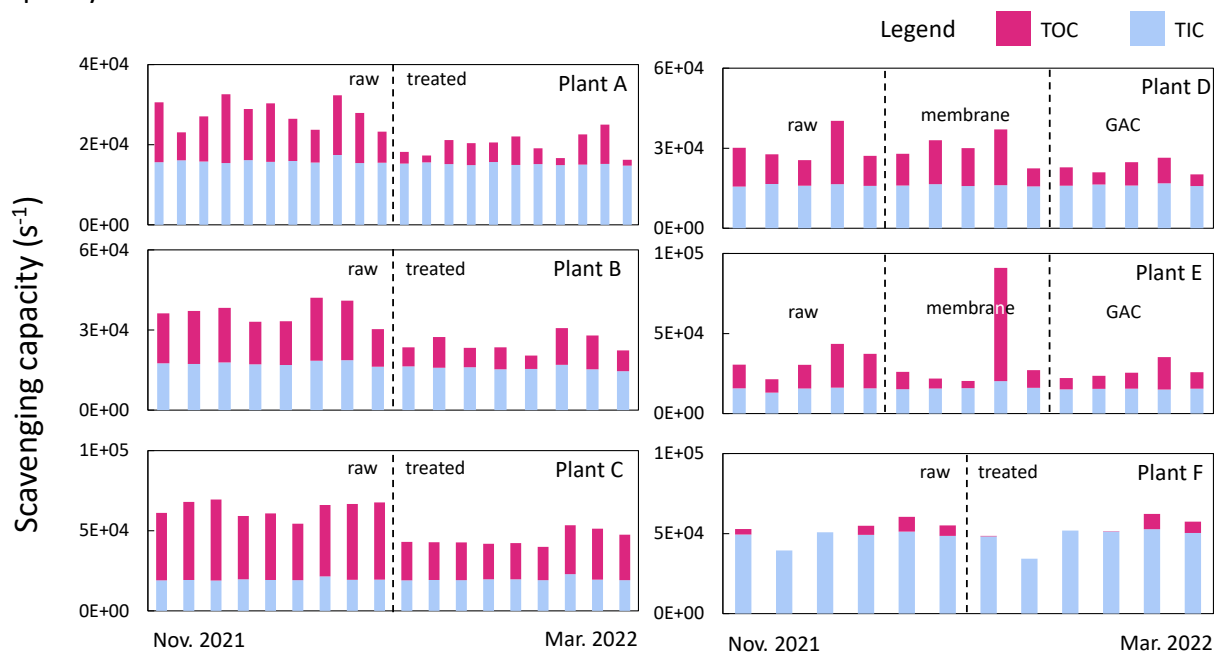


Figure D1-3. The Contribution of Total Organic Carbon (TOC) and Total Inorganic Carbon (TIC) to Total Scavenging Capacity of the Raw and Treatment Water Samples from Plant A-F over 5 months.

D1.5 TOC Reactivity Towards Hydroxyl Radical ($k_{\text{TOC,OH}}$)

The scavenging capacity was removed by an average of 30% in the treatment processes (mainly by TOC removal), but the TOC removal averaged only 10%. This implies that the nature of the TOC was altered across the treatment to render it less reactive to the hydroxyl radical. The scavenging capacity contributed by TOC (found in Figure D-3) was normalized for TOC molar carbon concentration. A normalized factor, $k_{\text{TOC,OH}}$ ($\text{M}^{-1}\text{s}^{-1}$), was calculated to represent the reactivity of TOC towards hydroxyl radical per unit of TOC.

The $k_{\text{TOC,OH}}$ values for the collected water samples are shown (Figure D-4). In general, the specific TOC reactivity towards hydroxyl radical decreased after treatment by 3-80%. It is noteworthy that some $k_{\text{TOC,OH}}$ increased after filtration at Plant D and after GAC filtration at

Plant E. This may be attributed to the possible biological activity in the (GAC) filter. The $k_{\text{TOC,OH}}$ for Plant F (UV-treated groundwater) is not reliable as both the scavenging capacity from TOC and water TOC are very low, so the error in $k_{\text{TOC,OH}}$ may be large. Overall, the results suggest that the water treatment process may change the reactivity of NOM towards hydroxyl radical. Further analysis of NOM (e.g., fluorescence analysis) may help to investigate the change in NOM characteristics that is correlated with $k_{\text{TOC,OH}}$ change. The fluorescence excitation-emission matrices of the water samples were measured, but further data analysis (e.g., by PARAllel FACTor) remains to be conducted.

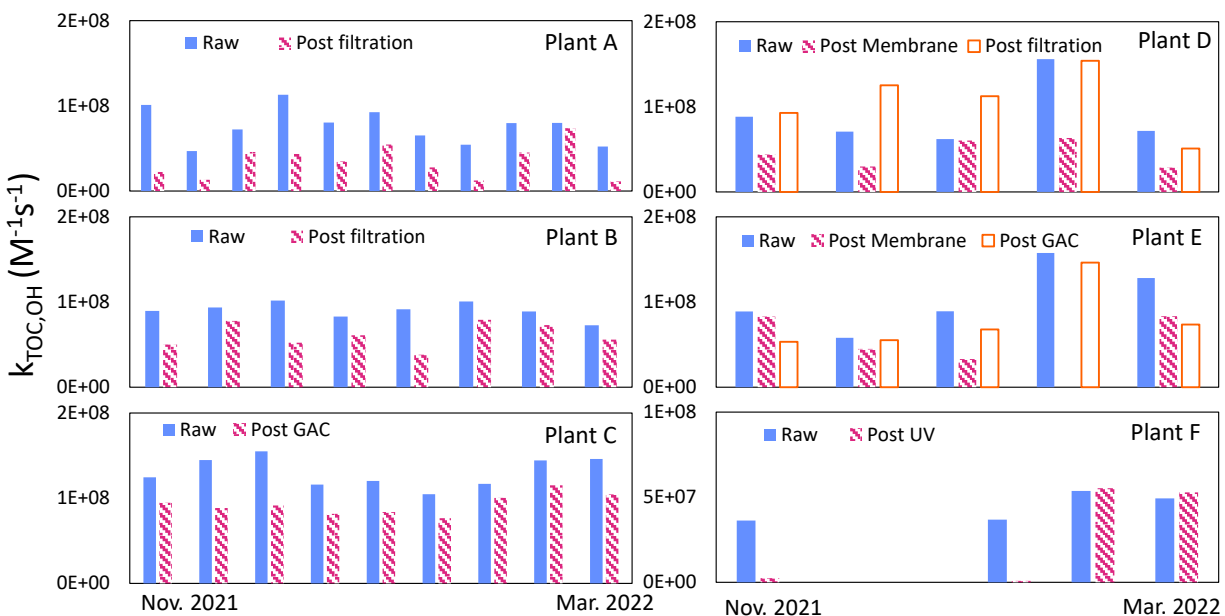


Figure D1-4. The Calculated Reactivity of Total Organic Carbon ($k_{\text{TOC,OH}}$) towards Hydroxyl Radical in Raw and Treated Water Samples from Plant A-F over 5 months.

D1.6 Conclusions

The hydroxyl radical scavenging capacity of water samples collected from water plants in Ontario was measured by a novel external calibration method. This method has been shown so far to be reliable, fast, and easy to conduct with the current prototype device. It has been demonstrated that this method has the potential to be applied in practice widely and frequently to provide the water scavenging capacity measurement to utilities or other stakeholders. However, several unknowns still exist with the method, such as how to properly handle water samples containing chemicals such as chlorine/chloramines. More field testing is also needed to verify the performance of the method and device in practice. The work conducted to date was in a university laboratory environment.

D1.7 References

- Hwang, T.-M., S. -H. Nam, J. Lee, J. -W. Koo, E. Kim, M. Kwon. 2020. "Hydroxyl Radical Scavenging Factor Measurement Using a Fluorescence Excitation-Emission Matrix and Parallel Factor Analysis an Ultraviolet Advanced Oxidation Processes." *Chemosphere*, 259: 127396. <https://doi.org/10.1016/j.chemosphere.2020.127396>.
- Kwon, M., S. Kim, Y. Jung, T. -M. Hwang, M. I. Stefan, J. -W. Kang. 2019. "The Impact of Natural Variation of OH Radical Demand of Drinking Water Sources on the Optimum Operation of the UV/H₂O₂ Process." *Environmental Science & Technology*, 53: 3177–3186. <https://doi.org/10.1021/acs.est.8b05686>.
- Kwon, M., S. Kim, Y. Yoon, Y. Jung, T. M. Hwang, J. W. Kang. 2014. "Prediction of the Removal Efficiency of Pharmaceuticals by a Rapid Spectrophotometric Method Using Rhodamine B in the UV/H₂O₂ Process." *Chem. Eng. Journal*, 236: 438–447. <https://doi.org/10.1016/J.CEJ.2013.10.064>.
- Lee, Y., and U. von Gunten. 2010. "Oxidative Transformation of Micropollutants during Municipal Wastewater Treatment: Comparison of Kinetic Aspects of Selective (Chlorine, Chlorine Dioxide, Ferratevi, and Ozone) and Non-Selective Oxidants (Hydroxyl Radical)." *Water Research*, 44: 555–566. <https://doi.org/10.1016/j.watres.2009.11.045>.
- Rosenfeldt, E. J., and K. G. Linden. 2007. "The R_{OH,UV} Concept to Characterize and the Model UV/H₂O₂ Process in Natural Waters." *Environmental Science & Technology*, 41: 2548–2553. <https://doi.org/10.1021/ES062353P>.
- Sawyer, C. N. 2003. *Chemistry for Environmental Engineering and Science*. McGraw-Hill.
- Wagner, I., J. Karthäuser, and H. Strehlow. 1986. "On the Decay of the Dichloride Anion Cl₂⁻ in Aqueous Solution." *Berichte der Bunsengesellschaft für Phys. Chemie*, 90: 861–867. <https://doi.org/10.1002/bbpc.19860901007>.
- Wang, C., E. Rosenfeldt, Y. Li, and R. Hofmann. 2020. "External Standard Calibration Method to Measure the Hydroxyl Radical Scavenging Capacity of Water Samples." *Environmental Science & Technology*, 54: 1929–1937. <https://doi.org/10.1021/acs.est.9b06273>.
- Yang, Y., J. J. Pignatello, J. Ma, and W. A. Mitch. 2016. "Effect of Matrix Components on UV/H₂O₂ and UV/S₂O₈²⁻ Advanced Oxidation Processes for trace Organic Degradation in Reverse Osmosis Brines from Municipal Wastewater Reuse Facilities." *Water Research*, 89: 192–200. <https://doi.org/10.1016/J.WATRES.2015.11.049>.

Appendix E: DBPs and Toxicity

Prepared by:

**Nathan Moore, Liz Taylor-Edmonds, Tianyi Chen, Latif Abdalrhman, Susan Andrews,
and Ron Hofmann**

University of Toronto, Department of Civil & Mineral Engineering

Contents

Chapter E1: DBPs and Toxicity	233
E1.1 Executive Summary	233
E1.2 Introduction.....	234
E1.3 Normal Sampling Campaign	235
E1.3.1 Description	235
E1.3.2 Results	237
E1.4 Enhanced Sampling Campaign.....	244
E1.4.1 Results	247
E1.5 Quality Assurance/Quality Control	257
E1.5.1 Supplemental Information for the DBP Analysis.....	258
E1.5.2 Chromatographic Separation and DBP Reporting.....	260
E1.5.3 Supplemental Information for the Bioassays.....	261
E1.6 Complete “Normal” Campaign Results.....	264
E1.7 Complete “Enhanced” Campaign Results	272
E1.8 References.....	278

Tables

E1-1	List of Monitored DPBs	236
E1-2	Toxicity Assays	236
E1-3	Summary of Water Utilities and Sampling Details for the "Normal" DBP Survey	237
E1-4	UV Reactor Influent Parameters	237
E1-5	Enhanced Campaign Sampling Locations	245
E1-6	List of Monitored DPBs	246
E1-7	Toxicity Assays	247
E1-8	Water Quality Parameters of the Enhanced Sampling Campaign Waters as Tested in the Lab	247
E1-9	QAQC Summary for the Measured DBPs	259
E1-10	Bottle Preparation and Sample Handling – Enhanced Lab Experiments	260
E1-11	Sample Preservation Reagents.	260
E1-12	Broad Spectrum Bioassays Used for the Effect of UV-AOPs	261
E1-13	Disinfection Byproduct Concentrations Plant A	264
E1-14	Disinfection Byproduct Concentrations at Plant B	266
E1-15	Disinfection Byproduct Concentrations Plant C	268
E1-16	Disinfection Byproduct Concentrations Plant D	270
E1-17	Disinfection Byproduct Concentrations in the Treated Surface Water	272
E1-18	Disinfection Byproduct Concentrations in the Treated Carbon-Based Reuse Water	274
E1-19	Disinfection Byproduct Concentrations in the Treated RO-Based Reuse Water	276

Figures

E1-1	Normal Campaign THM4 Results	238
E1-2	Normal Campaign HAA9 Results.....	239
E1-3	Normal Campaign AOX Results.....	239
E1-4	Normal Campaign DIAA Results.....	240
E1-5	Normal Campaign DCAN Results	241
E1-6	Normal Campaign HAL Results	241
E1-7	Normal Campaign TCP Results.....	242
E1-8	Normal Campaign Chlorate Results	242
E1-9	Normal Campaign NDMA Results	243
E1-10	Normal Campaign Cell Viability Results	244
E1-11	UV Batch Reactor.....	246
E1-12	Lab-Scale AOX Results.	248
E1-13	Lab-Scale THM4 Results.....	249
E1-14	Lab-Scale HAA9 Results.	249
E1-15	Lab-Scale HK Results	250
E1-16	Lab-Scale HAN Results	251
E1-17	Lab-Scale HNM Results	251
E1-18	Lab-Scale HAL Results	252
E1-19	Lab-Scale HAM Results.	252
E1-20	Lab-Scale MX Results	253
E1-21	Lab-Scale MCA Results.....	253
E1-22	Lab-Scale Chlorate Results.....	254
E1-23	Oxidative Stress Response Activity Expressed as Toxicity Units in the Nrf2 Assay	255
E1-24	Genotoxicity of Samples Expressed as Toxicity Units in the SOS assay	256

CHAPTER E1

DBPs and Toxicity

E1.1 Executive Summary

There is growing interest in using UV-chlorine advanced oxidation (UV-AOPs) to control chemical contaminants in reuse and drinking water treatment. Questions remain, however, about the potential formation of byproducts that might affect health. A survey is being conducted to gather information on the concentration and types of byproducts that might be expected during UV-chlorine treatment. The survey is funded jointly by the Water Research Foundation, the State of California, and the (Canadian) Natural Science and Engineering Research Council (NSERC) through project CRDPJ 543834-19. This report presents interim results of this collaborative effort (the portion funded by California and WRF), with project completion expected in early 2023. The reader is referred to the expected subsequent journal publications for the final data analysis.

In the first part of this 2-part survey, water is collected from 4 utilities currently operating full- or large demonstration-scale UV-chlorine advanced oxidation for water reuse or drinking water treatment. The water is collected at the UV influent, the UV effluent, and at a site-specific distance downstream, representing finished or distributed water. The sampled waters are analyzed for approximately 40 regulated and emerging disinfection byproducts (DBPs), cellular cytotoxicity and genotoxicity, and relevant water quality parameters. The results presented in this report are from sampling conducted in June/July 2021 and in September 2021. From those periods, the trihalomethanes and haloacetic acids were below U.S. Environmental Protection Agency (U.S. EPA) regulatory limits for each site and sample. The emerging and nitrogenous DBPs were generally present at low levels, less than 5 µg/L. Approximately 100-800 µg/L of chlorate formed from UV transforming the free chlorine. For all reuse samples, the toxicity assays were well-below typical finished drinking water values.

In the second part of the 2-part survey, water is collected from a variety of water reuse-relevant sources and treated with lab-scale UV-chlorine, as well as chlorine and UV alone, UV/H₂O₂, and both UV-chlorine and UV/H₂O₂ followed by secondary disinfection. The 3 waters presented in this report are: (1) reverse osmosis permeate sampled from a full-scale water reuse facility, (2) granular activated carbon filtrate from a full-scale ozone-based advanced treatment facility, and (3) untreated river water (representing a relatively high organic source water). The treated waters are monitored for the same suite of analytes as in the first part of the survey, as well as 2 additional toxicity assays for a more comprehensive understanding of the overall byproduct formation (one bioassay for detecting byproducts causing oxidative stress, and another for byproducts causing general cellular stress). In the 3 waters, little-to-no byproducts were detected in the reverse osmosis permeate treated by UV-chlorine advanced oxidation. For the ozone-based reuse water and the surface water, UV-chlorine initially formed more byproducts than chlorine alone or UV/H₂O₂, but the regulated byproducts were below U.S. EPA limits. Several emerging or nitrogenous DBP classes did form (generally <10 µg/L) either during UV-chlorine or following secondary disinfection of water treated by UV-chlorine

or UV/H₂O₂. These included haloacetonitriles, halonitromethanes, and halo ketones. The toxicities measured by the bioassays were well-below typical drinking water values.

The purpose of this report is to present the initial results of this UV-chlorine byproduct survey. As expected, UV-chlorine did form trihalomethanes and haloacetic acids in high-precursor waters (e.g., in a drinking water context), and formed little of those compounds (zero to low- $\mu\text{g/L}$ levels) in reverse osmosis osmosis-treated source waters. Likewise, there was evidence that several unregulated DBPs can form during the UV-chlorine treatment of ground water, surface water, and ozone-based reuse water. These compounds were occasionally present in the AOP influent and remained through the UV reactor and downstream, including for reverse osmosis-treated source waters. Regardless, the DBPs concentrations and toxicities measured were similar to or less than what has been reported in U.S. nation-wide drinking water surveys. Accordingly, in this work to-date there has been no compelling evidence of toxic byproduct formation above the levels typically found in drinking water. This survey is, however, ongoing. Several additional source waters are being monitored and additional byproduct data being collected. Readers are invited to look for the final peer reviewed publication(s) for complete information

E1.2 Introduction

The UV-chlorine advanced oxidation process may use chlorine doses that are relatively large compared to conventional drinking water disinfection, and it also generates reactive chlorine species (RCS). It is understandable that there may therefore be concern about the potential to form byproducts or transformation products that may be of relevance to human health. For example, up to approximately 20% of chlorine photolyzed during the process may be converted to chlorate and up to 50% of bromide present has been found to convert to bromate under certain conditions (Buxton and Subhani, 1972; Fang et al., 2017; Feng et al., 2010; Gao et al., 2019; Kamath and Minakata, 2018; Wang et al., 2019). Various trihalomethanes and haloacetic acids have been reported following UV-chlorine (Wang et al., 2015).

Since it is not currently possible to measure all byproducts that are formed, accompanying traditional byproduct analysis with more holistic strategies can be beneficial. An increasingly common research tool is the toxicity assay, whereby the cumulative toxic effect of a mixture of DBPs in one sample can be compared to a reference sample (such as normal tap water), without knowing the exact and complete composition of the DBPs in the samples (Escher et al., 2013; Sun et al., 2019; Zheng et al., 2015; Neale and Escher, 2019). Such bioanalytical tools are already being used or investigated for water reuse applications: in 2018 the Science Advisory Panel for *Monitoring Strategies for Constituents of Emerging Concern (CECs) in Recycled Water* (convened by the California State Water Resources Control Board) made recommendations for the use of bioanalytical screening tools to assess estrogenic and dioxin-like biological activities in recycled water (Drewes et al., 2018).

In the context of UV-chlorine, there is very limited information on the extent and significance of any byproduct formation. Several of the existing studies that have investigated specific byproduct formation have been referenced herein. These studies have not investigated a wide enough variety of source waters or treatment trains to provide general guidance on UV-

chlorine operation, nor have they accounted for many of the nitrogenous classes of known DBPs. There are a few reported applications of bioanalytical tools to the study of UV-chlorine. However, these have generally been directed at observing the effects of specific micropollutants and their transformation products, and not on overall treated water quality in terms of potential toxic byproducts (Huang et al., 2017; Li et al., 2016). More data would be valuable in helping stakeholders to evaluate the safety of UV-chlorine relative to other treatment options.

This section of the report describes the findings of a byproduct survey conducted to gain an improved understanding of byproduct formation during and after UV-chlorine. Two DBP sampling campaigns were conducted for this survey: a “normal” campaign targeting utilities already using UV-chlorine and an “enhanced” campaign where water was collected for laboratory-scale AOP treatments. Sections E.3 and E.4 contain descriptions and results for the two respective sampling campaigns. Section E.5 contains supplementary information on the sampling methods, quality assurance and quality control procedures, and other relevant details as well as the full survey data in table format

E1.3 Normal Sampling Campaign

E1.3.1 Description

The purpose of the “normal” campaign was to survey byproduct levels at UV-chlorine facilities currently in operation. Water was sampled from 4 utilities currently operating full- or large pilot-scale UV-chlorine treatment. Samples were collected in duplicate before, after, and downstream of UV-chlorine and were transported to the University of Toronto for the analysis of regulated and emerging DBPs (Table E-1), as well as the relevant water quality parameters such as TOC and UV₂₅₄. Samples were also analyzed using bioassays for genotoxicity and cytotoxicity (Table E-7). This sampling was conducted twice, once in June or July 2021 and once in September 2021, to capture potential variations in water quality. The details of the utilities and sampling locations are provided in Table E-3.

Table E1-1. List of Monitored DPBs.

Trihalomethanes (THMs)		Inorganics	
Trichloromethane (TCM)	Bromochloriodomethane (BCIM)	Chlorite	
Bromodichloromethane (BDCM)	Dibromiodomethane (DBIM)	Chlorate	
Dibromochloromethane (DBCM)	Bromodiiodomethane (BDIM)	Bromate	
Tribromomethane (TBM)	Dichloriodomethane (DCIM)		
Chlorodiiodomethane (CDIM)	Triiodomethane (TIM)		
Haloacetic Acids (HAAs)		Haloacetonitriles (HANs)	
Chloroacetic acid (MCAA)	Bromodichloroacetic acid (BDCAA)	Trichloroacetonitrile (TCAN)	
Dichloroacetic acid (DCAA)	Chlorodibromoacetic acid (CDBAA)	Dichloroacetonitrile (DCAN)	
Trichloroacetic acid (TCAA)	Iodoacetic acid (IAA)	Bromochloroacetonitrile (BCAN)	
Bromoacetic acid (MBAA)	Diiodoacetic acid (DIAA)	Dibromoacetonitrile (DBAN)	
Dibromoacetic acid (DBAA)	Bromiodoacetic acid (BIAA)	Haloacetamides	
Tribromoacetic acid (TBAA)	Chloriodoacetic acid (CIAA)	Dibromoacetamide (DBAM)	
Bromochloroacetic acid (BCAA)		Trichloroacetamide (TCAM)	
Halonitromethanes (HNMs)	Halofuranones	Haloacetaldehydes (HALs)	
Trichloronitromethane (TCNM)	3-Chloro-4-(dichloromethyl)-5-hydroxy-2(5H)-furanone (MX)	Dichloroacetaldehyde (DCAL)	
Bromodichloronitromethane (BDCNM)		Trichloroacetaldehyde (TCAL)	
Dibromochloronitromethane (DBCNM)	Mucochloric acid (MCA)	Tribromoacetaldehyde (TBAL)	
Nitrosamines	Haloketones (HKs)	Other	
N-Nitrosodimethylamine (NDMA)	1,1-Dichloro-2-propanone (DCP)	Adsorbable Organohalides (AOX)	
	1,1,1-Trichloro-2-propanone (TCP)		

Table E1-2. Toxicity Assays.

Cell Viability
Alkaline phosphatase activity in the SOS Chromotest™ assay: <i>E. coli</i> cells
Genotoxicity
Activation of SOS DNA repair pathway through direct (mutagenic) or indirect (oxidative) damage to DNA: <i>E. coli</i> cells

Table E1-3. Summary of Water Utilities and Sampling Details for the "Normal" DBP Survey.

Water Utility	Description	Sampling Dates	Sampling Locations
Plant A	Full-scale UV-chlorine system treating trichloroethylene in groundwater for drinking water supply.	June 29 th , 2021 September 20 th , 2021	Influent (Inf): UV influent Effluent (Eff): UV effluent Downstream (Down): reservoir in distribution system
Plant B	Full-scale microfiltration, reverse osmosis, UV-chlorine system for water reuse.	July 2, 2021 September 29, 2021	Influent (Inf): UV influent Effluent (Eff): UV effluent Downstream (Down): product water tank after dechlorination and decarbonation, before the water was sent to spreading grounds
Plant C	Full-scale microfiltration, reverse osmosis, UV/chlorine system for water reuse.	June 9 th , 2021 September 29 th , 2021	Influent (Inf): UV influent Effluent (Eff): UV effluent Downstream (Down): the end of the chlorine contact basin, before the water was pumped to a groundwater injection barrier
Plant D	Demonstration-scale ozone-biofiltration, microfiltration, reverse osmosis, UV-chlorine system for water reuse.	June 15 th , 2021 September 29 th , 2021	Influent (Inf): UV influent Effluent (Eff): UV effluent Downstream (Down): UV effluent was held in a container for an additional 6 hours before transferring to sample bottles

E1.3.2 Results

The UV reactor influent water quality for the 4 sampling locations is summarized in Table E1-4.

Table E1-4. UV Reactor Influent Parameters.

Parameters	A		B		C		D	
	June/July 2021	September 2021						
pH	7.7	7.3	7.7	6.1	6.6	6.5	6.3	5.7
TOC (mg/L)	1.4	1.4	0.3	<MDL	0.3	0.09	<MDL	<MDL
UV ₂₅₄ (cm ⁻¹)	0.046	0.038	0.082	0.002	0.016	0.005	0.001	0.001
UVT (cm ⁻¹)	90%	97%	83%	100%	96%	99%	100%	100%

AOX and conventional DBPs

Figures E1 to E-3 show progression of the regulated THMs, HAAs, and adsorbable organohalides (AOX), across the 4 treatment trains. There was considerably more byproduct formation at Plant A than at the other 3 plants. This is because it is a groundwater source with more TOC in the AOP influent than at the other 3 plants, for which the influent is RO permeate (approximately 1.5 mg-C/L vs. <0.4 mg-C/L). Following UV-chlorine at Plant A the maximum observed THM4 concentration was 58.1 µg/L and HAA9 was 44.6 µg/L. Amongst the 3 RO-based treatment facilities, following UV-chlorine the maximum observed THM4 concentration was

36.7 $\mu\text{g/L}$ (a decrease from the 43.9 $\mu\text{g/L}$ in the influent at Plant B) and HAAs = 13.0 $\mu\text{g/L}$ at Plant C.

There is a small observed loss of THMs across the UV reactors in the first sampling at Plants ‘B,’ ‘C,’ and ‘D’ (influent vs. effluent). Mechanistically, this is not expected since THMs are conservative across a UV-AOP reactor. One possibility is that sample collection was taken from a tap that was fast-flowing and exposed to air, leading to volatile losses of THMs (no similar reduction from influent to effluent was observed for HAAs at the same Plants, and HAAs are not volatile). Similarly, there is a reduction in THMs from UV reactor effluent to the “downstream” point at Plant ‘D,’ which is following a reservoir where THMs might be lost through aeration—and again, no such reduction is observed for HAAs at this location. The HAA results suggest minor formation across the UV-chlorine AOP reactor. Overall, the amounts at the 3 reuse facilities remain small when compared to typical drinking water concentrations.

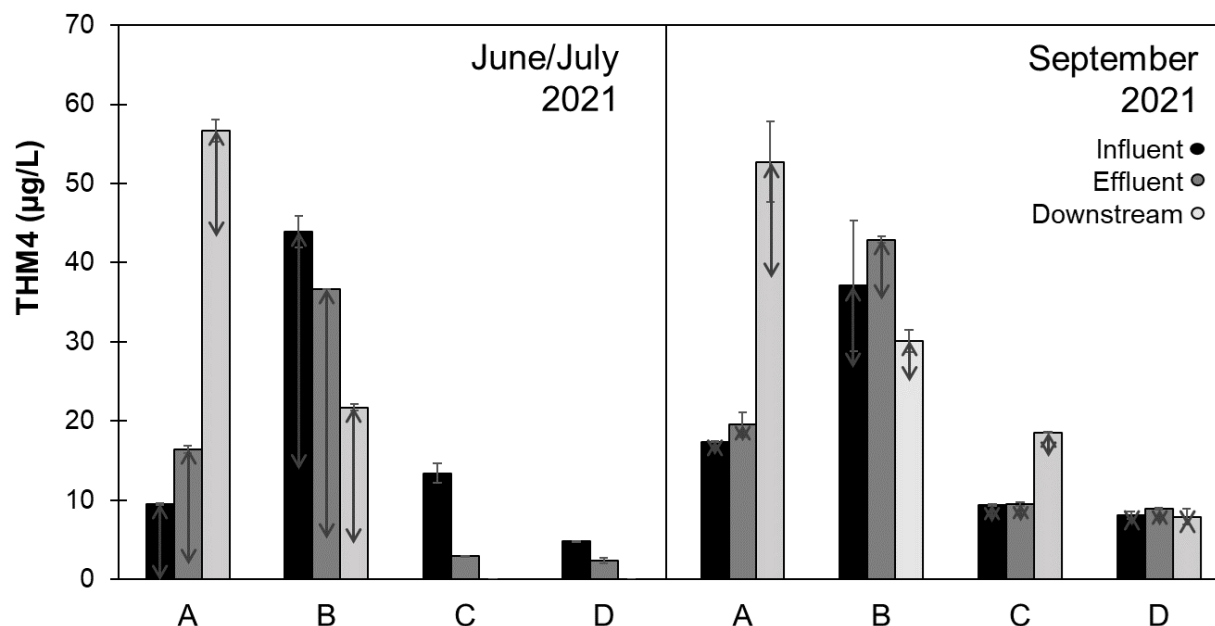


Figure E1-1. Normal Campaign THM4 Results

(June/July 2021 Plant ‘C’ Downstream sample lost). Error bars represent the range of experimental duplicates. The grey arrows represent the range in THM4 concentration that may instead be haloacetaldehydes (see Section E.5.2 for more information).

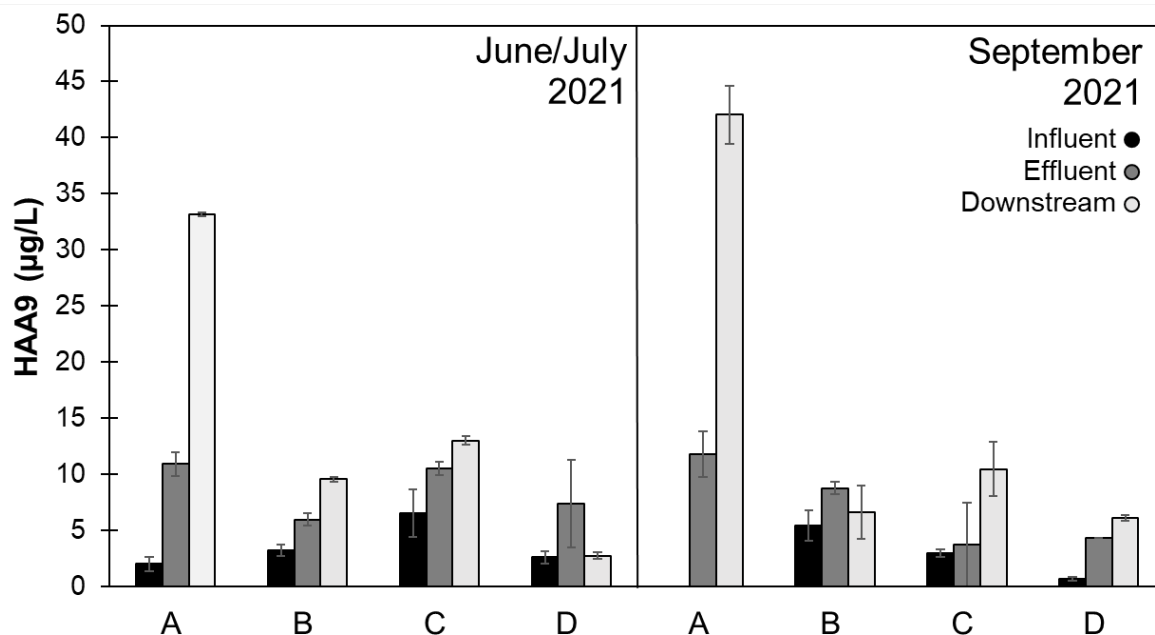


Figure E1-2. Normal Campaign HAA9 Results.
Error bars represent the range of experimental duplicates.

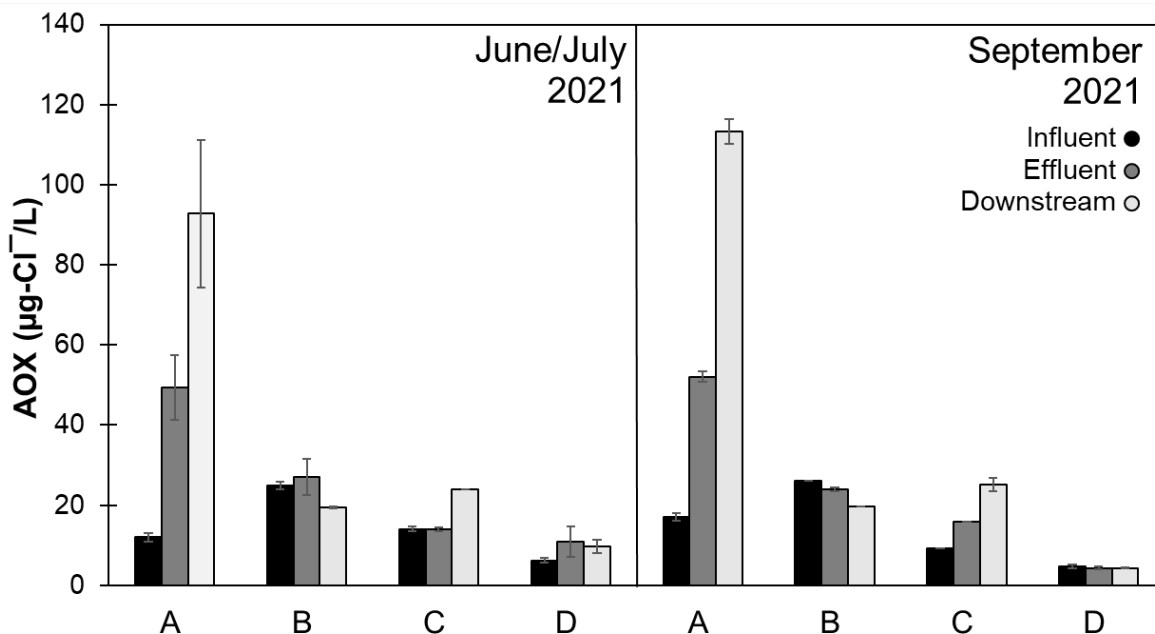


Figure E1-3. Normal Campaign AOX Results.
Error bars represent the range of experimental duplicates.

Emerging DBPs

Emerging and nitrogenous byproducts, such as the haloacetonitriles and haloacetamides, were generally below or near the detection limits (Table E-9). There were 1-2 µg/L of diiodoacetic acid measured across the AOP at Plants 'B' and 'D' during the second sampling, and there were

3-4 µg/L of DCAN (or DCP) present in the UV influent at Plant 'B' which was unaffected by the AOP. Up to 4.4 µg/L of total haloacetaldehydes formed during UV-chlorine at Plant 'A.' Also, 2.6 µg/L of TCP formed during UV-chlorine at Plant A during the first sampling, and an additional 1-3 µg/L formed after the AOP. Chlorate forms from the photolysis of free chlorine, often in the 5-20% yield (by mass) range of photolyzed chlorine. This was consistent here, given the 1.5-3 mg/L free chlorine doses applied at these locations which led to generally 0.1-0.8 mg/L chlorate. No chlorite or bromate was detected. NDMA tended to be consistently destroyed across the UV reactor However, Plants B and C showed some NDMA formation downstream of the AOP for the June/July sampling, a phenomenon which has been discussed by McCurry et al. (2017) and Sgroi et al. (2015). A similar increase in NDMA levels downstream of Plant A in the first sampling could be within experimental error of a non-effect, especially given that the first sampling event's results may be affected by an approximately 6 ng/L elevated background, a possible analytical artifact that is being investigated.

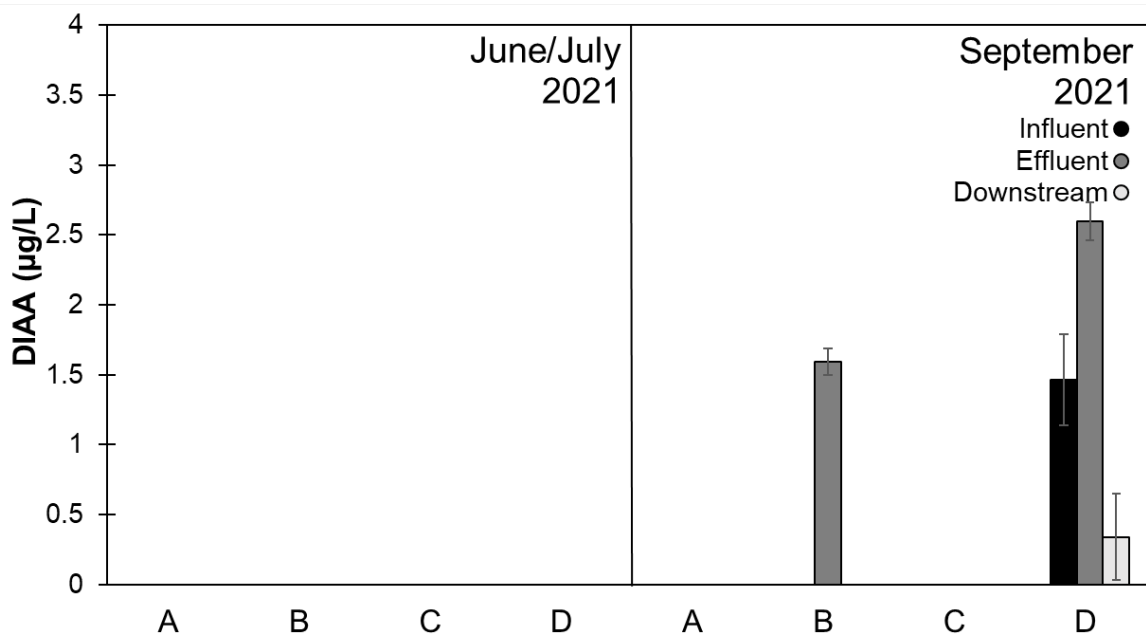


Figure E1-4. Normal Campaign DIAA Results.
Error bars represent the range of experimental duplicates.

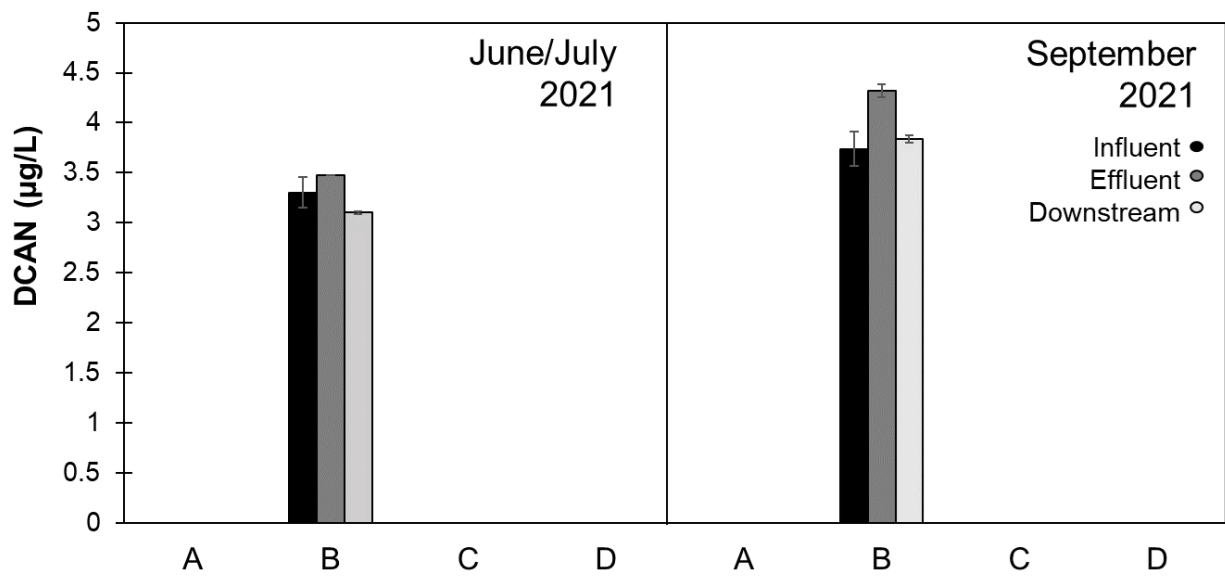


Figure E1-5. Normal Campaign DCAN Results.
 Error bars represent the range of experimental duplicates.

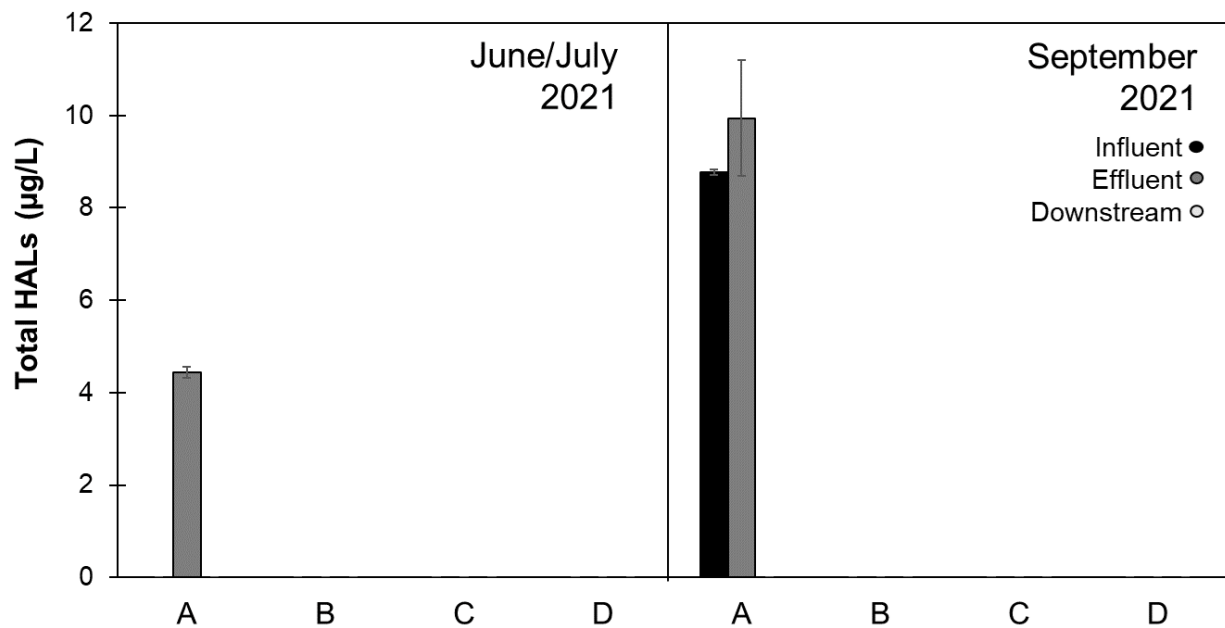


Figure E1-6. Normal Campaign HAL Results.
 Error bars represent the range of experimental duplicates.

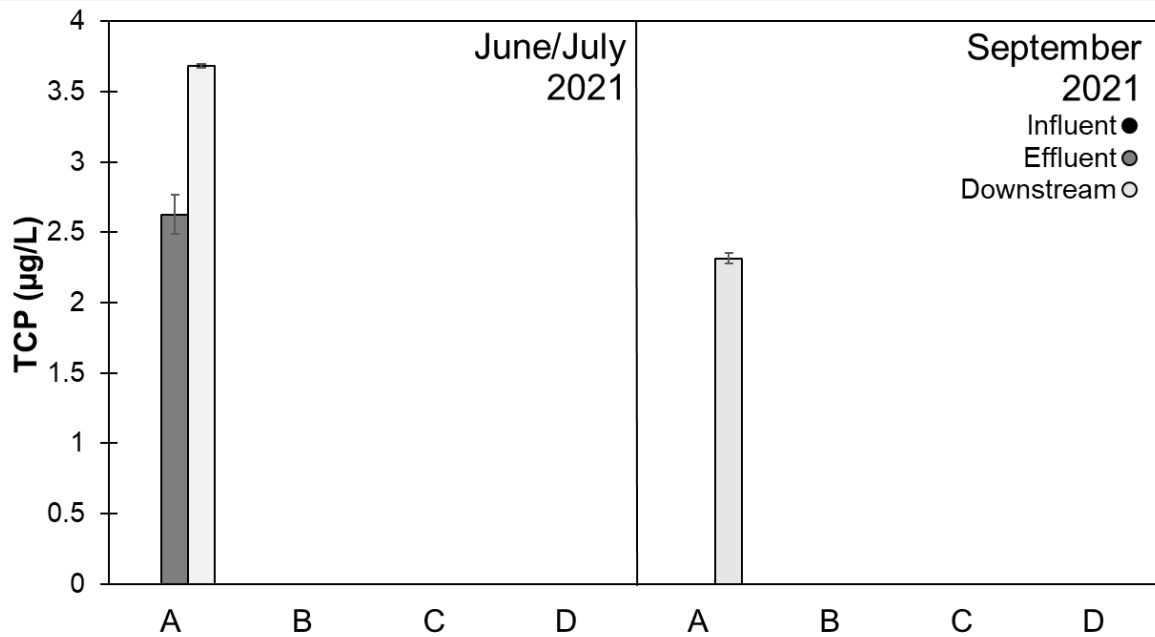


Figure E1-7. Normal Campaign TCP Results.
Error bars represent the range of experimental duplicates.

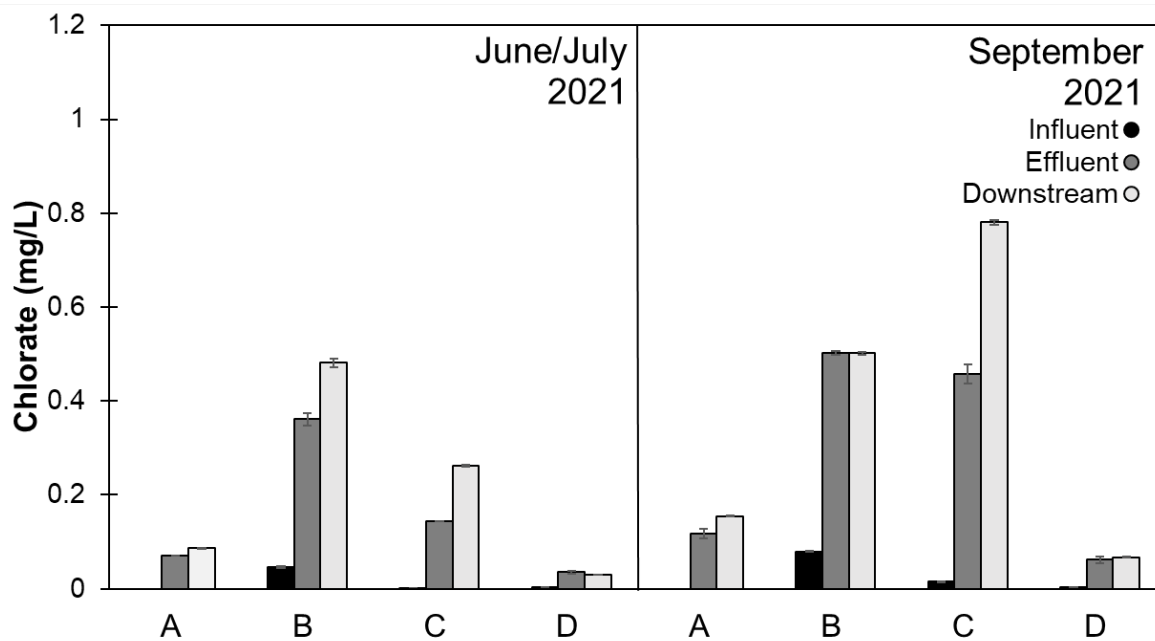


Figure E1-8. Normal Campaign Chlorate Results.
Error bars represent the range of experimental duplicates.

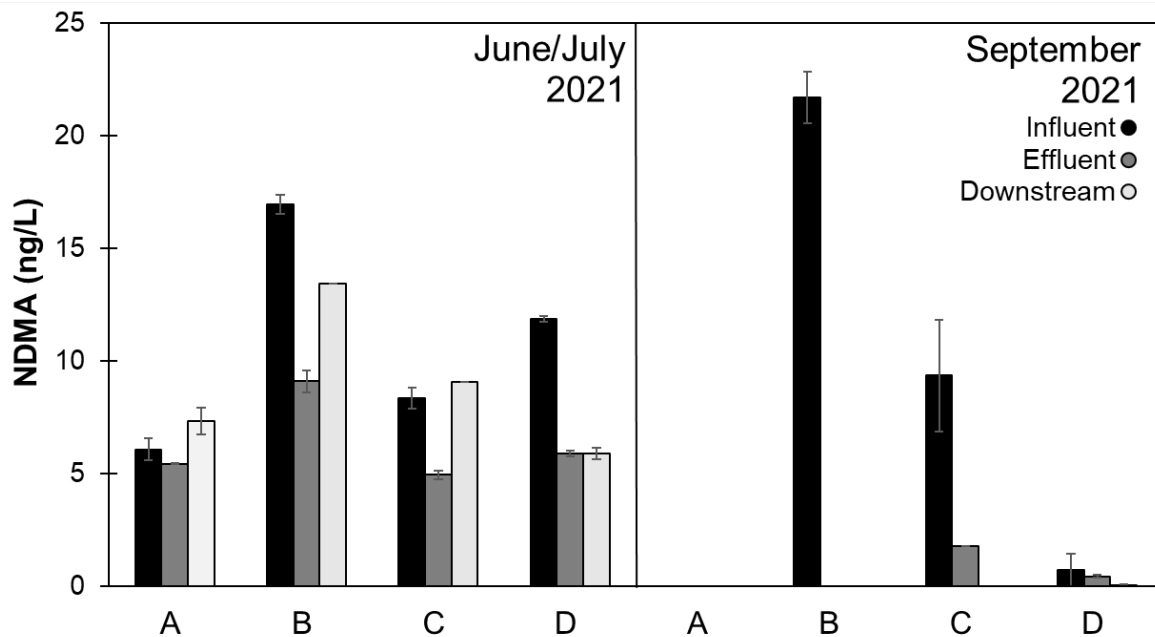


Figure E1-9. Normal Campaign NDMA Results.
 Error bars represent the range of experimental duplicates.

Cytotoxicity and genotoxicity

Cytotoxicity of the full-scale samples was assessed by measuring the activity of a metabolic enzyme, alkaline phosphatase, which functions independently of the genotoxicity pathway. Inhibition of enzyme activity reflects metabolic impairment, which is a hallmark feature of general cellular cytotoxicity. Cell viability is presented in Figure E-10 for the highest dose tested in the assay, a relative enrichment factor of 80-fold. Cell viability higher than 80% is considered to be non-cytotoxic. All of the samples are considered viable (non-cytotoxic) for the June/July 2021 sampling event. In the September 2021 sample set, the Plant A influent slightly breached the <80% threshold with a cell viability of 78% for raw untreated groundwater; with treatment, the value increased to 79%, and again to 80% during distribution, suggesting some improvement in water quality. Additionally, at Plant C the cell viability decreased from 81.5% to 79.9% during UV-chlorine but rose above the 80% threshold to 84.4% downstream.

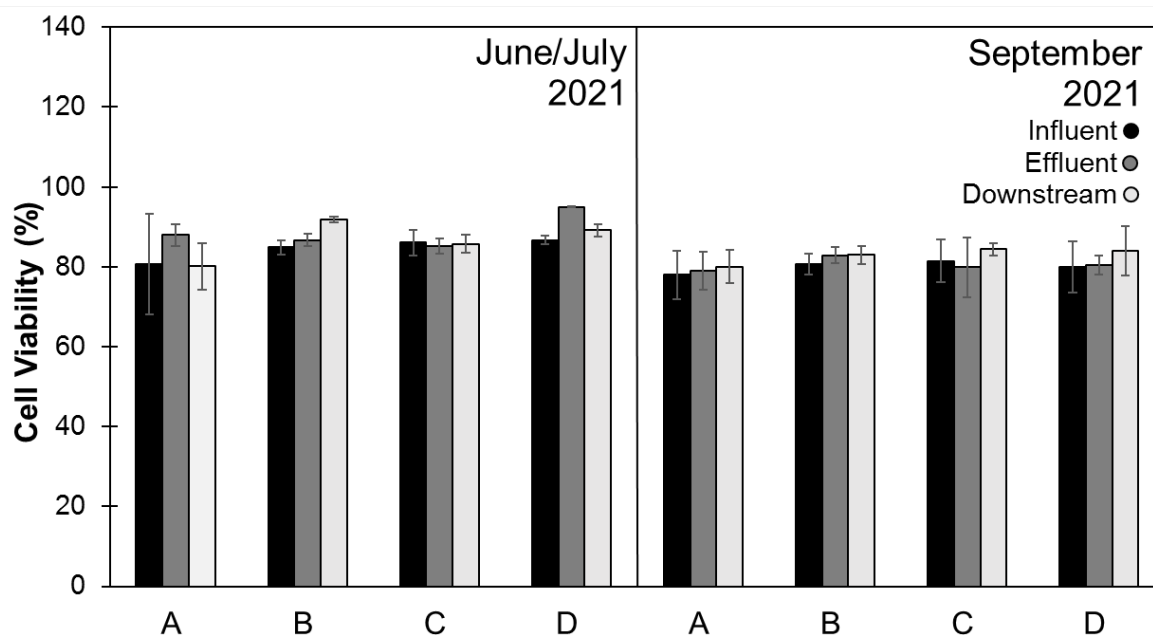


Figure E1-10. Normal Campaign Cell Viability Results.

Error bars represent the standard deviation of experimental duplicates analyzed in duplicate.

The SOS genotoxicity assay detects the activation of DNA repair genes in response to oxidative or mutagenic impacts on the genome. The downstream sample from Plant A (treats groundwater and is chlorinated) during June/July 2021 was the only sample that activated the genotoxicity pathway and did so only slightly. That is, the response (toxicity unit, $1/\text{REF IF } 1.5 = 0.014$) was well-below reported values for drinking water and reverse osmosis permeate (toxicity unit = 0.037) (Escher et al., 2014). The metrics for assessing toxicity, including the toxicity units, are described in Section E.5.3.

E1.4 Enhanced Sampling Campaign

The purpose of the “enhanced” campaign was to assess byproduct concentrations from several relevant source waters under lab-generated UV-chlorine treatment and parallel control conditions to better understand the range of byproduct formation that might occur. Water samples were shipped from 3 utilities to the University of Toronto where each water underwent lab-scale UV-chlorine, UV/H₂O₂, and UV or chlorine alone treatments. The details of the sampling locations are provided in Table E-5. The conditions tested are as follows:

- **Raw:** Water collected from the utility, having the characteristics described in Table E-5 and with no lab-scale treatment applied.
- **UV alone (UV):** A medium pressure UV dose consistent with achieving 0.5-log 1,4-dioxane destruction in the UV-chlorine system.
- **Chlorine alone (Cl):** A free chlorine dose of 6 mg/L quenched following the same contact time experienced in the UV-chlorine system (about 20 seconds).

- **Medium pressure UV-chlorine (UV/Cl):** Combined UV and 6 mg/L of chlorine at a UV dose to achieve approximately 0.5-log 1,4-dioxane destruction. The chlorine is quenched after 20-120 seconds, depending on practical considerations.
- **Medium pressure UV-chlorine followed by DBP formation potential testing (UV/Cl-FP):** The same UV-chlorine experiment described above, followed by additional free chlorine dosed to yield a 1 mg/L residual after 24 hours.
- **UV/H₂O₂:** Combined UV and 3 mg/L H₂O₂ at a UV dose to achieve approximately 0.5-log 1,4-dioxane destruction. The H₂O₂ is quenched following AOP treatment.
- **UV/H₂O₂-FP:** The same UV/H₂O₂ experiment described above, followed by quenching the H₂O₂ using free chlorine at a dose that also yields a 1 mg/L free chlorine residual after 24 hours

Table E1-5. Enhanced Campaign Sampling Locations.

Source water	Description
Surface water	Relatively high TOC, highly impacted river water sampled at the intake of a drinking water treatment plant.
Carbon-based reuse	Demonstration-scale carbon-based advanced treatment (CBAT) system treating wastewater for reuse. The water was sampled after ozone, biofiltration, and granular activated carbon filtration.
Reverse osmosis (RO)-based reuse	Full-scale microfiltration, reverse osmosis, UV-AOP system using UV-chlorine treating wastewater for reuse. The water was sampled after reverse osmosis.

The UV, Cl, UV/Cl, UV/Cl-FP, UV/H₂O₂, and UV/H₂O₂-FP treatments were conducted (all in duplicate) in a batch reactor (Figure E-11) using a medium pressure lamp to allow AOP doses to be applied within approximately 30 seconds, at which point residual oxidant is quenched using methods explained in Section E.5.1. This simulates the general contact time of chlorine in a full-scale UV reactor, as opposed to collimated beam tests where UV exposures in the order of many minutes or hours might be needed to achieve AOP conditions, resulting in non-representative chlorine DBP formation. The UV fluence is adjusted to yield approximately 0.5-log 1,4-dioxane reduction, measured at the start of the test in that water matrix, to be representative of a common AOP dose. For each test condition, the suite of DBPs and toxicity assays listed in Tables E-6 and E-7 were analyzed.

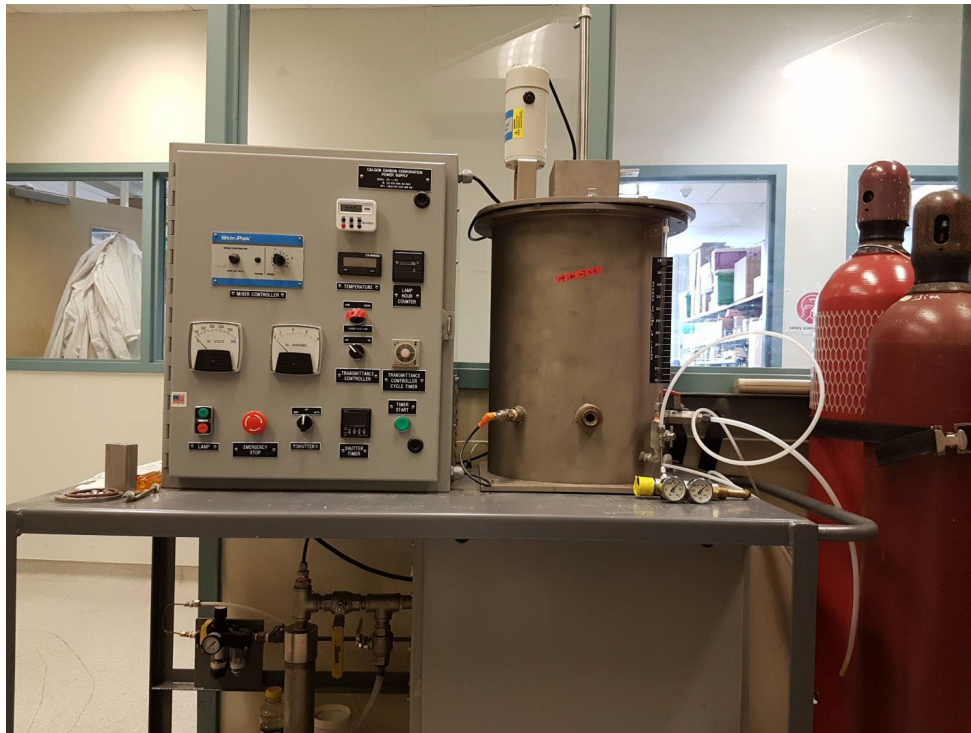


Figure E1-11. UV Batch Reactor.

Table E1-6. List of Monitored DPBs.

Trihalomethanes (THMs)		Inorganics	
Trichloromethane (TCM)	Bromochloriodomethane (BCIM)	Chlorite	
Bromodichloromethane (BDCM)	Dibromiodomethane (DBIM)	Chlorate	
Dibromochloromethane (DBCM)	Bromodiiodomethane (BDIM)	Bromate	
Tribromomethane (TBM)	Dichloriodomethane (DCIM)		
Chlorodiiodomethane (CDIM)	Triiodomethane (TIM)		
Haloacetic Acids (HAAs)		Haloacetonitriles (HANs)	
Chloroacetic acid (MCAA)	Bromodichloroacetic acid (BDCAA)	Trichloroacetonitrile (TCAN)	
Dichloroacetic acid (DCAA)	Chlorodibromoacetic acid (CDBAA)	Dichloroacetonitrile (DCAN)	
Trichloroacetic acid (TCAA)	Iodoacetic acid (IAA)	Bromochloroacetonitrile (BCAN)	
Bromoacetic acid (MBAA)	Diiodoacetic acid (DIAA)	Dibromoacetonitrile (DBAN)	
Dibromoacetic acid (DBAA)	Bromiodoacetic acid (BIAA)	Haloacetamides	
Tribromoacetic acid (TBAA)	Chloriodoacetic acid (CIAA)	Dibromoacetamide (DBAM)	Trichloroacetamide (TCAM)
Bromochloroacetic acid (BCAA)			
Halonitromethanes (HNMs)		Halofuranones	Haloacetaldehydes (HALs)
Trichloronitromethane (TCNM)	3-Chloro-4-(dichloromethyl)-5-hydroxy-2(5H)-furanone (MX)	Dichloroacetaldehyde (DCAL)	Trichloroacetaldehyde (TCAL)
Bromodichloronitromethane (BDCNM)	Mucochloric acid (MCA)	Trichloroacetaldehyde (TCAL)	Tribromoacetaldehyde (TBAL)
Dibromochloronitromethane (DBCNM)			
Haloketones (HKs)		Other	
1,1-Dichloro-2-propanone (DCP)		Adsorbable Organohalides (AOX)	
1,1,1-Trichloro-2-propanone (TCP)			

Table E1-7. Toxicity Assays.

Oxidative stress response
Activation of Nrf2 mediates antioxidant response element: MCF7 cells (human breast cancer)
Genotoxicity
Activation of SOS DNA repair pathway through direct (mutagenic) or indirect (oxidative) damage to DNA: <i>E. coli</i> cells
Cytotoxicity
MTT dye indicates cell proliferation: HeLa cells (human cervical cancer)
General cellular stress
Activation of p53: HeLa cells (human cervical cancer)

E1.4.1 Results

The sampled (Raw) water quality for the 3 sampling locations is summarized in Table E-8.

Table E1-8. Water Quality Parameters of the Enhanced Sampling Campaign Waters as Tested in the Lab
(not necessarily identical to when sampled at the plant).

Parameters	RO-based reuse	Carbon-based reuse	Surface water
pH	5.8	7.2	8.8
TOC (mg/L)	0.3	3.2	2.9
UV ₂₅₄ (cm ⁻¹)	0.008	0.05	0.2
UVT (% cm ⁻¹)	98	88	68

AOX and conventional DBPs

Low levels of AOX (10-60 µg-Cl⁻/L) were present in the untreated water, UV, and UV/H₂O₂ samples for all three source waters. This is presumably due to AOX present in the plant influent or AOX formed during chlor(am)ination upstream of membranes at the reuse plants.

For the RO-based reuse water, there was little change in AOX and THM4 for any treatment: ± 12.9 µg-Cl⁻/L and ± 3.8 µg/L amongst all treatments, respectively. However, UV-chlorine did roughly double the HAA9 concentration relative to Cl alone at the same chlorine dose (4.0 µg/L to 8.5 µg/L). The HAA9 concentration was doubled again (to 20.6 µg/L) by the formation potential testing. UV/H₂O₂ treatment led to similar HAA9 levels after formation potential testing (15.6 µg/L) suggesting similar productivity of both AOPs in generating HAA precursors even in low-TOC waters.

For the carbon-based reuse and surface water there was a 40-50% increase in AOX from the UV-chlorine AOP relative to Cl alone (again, at the same dose). The THM4 concentration increased from 13-15 µg/L to 21-23 µg/L and HAA9 from 7-13 µg/L to 28-30 µg/L. This suggests a possible role of UV-chlorine radicals in promoting these byproducts. Still, both THM4 and HAA9 were low compared to regulatory drinking water limits. Formation potential testing after UV-chlorine caused a roughly 2-fold increase in AOX when compared to UV-chlorine alone (i.e., AOX formation from the 6 mg/L chlorine within the UV reactor was half the eventual AOX measured 24 hours later after exposed to chlorine as a secondary disinfectant). AOX formation during the 24-hour formation potential tests were reasonably similar for both UV-chlorine and

UV-H₂O₂ treatment. THM4 and HAA9 were near to or exceeded drinking water regulatory limits after formation potential testing for both AOPs when treating the raw river water and the ozone-CBAT wastewater: 100.8-161.6 µg/L for THM4 and 45.8-113.1 µg/L for HAA9. This is not unexpected since the TOC in these two waters was near 3 mg-C/L, and a reasonably high chlorine dose was applied (1 mg/L residual at 24 hours). Unlike in the RO-based reuse water, UV-chlorine generated more THM precursors than HAA precursors (>5-times increase in THM4 after formation potential testing vs. a roughly 3-times increase in HAAs). The RO may have preferentially removed certain THM4 precursor compounds. In addition, UV-chlorine tended to generate more THM and HAA than UV/H₂O₂, as downstream THM4 and HAA9 concentrations ranged from 13-73% greater downstream of UV-chlorine than of UV/H₂O₂.

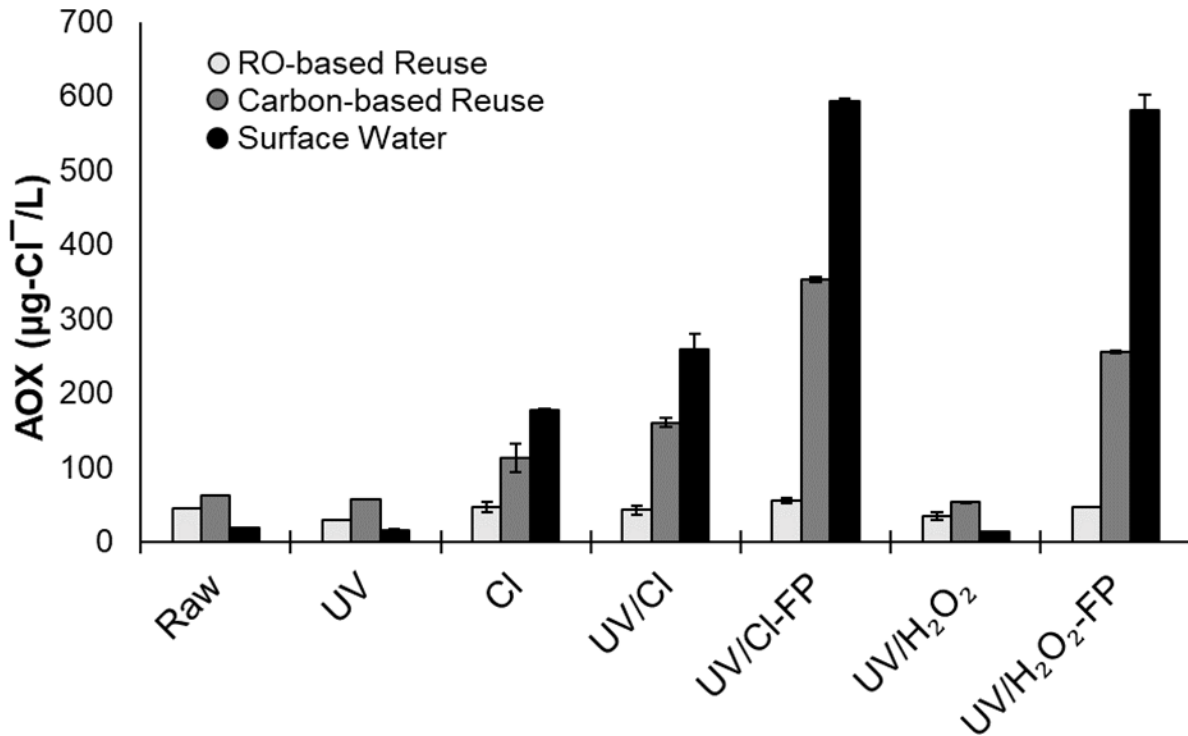


Figure E1-12. Lab-Scale AOX Results.
Error bars represent the range of experimental duplicates.

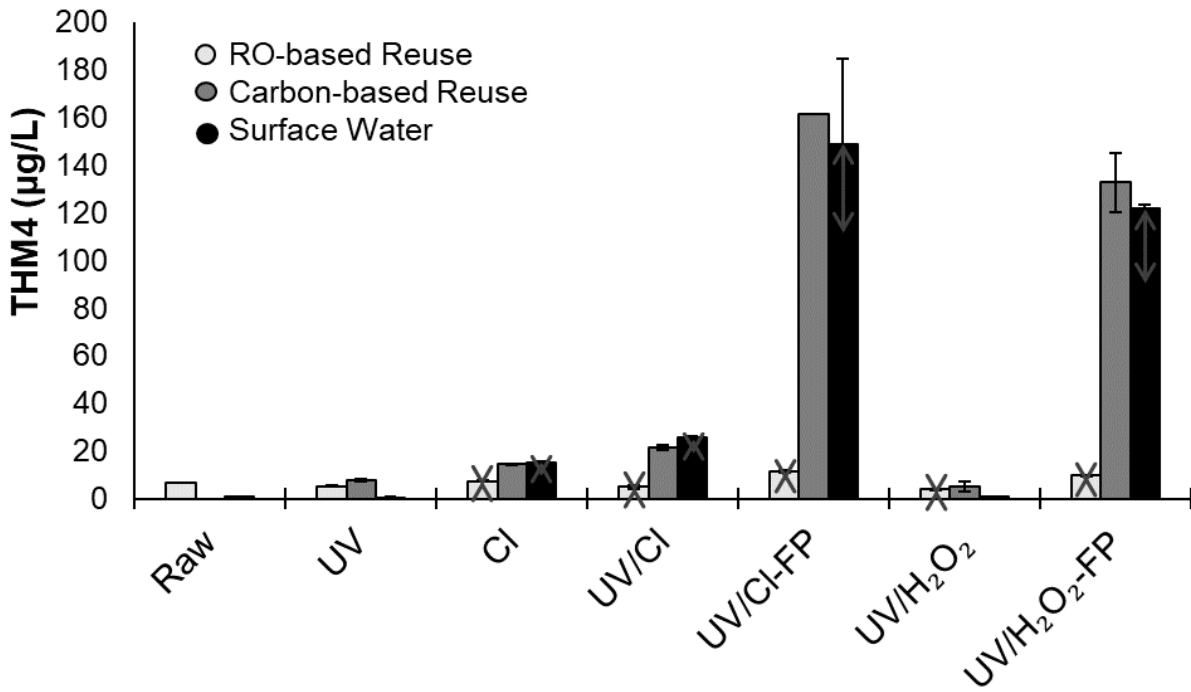


Figure E1-13. Lab-Scale THM4 Results.

Error bars represent the range of experimental duplicates. The grey arrows represent the range in THM4 concentration that may instead be haloacetaldehydes (see Section E.5.2 for more information).

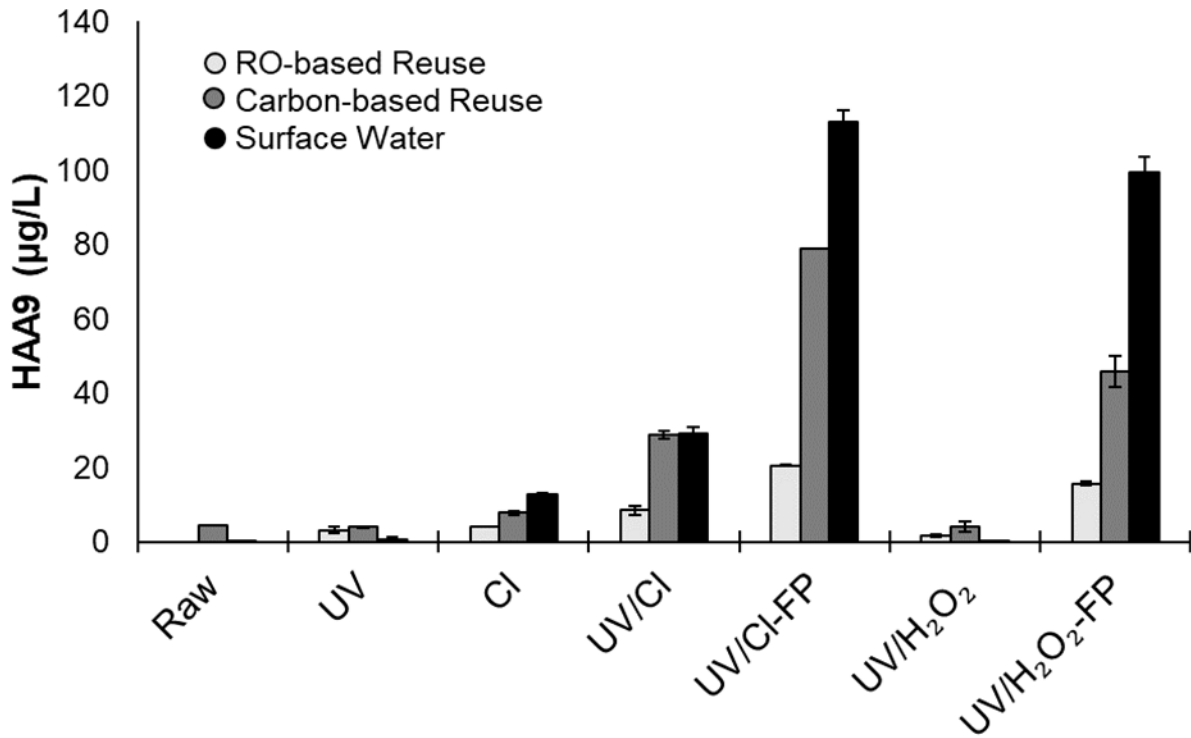


Figure E-14. Lab-Scale HAA9 Results.

Error bars represent the range of experimental duplicates.

Emerging DBPs

The majority of emerging and nitrogenous DBPs were below detection limits in the RO-treated water. There were approximately 2 µg/L of TCP formed during subsequent chlorination of water treated by either AOP. Additionally, 31.8 ng/L of MCA formed during UV-chlorine and an additional 157.2 ng/L formed during subsequent chlorination, which was greater than the 14.6 ng/L which formed during subsequent chlorination of the UV/H₂O₂-treated water. For the other 2 source waters, there was evidence to suggest that UV-chlorine may lead to increased concentrations of several emerging and nitrogenous DBP species, with the greatest concentrations occurring after post-chlorination (formation potential). UV-chlorine formed 4.1 µg/L of HANs (surface water only), 4.6 µg/L of HNMs (surface water only), 2.1-6.6 µg/L of HKs, 1.7-4.3 µg/L of HALs, and as much as 5.4 ng/L of MX and 225.7 ng/L of MCA compared to chlorine alone. An additional 4.1-12.4 µg/L of HANs, 2.3-3.4 µg/L of HNMs, 16 µg/L of HKs (carbon-based reuse only), and 9.1 µg/L of HALs (surface water only) were formed through post-chlorination. MX concentrations remained within roughly 1 ng/L of UV reactor effluent levels, but the MCA concentration rose by as much as 1326.1 ng/L. The HAMs were below the detection limit before and immediately after UV-chlorine; however, the total HAM concentration increased to 3.5 µg/L after post-chlorination of the UV-chlorine treated surface water (no HAMs were detected downstream of UV-chlorine for the carbon-based reuse water). Most of these compounds are not regulated, but they are considered to be more toxic than conventional THMs and HAAs (Wagner and Plewa, 2017). Accordingly, the formation of such compounds may warrant consideration even at the generally low-µg/L levels observed here. Chlorate varied from 0 to 13% of the photolyzed chlorine. No chlorite or bromate was detected.

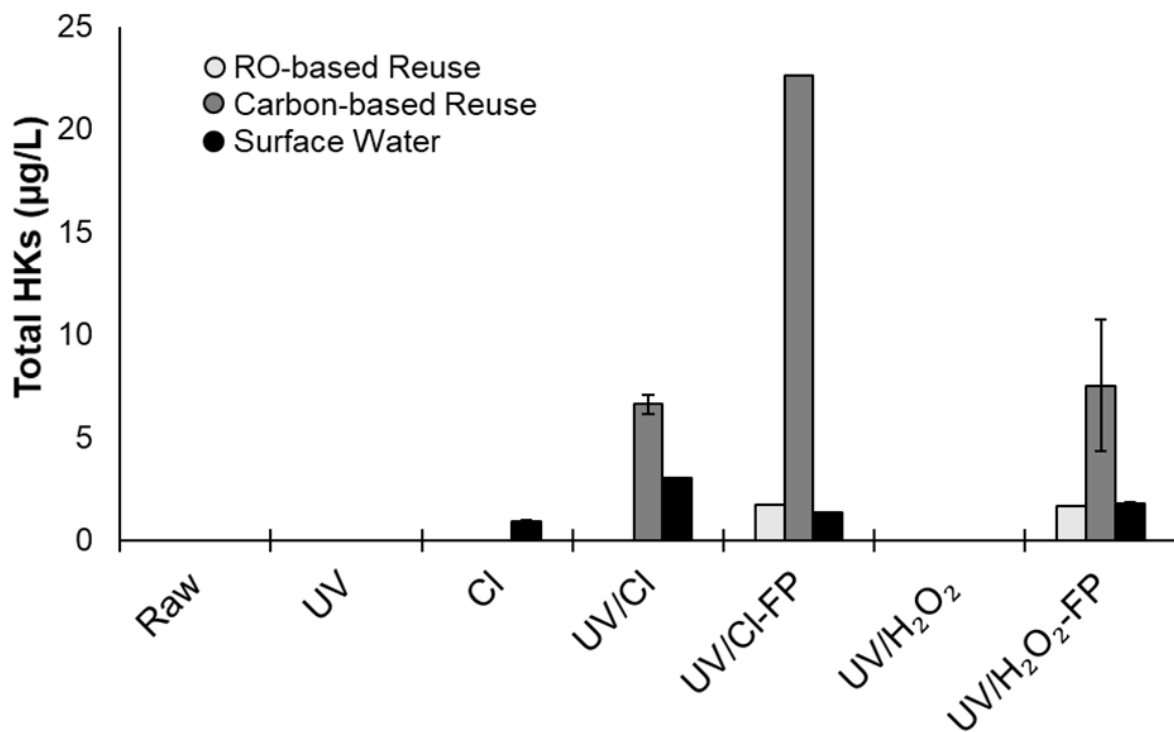


Figure E1-15. Lab-Scale HK Results.

Error bars represent the range of experimental duplicates.

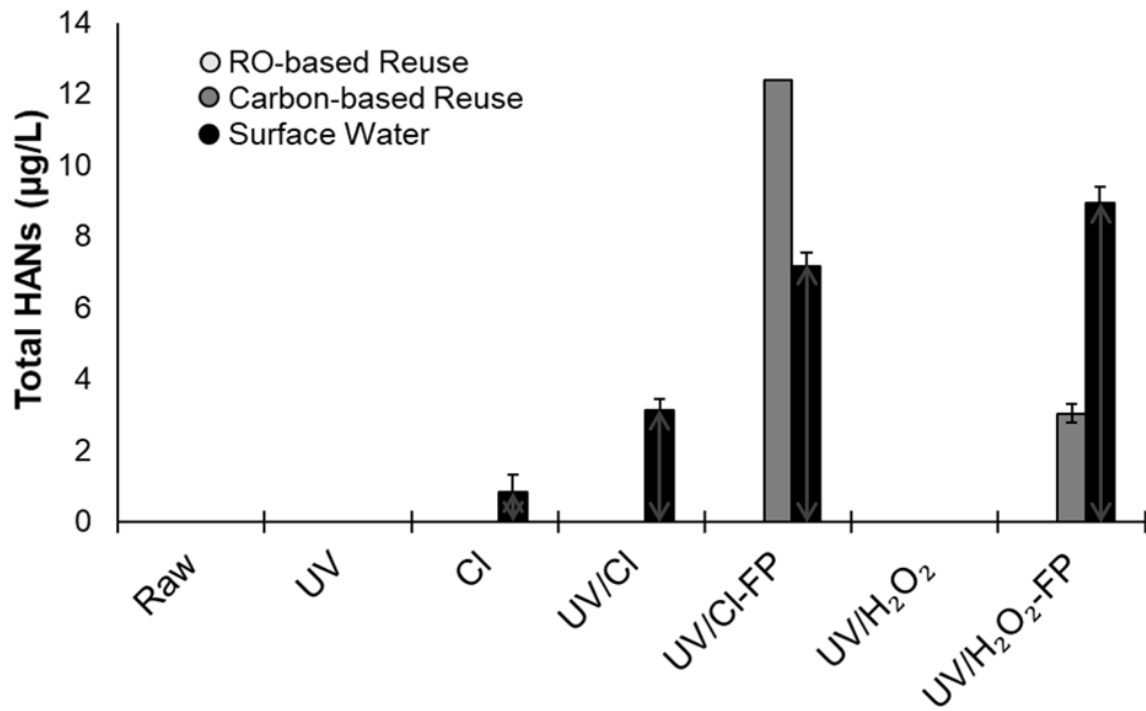


Figure E1-16. Lab-Scale HAN Results.

Error bars represent the range of experimental duplicates. The grey arrows represent the range in HAN concentration that may instead be DCIM or DCP (see Section E.5.2 for more information).

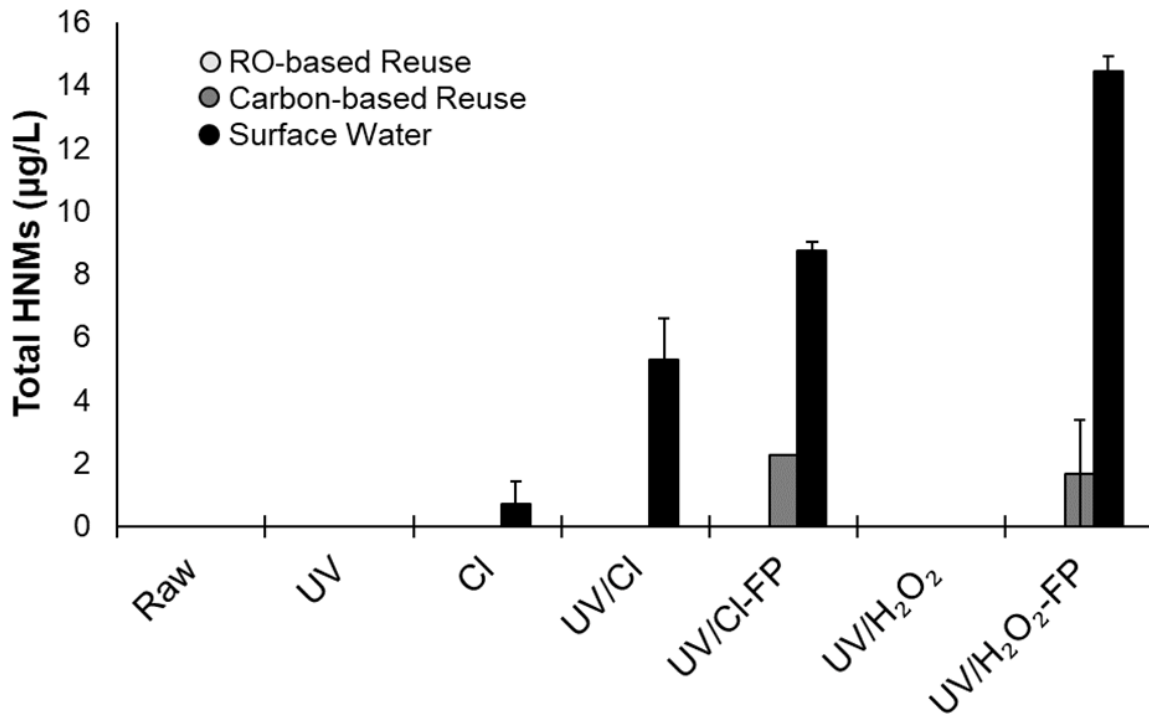


Figure E1-17. Lab-Scale HNM Results.

Error bars represent the range of experimental duplicates.

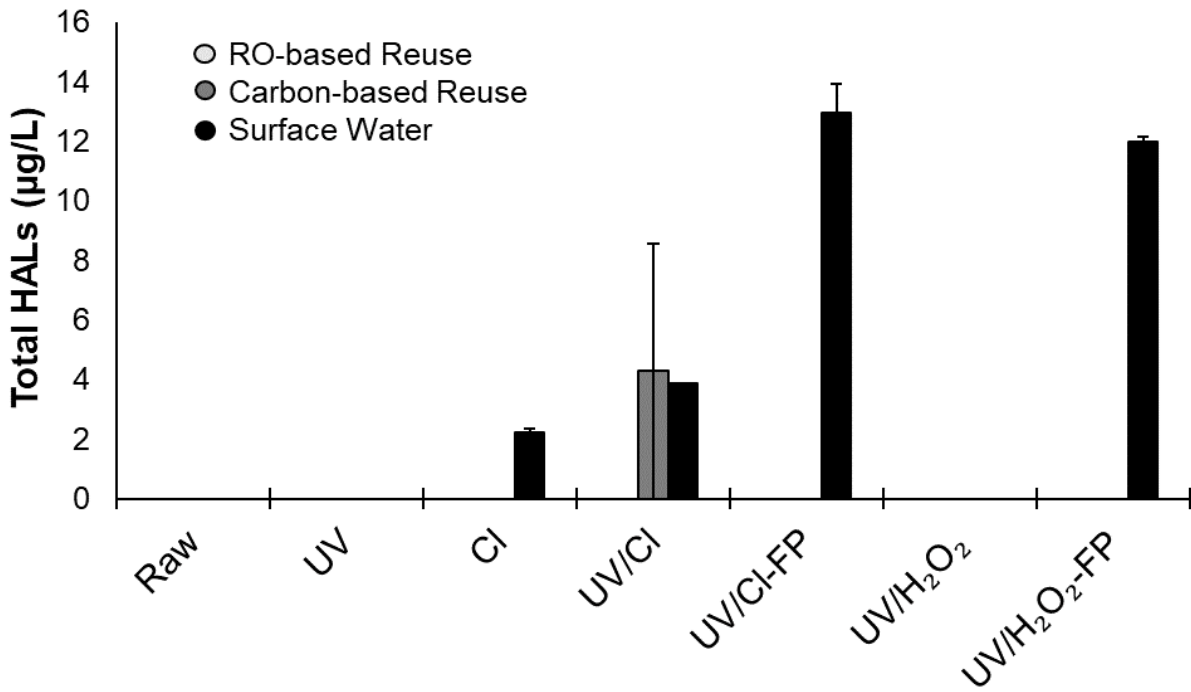


Figure E1-18. Lab-Scale HAL Results.
 Error bars represent the range of experimental duplicates.

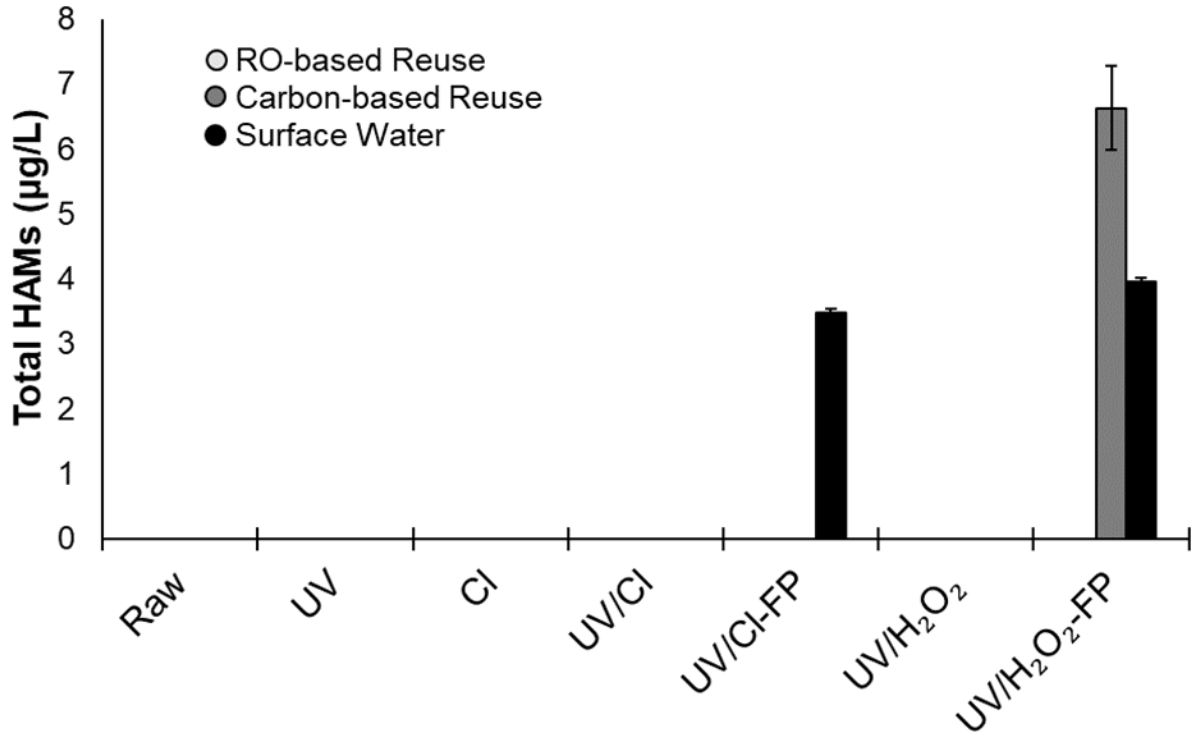


Figure E1-19. Lab-Scale HAM Results.
 Error bars represent the range of experimental duplicates.

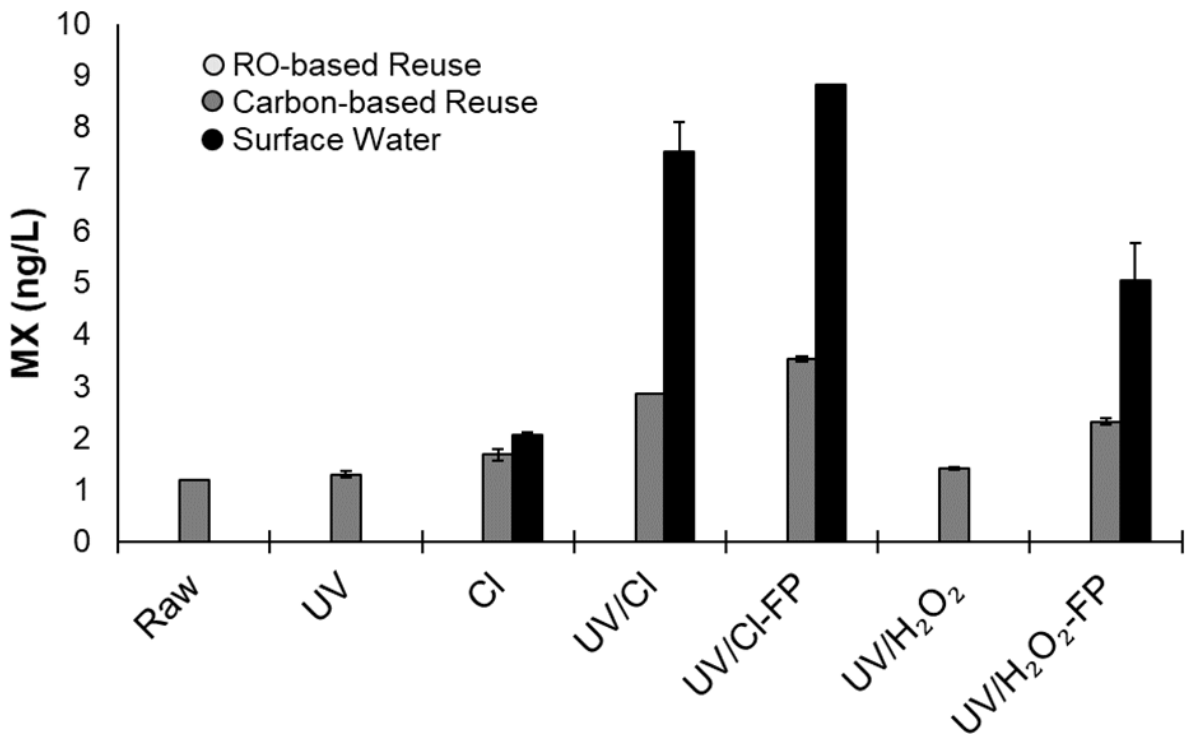


Figure E1-20. Lab-Scale MX Results.
Error bars represent the range of experimental duplicates.

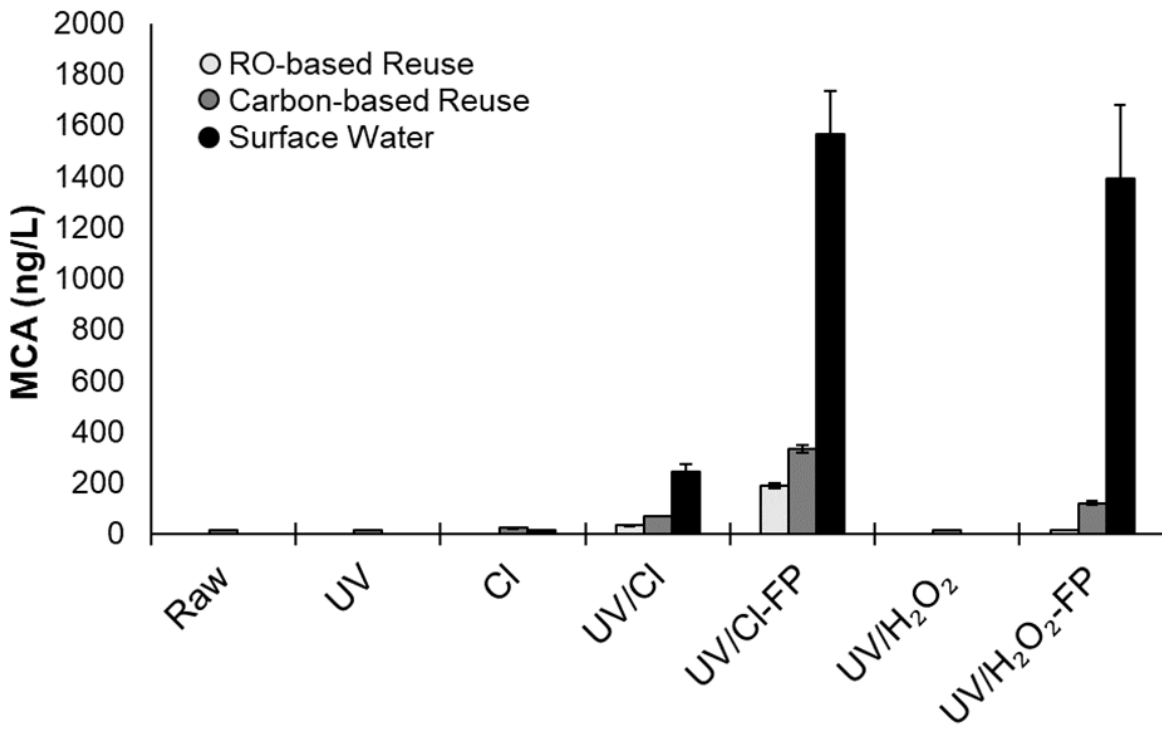


Figure E1-21. Lab-Scale MCA Results.
Error bars represent the range of experimental duplicates.

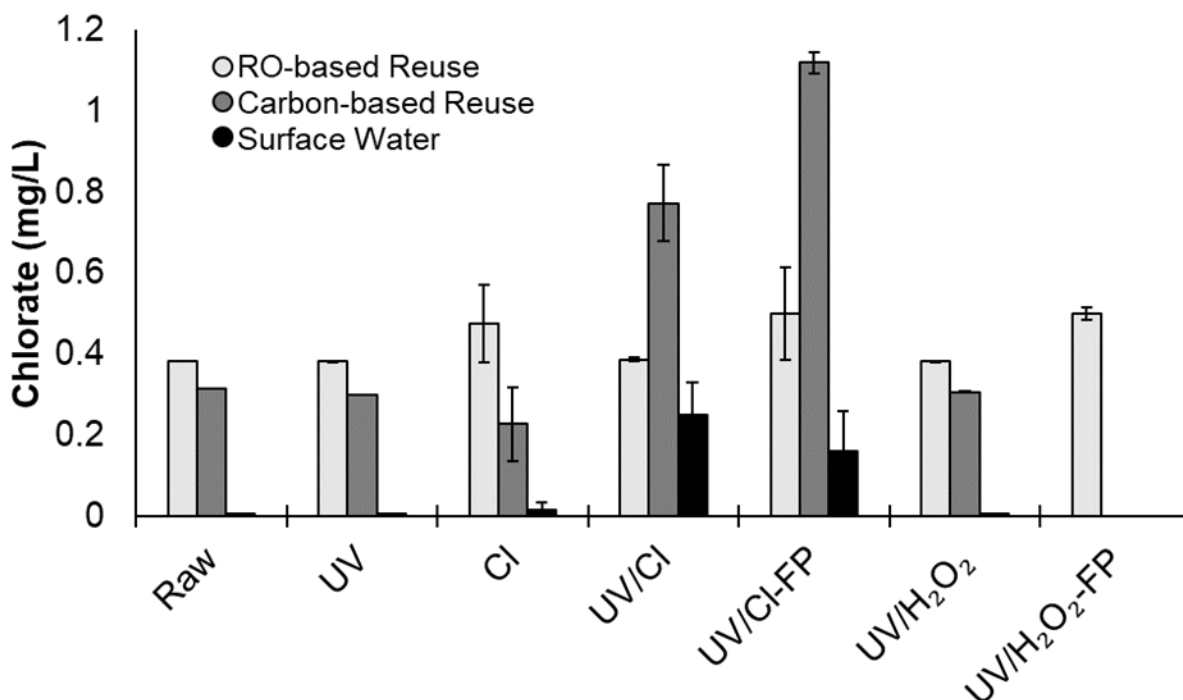


Figure E1-22. Lab-Scale Chlorate Results.
Error bars represent the range of experimental duplicates.

Oxidative stress

The Nrf2 assay detects the activation of the adaptive oxidative stress response system. This pathway serves as the first line defense to electrophilic attack of proteins and serves to restore homeostasis in the cell. This pathway is sensitive to both micropollutants and disinfection by-products. The results of this assay are shown in Figure E-23.

For the surface water, samples subject to chlorination (24-hour chlorination formation potential test) following either UV-chlorine or UV/H₂O₂ elicited the highest responses amongst the treated samples. The raw river water also elicited a positive response, which may reflect agricultural impacts on this water shed. The application of chlorine, UV, or UV in combination with chlorine or hydrogen peroxide, attenuated the raw water response, perhaps due to micropollutant destruction.

The chlorination (formation potential) samples also elicited the greatest Nrf2 activity for the carbon-based reuse water, though the activity level was roughly 4-times lower than for the surface water. In this case, the oxidative stress response was smallest in the raw water and increased with treatment, trending well with the conventional DBP results. The response from UV-chlorine, though small, was roughly twice that of UV/H₂O₂.

For the RO-based reuse, very minimal Nrf2 activity was measured where many samples were below the reporting limit. For context, a typical Nrf2 toxicity unit value for conventionally treated drinking water is 0.37 (Escher et al., 2014). Both the RO- and carbon-based reuse waters are well below this threshold.

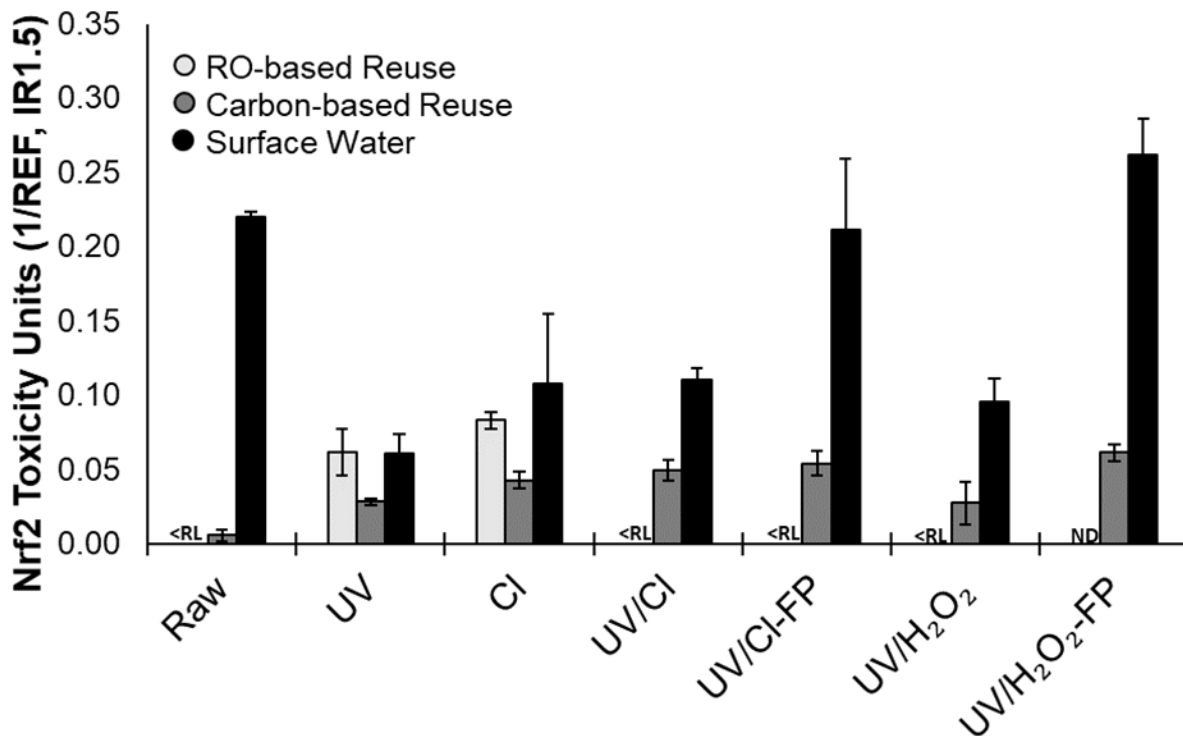


Figure E1-23. Oxidative Stress Response Activity Expressed as Toxicity Units in the Nrf2 Assay.
 Samples below the reporting limit are indicated by <RL and non-detects in the assay by ND.
 Error bars represent the standard deviation of experimental duplicates and analytical triplicates.

Genotoxicity

The DNA repair mechanism is mediated by a suite of genes known as SOS which represents the cell's response to oxidative or mutagenic damage of the genome. This mechanism is a downstream event from the oxidative stress response, meaning higher concentrations are needed to activate the SOS response (and the toxicity units, which represent the dose response, are smaller). In fact, most of the samples shown in Figure E-24 were considered non-detectable (no statistical difference from the negative control) or below the reporting limit. The surface water was the only source water to yield quantifiable genotoxicity. For that water, the application of UV-chlorine increased activity levels above chlorine alone by roughly 50%. The further application of secondary disinfection decreased the activity levels, compared to that from UV-chlorine; and the activity following secondary disinfection of the UV-chlorine-treated water was roughly 33% less than that after secondary disinfection of the UV/H₂O₂-treated water.

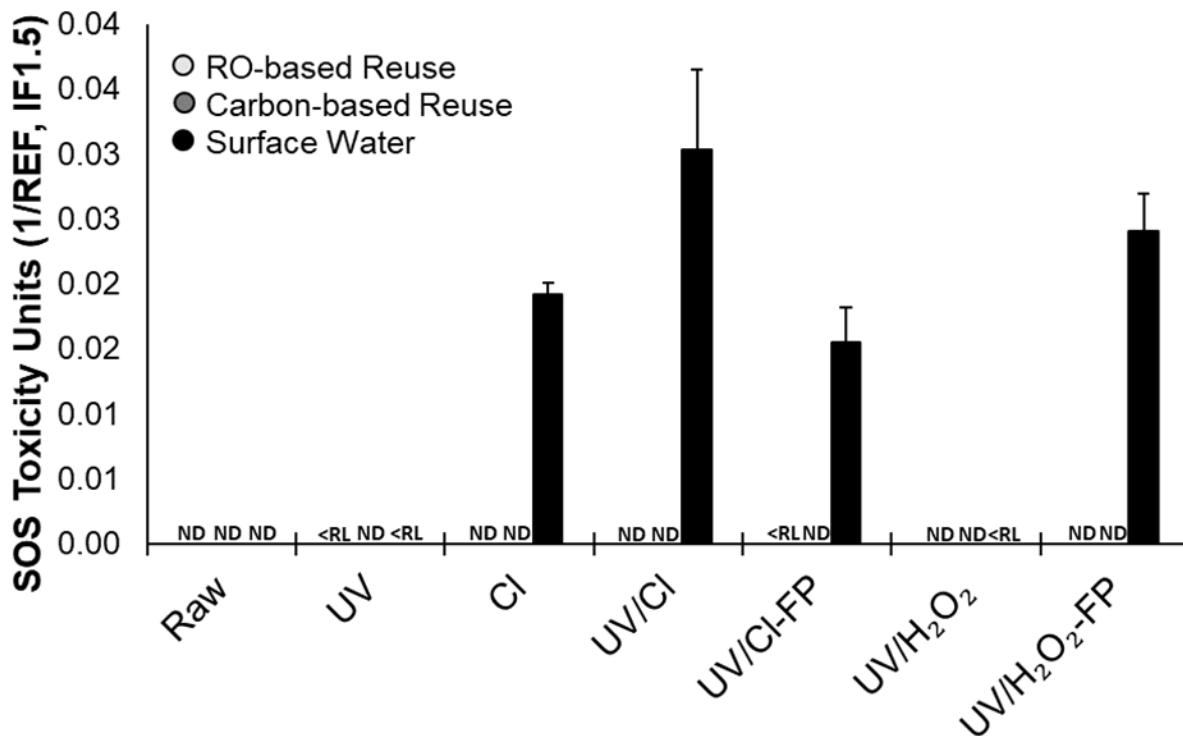


Figure E1-24. Genotoxicity of Samples Expressed as Toxicity Units in the SOS Assay.

Red lines represent typical disinfected drinking waters; samples below RL (hatched) and non-detects in the assay (white bars) values are shown for comparison and not considered genotoxic. Error bars represent the standard deviation.

Cytotoxicity and general cellular stress

The MTT dye conversion test was assayed for all of the enhanced samples to determine the metabolic status of the cells (cytotoxicity). All of the samples were considered viable (greater than 80% cellular activity), which means that there was no observed cytotoxicity in the samples.

The p53 pathway is responsive to general cellular stress and mediates cell death. No sample for any of the three waters was observed to activate this cellular defense pathway (i.e., all were non-detect).

E1.5 Quality Assurance/Quality Control

The University of Toronto lab is not licensed. All analyses are completed according to their respective standard methods (APHA et al., 2012) or manufacturer's instructions, as applicable. In addition, strict quality assurance/quality control (QA/QC) procedures are followed, including appropriate sample collection, determination of method detection limits (MDLs) and calibration control charts (CCCs).

Sample Collection. Sampling instruction sheets and sample information and chain of custody sheets are part of our sample collection program to ensure that samples are properly collected, along with relevant operational and water quality information.

Method Detection Limit (MDL). An MDL is defined as the minimum concentration of an analyte that can be identified, measured, and reported with 99% confidence that the value obtained is greater than zero. Prior to any analysis of samples, the MDLs are determined. MDLs are obtained through the analysis of seven replicates of a solution of reagent water containing the target analytes at or near the reporting limit over at least three days. MDLs are a statistical determination based on the standard deviation of the quantitation of the analytes using a student t distribution with 6 degrees of freedom and 99% confidence level. The calculated MDL is then compared with previously calculated MDLs on a given instrument and relevant literature to ensure that an acceptable precision has been achieved.

Calibration Control Charts. A calibration check standard is prepared at a known concentration to assess the accuracy of an analyzer during an analytical run. Check standards are analyzed before every sampling run, after every tenth sample (along with a blank), and at the end of each run. For the calibration curve to be deemed to be applicable, the calibration check standards must meet a number of requirements. The results of the MDL test are used to determine the mean and the standard deviation of the results. The calibration curve is deemed unacceptable if:

- 7 consecutive measurements are greater or less than the mean
- 5 out of the 6 previous samples show an increasing or decreasing trend
- 5 out of the 6 previous samples were more than 1 standard deviation from the mean
- 3 out of the 4 previous samples were more than 2 standard deviations from the mean, or
- 2 consecutive measurements were greater than 3 standard deviations from the mean

If a calibration curve is deemed to be unacceptable, the results of all subsequent samples are discarded. A new calibration curve is then prepared, and the samples are reanalyzed using the conforming calibration curve.

Standard additions. Laboratory-fortified matrix (LFM) samples are prepared for each water source to evaluate the recovery of each byproduct in that specific water and to account for any matrix-induced analyte bias. If the accuracy or percent recovery of the LFM samples fall outside of the method's specified acceptance criteria, that batch of samples will be analyzed using the method of standard addition (APHA et al., 2012). Moreover, any discovered bias will be noted in the final results.

E1.5.1 Supplemental Information for the DBP Analysis

The THMs, HAAs, HANs, HNMs, HKs, HALs, and HAMs were extracted and analyzed using liquid-liquid extraction and gas chromatography-electron capture detection, according to EPA Method 551.1. AOX was determined using an AOX analyzer (Model: Xplorer, TE Instruments, Amsterdam, Netherlands). The MX compounds and NDMA were extracted and analyzed by solid phase extraction and gas chromatography-mass spectrometry following the methods described by McKie et al. (2015) and Shen and Andrews (2011), respectively. The ions and inorganic oxyhalide byproducts were measured using ion chromatography based on EPA Method 300. Sampling and sample reservation methods are described in Table E-10.

Table E1-9. QAQC Summary for the Measured DBPs.

Italicized Detection Limits are Preliminary and are Being Assessed throughout the Study.

Analyte	Calibration			Method Detection Limit
	Retention Time (min)	Slope	R ²	
TCM	3.19-3.20	0.0106	0.9994	0.70 µg/L
BDCM	4.78	0.0597	0.9949	0.38 µg/L
DBCM	8.57	0.0533	0.9977	0.37 µg/L
TBM	14.67	0.0229	0.9974	0.44 µg/L
DCIM	10.80	0.0092	0.9987	1.05 µg/L
BCIM	16.54	0.0038	0.999	0.95 µg/L
DBIM	19.79	0.0042	0.9979	0.93 µg/L
CDIM	20.41	0.0189	0.9969	0.71 µg/L
BDIM	22.24	0.0170	0.9966	0.60 µg/L
TIM	23.59	0.0206	0.9967	0.65 µg/L
BDCNM	6.44	0.0086	0.9989	1.26 µg/L
TCNM	7.29	0.0896	0.9927	0.73 µg/L
DBCNM	12.25	0.0351	0.9959	0.96 µg/L
TCAN	3.88	0.0810	0.9846	0.32 µg/L
DCAN	5.39	0.0935	0.9992	0.22 µg/L
BCAN	10.67	0.0704	0.9990	0.23 µg/L
DBAN	16.91	0.0766	0.9988	0.25 µg/L
DCAL	3.41	0.0123	0.9990	0.73 µg/L
TCAL	4.82	0.0776	0.9980	0.57 µg/L
TBAL	19.65	0.0189	0.9996	1.02 µg/L
DCP	5.45	0.0501	0.9968	0.34 µg/L
TCP	11.34	0.0866	0.9963	0.28 µg/L
TCAM	22.34	0.0372	0.9994	1.96 µg/L
DBAM	22.94-23.02	0.0102	0.9949	1.76 µg/L
MCAA	6.38-6.41	0.0011	0.9997	1.80 µg/L
MBAA	10.51-10.57	0.0111	0.9998	1.49 µg/L
DCAA	11.46-11.50	0.0141	0.9999	0.8 µg/L
TCAA	17.21-17.26	0.0526	0.9982	0.69 µg/L
BCAA	17.75-17.77	0.0361	0.9992	0.69 µg/L
DBAA	23.20-23.21	0.0453	0.9994	0.87 µg/L
BDCAA	23.47-23.48	0.0728	0.9990	1.26 µg/L
CDBAA	26.07	0.0604	0.9991	2.30 µg/L
TBAA	27.42	0.0298	0.9858	2.50 µg/L
IAA	17.57	0.0295	0.9995	2.50 µg/L
CIAA	24.67	0.0115	0.9995	2.50 µg/L
BIAA	26.34	0.0145	0.9997	2.50 µg/L
DIAA	27.77	0.0188	0.9997	2.50 µg/L
NDMA	8.4	0.0182	0.9956	1.26 ng/L
MX	16.21	0.00258	0.9913	1.39 ng/L
MCA	10.88	0.00181	0.9970	5 ng/L
Chlorite	6.8	0.00171	0.9969	50 µg/L
Chlorate	11.3	0.3032	0.9984	16 µg/L
Bromate	10.4	0.000961	0.9998	2 µg/L
AOX	Not applicable	Not applicable	Not applicable	30 µg-Cl/L
TOC	Not applicable	Not applicable	Not applicable	0.1 mg/L

Table E1-10. Bottle Preparation and Sample Handling – Enhanced Lab Experiments.

Refer to Table E1-11. for quenching and acidification reagent descriptions.

Analyte	Sample bottle Volume (mL)	Preparation (e.g., quenching)	Post-treatment (e.g., acidification)
THMs et al.	125	Add 12.5 mg ascorbic acid Add 2 g of phosphate buffer	-
AOX	250	Add 25 mg sodium sulfite	Acidify to pH < 2 with 0.5 mL H ₂ SO ₄
HAAs	40	Add 4 mg ascorbic acid	-
Inorganics	40	Add 20 µL EDA	-
NDMA	500	Add 50 mg ascorbic acid	-
MX	1000	Add 100 mg ascorbic acid	Acidify to pH < 2 with 1.5 mL (20 drops) H ₂ SO ₄
Toxicity	2000	Add 200 mg ascorbic acid	Acidify to pH < 2 with 3 mL (40 drops) H ₂ SO ₄
General Water quality parameters	40	Add 4 mg sodium sulfite	-

All collected samples stored in the dark at 4 °C until analyzed.

Table E1-11. Sample Preservation Reagents.

Ascorbic Acid	(add solid directly to vial at 100 mg/L; approximately 5:1 molar ratio with chlorine) ACS Reagent grade.
Ethylenediamine (EDA) preservation solution, 100 mg/mL (source: EPA 300.1)	(add to final concentration of 50 mg/L; 0.5 mL per 1 L of sample) Dilute 2.8 mL of ethylenediamine (99%) (CASRN 107-15-3) to 25 mL with reagent water. Prepare fresh monthly.
Phosphate Buffer (source: EPA 551.1)	(add 1 g into 60 mL of sample) Used to lower the sample matrix pH to 4.8 to 5.5 in order to inhibit base catalyzed degradation of the haloacetonitriles, some of the chlorinated solvents, and to standardize the pH of all samples. Prepare a dry homogeneous mixture of 1% Sodium Phosphate, dibasic (Na ₂ HPO ₄)/99% Potassium Phosphate, monobasic (KH ₂ PO ₄) by weight (example: 2 g Na ₂ HPO ₄ and 198 g KH ₂ PO ₄ to yield a total weight of 200 g) Both of these buffer salts should be in granular form and of ACS grade or better. Powder would be ideal but would require extended cleanup time (outlined in Section 7.1.7.5 of EPA 551.1) to allow for buffer/solvent settling.
Sodium Sulfite	(add solid directly to vial at 100 mg/L; approximately 5:1 molar ratio with chlorine) ACS Reagent grade Na ₂ SO ₃ .

E1.5.2 Chromatographic Separation and DBP Reporting

TCM and DCAL could not be chromatographically separated by the analytical method used during the June and July 2021 ‘normal’ sampling. Accordingly, the sum of all TCM plus DCAL is reported as TCM for that period. TCM was selected for reporting because it is more abundant in chlorinated drinking water and drinking water regulations (Richardson et al., 2007).

DCAN and DCP could not be chromatographically separated by the analytical method used during the two ‘normal’ sampling campaigns and the ‘enhanced’ sampling for the surface water. Accordingly, the sum of all DCAN plus DCP is reported as DCAN for those datasets. DCAN was selected for reporting because it is more abundant in chlorinated drinking water (Krasner et al., 1989).

BCAN and DCIM could not be chromatographically separated by the analytical method used during the September 2021 ‘normal’ sampling and the ‘enhanced’ sampling for the surface water. Accordingly, the sum of all BCAN plus DCIM is reported as BCAN for those datasets. BCAN was selected for reporting because of its greater genotoxic potency (Wagner and Plewa, 2017).

BDCM and TCAL could not be chromatographically separated by the analytical method used during the September 2021 ‘normal’ sampling and the ‘enhanced’ sampling for the surface water and RO-based reuse water. Accordingly, the sum of all BDCM plus TCAL is reported as BDCM for those datasets. BDCM was selected for reporting because of its regulatory status (U.S. EPA, 2006).

E1.5.3 Supplemental Information for the Bioassays

Table E1-12. Broad Spectrum Bioassays used for the Effect of UV-AOPs

OD = optical density; RLU = relative light units.

Bioassay	Test (strain/cell line)	Species	Endpoint	Detected Signal
p53 assay	Luciferase reporter gene under the control of the p53 response element in HeLa stable cell line		Monitor activation of p53 by treatment; responsive to DNA damage and cellular stress.	Luciferase RLU of treated cells compared to negative control
SOS-Chromotest™	B-galactosidase reporter gene under the control of SOS response element in <i>E. coli</i> PQ17 bacterial strain		Activation of the DNA repair pathway to direct (mutagenic) and indirect (oxidative) in response to DNA damage	Ratio of blue (OD at 450nm) to green fluorescence emission (OD at 620 nm) in excitation of reporter enzyme substrates
ARE-Nrf2	Luciferase reporter under the control of the Nrf2 anti-oxidant response element in human breast cancer cell line MCF7		Activation of the oxidative stress response pathway Nrf2-ARE	Luciferase RLU of treated cells compared to negative control
MTT cell viability	MTT dye added to exposed HeLa stable cell line		Indicates metabolic activity and cell viability	OD at 540 nm as marker for MTT cell viability

Solid phase extraction was performed for duplicate water samples using 200 mg HLB Oasis columns (Waters Corporation). Two liters of acidified sample (pH ~2) was loaded on the cartridge, eluted with 10 mLs of acetone, and evaporated under a gentle nitrogen stream. Samples were reconstituted in 60 µL DMSO for subsequent cellular testing. Further details are provided in Zheng et al. (2015).

The human MCF7 cell-based ARE-Nrf2 assay targets the activation of the oxidative stress response pathway, detailed methods are described by Sun et al. (2017). General stress activation through p53 pathway is assayed in HeLa human cervical cancer cells and is regarded as a sensitive indicator for chemicals with genotoxic properties, where methods are described in Sun et al. (2017). During propagation, human cell lines were seeded with 104 cells per well and incubated at 37 °C with 5% CO₂ in 200 µL of media. For exposure studies, media was diluted 1000-fold with the concentrated eluent, serially diluted on the plate, and incubated for 16-18 hours. The positive control (iodoacetamide for ARE-Nrf2; doxorubicin for p53) and negative control (DMSO with 10% saline) was tested on every plate, alongside samples. The media was replaced with PBS and Steadylite™ luciferase for colorimetric evaluation.

Activation of the DNA repair pathway mediated by the SOS-response pathway was performed to detect the global response to DNA damage, using the SOS-Chromotest™ (EBPI Inc, Mississauga, ON) assay, detailed methods are described in Zheng et al. (2015). Briefly, SOS lyophilized bacteria was hydrated overnight and diluted to 10⁶ cells (OD₆₀₀ of 0.05). Sample concentrates were diluted 5-fold in the first well, serially diluted (50% step-wise) for a total of 8 concentrations and run in duplicate on the plate. The positive control (4-NQO) and negative control (MQ blank and DMSO with 10% saline) was tested on every plate, alongside samples. 100 µL of bacterial culture was incubated for 2 hours at room temperature prior to colorimetric measurements. Detailed methods can be found in Zheng et al. (2015).

For adaptive stress response bioassays that use reporter genes, the response is determined as an induction ratio (IR), where an IR 1.5 (or greater) is considered genotoxic. For genotoxic samples, effect concentration (EC) for IR 1.5 is derived from the linear slope of dose-response curve, where the concentration corresponds to the relative enrichment factor (REF). Further details are presented in Escher et al. (2012). The EC_{IR1.5} corresponds to how many times the sample must be concentrated or diluted to elicit an IR of 1.5. This is considered to be a sensitive benchmark parameter (Reungoat et al., 2010). The results are expressed as 1/EC_{IR1.5} and referred to as Toxicity Units; therefore, a higher number represents a higher genotoxic effect.

For the ARE-Nrf2, p53 and MTT assay, sample concentrates were serially diluted such that 4 concentrations were tested in triplicate. Cells were exposed for 16-18 hours prior to spectrophotometric quantification. Detailed methods can be found in Sun et al. (2017). Cytotoxicity of fractions was measured by conversion of MTT dye, detailed procedure is presented in Sun et al. (2017). Cells were plated and exposed the same as in measurements of ARE-Nrf2 and p53 potency, where samples with cell viability greater than 80% were considered for toxicity bioassay assessment. In the SOS assay, duplicate samples were serially diluted such that 8 concentrations were tested in duplicate, with an exposure time of 2 hours prior to substrate additions and spectrophotometric quantification. Detailed methods can be found in Zheng et al. (2015).

The limit of detection (LOD) corresponds to 3 times the standard deviation of the positive controls that elicited a significantly different response from the controls, while the limit of reporting corresponds to 3 times the standard deviation of the negative controls. For example, the standard deviation of the positive control for the SOS (4-NQO) was 0.15 (i.e., the LOD was

at an IR of 1.43) and the limit of reporting (LOR) was IR 1.19. For the ARE-NRF2 assay, the LOD was 1.28 (where the positive control was iodoacetamide) and the LOR was 1.26. That means that the IR of 1.5 used to derive the ECIR1.5 is relatively close to the threshold of effect and correspondingly, the ECIR1.5 is close to the LOEC (lowest observed effect concentration). An EC IR 1.5 is also defined by the International Organization for Standardization as the threshold of genotoxic effect (International Organization for Standardization, 2000), providing the sample was not cytotoxic (growth < 0.5). As such, ECIR1.5 should always be preferred over a LOEC value (Macova et al., 2011).

E1.6 Complete “Normal” Campaign Results

Table E1-13. Disinfection Byproduct Concentrations Plant A.

Average ± range in µg/L or mg/L. <MDL = below method detection limit; - = no data/not applicable.

DBP Class and units	DBP	A					
		Influent		Effluent		Downstream	
		June/July 2021	September 2021	June/July 2021	September 2021	June/July 2021	September 2021
Trihalomethanes (THMs) µg/L	Trichloromethane	9.5 ± 0.08 ^a	12.6 ± 0.06	13.9 ± 0.67 ^a	13.8 ± 1.3	13.4 ± 0.9 ^a	20.2 ± 2.2
	Bromodichloromethane	<MDL	1.5 ± 0.02 ^d	<MDL	2.0 ± 0.09 ^d	19.9 ± 0.8	14.7 ± 1.4 ^d
	Dibromochloromethane	<MDL	3.4 ± 0.03	2.6 ± 0.1	3.8 ± 0.2	17.9 ± 0.3	15.0 ± 1.2
	Tribromomethane	<MDL	<MDL	<MDL	<MDL	5.5 ± 0.09	2.8 ± 0.18
Iodinated Trihalomethanes (I-THMs) µg/L	Triiodomethane	<MDL	<MDL	<MDL	<MDL	<MDL	<MDL
	Bromochloroiodomethane	<MDL	<MDL	<MDL	<MDL	<MDL	<MDL
	Chlorodiiodomethane	<MDL	<MDL	<MDL	<MDL	<MDL	<MDL
	Dibromoiodomethane	<MDL	<MDL	<MDL	<MDL	<MDL	<MDL
	Bromodiiodomethane	<MDL	<MDL	<MDL	<MDL	<MDL	<MDL
	Dichloroiodomethane	<MDL	- ^c	<MDL	- ^c	<MDL	- ^c
Haloacetic Acids (HAAs) µg/L	Chloroacetic acid	-	-	-	-	-	-
	Bromoacetic acid	<MDL	<MDL	<MDL	<MDL	<MDL	3.6 ± 0.4
	Dichloroacetic acid	<MDL	<MDL	2.8 ± 0.5	1.8 ± 1.8	14.1 ± 0.03	10.6 ± 0.1
	Trichloroacetic acid	<MDL	<MDL	1.2 ± 0.06	1.3 ± 0.005	3.8 ± 0.01	3.6 ± 0.03
	Bromochloroacetic acid	<MDL	<MDL	1.3 ± 0.2	1.6 ± 0.01	6.1 ± 0.04	5.2 ± 0.04
	Dibromoacetic acid	<MDL	<MDL	1.3 ± 0.1	1.6 ± 0.02	4.4 ± 0.01	3.9 ± 0.01
	Bromodichloroacetic acid	<MDL	<MDL	1.5 ± 0.02	2.0 ± 0.1	1.5 ± 0.005	5.1 ± 0.6
	Chlorodibromoacetic acid	<MDL	<MDL	<MDL	2.7 ± 0.1	<MDL	10.1 ± 1.4
	Tribromoacetic acid	<MDL	<MDL	<MDL	<MDL	<MDL	<MDL
Iodinated Haloacetic Acids (I-HAAs) µg/L	Iodoacetic acid	<MDL	<MDL	<MDL	<MDL	<MDL	<MDL
	Diiodoacetic acid	<MDL	<MDL	<MDL	<MDL	<MDL	<MDL
	Bromoiiodoacetic acid	<MDL	<MDL	<MDL	<MDL	<MDL	<MDL
	Chloroiiodoacetic acid	-	-	-	-	-	-
Haloacetonitriles (HANs) µg/L	Trichloroacetonitrile	<MDL	<MDL	<MDL	<MDL	<MDL	<MDL
	Dichloroacetonitrile	<MDL	<MDL ^b	<MDL	<MDL ^b	<MDL	1.8 ± 0.2 ^b
	Dibromoacetonitrile	<MDL	<MDL	<MDL	<MDL	<MDL	1.8 ± 0.1
	Bromochloroacetonitrile	<MDL	<MDL ^c	<MDL	<MDL ^c	<MDL	<MDL ^c

Continued on next page

Continued from previous page

Haloketones (HKs) µg/L	1,1-Dichloro-2-propanone	^a	^b	^b	^b	^b	^b
	1,1,1-Trichloro-2-propanone	<MDL	<MDL	2.6 ± 0.1	<MDL	3.7 ± 0.01	2.3 ± 0.03
Halonitromethanes (HNMs) µg/L	Trichloronitromethane	<MDL	<MDL	<MDL	<MDL	<MDL	<MDL
	Bromodichloronitromethane	<MDL	<MDL	<MDL	<MDL	<MDL	<MDL
	Dibromochloronitromethane	-	-	-	-	-	-
Haloacetamides (HAMs) µg/L	Trichloroacetamide	<MDL	<MDL	<MDL	<MDL	<MDL	<MDL
	Dibromoacetamide	<MDL	<MDL	<MDL	<MDL	<MDL	1.8 ± 0.1
Haloacetaldehydes (HALs) µg/L	Dichloroacetaldehyde	^a	8.8 ± 0.1	^a	9.9 ± 1.2	^a	<MDL
	Trichloroacetaldehyde	<MDL	^d	4.4 ± 0.1	^d	<MDL	^d
	Tribromoacetaldehyde	<MDL	<MDL	<MDL	<MDL	<MDL	<MDL
Halogenated Furanones (MX Compounds) ng/L	3-Chloro-4-(dichloromethyl)-5-hydroxy-2(5H)-furanone	<MDL	<MDL	1.5 ± 0.05	1.9 ± 0.1	4.7 ± 0.5	3.6 ± 0.01
	2,3-Dichloro-4-oxobutenoic acid	<MDL	<MDL	33.8 ± 1.88	11.2 ± 1.1	336 ± 22.5	163.1 ± 27
Nitrosamines ng/L	N-nitrosodimethylamine	6.1 ± 0.5	<MDL	5.4 ± 0.02	<MDL	7.3 ± 0.6	<MDL
Inorganic DBPs mg/L	Chlorite	<MDL	<MDL	<MDL	<MDL	<MDL	<MDL
	Chlorate	<MDL	<MDL	0.07	0.1 ± 0.01	0.09 ± 0.001	0.1 ± 0.001
	Bromate	<MDL	<MDL	<MDL	<MDL	<MDL	<MDL
Other	Adsorbable organohalides (µg-Cl/L)	<MDL	<MDL	49.3 ± 8.1	52 ± 1.3	93 ± 18.3	113.1 ± 3.1
	Bromide (mg/L)	<MDL	3.8 ± 0.1	<MDL	3.5 ± 0.1	<MDL	3.8 ± 0.2
	Chloride (mg/L)	212.7 ± 0.4	227.7 ± 1.2	218.7 ± 0.5	222.1 ± 9.7	248.0 ± 0.3	224.5 ± 6.7
	Phosphate (mg/L)	<MDL	0.009	<MDL	0.006 ± 0.002	3 ± 0.7	0.01
	Sulfate (mg/L)	207.3 ± 0.5	155.5 ± 0.8	208.2 ± 0.3	148.3 ± 9	185 ± 2.7	156.6 ± 5.8
	Conductivity (µS/cm)	1862	1626	2332	1607	1983	-
	TOC (mg/L)	1.4 ± 0.004	1.4 ± 0.007	1.4 ± 0.0002	11.3 ± 2.6	1.5 ± 0.1	1.2 ± 0.03
	DOC (mg/L)	1.1	2.5	1.1	8.7	1.3	2.6
	Ammonia (mg/L)	0.02 ± 0.0013	0.2 ± 0.014	0.02 ± 0.0008	0.02 ± 0.003	0.03 ± 0.002	0.05 ± 0.006
	Nitrate (mg/L)	0.5 ± 0.02	0.3 ± 0.0006	0.5 ± 0.01	0.3 ± 0.005	0.6 ± 0.003	0.3 ± 0.004
	Nitrite (mg/L)	0.02 ± 0.0005	<MDL	<MDL	<MDL	<MDL	<MDL
	pH	7.7 ± 0.2	7.3 ± 0.04	7.8 ± 0.05	7.2 ± 0.07	7.8 ± 0.02	7.3 ± 0.07
	UV ₂₅₄ (cm ⁻¹)	0.05 ± 0.01	0.04 ± 0.001	0.05 ± 0.001	0.9 ± 0.004	0.05 ± 0.002	0.03 ± 0.005

- TCM+DCAL reported as TCM. See Chromatographic separation and DBP reporting for more information.
- DCAN+DCP reported as DCAN. See Chromatographic separation and DBP reporting for more information.
- BCAN+DCIM reported as BCAN. See Chromatographic separation and DBP reporting for more information.
- BDCM+TCAL reported as BDCM. See Chromatographic separation and DBP reporting for more information.

Table E1-14. Disinfection Byproduct Concentrations at Plant B.

Average ± range in µg/L or mg/L. <MDL = below method detection limit; - = no data/not applicable.

DBP Class and units	DBP	B					
		Influent		Effluent		Downstream	
		June/July 2021	September 2021	June/July 2021	September 2021	June/July 2021	September 2021
Trihalomethanes (THMs) µg/L	Trichloromethane	31.6 ± 1.2 ^a	24.1 ± 5.9	30.3 ^a	30.4 ± 0.2	16.5 ± 0.4 ^a	20.9 ± 1.03
	Bromodichloromethane	9.3 ± 0.6	8.5 ± 2.0 ^d	6.4	9.3 ± 0.2 ^d	5.2 ± 0.03	6.1 ± 0.3 ^d
	Dibromochloromethane	3.0 ± 0.1	4.5 ± 0.4	<MDL	3.2 ± 0.04	<MDL	3.1 ± 0.06
	Tribromomethane	<MDL	<MDL	<MDL	<MDL	<MDL	<MDL
Iodinated Trihalomethanes (I-THMs) µg/L	Triiodomethane	<MDL	<MDL	<MDL	<MDL	<MDL	<MDL
	Bromochloroiodomethane	<MDL	<MDL	<MDL	<MDL	<MDL	<MDL
	Chloroiodomethane	<MDL	<MDL	<MDL	<MDL	<MDL	<MDL
	Dibromoiodomethane	<MDL	<MDL	<MDL	<MDL	<MDL	<MDL
	Bromodiiodomethane	<MDL	<MDL	<MDL	<MDL	<MDL	<MDL
	Dichloroiodomethane	<MDL	- ^c	<MDL	- ^c	<MDL	- ^c
	Bromoacetic acid	<MDL	1.7 ± 0.2	<MDL	1.5 ± 0.01	<MDL	<MDL
	Dichloroacetic acid	<MDL	1.3 ± 0.3	2.7 ± 0.09	3.2 ± 0.3	4.0 ± 0.1	1.7 ± 0.3
	Trichloroacetic acid	<MDL	1.1 ± 0.02	1.0 ± 0.001	1.1	1.2 ± 0.01	1.3 ± 0.005
	Bromochloroacetic acid	<MDL	<MDL	<MDL	<MDL	<MDL	<MDL
	Dibromoacetic acid	<MDL	<MDL	<MDL	<MDL	<MDL	<MDL
	Bromodichloroacetic acid	<MDL	<MDL	<MDL	<MDL	1.5 ± 0.002	<MDL
	Chlorodibromoacetic acid	<MDL	<MDL	<MDL	2.8 ± 0.3	<MDL	<MDL
	Tribromoacetic acid	<MDL	<MDL	<MDL	<MDL	<MDL	<MDL
Iodinated Haloacetic Acids (I-HAAs) µg/L	Iodoacetic acid	<MDL	<MDL	<MDL	<MDL	<MDL	<MDL
	Diiodoacetic acid	<MDL	<MDL	<MDL	<MDL	<MDL	<MDL
	Bromoiodoacetic acid	<MDL	<MDL	<MDL	<MDL	<MDL	<MDL
	Chloroiodoacetic acid	-	-	-	-	-	-
Haloacetonitriles (HANs) µg/L	Trichloroacetonitrile	<MDL	<MDL	<MDL	<MDL	<MDL	<MDL
	Dichloroacetonitrile	3.3 ± 0.2	3.7 ± 0.2 ^b	1.7 ± 1.7	4.3 ± 0.07 ^b	3.1 ± 0.02	3.8 ± 0.4 ^b
	Dibromoacetonitrile	<MDL	<MDL	<MDL	<MDL	<MDL	<MDL
	Bromochloroacetonitrile	<MDL	<MDL ^c	<MDL	<MDL ^c	<MDL	<MDL ^c

Continued on next page

Continued from previous page

Haloketones (HKs) µg/L	1,1-Dichloro-2-propanone	- ^b					
	1,1,1-Trichloro-2-propanone	<MDL	<MDL	<MDL	<MDL	<MDL	<MDL
Halonitromethanes (HNMs) µg/L	Trichloronitromethane	<MDL	<MDL	<MDL	<MDL	<MDL	<MDL
	Bromodichloronitromethane	<MDL	<MDL	<MDL	<MDL	<MDL	<MDL
	Dibromochloronitromethane	-	-	-	-	-	-
Haloacetamides (HAMs) µg/L	Trichloroacetamide	<MDL	<MDL	<MDL	<MDL	<MDL	<MDL
	Dibromoacetamide	<MDL	<MDL	<MDL	<MDL	<MDL	<MDL
Haloacetaldehydes (HALs) µg/L	Dichloroacetaldehyde	- ^a	<MDL	- ^a	<MDL	- ^a	<MDL
	Trichloroacetaldehyde monohydrate	<MDL	- ^d	<MDL	- ^d	<MDL	- ^d
	Tribromoacetaldehyde	<MDL	<MDL	<MDL	<MDL	<MDL	<MDL
Halogenated Furanones (MX Compounds) ng/L	3-Chloro-4-(dichloromethyl)-5-hydroxy-2(5H)-furanone	<MDL	<MDL	<MDL	1.9 ± 0.08	<MDL	<MDL
	2,3-Dichloro-4-oxobutenoic acid	<MDL	<MDL	<MDL	11.3 ± 1.09	<MDL	<MDL
Nitrosamines ng/L	N-nitrosodimethylamine	17.0 ± 0.4	22.0 ± 1.1	9.1 ± 0.5	<MDL	13.4	<MDL
Inorganic DBPs mg/L	Chlorite	<MDL	<MDL	<MDL	<MDL	<MDL	<MDL
	Chlorate	<MDL	0.08 ± 0.0006	0.4 ± 0.01	0.5 ± 0.005	0.5 ± 0.01	0.5 ± 0.002
	Bromate	<MDL	<MDL	<MDL	<MDL	<MDL	<MDL
Other	Adsorbable organohalides (µg-Cl-/L)	<MDL	<MDL	<MDL	52.0 ± 1.3	<MDL	<MDL
	Bromide (mg/L)	0.006 ± 0.0001	0.003 ± 0.0004	0.008 ± 0.0005	3.5 ± 0.1	0.005 ± 0.0002	0.003 ± 0.0005
	Chloride (mg/L)	8.8 ± 0.3	6.9 ± 0.2	17.3 ± 0.9	222.1 ± 10	15.1 ± 0.2	11.8 ± 0.03
	Phosphate (mg/L)	<MDL	0.2 ± 0.2	<MDL	0.005 ± 0.002	<MDL	<MDL
	Sulfate (mg/L)	0.2 ± 0.01	0.3 ± 0.09	0.4 ± 0.04	148.3 ± 8.9	5.9 ± 0.07	5.5 ± 0.06
	Conductivity (µS/cm)	944.5	267.5	1406	272.2	1025	342
	TOC (mg/L)	0.3 ± 0.04	<MDL	0.3 ± 0.03	<MDL	0.2 ± 0.01	<MDL
	DOC mg/L	0.3	<MDL	0.3	<MDL	0.2	<MDL
	Ammonia mg/L	0.3 ± 0.07	0.5 ± 0.1	0.03 ± 0.004	0.02 ± 0.003	0.063 ± 0.005	0.05 ± 0.003
	Nitrate mg/L	0.4 ± 0.03	0.5 ± 0.006	0.9 ± 0.04	0.3 ± 0.005	0.7 ± 0.02	0.5 ± 0.006
	Nitrite mg/L	0.3 ± 0.002	0.02 ± 0.0006	0.003 ± 0.0001	<MDL	0.003 ± 0.0002	<MDL
	pH	7.7 ± 0.2	6.1 ± 0.07	7.5 ± 0.1	7.3 ± 0.07	8.4 ± 0.1	7.0 ± 0.09
	UV ₂₅₄ cm ⁻¹	0.08 ± 0.03	0.002 ± 0.001	0.03 ± 0.01	0.9 ± 0.004	0.04 ± 0.008	0.005 ± 0.0005

- TCM+DCAL reported as TCM. See Chromatographic separation and DBP reporting for more information.
- DCAN+DCP reported as DCAN. See Chromatographic separation and DBP reporting for more information.
- BCAN+DCIM reported as BCAN. See Chromatographic separation and DBP reporting for more information.
- BDCM+TCAL reported as BDCM. See Chromatographic separation and DBP reporting for more information.

Table E1-15. Disinfection Byproduct Concentrations Plant C.
Average ± range in µg/L or mg/L. <MDL = below method detection limit; - = no data/not applicable.

DBP Class and units	DBP	C					
		Influent		Effluent		Downstream	
		June/July 2021	September 2021	June/July 2021	September 2021	June/July 2021	September 2021
Trihalomethanes (THMs) µg/L	Trichloromethane	<MDL ^a	4.1 ± 0.007	<MDL ^a	4.7 ± 0.2	-	4.8 ± 0.06
	Bromodichloromethane	<MDL	1.9 ± 0.08 ^d	<MDL	1.8 ± 0.01 ^d	-	3.9 ± 0.06 ^d
	Dibromochloromethane	5.3 ± 0.5	3.4 ± 0.003	2.9 ± 0.023	3.0 ± 0.04	-	6.6 ± 0.04
	Tribromomethane	8.1 ± 0.7	<MDL	<MDL	<MDL	-	3.2 ± 0.01
Iodinated Trihalomethanes (I-THMs) µg/L	Triiodomethane	<MDL	<MDL	<MDL	<MDL	-	<MDL
	Bromochloroiodomethane	<MDL	<MDL	<MDL	<MDL	-	<MDL
	Chloroiodomethane	<MDL	<MDL	<MDL	<MDL	-	<MDL
	Dibromoiodomethane	<MDL	<MDL	<MDL	<MDL	-	<MDL
	Bromodiiodomethane	<MDL	<MDL	<MDL	<MDL	-	<MDL
	Dichloroiodomethane	<MDL	- ^c	<MDL	- ^c	-	- ^c
Haloacetic Acids (HAAs) µg/L	Chloroacetic acid	-	-	-	-	-	-
	Bromoacetic acid	1.6 ± 1.6	<MDL	4.5 ± 0.08	1.9	3.3 ± 0.1	<MDL
	Dichloroacetic acid	<MDL	0.9 ± 0.2	<MDL	<MDL	<MDL	1.1 ± 1.1
	Trichloroacetic acid	<MDL	1.1 ± 0.005	<MDL	1.1	1.0 ± 0.005	1.1
	Bromochloroacetic acid	<MDL	<MDL	<MDL	0.9	1.5 ± 0.01	1.3 ± 0.005
	Dibromoacetic acid	<MDL	<MDL	1.0 ± 0.01	1.0	1.6 ± 0.02	1.6 ± 0.01
	Bromodichloroacetic acid	<MDL	<MDL	1.5 ± 0.002	1.8	1.5 ± 0.007	1.9
	Chlorodibromoacetic acid	<MDL	<MDL	<MDL	<MDL	<MDL	<MDL
	Tribromoacetic acid	2.7 ± 0.9	<MDL	<MDL	<MDL	2.8 ± 0.2	<MDL
	Iodinated Haloacetic Acids (I-HAAs) µg/L	Iodoacetic acid	<MDL	<MDL	<MDL	<MDL	<MDL
Diiodoacetic acid		<MDL	<MDL	<MDL	<MDL	<MDL	<MDL
Bromiodoacetic acid		<MDL	<MDL	<MDL	<MDL	<MDL	<MDL
Chloriodoacetic acid		-	-	-	-	-	-

Continued on next page

Continued from previous page

Haloacetonitriles (HANs) µg/L	Trichloroacetonitrile	<MDL	<MDL	<MDL	<MDL	-	<MDL
	Dichloroacetonitrile	<MDL	<MDL ^b	<MDL	<MDL ^b	-	<MDL ^b
	Dibromoacetonitrile	<MDL	<MDL	<MDL	<MDL	-	1.5 ± 0.1
	Bromochloroacetonitrile	<MDL	<MDL ^c	<MDL	<MDL ^c	-	<MDL ^c
Haloketones (HKs) µg/L	1,1-Dichloro-2-propanone	- ^b	- ^b	- ^b	- ^b	-	- ^b
	1,1,1-Trichloro-2-propanone	<MDL	<MDL	<MDL	<MDL	-	<MDL
Halonitromethanes (HNMs) µg/L	Trichloronitromethane	<MDL	<MDL	<MDL	<MDL	-	<MDL
	Bromodichloronitromethane	<MDL	<MDL	<MDL	<MDL	-	<MDL
	Dibromochloronitromethane	-	-	-	-	-	-
Haloacetamides (HAMs) µg/L	Trichloroacetamide	<MDL	<MDL	<MDL	<MDL	-	<MDL
	Dibromoacetamide	<MDL	<MDL	<MDL	<MDL	-	<MDL
Haloacetaldehydes (HALs) µg/L	Dichloroacetaldehyde	- ^a	<MDL	- ^a	<MDL	-	<MDL
	Trichloroacetaldehyde	<MDL	- ^d	<MDL	- ^d	-	- ^d
	Tribromoacetaldehyde	<MDL	<MDL	<MDL	<MDL	-	<MDL
Halogenated Furanones (MX Compounds) ng/L	3-Chloro-4-(dichloromethyl)-5-hydroxy-2(SH)-furanone	<MDL	<MDL	<MDL	<MDL	<MDL	<MDL
	2,3-Dichloro-4-oxobutenoic acid	<MDL	<MDL	39.8 ± 0.8	-	-	41.5 ± 8.1
Nitrosamines ng/L	N-nitrosodimethylamine	8.3 ± 0.5	9.3 ± 2.5	4.9 ± 0.2	1.8	9.0	<MDL
Inorganic DBPs mg/L	Chlorite	<MDL	<MDL	<MDL	<MDL	<MDL	<MDL
	Chlorate	<MDL	<MDL	0.1	0.4 ± 0.02	0.3 ± 0.001	0.8 ± 0.004
	Bromate	<MDL	<MDL	<MDL	<MDL	<MDL	<MDL
Other	Adsorbable organohalides (µg-Cl/L)	<MDL	<MDL	<MDL	<MDL	<MDL	<MDL
	Bromide (mg/L)	0.2 ± 0.002	0.2 ± 0.001	0.2 ± 0.001	0.2 ± 0.005	0.2 ± 0.003	0.2 ± 0.0008
	Chloride (mg/L)	72.3 ± 0.7	80 ± 0.61	76.8 ± 0.3	85.3 ± 0.3	178.8 ± 0.8	167.7 ± 1.9
	Phosphate (mg/L)	<MDL	-	<MDL	<MDL	<MDL	0.009
	Sulfate (mg/L)	11.4 ± 0.1	14.0 ± 0.3	11.4 ± 0.1	13.6 ± 0.1	12.1 ± 0.04	13.9 ± 0.2
	Conductivity (µS/cm)	557.7	541.4	995.4	551.5	919.6	856.8
	TOC (mg/L)	0.3	0.09 ± 0.02	0.4	0.08 ± 0.03	0.6	0.1 ± 0.004
	DOC (mg/L)	0.3	0.2	0.4	0.2	0.6	0.3
	Ammonia (mg/L)	0.1 ± 0.03	0.6	0.02 ± 0.0008	0.1 ± 0.02	0.05 ± 0.01	0.05 ± 0.004
	Nitrate (mg/L)	0.8 ± 0.003	0.9 ± 0.01	0.9 ± 0.03	1.1 ± 0.001	1.0 ± 0.007	1.0 ± 0.02
	Nitrite (mg/L)	0.07 ± 0.001	0.03 ± 0.0003	0.002	<MDL	0.001 ± 0.0002	<MDL
	pH	6.6 ± 0	6.5 ± 0	7.6 ± 0	6.5 ± 0.03	8.1 ± 0	7.7 ± 0.3
	UV ₂₅₄ (cm ⁻¹)	0.02 ± 0.01	0.004 ± 0.0007	0.004 ± 0.001	0.001 ± 0.0001	-	0.01 ± 0.001

- TCM+DCAL reported as TCM. See Chromatographic separation and DBP reporting for more information.
- DCAN+DCP reported as DCAN. See Chromatographic separation and DBP reporting for more information.
- BCAN+DCIM reported as BCAN. See Chromatographic separation and DBP reporting for more information.
- BDCM+TCAL reported as BDCM. See Chromatographic separation and DBP reporting for more information.

Table E1-16. Disinfection Byproduct Concentrations Plant D.
Average ± range in µg/L or mg/L. <MDL = below method detection limit; - = no data/not applicable.

DBP Class and units	DBP	D					
		Influent		Effluent		Downstream	
		June/July 2021	September 2021	June/July 2021	September 2021	June/July 2021	September 2021
Trihalomethanes (THMs) µg/L	Trichloromethane	<MDL ^a	4.3 ± 0.2	<MDL ^a	4.4 ± 0.1	<MDL ^a	4.2 ± 0.06
	Bromodichloromethane	2.7 ± 0.01	0.76 ± 0.76 ^d	2.4 ± 0.3	1.7 ± 0.03 ^d	<MDL	0.89 ± 0.89 ^d
	Dibromochloromethane	2.1 ± 0.05	3.0 ± 0.07	<MDL	2.8 ± 0.02	<MDL	2.8 ± 0.04
	Tribromomethane	<MDL	<MDL	<MDL	<MDL	<MDL	<MDL
Iodinated Trihalomethanes (I-THMs) µg/L	Triiodomethane	<MDL	<MDL	<MDL	<MDL	<MDL	<MDL
	Bromochloroiodomethane	<MDL	<MDL	<MDL	<MDL	<MDL	<MDL
	Chloroiodomethane	<MDL	<MDL	<MDL	<MDL	<MDL	<MDL
	Dibromoiodomethane	<MDL	<MDL	<MDL	<MDL	<MDL	<MDL
	Bromodiiodomethane	<MDL	<MDL	<MDL	<MDL	<MDL	<MDL
	Dichloroiodomethane	<MDL	- ^c	<MDL	- ^c	<MDL	- ^c
Haloacetic Acids (HAAs) µg/L	Chloroacetic acid	-	-	-	-	-	-
	Bromoacetic acid	<MDL	<MDL	2.2 ± 2.2	<MDL	<MDL	<MDL
	Dichloroacetic acid	<MDL	<MDL	<MDL	1.6 ± 0.2	<MDL	1.2 ± 1.2
	Trichloroacetic acid	<MDL	<MDL	<MDL	<MDL	<MDL	<MDL
	Bromochloroacetic acid	<MDL	<MDL	<MDL	<MDL	<MDL	<MDL
	Dibromoacetic acid	<MDL	<MDL	<MDL	<MDL	<MDL	<MDL
	Bromodichloroacetic acid	<MDL	<MDL	<MDL	<MDL	<MDL	<MDL
	Chlorodibromoacetic acid	<MDL	<MDL	<MDL	2.7 ± 0.2	<MDL	2.8 ± 0.3
	Tribromoacetic acid	<MDL	<MDL	<MDL	<MDL	<MDL	<MDL
Iodinated Haloacetic Acids (I-HAAs) µg/L	Iodoacetic acid	<MDL	<MDL	<MDL	<MDL	<MDL	<MDL
	Diiodoacetic acid	<MDL	<MDL	<MDL	2.6 ± 0.1	<MDL	<MDL
	Bromiodoacetic acid	<MDL	<MDL	<MDL	<MDL	<MDL	<MDL
	Chloriodoacetic acid	-	-	-	-	-	-
Haloacetonitriles (HANs) µg/L	Trichloroacetonitrile	<MDL	<MDL	<MDL	<MDL	<MDL	<MDL
	Dichloroacetonitrile	<MDL	<MDL ^b	<MDL	<MDL ^b	<MDL	<MDL ^b
	Dibromoacetonitrile	<MDL	<MDL	<MDL	<MDL	<MDL	<MDL
	Bromochloroacetonitrile	<MDL	<MDL ^c	<MDL	<MDL ^c	<MDL	<MDL ^c
Haloketones (HKs) µg/L	1,1-Dichloro-2-propanone	- ^b	- ^b	- ^b	- ^b	- ^b	- ^b
	1,1,1-Trichloro-2-propanone	<MDL	<MDL	<MDL	<MDL	<MDL	<MDL
Halonitromethanes (HNMs) µg/L	Trichloronitromethane	<MDL	<MDL	<MDL	<MDL	<MDL	<MDL
	Bromodichloronitromethane	<MDL	<MDL	<MDL	<MDL	<MDL	<MDL
	Dibromochloronitromethane	-	-	-	-	-	-
Haloacetamides (HAMs) µg/L	Trichloroacetamide	<MDL	<MDL	<MDL	<MDL	<MDL	<MDL
	Dibromoacetamide	<MDL	<MDL	<MDL	<MDL	<MDL	<MDL

Continued on next page

Continued from previous page

Haloacetaldehydes (HALs) µg/L	Dichloroacetaldehyde	- ^a	<MDL	- ^a	<MDL	- ^a	<MDL
	Trichloroacetaldehyde	<MDL	- ^d	<MDL	- ^d	<MDL	- ^d
	Tribromoacetaldehyde	<MDL	<MDL	<MDL	<MDL	<MDL	<MDL
Halogenated Furanones (MX Compounds) ng/L	3-Chloro-4-(dichloromethyl)-5-hydroxy-2(5H)-furanone	<MDL	<MDL	<MDL	<MDL	<MDL	<MDL
	2,3-Dichloro-4-oxobutenoic acid	<MDL	<MDL	<MDL	<MDL	<MDL	<MDL
Nitrosamines ng/L	N-nitrosodimethylamine	11.9 ± 0.1	<MDL	5.9 ± 0.1	<MDL	5.9 ± 0.2	<MDL
Inorganic DBPs mg/L	Chlorite	<MDL	<MDL	<MDL	<MDL	<MDL	<MDL
	Chlorate	<MDL	<MDL	0.03 ± 0.002	0.06 ± 0.006	0.03	0.07 ± 0.001
	Bromate	<MDL	<MDL	<MDL	<MDL	<MDL	<MDL
Other	Adsorbable organohalides (µg-Cl ⁻ /L)	<MDL	<MDL	<MDL	<MDL	<MDL	<MDL
	Bromide (mg/L)	0.02 ± 0.001	0.01 ± 0.0008	0.02 ± 0.0004	0.01 ± 0.0005	0.02 ± 0.0005	0.009 ± 0.0002
	Chloride (mg/L)	9.1 ± 0.2	10.7 ± 0.08	11.8 ± 0.08	11.8 ± 0.2	10.6 ± 0.2	11.7 ± 0.04
	Phosphate (mg/L)	<MDL	<MDL	<MDL	<MDL	<MDL	<MDL
	Sulfate (mg/L)	0.8 ± 0.02	0.5 ± 0.01	0.9 ± 0.01	0.6 ± 0.02	0.9 ± 0.06	0.6 ± 0.005
	Conductivity (µS/cm)	821.1	268.9	924.5	281.3	921.4	282.2
	TOC (mg/L)	0.05 ± 0.01	<MDL	0.2 ± 0.003	<MDL	0.07 ± 0.002	<MDL
	DOC (mg/L)	0.25	<MDL	0.33	<MDL	0.22	<MDL
	Ammonia (mg/L)	0.4 ± 0.008	0.1 ± 0.03	0.09 ± 0.002	0.03 ± 0.002	0.1 ± 0.05	0.03 ± 0.001
	Nitrate (mg/L)	2.2 ± 0.06	2.7 ± 0.04	2.4 ± 0.005	2.7 ± 0.009	1.9 ± 0.05	2.6 ± 0.01
	Nitrite (mg/L)	0.004	0.009 ± 0.0005	0.004 ± 0.001	<MDL	0.007 ± 0.0001	0.0001 ± 0.0001
	pH	6.3 ± 0.02	5.7 ± 0.01	7.0 ± 0.2	5.8 ± 0.04	7.1 ± 0.01	6.5 ± 0
	UV ₂₅₄ (cm ⁻¹)	0.0013	0.001 ± 0.0003	0.04	0.002 ± 0.0009	0.01 ± 0.0007	0.0005 ± 0.0002

- TCM+DCAL reported as TCM. See Chromatographic separation and DBP reporting for more information.
- DCAN+DCP reported as DCAN. See Chromatographic separation and DBP reporting for more information.
- BCAN+DCIM reported as BCAN. See Chromatographic separation and DBP reporting for more information.
- BDCM+TCAL reported as BDCM. See Chromatographic separation and DBP reporting for more information.

E1.7 Complete “Enhanced” Campaign Results

Table E1-17. Disinfection Byproduct Concentrations in the Treated Surface Water.
Average ± range in µg/L or mg/L. <MDL = below method detection limit; - = no data/not applicable.

DBP Class and units	DBP	Surface water						
		Raw	UV	Cl	UV/Cl	UV/Cl - FP	UV/H ₂ O ₂	UV/H ₂ O ₂ - FP
Trihalomethanes (THMs) µg/L	Trichloromethane	<MDL	<MDL	12.4 ± 0.4	20.5 ± 0.5	114.8 ± 34.6	<MDL	98.1 ± 0.7
	Bromodichloromethane ^c	<MDL	<MDL	1.4 ± 0.1	3.4 ± 0.02	30.2 ± 0.7	<MDL	20.9 ± 0.7
	Dibromochloromethane	0.9	0.4 ± 0.4	1.3 ± 0.04	1.5 ± 0.04	4.0 ± 0.4	0.9 ± 0.009	2.6 ± 0.1
	Tribromomethane	<MDL	<MDL	<MDL	<MDL	<MDL	<MDL	<MDL
Iodinated Trihalomethanes (I-THMs) µg/L	Triiodomethane	<MDL	<MDL	<MDL	<MDL	<MDL	<MDL	<MDL
	Bromochloroiodomethane	<MDL	<MDL	<MDL	<MDL	<MDL	<MDL	<MDL
	Chloroiodomethane	<MDL	<MDL	<MDL	<MDL	<MDL	<MDL	<MDL
	Dibromoiodomethane	<MDL	<MDL	<MDL	<MDL	<MDL	<MDL	<MDL
	Bromodiiodomethane	<MDL	<MDL	<MDL	<MDL	<MDL	<MDL	<MDL
Haloacetic Acids (HAAs) µg/L	Dichloroiodomethane ^a	-	-	-	-	-	-	-
	Chloroacetic acid	-	-	-	-	-	-	-
	Bromoacetic acid	<MDL	<MDL	<MDL	<MDL	<MDL	<MDL	<MDL
	Dichloroacetic acid	<MDL	<MDL	6.0 ± 0.07	17.8 ± 1.3	63.8 ± 2.5	<MDL	43.3 ± 1.6
	Trichloroacetic acid	<MDL	<MDL	4.5 ± 0.2	7.5 ± 0.6	40.2 ± 0.1	<MDL	48.9 ± 3.0
	Bromochloroacetic acid	<MDL	<MDL	1.0 ± 0.08	2.4 ± 0.03	7.3 ± 0.3	<MDL	4.2 ± 0.2
	Dibromoacetic acid	<MDL	<MDL	<MDL	1.0 ± 0.02	1.6 ± 0.2	<MDL	1.1 ± 0.1
	Bromodichloroacetic acid	<MDL	<MDL	<MDL	<MDL	<MDL	<MDL	1.5 ± 0.5
	Chlorodibromoacetic acid	-	-	-	-	-	-	-
Iodinated Haloacetic Acids (I-HAAs) µg/L	Tribromoacetic acid	-	-	-	-	-	-	-
	Iodoacetic acid	<MDL	<MDL	<MDL	<MDL	<MDL	<MDL	<MDL
	Diiodoacetic acid	-	-	-	-	-	-	-
	Bromoiodoacetic acid	<MDL	<MDL	<MDL	<MDL	<MDL	<MDL	<MDL
	Chloroiodoacetic acid	-	-	-	-	-	-	-

Continued on next page

Continued from previous page

Haloacetonitriles (HANs) µg/L	Trichloroacetonitrile	<MDL	<MDL	<MDL	<MDL	<MDL	<MDL	<MDL
	Dichloroacetonitrile ^b	<MDL	<MDL	0.4 ± 0.08	2.7 ± 0.06	5.7 ± 0.3	<MDL	8.3 ± 0.1
	Dibromoacetonitrile	<MDL	<MDL	<MDL	<MDL	<MDL	<MDL	<MDL
	Bromochloroacetonitrile ^a	<MDL	<MDL	0.3 ± 0.3	0.4 ± 0.4	1.4 ± 0.09	<MDL	0.6 ± 0.6
Haloketones (HKs) µg/L	1,1-Dichloro-2-propanone ^b	-	-	-	-	-	-	-
	1,1,1-Trichloro-2-propanone	<MDL	<MDL	0.9 ± 0.06	3.0 ± 0.04	1.3 ± 0.02	<MDL	1.8 ± 0.08
Halonitromethanes (HNMs) µg/L	Trichloronitromethane	<MDL	<MDL	<MDL	1.1 ± 1.1	3.5 ± 0.3	<MDL	3.3 ± 0.8
	Bromodichloronitromethane	<MDL	<MDL	<MDL	4.1 ± 0.2	5.1 ± 0.6	<MDL	11.1 ± 0.3
	Dibromochloronitromethane	<MDL	<MDL	<MDL	<MDL	<MDL	<MDL	<MDL
Haloacetamides (HAMs) µg/L	Trichloroacetamide	<MDL	<MDL	<MDL	<MDL	3.4 ± 0.06	<MDL	4.0 ± 0.06
	Dibromoacetamide	<MDL	<MDL	<MDL	<MDL	<MDL	<MDL	<MDL
Haloacetaldehydes (HALs) µg/L	Dichloroacetaldehyde	<MDL	<MDL	2.2 ± 0.1	3.8 ± 0.02	12.9 ± 0.9	0	12.0 ± 0.1
	Trichloroacetaldehyde ^c	-	-	-	-	-	-	-
	Tribromoacetaldehyde	<MDL	<MDL	<MDL	<MDL	<MDL	<MDL	<MDL
Halogenated Furanones (MX Compounds) ng/L	3-Chloro-4-(dichloromethyl)-5-hydroxy-2(5H)-furanone	<MDL	<MDL	2.0 ± 0.04	7.5 ± 0.5	8.8 ± 0.004	<MDL	5.0 ± 0.7
	2,3-Dichloro-4-oxobutenoic acid	<MDL	<MDL	16.1 ± 0.4	241.8 ± 32.2	1567.9 ± 168.4	<MDL	1389.5 ± 290.0
Inorganic DBPs mg/L	Chlorite	<MDL	<MDL	<MDL	<MDL	<MDL	<MDL	<MDL
	Chlorate	<MDL	<MDL	16.1 ± 16.1	248.5 ± 82.2	158.9 ± 98.8	<MDL	<MDL
	Perchlorate	-	-	-	-	-	-	-
	Bromate	<MDL	<MDL	<MDL	<MDL	<MDL	<MDL	<MDL
Other	Adsorbable organohalides µg-Cl ⁻¹ /L	<MDL	<MDL	177.8 ± 1.0	258.9 ± 20.8	592.7 ± 4.5	<MDL	581.9 ± 20.9
	Free chlorine residual mg/L as Cl ₂	-	-	5.5	1.3 ± 0.07	-	-	-
	Bromide mg/L	0.04	0.04 ± 0.0007	0.004 ± 0.001	0.01 ± 0.0001	<MDL	0.03 ± 0.001	0.02 ± 0.02
	Chloride mg/L	83.6	83.3 ± 0.6	93.9 ± 4.0	97.6 ± 1.7	100.7 ± 0.3	82.5 ± 0.4	103.1 ± 2.3
	Phosphate mg/L	<MDL	0.0003 ± 0.0003	<MDL	<MDL	0.08 ± 0.07	0.0002 ± 0.0002	0.03 ± 0.03
	Sulfate mg/L	40.9	38.9 ± 1.0	40.8 ± 3.9	42.3 ± 1.1	40.3 ± 0.5	39.5 ± 0.2	39.2 ± 1.1
	Conductivity µS cm ⁻¹	-	-	-	1120	1179 ± 12	1026.5 ± 7.5	1141 ± 2
	TOC mg/L	2.9	-	-	3.4	2.7 ± 0.1	2.9 ± 0.03	2.8 ± 0.1
	DOC mg/L	-	-	-	2.7	2.4 ± 0.02	2.7 ± 0.1	2.7 ± 0.1
	Ammonia mg/L	0.01	0.01 ± 0.0009	0.02 ± 0.01	0.01 ± 0.003	0.01 ± 0.003	0.01 ± 0.001	0.01 ± 0.0007
	Nitrate mg/L	5.9	5.8 ± 0.05	6.0 ± 0.3	6.1 ± 0.1	6.0 ± 0.1	5.7 ± 0.06	5.8 ± 0.2
	Nitrite mg/L	0.04	0.1 ± 0.002	0.006 ± 0.0008	0.002 ± 0.0004	0.0002	0.2 ± 0.0002	0.0004
	Treated water temperature °C	-	23 ± 0	15 ± 0	24 ± 0	25.5 ± 1.5	-	-
	pH	8.8	-	-	8.6 ± 0	8.7 ± 0.06	8.7 ± 0.05	8.7 ± 0.01
	UV ₂₅₄ cm ⁻¹	0.1	0.1 ± 0.002	0.1 ± 0.0002	0.1 ± 0.0008	0.1 ± 0.005	0.1 ± 0.007	0.1 ± 0.001

- BCAN+DCIM reported as BCAN. See Chromatographic separation and DBP reporting for more information.
- DCAN+DCP reported as DCAN. See Chromatographic separation and DBP reporting for more information.
- BDCM+TCAL reported as BDCM. See Chromatographic separation and DBP reporting for more information.

Table E1-18. Disinfection Byproduct Concentrations in the Treated Carbon-Based Reuse Water.
Average ± range in µg/L or mg/L. <MDL = below method detection limit; - = no data/not applicable.

DBP Class and units	DBP	Carbon-based reuse						
		Raw	UV	Cl	UV/Cl	UV/Cl - FP	UV/H ₂ O ₂	UV/H ₂ O ₂ - FP
Trihalomethanes (THMs) µg/L	Trichloromethane	<MDL	4.0 ± 0.3	4.7 ± 0.3	10.0 ± 0.7	15.9	3.5 ± 0.31	31.4 ± 3.2
	Bromodichloromethane	<MDL	3.6 ± 0.1	4.5 ± 0.1	6.9 ± 0.3	82.1	1.7 ± 1.7	53.4 ± 4.8
	Dibromochloromethane	<MDL	<MDL	4.2 ± 0.1	4.3 ± 0.02	36.7	<MDL	35.6 ± 3.2
	Tribromomethane	<MDL	<MDL	0.9 ± 0.9	0	26.8	<MDL	12.1 ± 1.1
Iodinated Trihalomethanes (I-THMs) µg/L	Triiodomethane	<MDL	<MDL	<MDL	<MDL	<MDL	<MDL	<MDL
	Bromochloroiodomethane	<MDL	<MDL	<MDL	<MDL	<MDL	<MDL	<MDL
	Chlorodiiodomethane	<MDL	<MDL	<MDL	<MDL	<MDL	<MDL	<MDL
	Dibromiodomethane	<MDL	<MDL	<MDL	<MDL	<MDL	<MDL	<MDL
	Bromodiiodomethane	<MDL	<MDL	<MDL	<MDL	<MDL	<MDL	<MDL
	Dichloroiodomethane	-	-	-	-	-	-	-
Haloacetic Acids (HAAs) µg/L	Chloroacetic acid	-	-	-	-	-	-	-
	Bromoacetic acid	<MDL	<MDL	<MDL	<MDL	3.4 ± 0.05	<MDL	1.6 ± 0.01
	Dichloroacetic acid	4.3	<MDL	<MDL	15.9 ± 0.7	47.7 ± 1.3	<MDL	22.3 ± 3.1
	Trichloroacetic acid	<MDL	<MDL	1.3 ± 0.03	2.1 ± 0.03	5.4 ± 0.03	<MDL	4.5 ± 0.09
	Bromochloroacetic acid	<MDL	<MDL	1.1 ± 0.01	4.1 ± 0.1	13.6 ± 0.05	1.1 ± 0.1	8.2 ± 0.2
	Dibromoacetic acid	<MDL	<MDL	1.4 ± 0.2	2.0 ± 0.1	6.3 ± 0.9	<MDL	5.9 ± 0.9
	Bromodichloroacetic acid	<MDL	<MDL	<MDL	<MDL	<MDL	<MDL	<MDL
	Chlorodibromoacetic acid	<MDL	<MDL	<MDL	<MDL	<MDL	<MDL	<MDL
	Tribromoacetic acid	<MDL	3.9 ± 0.2	3.9 ± 0.6	4.5 ± 0.1	<MDL	3.0 ± 1.3	3.1 ± 0.2
	Iodoacetic acid	<MDL	<MDL	<MDL	<MDL	<MDL	<MDL	<MDL
Iodinated Haloacetic Acids (I-HAAs) µg/L	Diiodoacetic acid	<MDL	<MDL	<MDL	<MDL	<MDL	<MDL	<MDL
	Bromoiodoacetic acid	<MDL	<MDL	<MDL	<MDL	<MDL	<MDL	<MDL
	Chloroiodoacetic acid	-	-	-	-	-	-	-
Haloacetonitriles (HANs) µg/L	Trichloroacetonitrile	<MDL	<MDL	<MDL	<MDL	6.8	<MDL	<MDL
	Dichloroacetonitrile	<MDL	<MDL	<MDL	<MDL	<MDL	<MDL	0.23 ± 0.23
	Dibromoacetonitrile	<MDL	<MDL	<MDL	<MDL	<MDL	<MDL	<MDL
	Bromochloroacetonitrile	<MDL	<MDL	<MDL	<MDL	5.5	<MDL	2.8 ± 0.03

Continued on next page

Continued from previous page

Haloketones (HKs) $\mu\text{g/L}$	1,1-Dichloro-2-propanone	<MDL	<MDL	<MDL	4.5 \pm 0.3	14.1	<MDL	3.6 \pm 2.8
	1,1,1-Trichloro-2-propanone	<MDL	<MDL	<MDL	2.0 \pm 0.1	8.4	<MDL	3.8 \pm 0.4
Halonitromethanes (HNMs) $\mu\text{g/L}$	Trichloronitromethane	<MDL	<MDL	<MDL	<MDL	2.2	<MDL	<MDL
	Bromodichloronitromethane	<MDL	<MDL	<MDL	<MDL	<MDL	<MDL	1.6 \pm 1.6
	Dibromochloronitromethane	<MDL	<MDL	<MDL	<MDL	<MDL	<MDL	<MDL
Haloacetamides (HAMs) $\mu\text{g/L}$	Trichloroacetamide	<MDL	<MDL	<MDL	<MDL	<MDL	<MDL	<MDL
	Dibromoacetamide	<MDL	<MDL	<MDL	<MDL	<MDL	<MDL	6.6 \pm 0.6
Haloacetaldehydes (HALs) $\mu\text{g/L}$	Dichloroacetaldehyde	<MDL	<MDL	<MDL	4.2 \pm 4.2	<MDL	<MDL	<MDL
	Trichloroacetaldehyde	<MDL	<MDL	<MDL	<MDL	<MDL	<MDL	<MDL
	Tribromoacetaldehyde	<MDL	<MDL	<MDL	<MDL	<MDL	<MDL	<MDL
Halogenated Furanones (MX Compounds) ng/L	3-Chloro-4-(dichloromethyl)-5-hydroxy-2(5H)-furanone	<MDL	<MDL	1.6 \pm 0.1	2.9	3.5 \pm 0.04	1.4 \pm 0.04	2.3 \pm 0.07
	2,3-Dichloro-4-oxobutenoic acid	14.9 \pm 0	15.3 \pm 0.3	22.6 \pm 1.5	67.0	332.4 \pm 16.1	14.8 \pm 0.5	119.2 \pm 7.5
Inorganic DBPs mg/L	Chlorite	<MDL	<MDL	<MDL	<MDL	<MDL	<MDL	<MDL
	Chlorate	0.3	0.3 \pm 0.0009	0.2 \pm 0.09	0.7 \pm 0.09	1.1 \pm 0.02	0.3 \pm 0.001	<MDL
	Bromate	<MDL	<MDL	<MDL	<MDL	<MDL	<MDL	<MDL
Other	Adsorbable organohalides $\mu\text{g-Cl}^{-1}$	61.7	56.6 \pm 0.1	113.3 \pm 18.8	160.5 \pm 6.2	353.2 \pm 4.1	53.2 \pm 0.4	255.7 \pm 1.2
	Free chlorine residual mg/L as Cl_2	-	-	6.2 \pm 0.1	0	-	-	-
	Hydrogen Peroxide residual mg/L	-	-	-	-	-	2.6 \pm 0.01	2.7 \pm 0.005
	Bromide mg/L	0.2	0.2 \pm 0.007	0.1 \pm 0.0001	0.07 \pm 0.02	0.04 \pm 0.0008	0.2 \pm 0.01	0.04 \pm 0.001
	Chloride mg/L	205.6	201.9 \pm 0.01	202.5 \pm 6.7	202.6 \pm 2.3	227.0 \pm 2.5	206.6 \pm 1.1	226.0 \pm 0.3
	Phosphate mg/L	0.02	0.1 \pm 0.1	0.09 \pm 0.08	0.1 \pm 0.03	0.1 \pm 0.08	0.008 \pm 0.002	0.03 \pm 0.002
	Sulfate mg/L	80.8	80.2 \pm 0.1	76.0 \pm 3.0	76.3 \pm 1.1	81.0 \pm 1.2	81.0 \pm 0.06	81.4 \pm 0.4
	Conductivity $\mu\text{S cm}^{-1}$	1558	339.8 \pm 156.6	1578.5 \pm 86.5	1529.5 \pm 3.5	1575.5 \pm 141.5	1214 \pm 52.0	1603 \pm 18.0
	TOC mg/L	3.2	3.0 \pm 0.02	3.2 \pm 0.05	3.1 \pm 0.08	3.1 \pm 0.07	3.0 \pm 0.03	2.9 \pm 0.01
	DOC mg/L	3.1	2.7 \pm 0.05	3.0 \pm 0.07	3.0 \pm 0.1	3.0 \pm 0.04	3.1 \pm 0.04	2.8 \pm 0.03
	Ammonia mg/L	0.01	0.02 \pm 0.004	0.01 \pm 0.001	0.03 \pm 0.001	0.01 \pm 0.0007	0.2 \pm 0.1	0.01
	Nitrate mg/L	3.2	2.9 \pm 0.01	2.8 \pm 0.005	2.9 \pm 0.05	3.2 \pm 0.03	3.0 \pm 0.04	3.1 \pm 0.04
	Nitrite mg/L	<MDL	0.1 \pm 0.001	<MDL	<MDL	<MDL	0.1 \pm 0.0001	<MDL
	Treated water temperature $^{\circ}\text{C}$	21.0	27.5 \pm 0.5	13.0 \pm 0	27.0 \pm 0	27.0 \pm 0	25.7 \pm 0.7	26.5 \pm 0.5
	pH	7.2	7.2 \pm 0.07	7.7 \pm 0.1	7.5 \pm 0.01	7.2 \pm 0	7.2 \pm 0	7.1 \pm 0.05
	UV ₂₅₄ cm^{-1}	0.05	0.1 \pm 0.07	0.1 \pm 0.005	0.1 \pm 0.01	0.09 \pm 0.009	0.09 \pm 0.01	0.1 \pm 0.03

Table E1-19. Disinfection Byproduct Concentrations in the Treated RO-Based Reuse Water.
Average ± range in µg/L or mg/L. <MDL = below method detection limit; “-” = no data/not applicable.

DBP Class and units	DBP	RO-based reuse						
		Raw	UV	Cl	UV/Cl	UV/Cl - FP	UV/H ₂ O ₂	UV/H ₂ O ₂ - FP
Trihalomethanes (THMs) µg/L	Trichloromethane	<MDL	0.7 ± 0.1	<MDL	<MDL	1.1 ± 0.08	<MDL	1.3 ± 0.1
	Bromodichloromethane ^a	2.3	2.2 ± 0.007	2.2 ± 0.008	2.2 ± 0.04	4.7 ± 0.2	2.1 ± 0.03	3.9 ± 0.1
	Dibromochloromethane	1.9	1.5 ± 0.1	2.0 ± 0.005	1.4 ± 0.3	3.5 ± 0.3	1.3 ± 0.06	2.8 ± 0.4
	Tribromomethane	2.7	0.6 ± 0.09	2.7 ± 0.008	0.7 ± 0.02	2.0 ± 0.05	<MDL	1.7 ± 0.004
Iodinated Trihalomethanes (I-THMs) µg/L	Triiodomethane	<MDL	<MDL	<MDL	<MDL	<MDL	<MDL	<MDL
	Bromochloroiodomethane	<MDL	<MDL	<MDL	<MDL	<MDL	<MDL	<MDL
	Chlorodiiodomethane	<MDL	<MDL	<MDL	<MDL	<MDL	<MDL	<MDL
	Dibromoiodomethane	<MDL	<MDL	<MDL	<MDL	<MDL	<MDL	<MDL
	Bromodiiodomethane	<MDL	<MDL	<MDL	<MDL	<MDL	<MDL	<MDL
	Dichloroiodomethane	<MDL	<MDL	<MDL	<MDL	<MDL	<MDL	<MDL
Haloacetic Acids (HAAs) µg/L	Chloroacetic acid	-	-	-	-	-	-	-
	Bromoacetic acid	<MDL	<MDL	<MDL	1.8 ± 0.02	3.9 ± 0.05	<MDL	1.9 ± 0.05
	Dichloroacetic acid	<MDL	<MDL	<MDL	<MDL	3.8 ± 0.1	<MDL	2.5 ± 0.1
	Trichloroacetic acid	<MDL	1.1 ± 0.05	1.1 ± 0.004	1.2 ± 0.03	1.6 ± 0.1	<MDL	1.5 ± 0.003
	Bromochloroacetic acid	<MDL	<MDL	<MDL	1.0 ± 0.02	2.8 ± 0.04	<MDL	1.8 ± 0.02
	Dibromoacetic acid	<MDL	1.0 ± 0.003	1.0 ± 0.006	1.2 ± 0.004	2.1 ± 0.03	<MDL	1.8 ± 0.009
	Bromodichloroacetic acid	<MDL	<MDL	1.8 ± 0.003	1.9 ± 0.008	2.4 ± 0.04	<MDL	2.3 ± 0.0008
	Chlorodibromoacetic acid	<MDL	<MDL	<MDL	<MDL	3.6 ± 0.02	<MDL	3.6 ± 0.2
	Tribromoacetic acid	<MDL	<MDL	<MDL	<MDL	<MDL	<MDL	<MDL
Iodinated Haloacetic Acids (I-HAAs) µg/L	Iodoacetic acid	<MDL	<MDL	<MDL	<MDL	<MDL	<MDL	<MDL
	Diiodoacetic acid	<MDL	<MDL	<MDL	<MDL	<MDL	<MDL	<MDL
	Bromiodoacetic acid	<MDL	<MDL	<MDL	<MDL	<MDL	<MDL	<MDL
	Chloriodoacetic acid	-	-	-	-	-	-	-
Haloacetonitriles (HANs) µg/L	Trichloroacetonitrile	<MDL	<MDL	<MDL	<MDL	<MDL	<MDL	<MDL
	Dichloroacetonitrile	<MDL	<MDL	<MDL	<MDL	<MDL	<MDL	<MDL
	Dibromoacetonitrile	<MDL	<MDL	<MDL	<MDL	3.0 ± 0.001	<MDL	3.0 ± 0.005
	Bromochloroacetonitrile	-	-	-	-	-	-	-

Continued on next page

Haloketones (HKs) µg/L	1,1-Dichloro-2-propanone	<MDL	<MDL	<MDL	<MDL	<MDL	<MDL	<MDL
	1,1,1-Trichloro-2-propanone	<MDL	<MDL	<MDL	<MDL	1.8 ± 0.008	<MDL	1.7 ± 0.002
Halonitromethanes (HNMs) µg/L	Trichloronitromethane	<MDL	<MDL	<MDL	<MDL	<MDL	<MDL	<MDL
	Bromodichloronitromethane	<MDL	<MDL	<MDL	<MDL	<MDL	<MDL	<MDL
	Dibromochloronitromethane	-	-	-	-	-	-	-
Haloacetamides (HAMs) µg/L	Trichloroacetamide	<MDL	<MDL	<MDL	<MDL	<MDL	<MDL	<MDL
	Dibromoacetamide	<MDL	<MDL	<MDL	<MDL	<MDL	<MDL	<MDL
Haloacetaldehydes (HALs) µg/L	Dichloroacetaldehyde	<MDL	<MDL	<MDL	<MDL	<MDL	<MDL	<MDL
	Trichloroacetaldehyde ^a	-	-	-	-	-	-	-
	Tribromoacetaldehyde	<MDL	<MDL	<MDL	<MDL	<MDL	<MDL	<MDL
Halogenated Furanones (MX Compounds) ng/L	3-Chloro-4-(dichloromethyl)-5-hydroxy-2(5H)-furanone	<MDL	<MDL	<MDL	<MDL	<MDL	<MDL	<MDL
	2,3-Dichloro-4-oxobutenoic acid	<MDL	<MDL	<MDL	31.8 ± 3.0	189.9 ± 10.6	<MDL	14.7 ± 0.6
Inorganic DBPs mg/L	Chlorite	<MDL	<MDL	<MDL	<MDL	<MDL	<MDL	<MDL
	Chlorate	0.3	0.3 ± 0.0008	0.4 ± 0.09	0.4 ± 0.005	0.5 ± 0.1	0.3 ± 0.0007	0.5 ± 0.01
	Bromate	-	-	-	-	-	2.77	-
Other	Adsorbable organohalides µg-Cl ⁻¹	45.0	<MDL	46.5 ± 7.1	42.7 ± 6.3	55.3 ± 4.2	34.3 ± 5.6	47.5 ± 0.005
	Free chlorine residual mg/L as Cl ₂	0.02	-	2.4 ± 0.08	1.1 ± 0.06	1.5 ± 0.04	-	0.8 ± 0.03
	Hydrogen Peroxide residual mg/L	-	-	-	-	-	2.8	-
	Bromide mg/L	0.2	0.2 ± 0.002	0.1 ± 0.01	0.2 ± 0.004	0.1 ± 0.006	0.2 ± 0.004	0.1 ± 0.001
	Chloride mg/L	86.3	83.2 ± 2.6	94.7 ± 4.7	90.2 ± 0.2	94.1 ± 4.0	80.9 ± 0.4	95.4 ± 0.06
	Phosphate mg/L	3.6	3.2 ± 0.1	3.4 ± 0.2	3.3 ± 0.02	3.3 ± 0.2	3.3 ± 0.06	3.1 ± 0.004
	Sulfate mg/L	33.2	31.2 ± 0.1	33.4 ± 0.8	30.5 ± 0.09	36.9 ± 1.5	30.5 ± 0.3	32.9 ± 0.6
	Conductivity µS cm ⁻¹	558.0	551.2 ± 1.9	588.6 ± 0.5	584.9 ± 9.3	600.0 ± 0.2	556.1 ± 8.8	607.1 ± 4.7
	TOC mg/L	0.5	0.4 ± 0.02	0.5 ± 0.08	0.6 ± 0.03	0.4 ± 0.05	0.4 ± 0.04	0.4 ± 0.04
	DOC mg/L	0.4	0.4 ± 0.02	0.5 ± 0.1	0.4 ± 0.02	0.4 ± 0.002	0.4 ± 0.01	0.4 ± 0.02
	Ammonia mg/L	0.1	0.08 ± 0.004	0.04 ± 0.005	0.009 ± 0.009	0.02 ± 0.008	0.2 ± 0.003	<MDL
	Nitrate mg/L	1.1	1.1 ± 0.01	1.1 ± 0.03	1.1 ± 0.02	1.3 ± 0.09	1.1 ± 0.02	1.1 ± 0.01
	Nitrite mg/L	0.04	0.05 ± 0.004	0.007 ± 0.0005	<MDL	<MDL	0.05 ± 0.002	<MDL
	Treated water temperature °C	14.1	29.5 ± 0.5	15.3 ± 1.1	29.3 ± 0.3	22.5 ± 0.2	27.3 ± -3.3	22.5 ± 0.1
	pH	5.8	6.1 ± 0.2	6.0 ± 0.1	6.1 ± 0.1	6.2 ± 0.01	5.9 ± 0.2	6.2 ± 0.005
	UV ₂₅₄ cm ⁻¹	0.008	0.006 ± 0.0002	0.009 ± 0.001	0.003 ± 0.0003	0.004 ± 0.001	0.004 ± 0.0004	0.005 ± 0.001

^aBDCM+TCAL reported as BDCM. See Chromatographic separation and DBP reporting for more information.

E1.8 References

APHA, AWWA, and WEF. 2012. *Standard Methods for the Examination of Water & Wastewater, 22nd ed.* American Public Health Association, American Water Works Association, and Water Environment Federation: Washington, D.C., USA.

Buxton, G. V., and M. S. Subhani. 1972. "Radiation Chemistry and Photochemistry of Oxychlorine Ions. Part 2.-Photodecomposition of Aqueous Solutions of Hypochlorite Ions." *J. Chem. Soc. Faraday Trans. 1 Phys. Chem. Condens. Phases* 68: 958–969. doi:10.1039/F19726800958.

Drewes, J. E., P. Anderson, N. Denslow, W. Jakubowski, A. Olivieri, D. Schlenk, and S. Snyder. 2018. *Monitoring Strategies for Constituents of Emerging Concern (CECs) in Recycled Water. Recommendations of a Science Advisory Panel.* SCCWRP Technical Report 1032.

Escher, B. I., M. Allinson, R. Altenburger, P. A. Bain, P. Balaguer, W. Busch, J. Crago, N. D. Denslow, E. Dopp, K. Hilscherova, A. R. Humpage, A. Kumar, M. Grimaldi, B. S. Jayasinghe, B. Jarosova, A. Jia, S. Makarov, K. A. Maruya, A. Medvedev, A. C. Mehinto, J. E. Mendez, A. Poulsen, E. Prochazka, J. Richard, A. Schifferli, D. Schlenk, S. Scholz, F. Shiraishi, S. Snyder, G. Su, J. Y. M. Tang, B. Burg, S. C. Van Der Linden, I. Van Der Werner, S. D. Westerheide, C. K. C. Wong, M. Yang, B. H. Y. Yeung, X. Zhang, and F. D. L. Leusch. 2014. "Benchmarking Organic Micropollutants in Wastewater, Recycled Water and Drinking Water with in Vitro Bioassays." *Environmental Science & Technology*, 48: 1940–1956. doi:10.1021/es403899t.

Escher, B. I., M. Dutt, E. Maylin, J. Y. M. Tang, S. Toze, C. R. Wolf, and M. Lang. 2012. "Water Quality Assessment Using the Arec32 Reporter Gene Assay Indicative of the Oxidative Stress Response Pathway." *J. Environ. Monit.*, 14: 2877–2885. doi:10.1039/c2em30506b.

Escher, B. I., C. van Daele, M. Dutt, J. Y. Tang, and R. Altenburger. 2013. "Most Oxidative Stress Response in Water Samples Comes from Unknown Chemicals: The Need for Effect-Based Water Quality Trigger Values." *Environmental Science & Technology*, 47 (13): 7002-7011.

Fang, J., Q. Zhao, C. Fan, C. Shang, Y. Fu, and X. Zhang. 2017. "Bromate Formation from the Oxidation of Bromide in the UV/Chlorine Process with Low Pressure and Medium Pressure UV Lamps." *Chemosphere* 183: 582–588. doi:10.1016/j.chemosphere.2017.05.136.

Feng, Y. G., D. W. Smith, and J. R. Bolton. 2010. "A Potential New Method for Determination of the Fluence (UV Dose) Delivered in UV Reactors Involving the Photodegradation of Free Chlorine." *Water Environ. Res.*, 82: 328–334. doi:10.2175/106143009X447920.

Gao, Z. -C., Y. -L. Lin, B. Xu, Y. Xia, C. -Y. Hu, T. -Y. Zhang, T. -C. Cao, W. -H. Chu, and N. -Y. Gao. 2019. "Effect of UV Wavelength on Humic Acid Degradation and Disinfection By-Product Formation during the UV/Chlorine Process." *Water Research*, 154: 199–209. doi:10.1016/j.watres.2019.02.004

Huang, N., T. Wang, W. -L. L. Wang, Q. -Y. Y. Wu, A. Li, and H. -Y. Y. Hu. 2017. "UV/Chlorine As an Advanced Oxidation Process for the Degradation of Benzalkonium Chloride: Synergistic

Effect, Transformation Products and Toxicity Evaluation." *Water Research*, 114: 246–253. doi:10.1016/j.watres.2017.02.015.

International Organization for Standardization. 2000. "Water quality — Determination of the Genotoxicity of Water and Waste Water Using the Umu-Test." ISO 13829:2000: Vernier, Switzerland.

Kamath, D., and D. Minakata. 2018. "Emerging Investigators Series: Ultraviolet and Free Chlorine Aqueous-Phase Advanced Oxidation Process: Kinetic Simulations and Experimental Validation." *Environ. Sci. Water Res. Technol.*, 4: 1231–1238. doi:10.1039/c8ew00196k.

Krasner, S. W., M. J. McGuire, J. G. Jacangelo, N. L. Patania, K. M. Reagan, and E. M. Aieta. 1989. "The Occurrence of Disinfection By-products in US Drinking Water." *Journal American Water Works Association*, 81: 41–53. doi:10.2307/41292789.

Li, M., B. Xu, Z. Liungai, H. Y. Hu, C. Chen, J. Qiao, and Y. Lu. 2016. "The Removal of Estrogenic Activity with UV/Chlorine Technology and Identification of Novel Estrogenic Disinfection By-Products." *Journal of Hazardous Materials*, 307: 119–126. doi:10.1016/j.jhazmat.2016.01.003

Macova, M., S. Toze, L. Hodgers, J. F. Mueller, M. Bartkow, and B. I. Escher. 2011. "Bioanalytical Tools for the Evaluation of Organic Micropollutants during Sewage Treatment, Water Recycling and Drinking Water Generation." *Water Research*, 45: 4238–4247. doi:10.1016/j.watres.2011.05.032.

McCurry, D. L., K. P. Ishida, G. L. Oelker, and W. A. Mitch. 2017. "Reverse Osmosis Shifts Chloramine Speciation Causing Re-Formation of NDMA during Potable Reuse of Wastewater." *Environmental Science & Technology*, 51: 8589–8596. doi:10.1021/acs.est.7b01641.

McKie, M. J., L. Taylor-Edmonds, S. A. Andrews, and R. C. Andrews. 2015. "Engineered Biofiltration for the Removal of Disinfection By-Product Precursors and Genotoxicity." *Water Research*, 81: 196–207. doi:10.1016/j.watres.2015.05.034.

Neale, P. A., and B. I. Escher. 2019. "In Vitro Bioassays to Assess Drinking Water Quality." *Current Opinion in Environmental Science & Health*, 7: 1-7.

Reungoat, J., M. Macova, B. I. Escher, S. Carswell, J. F. Mueller, and J. Keller. 2010. "Removal of Micropollutants and Reduction of Biological Activity in a Full Scale Reclamation Plant Using Ozonation and Activated Carbon Filtration." *Water Research*, 44: 625–637. doi:10.1016/j.watres.2009.09.048.

Richardson, S. D., M. J. Plewa, E. D. Wagner, R. Schoeny, D. M. DeMarini. 2007. "Occurrence, Genotoxicity, and Carcinogenicity of Regulated and Emerging Disinfection By-Products in Drinking Water: A Review and Roadmap for Research." *Mutat. Res. - Rev. Mutat. Res.*, 636: 178–242. doi:10.1016/j.mrrev.2007.09.001.

Sgroi, M., P. Roccaro, G. L. Oelker, S. A. Snyder. 2015. "N-Nitrosodimethylamine (NDMA) Formation at an Indirect Potable Reuse Facility." *Water Research*, 70: 174–183. doi:10.1016/j.watres.2014.11.051.

- Shen, R., and S. A. Andrews. 2011. "Demonstration of 20 Pharmaceuticals and Personal Care Products (Ppcps) as Nitrosamine Precursors during Chloramine Disinfection." *Water Research*, 45: 944–952.
- Sun, J., D. Kong, E. Aghdam, J. Fang, Q. Wu, J. Liu, Y. Du, X. Yang, and C. Shang. 2019. "The Influence of the UV/Chlorine Advanced Oxidation of Natural Organic Matter for Micropollutant Degradation on the Formation of Dbps and Toxicity during Post-Chlorination." *Chemical Engineering Journal*, 373: 870-879.
- Sun, J., H. Peng, H. A. Alharbi, P. D. Jones, J. P. Giesy, and S. B. Wiseman. 2017. "Identification of Chemicals that Cause Oxidative Stress in Oil Sands Process-Affected Water." *Environmental Science & Technology*, 51 (15): 8773-8781. doi:10.1021/acs.est.7b01987.
- U.S. EPA. 2006. *National Primary Drinking Water Regulations: Stage 2 Disinfectants and Disinfection Byproducts Rule* (No. 71 FR 387), Federal Register.
- Wagner, E. D., and M. J. Plewa. 2017. "CHO Cell Cytotoxicity and Genotoxicity Analyses of Disinfection By-Products: An Updated Review." *J. Environ. Sci.*, 58: 64–76. doi:10.1016/j.jes.2017.04.021.
- Wang, C., N. Moore, K. Bircher, S. Andrews, and R. Hofmann. 2019. "Full-Scale Comparison of UV/H₂O₂ and UV/Cl₂ Advanced Oxidation: The Degradation of Micropollutant Surrogates and the Formation of Disinfection Byproducts." *Water Research*, 161: 448–458. doi:10.1016/j.watres.2019.06.033.
- Wang, D., J. R. Bolton, S. A. Andrews, and R. Hofmann. 2015. "Formation of Disinfection By-Products in the Ultraviolet/Chlorine Advanced Oxidation Process." *Sci. Total Environ.*, 518–519: 49–57. doi:10.1016/j.scitotenv.2015.02.094.
- Zheng, D., R. C. Andrews, S. A. Andrews, and L. Taylor-Edmonds. 2015. "Effects of Coagulation on the Removal of Natural Organic Matter, Genotoxicity, and Precursors to Halogenated Furanones." *Water Research*, 70: 118–129. doi:10.1016/j.watres.2014.11.039



THE
**Water
Research**
FOUNDATION

advancing the science of water®



1199 North Fairfax Street, Suite 900
Alexandria, VA 22314-1445

6666 West Quincy Avenue
Denver, CO 80235-3098

www.waterrf.org | info@waterrf.org